



UNIVERSITY of the
WESTERN CAPE

**Protein expression and antifungal effect of fluconazole-resistant
Candida species following effective *in vitro* treatment with K21, a
novel antifungal agent**

By

Cathy Nisha John

Student number - 2771795

Thesis submitted in fulfilment of the requirements for the degree of

Doctor of Philosophy (PhD)

Department of Medical Biosciences, Faculty of Natural Sciences

Supervisor: **Prof. Charlene WJ Africa**

Date: 11/12/2019

DECLARATION

I declare that this work “**Protein expression and antifungal effect of fluconazole-resistant *Candida* species following effective *in vitro* treatment with K21, a novel antifungal agent**” is my original work and all the sources that I have used or cited have been indicated and acknowledged by means of complete references, and that this document has not been submitted for degree purposes at any other academic institutions.

Cathy Nisha John

Student Number: 2771795

Signed: **CATHY NISHA JOHN**.....

Date:11/12/2019.....



UNIVERSITY of the
WESTERN CAPE

DEDICATION

I dedicate this thesis to my loving father A. D. John and mother Mary John, my dearest husband Arun and darling sons Dave and Neil for their unreserved encouragement, prayers, love and sacrifice for my success.



UNIVERSITY *of the*
WESTERN CAPE

ACKNOWLEDGEMENTS

This thesis would not be complete without the proper thank you to everyone that helped to accomplish this work.

First and foremost, I thank the **Almighty God** for listening to my prayers and for the health and strength he has given me throughout these years.

I take this opportunity to thank the **University of the Western Cape** and the faculty of **Natural Sciences** who has contributed positively to my PhD journey.

I would like to express my sincere gratitude to my mentor and supervisor, **Professor. Charlene Africa** who, despite her multiple academic, administrative and family occupations, accepted to guide this work. This thesis would not have been possible without her constant encouragement, support and the belief she had in me that motivated me to successfully complete this project. I want to thank her for the advice for many fruitful discussions and the expertise she has shared throughout the experiments. I admire her scientific rigor and dedication to science.

I would like to thank **KHG FiteBac Technology (Kimmerling Holding group)** for funding my study. My special gratitude to **Dr. Kirk Kimmerling** and **Dr. Dharam Ablashi** for giving me the opportunity to perform the study.

Special thanks to **Professor. Michel Monod**, Centre Hospitalier Universitaire Vaudois (CHUV), Lausanne, Switzerland, for taking his precious time to kindly prepare and provide the Sap antibodies for the research.

I thank Dr. Franscious Cummings, Department of Physics, University of the Western Cape, for assisting me with the Scanning electron microscopy techniques. I also thank Mohamed Jaffer, Centre for Imaging and Analysis, University of Cape Town, for the guidance in Transmission electron microscopy.

I thank my family for their unconditional love, prayers and motivations through my ups and downs that kept me going to achieve my goals.

My dear friends Shanly and Bifin and their loving kids and Dr. Sunil and family who made my stay in Cape Town pleasant.

I owe my gratitude to the colleagues of the Maternal Endogenous Infections studies (MEnIS) research lab, especially, Dr. Pedro Abrantes and Dr. Mohamed Shallouf for their assistance in my work at any time without hesitations.

The fulfilment of my thesis is the work of the good atmosphere around me as friends especially Felicia, Immanuel, Laila and Teresa. The time spent with my dear ones will stay forever in my memories.

Finally, I ask for the forgiveness of those whose contributions to this study I have inadvertently forgotten.

TABLE OF CONTENTS

DECLARATION.....	I
DEDICATION.....	II
ACKNOWLEDGEMENTS.....	III
ABSTRACT.....	IX
LIST OF FIGURES.....	XI
LIST OF TABLES.....	XIV
KEYWORDS.....	XV
RESEARCH OUTPUT.....	XVI
ABBREVIATIONS.....	XVII
CHAPTER 1: LITERATURE REVIEW.....	1
1.1 INTRODUCTION.....	1
1.2 Epidemiology of Candidiasis.....	2
1.3 Pathogenesis and virulence of <i>Candida albicans</i>	5
1.4 Current antifungal drugs and their mode of actions.....	10
1.5 Drug resistance and the need for novel antifungal drugs.....	11
1.6 Quaternary ammonium compounds (QAC) as possible alternatives to combat antimicrobial resistance.....	15
1.7 K21 antimicrobial compound.....	16
1.8 Summary.....	20
1.9 Study Hypothesis.....	21
1.10 Aims and Objectives.....	21

CHAPTER 2: A COMPARISON OF THE ANTIFUNGAL PROFILES OF *CANDIDA* USING FLUCONAZOLE AND A NOVEL QUATERNARY AMONIUM SILANE COMPOUND, K21.....23

2.1 INTRODUCTION.....23

2.2 MATERIALS AND METHODS.....24

2.2.1 Study design and Sample size.....24

2.2.2 Resuscitation and confirmation of purity of *Candida* isolates.....25

2.2.3 Antifungal susceptibility testing of K21.....25

2.2.3.1 Preparation of Roswell Park Memorial Institute-1640 media (RPMI-1640).....25

2.2.3.2 Preparation of K21 dilutions for assays.....26

2.2.3.3 Microdilution susceptibility assays.....27

2.2.4 Antifungal susceptibility testing of Fluconazole.....29

2.2.5 Comparison of the antimicrobial activity of FCZ, K21 and FCZ/K21.....30

2.2.5.1 Time kill and Synergy assay.....30

2.2.5.2 Checkerboard assay.....30

2.2.6 Statistical analysis.....33

2.3 RESULTS.....34

2.3.1 Confirmation of purity and distribution of *Candida* species.....34

2.3.2 Antifungal profiles of *Candida* species exposed to FCZ.....35

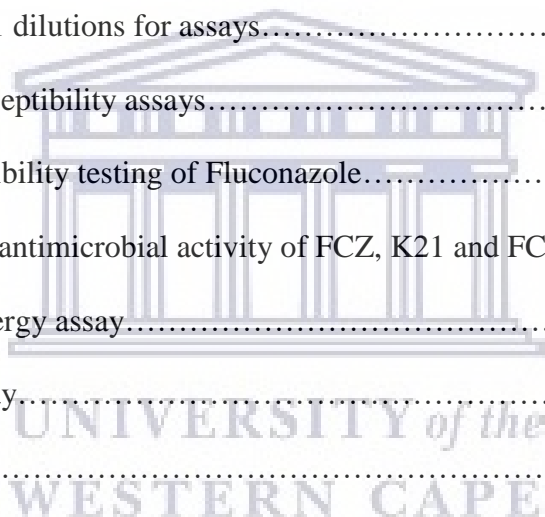
2.3.2.1 Broth microdilution assay for K21.....36

2.3.2.2 Effect of Fluconazole (FCZ).....39

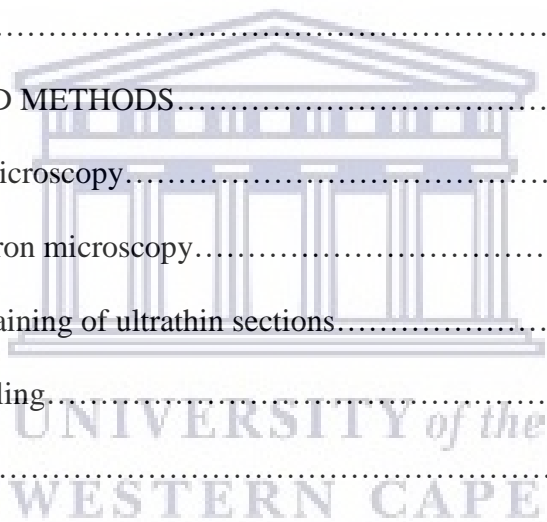
2.3.2.3 Effect of K21.....42

2.3.2.4 Comparison of FCZ with K21.....44

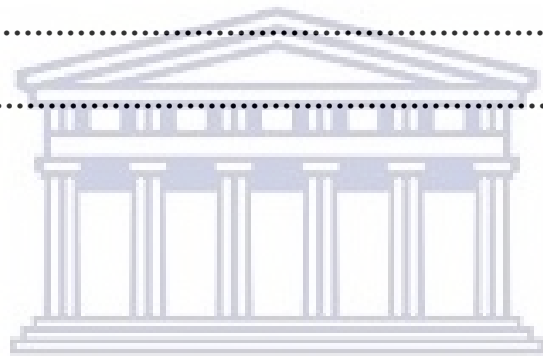
2.3.2.5 Synergistic effect of FCZ/K21.....45



2.3.2.6	Time-kill assay for K21.....	52
2.3.2.7	Time-kill assay for Synergy.....	54
2.3.2.7.1	Synergy of <i>C. albicans</i> (ATCC 90028 and NCPF 3281) determined by time-kill assay.....	55
2.3.2.7.2	Synergy of <i>C. glabrata</i> (ATCC 26512) determined by time-kill assay.....	59
2.3.2.7.3	Synergy of <i>C. dubliniensis</i> (NCPF 3949a) determine by time-kill assay.....	61
2.4	DISCUSSION.....	63
CHAPTER 3: MODE OF ACTION OF K21 AS OBSERVED BY ELECTRON MICROCOPY.....		67
3.1	INTRODUCTION.....	67
3.2	MATERIALS AND METHODS.....	67
3.2.1	Scannig electron microscopy.....	68
3.2.2	Transmission electron microscopy.....	69
3.2.2.1	Double contrast staining of ultrathin sections.....	71
3.2.2.2	Immunogold labelling.....	71
3.3	RESULTS.....	74
3.3.1	Scanning electron microscopy.....	74
3.3.1.1	Cell surface changes following K21 exposure.....	74
3.3.1.2	Cell surface changes following FCZ exposure.....	80
3.3.1.3	Cell surface changes following K21+FCZ exposure.....	85
3.3.2	Transmission electron microscopy.....	90
3.3.2.1	Ultrastructural changes at different time intervals of K21 exposure.....	90
3.3.2.2	Immunogold labelling of Sap after exposure to K21.....	93
3.4	DISCUSSION.....	102



CHAPTER 4: GENERAL DISCUSSION.....	109
4.1 BACKGROUND.....	109
4.2 Antifungal Susceptibility Testing.....	109
4.3 Electron microscopy and Sap protein expression of <i>Candida</i>	119
4.3.1 Scanning Electron Microscopy.....	119
4.3.2 Transmission Electron Microscopy.....	122
4.3.3 Effect of K21 on Sap expression in <i>Candida</i>	126
4.4 Limitations of the study.....	132
CHAPTER 5: CONCLUSION.....	134
REFERENCES.....	137
APPENDIX A.....	178



UNIVERSITY *of the*
WESTERN CAPE

ABSTRACT

Background: Oropharyngeal candidiasis, caused by the fungus *Candida*, is the most common opportunistic infection affecting the quality of life of immunocompromised patients. Fluconazole is widely used as the first line of treatment for fungal infections. However, the inappropriate and misguided use of the drug has led to the evolution of fluconazole-resistant *Candida* organisms. This arising resistance resulted in the urgent need for the development of new antimicrobial drugs. The aim of the present study was to investigate the antifungal action of K21, a novel antimicrobial quaternary ammonium compound, on fluconazole-resistant *Candida* species.

Materials and Methods: An *in vitro* study was conducted using a total of 143 *Candida* isolates obtained from HIV-positive patients. The ethical aspects of the study complied with the declaration of Helsinki (2013). The time-kill assay was used to evaluate the rate of action of K21 over time on *Candida* while the fungicidal effect of K21 against *C. albicans* (ATCC 90028) and *C. glabrata* (ATCC 26512) was observed at 2 hours. The minimum inhibitory concentration (MIC) of K21 was compared with the MICs of fluconazole. Synergy between K21 and fluconazole was evaluated by both the checkerboard microdilution method and time-kill assay. The modes of action of K21 and drug delivery were determined by performing postembedding immunogold labelling and for the site-specific target and protein expression of Sap 1-3 and Sap 4-6 within the *Candida* cell.

Results: Of the 143 isolates, 108 were fluconazole-resistant, 15 were fluconazole-intermediate and 20 were fluconazole-susceptible using the broth microdilution assay and breakpoint values recommended by the Clinical and Laboratory Standards Institute (CLSI).

The MIC of K21 was 31.24 µg/mL for *C. albicans* when determined by the broth microdilution assay. About 103 *Candida* species were resistant and 13 were categorised as intermediate to FCZ with a MIC range between 64 µg/mL - 256 µg/mL and 16 µg/mL - 32 µg/mL respectively. However, the majority of the *Candida* species (n = 86) showed intermediate susceptibility to K21 with a MIC range between 62.48 µg/mL - 124.95 µg/mL and only 9 of the *Candida* species were resistant to K21 with a MIC value of ≥ 249.89 µg/mL. A statistically significant (p value = 0.000) was observed when the MIC values of K21 and FCZ were compared.

No antagonism was observed in the study among the *Candida* strains. The time-kill and synergism assays showed significant differences over time with synergy between K21 and FCZ demonstrated for *C. albicans* (ATCC 90028 and NCPF 3281) *C. dubliniensis* (NCPF 3949a), *C. tropicalis* (ATCC 950) and *C. lusitaniae* (ATCC 34449).

Scanning electron microscopy displayed major alterations in the morphology of *Candida* species between 2 hours and 24 hours, exhibiting cell lysis and cell death. Transmission micrographs of *C. albicans* (ATCC 90028) treated with K21 showed shrunken nuclei with disruption of cell walls and cell membranes. Immunogold labelling of *C. albicans* (ATCC 90028) and *C. dubliniensis* (NCPF 3949a) with Sap 1-3 antibodies exhibited the presence of gold particles confined to the cell wall and cell membrane, but, when exposed to Sap 4-6 antibodies there were a few non-specific gold particles found in *C. albicans* (ATCC 90028) and an absence of gold particles in *C. dubliniensis* (NCPF 3949a). *C. tropicalis* (ATCC 950) showed few gold particles along the cell membrane when treated with Sap 1-3 antibodies and no gold particles were found when treated with Sap 4-6 antibodies.

Conclusion: The present study suggests that K21 acts as a potent antifungal agent and can be considered for development as an alternative treatment for fluconazole-resistant *Candida* species especially in immunocompromised patients.

LIST OF FIGURES

Figure 1.1: Diagrammatic representation of <i>Candida</i> virulence factors.....	9
Figure 1.2: Chemical structure of the K21 antimicrobial compound.....	18
Figure 1.3: Hydrolysis and condensation of K21.....	19
Figure 2.1: Flow diagram showing the dilution protocol of K21	27
Figure 2.2: Species distribution of the <i>Candida</i> species investigated.....	34
Figure 2.3: <i>Candida</i> species resistant to FCZ.....	35
Figure 2.4: <i>Candida</i> species intermediate to FCZ.....	36
Figure 2.5: <i>Candida</i> species susceptible to FCZ	36
Figure 2.7: Whisker Box-plot showing the variations of the data against K21 and FCZ.....	45
Figure 2.8: Broth microdilution checkerboard assay results of <i>C. albicans</i> (ATCC 90028).....	48
Figure 2.9: Broth microdilution checkerboard assay results of <i>C. albicans</i> (NCPF 3281) showing an indifferent effect.....	49
Figure 2.10: Broth microdilution checkerboard assay results of <i>C. dubliniensis</i> (NCPF 3949a) showing a synergistic effect.....	50
Figure 2.11: Broth microdilution checkerboard assay results of <i>C. lusitaniae</i> (ATCC 34449) showing a definite synergism.....	51
Figure 2.12: Broth microdilution checkerboard assay results of <i>C. glabrata</i> (ATCC 26512) showing an indifferent effect.....	52
Figure 2.13: Time-kill curve plotted for <i>C. albicans</i> (ATCC 90028).....	53
Figure 2.14: Time-kill curve plotted for <i>C. glabrata</i> (ATCC 26512).....	54
Figure 2.15: Time-kill curve of K21 and FCZ alone and in combinations against <i>C. albicans</i> (ATCC 90028).....	56

Figure 2.16: Time-kill curve of K21 and FCZ alone and in combinations against <i>C. albicans</i> (NCPF 3281).....	56
Figure 2.17: Time-kill curve of K21 and FCZ alone and in combinations for <i>C. glabrata</i> (ATCC 26512).....	60
Figure 2.18: Time-kill curve of K21 and FCZ alone and in combinations for <i>C. dubliniensis</i> (NCPF 3949a).....	62
Figure 3.1: Diagrammatic representation of Scanning electron microscopy.....	69
Figure 3.2: Post-embedding immunogold labelling.....	73
Figure 3.3: Primary antibody fixation.....	73
Figure 3.4: Scanning micrographs of <i>C. albicans</i> (ATCC 90028) without treatment and after 2, 4, 6 and 24 hours exposure to K21.....	76
Figure 3.5: Scanning micrographs of <i>C. krusei</i> (ATCC 2159) without treatment and after 2, 4, 6 and 24 hours exposure to K21.....	77
Figure 3.6: Scanning micrographs of <i>C. glabrata</i> (ATCC 26512) without treatment and after 2, 4, 6 and 24 hours exposure to K21.....	79
Figure 3.7: Scanning micrographs of <i>C. albicans</i> (ATCC 90028) treated with FCZ at 2, 4, 6 and 24 hours.....	81
Figure 3.8: Scanning micrographs of <i>C. krusei</i> (ATCC 2159) treated with FCZ at 2, 4, 6 and 24 hours.....	83
Figure 3.9: Scanning micrographs of <i>C. glabrata</i> (ATCC 26512) treated with FCZ at 2, 4, 6 and 24 hours.....	84
Figure 3.10: Scanning micrographs of <i>C. albicans</i> (ATCC 90028) treated with K21 + FCZ at 2, 4, 6 and 24 hours.....	86
Figure 3.11: Scanning micrographs of <i>C. krusei</i> (ATCC 2159) treated with K21 + FCZ at 2, 4, 6 and 24 hours.....	88
Figure 3.12: Scanning micrographs of <i>C. glabrata</i> (ATCC 26512) treated with K21 + FCZ at 2, 4, 6 and 24 hours.....	89

Figure 3.13: Transmission micrographs of *C. albicans* (ATCC 90028) without K21 treatment.....91

Figure 3.14: Transmission micrographs of *C. albicans* (ATCC 90028) treated with K21 at 2, 4, 6 and 24 hours.....92

Figure 3.15: Immunogold labelling of *C. albicans* (ATCC 90028) with Sap 1-3 antibodies.....94

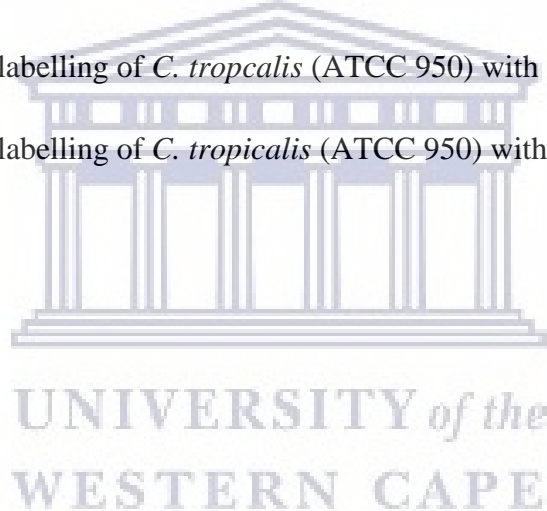
Figure 3.16: Immunogold labelling of *C. albicans* (ATCC 90028) with Sap 4-6 antibodies.....95

Figure 3.17: Immunogold labelling of *C. dubliniensis* (NCPF 3949a) with Sap 1-3 antibodies.....97

Figure 3.18: Immunogold labelling of *C. dubliniensis* (NCPF 3949a) with Sap 4-6 antibodies.....98

Figure 3.19: Immunogold labelling of *C. tropicalis* (ATCC 950) with Sap 1-3 antibodies.....100

Figure 3.20: Immunogold labelling of *C. tropicalis* (ATCC 950) with Sap 4-6 antibodies.....101



LIST OF TABLES

Table 2.1: Collective susceptibility patterns of <i>Candida</i> as determined by K21 and FCZ.....	39
Table 2.2: MIC ranges of FCZ-resistant <i>Candida</i>	40
Table 2.3: MIC ranges of FCZ-intermediate <i>Candida</i>	41
Table 2.4: MIC ranges of FCZ- susceptible <i>Candida</i>	42
Table 2.5: K21 MIC ranges for FCZ-resistant <i>Candida</i>	43
Table 2.6: K21 MIC ranges for FCZ intermediate <i>Candida</i>	43
Table 2.7: K21 MIC ranges of FCZ-susceptible <i>Candida</i>	44
Table 2.8: FCZ versus K21.....	45
Table 2.9: Microdilution checkerboard values to determine FCZ/K21 synergy.....	46
Table 2.10: K21 and FCZ concentrations over time for <i>C. albicans</i> (ATCC 90028).....	57
Table 2.11: K21 and FCZ concentrations relative to time for <i>C. albicans</i> (ATCC 90028).....	57
Table 2.12: K21 and FCZ concentrations over time for <i>C. albicans</i> (NCPF 3281).....	58
Table 2.13: K21 and FCZ concentrations relative to time for <i>C. albicans</i> (NCPF 3281).....	59
Table 2.14: K21 and FCZ concentrations over time for <i>C. glabrata</i> (ATCC 26512).....	61
Table 2.15: K21 and FCZ concentrations relative to time for <i>C. glabrata</i> (ATCC 26512).....	61
Table 2.16: K21 and FCZ concentrations over time for <i>C. dubliniensis</i> (NCPF 3949a).....	62
Table 2.17: K21 and FCZ concentrations relative to time for <i>C. dubliniensis</i> (NCPF 3949a).....	62

KEYWORDS

Quaternary ammonium compounds

K21 antimicrobial compound

Fluconazole

Candida

C. albicans

Antifungal susceptibility

Resistant

Broth microdilution assay

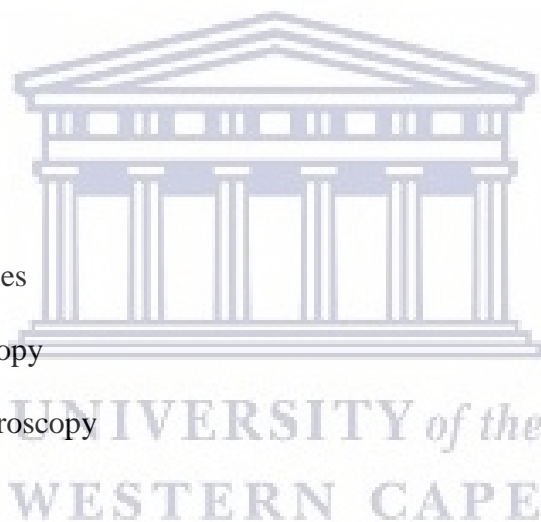
Time-kill assay

Synergy

Secreted aspartyl proteinases

Scanning electron microscopy

Transmission electron microscopy



RESEARCH OUTPUT

The following peer-reviewed conference proceedings and manuscripts were generated during the course of the study and published in scientific journals.

Conference Presentations:

Cathy NJ, Pedro MDSA, Kirk K, Dharam VA, Bhupesh KP, Charlene WJA. “Anti-fungal effect of K21 antimicrobial compound against fluconazole-resistant oral *Candida* isolates from HIV+ patients”. Oral presentation at 30th International Congress of Chemotherapy and Infection (ICC). Taipei, Taiwan, November 24-27, 2017.

Cathy NJ, Bhupesh KP, Dharam VA, Charlene WJA. “Ultrastructural analysis of fluconazole-resistant *Candida* species treated with K21 antimicrobial compound”. Poster presentation at the ASM microbe (American society for Microbiology), San Francisco, June 20-24, 2019.

Publications:

Cathy NJ, Pedro MDSA, Kirk K, Dharam VA, Bhupesh KP, Charlene WJA. 2017. “Anti-fungal effect of K21 antimicrobial compound against fluconazole-resistant oral *Candida* isolates from HIV+ patients”. *Int J Antimicrob agents*. 50(Suppl2), S49. p21.

Cathy NJ, Pedro MDSA, Bhupesh KP, Dharam VA and Charlene WJA, May2019. K21 compound, a potent antifungal agent: Implications for the treatment of fluconazole-resistant HIV-associated *Candida* species. *Frontiers in microbiology*. 10(1021).

<https://dx.doi.org/10.3389%2Ffmicb.2019.01021>

ABBREVIATIONS

AIDS: Acquired immunodeficiency syndrome

ATCC: American Type Culture Collection

ANOVA: Analysis of variance

ALS: Agglutinin-like sequence

BSA: Bovine Serum Albumin

CLSI: Clinical Laboratory Standards Institutes

CD4: Cluster of differentiation 4

cells/mm³: cells per millimetre cube

CFU/mL: Colony forming unit per millilitre

C: Carbon

DNA: Deoxyribonucleic acid

DRF: Damage Response Network

°C: Degree Celsius

ERG11: Ergosterol11

FCZ: Fluconazole

FICI: Fractional inhibitory Concentration Index

FIC: Fractional inhibitory concentration

FSG: Fish skin gelatin

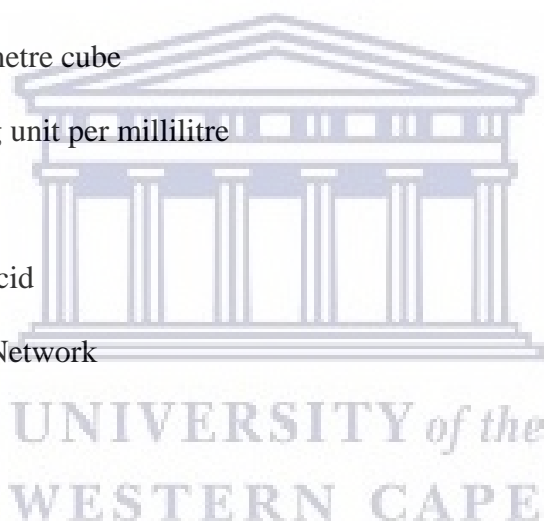
GPI: glycosylphosphatidylinositol

g: gram

g/mol: gram/mole

HIV: Human Immunodeficiency Virus

HHV: Human Herpes Virus



HBV: Hepatitis B virus

HCL: Hydrogen chloride

HSV: Herpes Simplex Virus

Hsp: Heat Shock Protein

HAART: Highly active antiretroviral therapy

IgA: Immunoglobulin A

IgG: Immunoglobulin G

INT: Iodonitrotetrazolium chloride

kDa: Kilodalton

kV: kilovolt

log: Logarithm

LR: London Resin

MIC: Minimum Inhibitory Concentration

M: Molarity

mL: Millilitre

µL: Microlitre

µM: Micromolar

µg: Microgram

mg: Milligram

µm: Micrometre

mm: Millimetre

NCAC: Non *Candida albicans Candida*

NCPF: National Collection of Pathogenic Fungi

NaCl: Sodium chloride

NAC: Non *albicans Candida*



N: Normality

nm: Nanometre

OPC: Oropharyngeal candidiasis

PBMCs: Peripheral blood mononuclear cells

PBS: Phosphate Buffer Saline

QAC: Quaternary Ammonium Compound

QAS: Quaternary Ammonium Silane

QAMS: Quaternary Ammonium Methacryloxy Silicate

RNA: Ribonucleic acid

SAP: Secreted Aspartyl Proteinase

SDA: Sabourauds Dextrose Agar

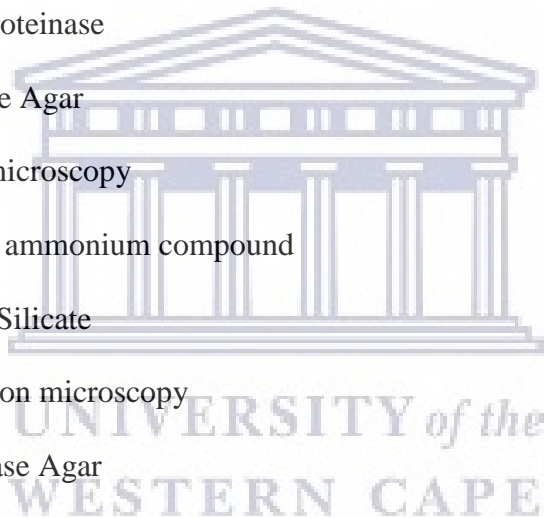
SEM: Scanning electron microscopy

SiQAC: Silica Quaternary ammonium compound

TEOS: Tetra Ethyl Ortho Silicate

TEM: Transmission electron microscopy

YNBA: Yeast Nitrogen Base Agar



CHAPTER 1

LITERATURE REVIEW

1.1 INTRODUCTION

The human oral cavity is colonized by various indigenous microorganisms. The diversity in the microorganisms harbouring the different structures of the oral mucosa is responsible for the various dental diseases. In a systematic review, it was reported that about 30-80% of HIV-positive patients suffer with oral infection of fungal, bacterial or viral origin (Reznik, 2005) with the HIV burden influencing the rate of progression of oral disease (Batavia *et al.*, 2016).

The most prevalent oral fungal infection among HIV patients is mucocutaneous candidiasis caused by *Candida* species. One of the most common forms of mucocutaneous candidiasis is oropharyngeal candidiasis which is reported in 90% of untreated HIV infected individuals (Fichtenbaum *et al.*, 2000). The predisposing factors for oral candidiasis can be classified into local and systemic host factors. The local host factors are the use of dentures, corticosteroid inhalers, increased sugar diet and reduced salivary flow while the systemic host factors include endocrine disorders (diabetes), immunosuppression (HIV, AIDS, leukaemia), use of broad spectrum antibiotics and nutritional deficiencies (Williams and Lewis, 2011). It is considered that the oral cavity may show the first signs and symptoms of HIV infection with a decline in the CD4 counts (<200 cells/mm³) indicating the presence of oral thrush caused by *C. albicans* (Hirata, 2015). The more immunosuppressed, the higher the incidence of opportunistic infections present among HIV patients, and thus oral candidiasis is considered an independent prognostic factor to determine the progression of HIV infection

(Konstantyner *et al.*, 2013). Sub-Saharan Africa is home to the world's largest population living with HIV/AIDS (29.4 million) with the majority being in South Africa, followed by Nigeria (UNAIDS, 2002). *Candida* species have been detected in about 75% of HIV-infected individuals in the Western Cape of South Africa, compared to 68% in HIV-negative individuals (Abrantes *et al.*, 2014).

Studies have proven the efficacy of fluconazole against *Candida* (Epstein *et al.*, 2002; Sholapurkar *et al.*, 2009). However, the widespread and repeated use of azoles has led to azole resistance, particularly fluconazole resistance amongst certain *Candida* strains in immunodeficient HIV patients, causing a dramatic increase in fungal infections (Fournier *et al.*, 2011; Osaigbovo II *et al.*, 2017) as well as an increase in mortality and morbidity (Sardi, *et al.*, 2013; Baddley *et al.*, 2008). *Candida* infections may be associated with up to 47% mortality (Pfaller *et al.*, 2011), with the mortality rate of bloodstream infections caused by *Candida* species ranging from 40% - 60% (Sun *et al.*, 2015). Increased *Candida* infections led to the use of antifungal agents in terms of prophylactic and treatment purposes (Belazi *et al.*, 2004). With fluconazole being the first choice of drug treatment against *C. albicans*, the development of new antimicrobial compounds to treat antifungal resistant strains is imperative.

1.2 Epidemiology of Candidiasis

The oral cavity acts as a reservoir for different microorganisms, many of which are implicated in various bacterial, viral, fungal, dental and systemic diseases. Fungi are eukaryotic organisms existing either as yeasts (round) or moulds (filamentous) or a combination of both types (dimorphic). *Candida* is a polygenic fungus which is determined by the polygenes, frequently found in the normal human microflora and is associated with

biofilm formation (Kumamoto, 2002). Various strains of *Candida* species are found in the oral cavity (Terezhalmay and Huber, 2011), and among the 163 acknowledged anamorphic species or intentionally distorted species of *Candida* present in the different oral habitats. *C. albicans*, *C. tropicalis*, *C. krusei*, *C. glabrata*, *C. guilliermondii*, *C. parapsilosis*, *C. lusitaniae*, *C. kefyr*, *C. rugosa*, *C. dubliniensis* and *C. viswanathii* are associated with human infections (Singh and Raksha, 2013; Williams and Lewis, 2011). *Candida* species may be recovered from up to one third of the mouths of healthy individuals, including geriatrics (Verma and Narang, 2014), constituting 17% - 75% colonisation rates (Mushi *et al.*, 2016), with colonisation in two thirds of those with advanced HIV disease (Fichtenbaum, 2000; Ruhnke, 2002). Non-*Candida albicans Candida* (NCAC) species facilitate infection in 20% - 40% of severely ill HIV patients (Mushi *et al.*, 2016). Approximately 80% - 90% of HIV-positive patients at some stage during their progression to AIDS develop oropharyngeal candidiasis (OPC) (Nemutandani *et al.*, 2016; Moyes and Naglik, 2011). Patil *et al.*, (2015) reported a mortality rate of 71% - 79% of patients with systemic candidiasis.

The persistence of *Candida* species on the oral mucosal surfaces of healthy individuals contributes to its virulence, disregarding the type of *Candida* causing the infection (Byadarahally and Rajappa, 2011). Besides the presence of highly common *C. albicans*, several non-*albicans Candida* species also differ widely in epidemiology, their ability to cause oral infections, and susceptibility to antifungal agents. About 50% of oral fungus infections are caused by *C. albicans* (Williams and Lewis, 2011) accounting for 95% of infections in immunocompromised HIV patients (Dupont *et al.*, 1992), whereas 80% of the infections are caused by *C. tropicalis* and *C. glabrata*, together with *C. albicans* (Greenberg *et al.*, 2008). Thompson *et al.*, (2010) reported *C. albicans* as the most common causative agent (54%) in advanced AIDS patients followed by *C. dubliniensis* (17%) and *C. glabrata* (16%) as the second and third most frequently isolated species. *C. glabrata* has been reported

in patients with increased use of immunosuppressive agents (Khan *et al.*, 2010). Multiple species of *Candida* from a single specimen have been reported in 5% - 10% of oral candidiasis and frequent combinations included the presence of *C. albicans* with *C. glabrata*, *C. krusei*, *C. dubliniensis*, or *C. tropicalis* (Vazquez, 2010). *Candida* infections in immunocompromised patients have become more frequently diagnosed as opportunistic infections.

In neonates with oral candidiasis, isolates of *C. albicans* followed by *C. glabrata*, *C. tropicalis* and *C. krusei* were reported (Tinoco-Araujo *et al.*, 2013). When triggered by factors such as an underlying pathology as in those with immunosuppressive chemotherapy, transplant patients, degenerative and neoplastic diseases (Karkowska-Kuleta *et al.*, 2009; Kim and Sudbery, 2011) as well as prolonged antibiotic use and poor nutrition, the *Candida* species shift from being commensal to opportunistic infectious agents, expressing pathogenicity (Soysa *et al.*, 2008; Wächtler *et al.*, 2011; Naglik *et al.*, 2011) by penetrating into the tissues, entering the blood stream (Mohandas and Ballal, 2011; Rao, 2012; Khan *et al.*, 2010) and eventually causing increased mortality and morbidity (Akpan and Morgan, 2002; Owotade *et al.*, 2013). Higher levels of HIV-1 RNA eventually lead to the development of systemic fungemia (Junqueira *et al.*, 2012; Shah *et al.*, 2014). The mortality rate of systemic candidiasis has been reported to be 38% (Gudlaugsson *et al.*, 2003) and 44% (Almirante *et al.*, 2005) in developed countries.

There are various types of oral manifestations of candidiasis such as pseudomembranous, erythematous, hyperplastic, mucocutaneous and angular cheilitis (Owotade and Patel, 2014). Oral candidiasis is also known as moniliasis (Scully, 2008), oral candidosis, oral thrush (James *et al.*, 2006), acute pseudomembranous candidiasis or oropharyngeal candidiasis. They appear as whitish plaques within the oropharynx or the buccal mucosa or palate or under surface of the tongue, the plaque leaves a reddish erosive area in the oral mucosa when

wiped away (Patil *et al.*, 2015). This is the most common form of candidiasis and accounts for almost 35% of oral candidiasis (Rhodus, 2012). The chronic form occurs in immunocompromised patients such as those with HIV or leukaemia (Treister and Bruch, 2010). The condition causes severe pain and discomfort on mastication, thus limiting the nutritional intake causing morbidity in elderly or immunocompromised patients (Sherman *et al.*, 2002).

A high incidence of *Candida* infection has been reported among hospitalized patients (Loeffler and Stevens, 2003), and studies have reported that the Non-*Candida albicans* *Candida* (NCAC) show varying virulence and drug sensitivity towards the principal antifungal drugs administered in hospitals (Schmalreck *et al.*, 2012; Tortorano *et al.*, 2012). A recent study documented by Mushi *et al.*, (2017) reported a prevalence of 33.5% oral candidiasis by NCAC species in AIDS patients in Sub-Saharan Africa between the years 2005-2015. However, fluconazole resistance by *C. albicans* was 44.7% compared to non-*albicans* *Candida* species exhibiting 21.9% resistance to fluconazole ($p < 0.001$). The limited antifungal arsenal and increased toxicity of the compounds contributed to a high frequency of mortality and morbidity due to fungal infections (Scorzoni *et al.*, 2017).

1.3 Pathogenesis and virulence of *Candida albicans*

Virulence of a pathogen refers to the ability of the microbe to infect the host tissue and multiply, causing danger to its host (Casadevall, 2007). Several virulence factors attribute to the capacity of *Candida* to cause fungal infections in host cells (Mason *et al.*, 2012). This includes the morphological transition between yeast and hyphal forms, the expression of adhesins and invasins on the cell surface, thigmotropism, biofilm formations, phenotypic switching, secretion of hydrolytic enzymes and environmental pH (Mayer *et al.*, 2013). In

HIV patients, the severe immunosuppression changes the pH, osmolarity and oxidative stress of the tissue environment which in turn is recognized by the *Candida* cell. This results in a disturbance in gene regulation causing the fungal transition from a commensal to opportunistic pathogen (Hube, 2004).

According to the Damage Response Framework (DRF) introduced by Casadevall and Pirofski in 1999, any damage to the host can be controlled by either the susceptible host or the pathogen and hence the interaction between a microbe and the host determines the microbial virulence (Calderone, 2002). In oropharyngeal candidiasis (OPC), the host responds with a T-helper cell 1 (Th1) and T-helper cell 17 (Th17) adaptive immune response (Jabra-Rizk *et al.*, 2016). The predominant host defence mechanism in HIV-infected individuals is the *C. albicans*-specific CD4 T-cell response (Cassone and Cauda, 2012). However, the impaired mucosal CD4+T cells, decreased salivary IgA levels and a shift to T-helper cell 2 (Th2) cytokine expression in saliva aggravates the colonisation of *Candida* (Liu *et al.*, 2016a; Nweze and Ogbonnaya, 2011).

Candida pathogenicity can be explained by mannoprotein derivatives on the cell wall with immunosuppressive properties against host defence mechanisms (Chaffin *et al.*, 1998); adhesins which are the first step in the internalization process and early stages of colonization (Staniszewska *et al.*, 2012a). Adhesins are glycosylphosphatidylinositol (GPI)-linked cell surface glycoproteins encoded by eight sets of agglutinin-like sequence (ALS) genes, some of which result in biofilm formation (Murciano *et al.*, 2012). These are important virulence factors since cells embedded within a biofilm can survive high antimicrobial concentrations forming drug resistant biofilms which facilitate the persistence of human infections (Rodrigues *et al.*, 2014) and protection from the host immune response (Lebeaux *et al.*, 2014). *Candida* forms part of the normal microflora of some individuals and certain inflammatory or immunocompromised host conditions or the use of antibiotics may cause an

imbalance in the normal microflora favouring an opportunistic infection (Ranjan and Dongari-Bagtzoglou, 2018).

Figure 1.1 represents a diagrammatic representation of the various virulence factors during the course of host invasion by *Candida* species (da Silva Dantas *et al.*, 2016). The virulence of *Candida* species, mainly *C. albicans*, depends on the site and stage of infection (Odds, 1994) and also on whether it is a mucosal or systemic type of infection (Naglik *et al.*, 2003).

Extracellular hydrolytic enzymes such as phospholipases and aspartyl proteinases (mainly by *C. albicans* and *C. tropicalis*) and haemolysin, secreted by the *Candida* facilitate the adherence and penetration of the species into the host tissues (Fotedar and Al-Hedaithy, 2005; Hube and Naglik, 2001; Li *et al.*, 2015; Park *et al.*, 2013; Schaller *et al.*, 2005; Tsang *et al.*, 2007).

Extracellular proteolytic activity of *C. albicans* was first understood by Staib in 1965, permitting the species to use protein as the sole nitrogen source (Staib, 1966). Among the extracellular hydrolytic enzymes produced by *C. albicans*, secreted aspartyl proteinase (Sap) is considered a key virulence factor in *Candida* infections (Dalle *et al.*, 2010; Tongchusak *et al.*, 2008) resulting in host tissue penetration and invasion (Jayatilake *et al.*, 2005; Melo *et al.*, 2004) and the transition of *Candida* from a commensal to opportunistic pathogen (Parra-Oreteg *et al.*, 2009). The abbreviations ‘SAP’ and ‘Sap’ describe the gene and the corresponding protein respectively (Schaller *et al.*, 2005).

The Saps of *C. albicans* encodes ten members of the SAP 1-10 multigene family (SAP 1 to SAP 3, SAP 4 to SAP 6, SAP 9, and SAP 10) based on amino acid sequence homology alignment (Monod *et al.*, 1994; 1998). However, SAP 7 and SAP 8, being divergent, are not represented as subfamily members (Chen *et al.*, 2002; Correia *et al.*, 2010). SAP 1-6 genes are responsible for the adherence, tissue damage and changes in the immune response,

however, functions of SAP 7 are not well discovered. SAP 9 and SAP 10 are considered to preserve the surface integrity of yeast cells. SAP gene expression may also depend on the type and stage of fungal infection (Abegg *et al.*, 2011) and is regulated during the morphological transition.

A relationship exists between the SAP isoenzymes family of *C. albicans* showing that Sap 1 to Sap 3 and Sap 4 to Sap 6 are up to 67% and 89% identical respectively, whereas, Sap 7 is only 20 to 27% identical to other Sap proteins (Stehr *et al.*, 2000; Naglik *et al.*, 2003). The size of mature Sap proteins 1-10 are in the range of 35-50 kDa (Felk *et al.*, 2002; Monod *et al.*, 1994; 1998) and hydrolyse both pure and conjugated proteins (Ruchel, 1981). Sap proteins are reported to be active at pH 3-4, though they show optimal activity at pH around 5 and also at neutral pH (Borg-von Zepelin *et al.*, 1998). Three major protease enzymes secreted *in vitro* by *C. albicans*, *C. parapsilosis* and *C. tropicalis* include Sap 2, Sapp 1 and Sapt 1 respectively (de Viragh *et al.*, 1993; Monod *et al.*, 1994; Togni *et al.*, 1991).

During host infection, the phospholipids broken down by the action of phospholipases and the degradation of substrates such as albumin, immunoglobulin by the Saps results in host tissue penetration and invasion (Jayatilake *et al.*, 2005; Melo *et al.*, 2004).

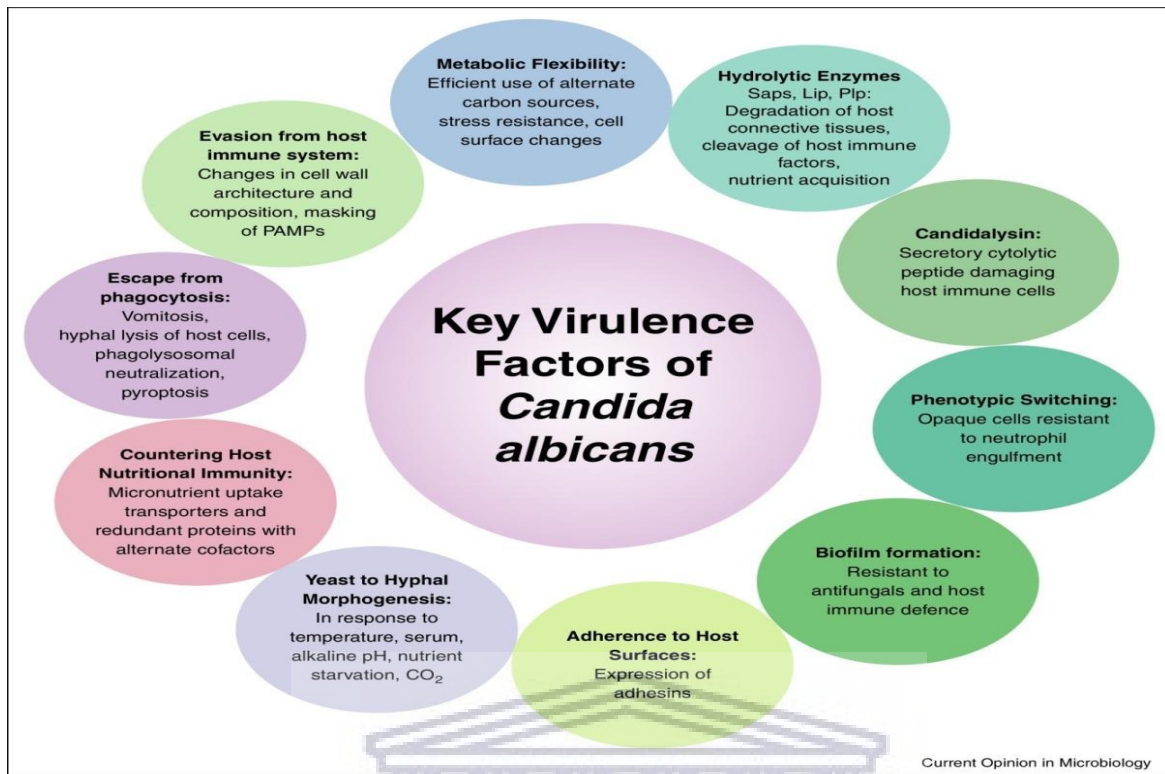


Figure 1.1: Diagrammatic representation of *Candida* virulence factors (da Silva Dantas *et al.*, 2016)

On the other hand, *C. glabrata*, *C. krusei* and *C. kefyr* have been reported to be non-proteolytic when tested in culture medium with bovine serum albumin as the sole nitrogen source (Dostál *et al.*, 2003; Desai *et al.*, 2011; Ruchel, *et al.*, 1992), and because *C. glabrata* does not form true hyphae, it is not considered to be as virulent as *C. albicans* (Li *et al.*, 2007).

The virulence mechanisms of *Candida*, such as secretion of hydrolytic enzymes, expression of adhesins, and phenotypic switching has prompted studies for the discovery of novel antifungal strategies to combat drug resistance. An urgent need for a focus on effective compounds which target different molecular biological components of the cell which may be involved in antifungal resistance is critical (Mayer *et al.*, 2013).

1.4 Current antifungal drugs and their mode of actions

The five main classes of antifungal agents for the treatment of fungal infections include the polyenes (nystatin and amphotericin B); the azoles (miconazole, clotrimazole, ketoconazole, itraconazole and fluconazole); the allylamines (naftifine and terbinafine)/thiocarbamates (tolnaftate and tolclolate); the fluoropyrimidines (5-fluorocytosine) and the echinocandins (caspofungin, micafungin, anidulafungin) (Maurya *et al.*, 2013; Pappas *et al.*, 2003).

The azoles and echinocandins target the fungal membranes and change the cell morphology, thus inhibiting growth of the cells (Tatsumi *et al.*, 2013). The azole groups inhibit the ergosterol biosynthesis in the fungal cell membrane and through their action on the cytochrome P450-dependent enzyme lanosterol 14 α -demethylase, catalyzes the conversion of lanosterol to ergosterol (Kathiravan *et al.*, 2012; Mayers *et al.*, 2017). Echinocandins demonstrate concentration-dependent fungicidal activity. They are inhibitors of the α -1, 3-D-glucan biosynthesis by the blockage of the (1, 3)- β -D-glucan synthase (Spampinato and Leonardi, 2013). The action of the drug results in the impairment of the fungal cell wall integrity leading to cell vulnerability to osmotic lysis (Grover, 2010).

Fluoropyrimidines impede protein synthesis (Martins *et al.*, 2015) by the formation of toxic fluorinated pyrimidine antimetabolites, while polyenes act on the fungal cell membranes and alter the cellular permeability causing leakage of cytosolic cytoplasmic components and eventually cell death (Sanglard and Odds, 2002). The allylamines and thiocarbamates impair ergosterol biosynthesis resulting in cell membrane disruption (Sanglard *et al.*, 2009).

The selection of suitable antifungal agents for superficial infections and systemic *Candida* infections is associated with the routes of administration and excretion of the drugs. Depending on the solubility of the drug, they are available as oral preparations (posaconazole and flucytosine) or intravenous preparations (caspofungin, micafungin and amphotericin B)

or available in both oral and intravenous preparations (fluconazole, itraconazole and voriconazole) (Ashley *et al.*, 2006).

Prophylactic use of antifungals (in the management of oral candidiasis in bone marrow transplant patients and immunocompromised patients, including leukaemia) and systemic azole antifungal therapy, mainly fluconazole and itraconazole, are found to be effective against superficial and chronic forms of candidosis (Wabe *et al.*, 2011). Studies have demonstrated the efficiency and safety of using fluconazole for the treatment of pseudomembranous candidiasis since it is better tolerated by the gastrointestinal tract than Amphotericin B and showed good adhesion to the oral mucosal surface with a rapid symptomatic response and patient compliance (Taillandier *et al.*, 2000; Goins *et al.*, 2002).

Being a first generation triazole, fluconazole has a longer half-life and a superior bioavailability when compared to itraconazole and voriconazole, the second and the third generation azoles respectively (Lipp, 2008). Fluconazole appears marginally lipophilic and is highly water-soluble exhibiting <2% low nephrotoxicity (Vadlapatla *et al.*, 2014). Fluconazoles are reported to demonstrate reduced rates of penetration to cerebrospinal fluid and reduced endocrinological toxic reactions to the host body (Como and Dismukes, 1994). Reported side effects of fluconazole administration include nausea, vomiting, diarrhoea, abdominal pain and alopecia (Garcia-Cuesta *et al.*, 2014).

1.5 Drug resistance and the need for novel antifungal drugs

Antimicrobial drug resistance is the ability of the microbes to grow in the presence of the drug which is meant to kill or inhibit their growth. Antimicrobial resistance occurs as a result of inappropriate use of antimicrobial agents and in patients those who do not adhere to

treatment plans and stop medications when they experience any side effects (Ayukekbong *et al.*, 2017; Lushniak, 2014). Based on the global report, the World Health Organisation predicted the evolvement of a 21st century post-antibiotic era due to antimicrobial crisis, where common infections can no longer be cured and the resistant bacteria, fungi and viruses were referred to as “superbugs” (WHO, 2014). Uncontrolled and persistent use of antimicrobials causes an intense selective pressure among the pathogens that creates a strong adaptive response in the world of microbes (Michael *et al.*, 2014), resulting in widespread resistance to antifungal therapies (Luque *et al.*, 2009; Manzano-Gayosso *et al.*, 2008). The existing challenges in the treatment of oral candidiasis are due to both antifungal drug resistance and the host’s underlying immune deficiency. Nanteza *et al.*, (2014) reported an association of oral candidiasis in HIV patients with low CD4 counts, while Moges *et al.*, (2016) reported the frequent isolation of fluconazole resistant *C. albicans* in HIV infected individuals regardless of HAART.

Fluconazole, the commonly prescribed triazole antifungal, demonstrates fungistatic rather than fungicidal activity leading to an acquired resistance of the drug and allows a trailing growth of *Candida* species even at higher concentrations of the drug (Berkow and Lockhart, 2017; Sagatova *et al.*, 2015). Even though FCZ is a teratogenic drug, it has been considered as the drug of choice for *Candida* infections due to its low toxicity and high efficiency compared with ketoconazole and amphotericin B (Lopez-Rangel and Van Allen, 2005). However, the administration of FCZ as a primary prophylaxis for oral candidiasis is not recommended in advanced HIV patients due to the risk of *Candida* species developing resistance (Patton *et al.*, 2001).

The mechanisms of antifungal drug resistance may occur as a result of the mutation of the azole target enzyme, changes or overexpression of the drug targets responsible for azole efflux from the cells and metabolic bypasses thereby reducing the effects of the drug

concentration (Read and Woods, 2014; Sanglard, 2016; Zavrel and White, 2015). Overexpression of ERG11 by resistant *Candida* species even in the presence or absence of fluconazole administration leads to increased concentrations of lanosterol 14 α -demethylase in turn resulting in an essential requirement of larger amounts of the antifungals to inhibit the enzyme (Cowen *et al.*, 2015). Risk factors for azole resistance in HIV/AIDS patients include poor compliance and dose administration for intermittent/therapeutic/prophylactic use (Mayers *et al.*, 2017).

Long term exposure to sub-inhibitory concentrations of azoles may lead to the development of acquired resistance in *C. albicans* and other species (Morschhäuser, 2016). Prolonged use of antifungals also reported the appearance of naturally resistant *C. glabrata* and *C. krusei* in HIV patients and a significant percentage of *C. dubliniensis* and *C. glabrata* in diabetes mellitus patients (Espinel-Ingroff *et al.*, 2014; Pfaller, 2012; Witaningrum *et al.*, 2018). Cross-resistance to ketoconazole, itraconazole and other imidazoles in fluconazole resistant isolates has been reported (Cuenca-Estrella *et al.*, 2002; Makarova *et al.*, 2003; Pfaller, 2012; Vazquez *et al.*, 1995). Non-*albicans Candida* species such as *C. glabrata*, showed a higher rate of fluconazole resistance (11-13%) followed by *C. tropicalis* and *C. parapsilosis* with a lower rate of 4-9% and 2-6% respectively (Cleveland *et al.*, 2012; Pfaller *et al.*, 2015). Several studies reported the resistance of *C. albicans* and non-*Candida albicans* species against the existing polyenes and 5-fluorocytosine (Kontoyiannis and Lewis, 2002; Souza *et al.*, 2010). Alexander *et al.*, (2013) reported co-resistance of clinical isolates of *C. glabrata* to both echinocandins and azoles.

Yeast biofilms possess persister or dormant cells to which drugs bind but are incompetent to inhibit the cell growth since the persister cells withstand both immune system and antifungal treatment due to the presence of the extracellular matrix (Lewis, 2007; Mukherjee and Chandra, 2004) which limits the drug penetration. A systematic analysis on infectious disease

detailed 9.2 million deaths in the year 2013 alone, most of which could be attributed to biofilm formation (Abubakar *et al.*, 2015; Salwiczek *et al.*, 2014). Echinocandins and Fluoropyrimidines are reported to be effective against *Candida* biofilms (Gonzales and Maisch, 2012).

Resistance to fluconazole has been reported in *C. glabrata* (Ajenjo *et al.*, 2011; Moran *et al.*, 2002) and *C. dubliniensis* (Pinjon *et al.*, 2005) with an increased incidence of non-*albicans* *Candida* infections reported in Latin American countries due to *C. parapsilosis* followed by *C. tropicalis* and *C. glabrata*, all of which were highly susceptible to Amphotericin B (Ajenjo *et al.*, 2011).

Increased resistance of *Candida* species to antifungal agents are associated with higher concentrations of the drugs to be used that may lead to invasive fungal infections in immunocompromised patients undergoing antifungal prophylaxis (Pfaller, 2012). This may in turn lead to poorer outcomes of the treatment. Moreover, limited antifungal drugs are available in oral and intravenous forms although the antifungals used in clinical treatments are diverse.

The severity of azole resistance differs between different geographical areas and the pattern of treatment and prophylaxis of invasive candidiasis (Oberoi *et al.*, 2012) with dose dependant and resistant *Candida* isolates as high as 50% in patients admitted in intensive care units (Guo *et al.*, 2013; Liao *et al.*, 2015).

The increase in multi drug resistance has led to the increase in the re-appearance of infectious diseases and death rates (Konate *et al.*, 2012). The need to explore alternative treatment methods to battle against the emerging drug resistant microorganisms has been mandatory.

Based on the epidemiological data, it appears that in future, fungal diseases may pose a dangerous hazard complicating the health of humans, animals and plants (Denning and

Bromley, 2015). The selective pressures exerted by the antifungal drugs exacerbate the urgent need and development of alternative novel antifungal drugs. The quest for new antifungal formulations and combination therapies may be recommended, especially since drug combinations have the advantage of using lower therapeutic doses, thus reducing the toxicity levels and increasing the drug efficiency due to the possible action on more than one target (Chen *et al.*, 2014).

With only five classes of antifungal agents currently available, there requires an urgent demand for the development of novel compounds with different mechanisms of action that may synergize with the present accessible drugs to achieve better fungicidal responses.

1.6. Quaternary ammonium compounds (QAC) as possible alternatives to combat antimicrobial resistance

Amongst the often used antimicrobial compounds are the QACs, chitosan, antimicrobial peptides (AMPs), antimicrobial enzymes (AMEs) and silver nanoparticles (AgNPs) (Jiao *et al.*, 2017).

QACs have been extensively used for industrial and cosmetic purposes, antifungal treatment in horticulture and in pharmaceutical or consumer products (Hegstad *et al.*, 2010). QACs are nitrogen containing compounds with a N (nitrogen) atom attached to four different covalent bonds. They are highly potent in combating antimicrobial resistance and may contribute to the critical need for the development of new and effective antimicrobial drugs incorporating QACs and are imperative to fight against resistant species (Jennings *et al.*, 2015a). In the early 1930s, QACs were applied as antiseptics and were considered as the first line of defence against pathogenic bacteria (Domagk, 1935; Jennings *et al.*, 2015b). They are potent

disinfectants of intact skin surfaces, mucous membranes and non-critical surfaces (Tischer *et al.*, 2012).

Fredell (1994) suggested that the antimicrobial activity of the QACs may be due to the disruption and denaturation of structural proteins and enzymes. Later studies showed that QACs are enhanced with broad spectrum antimicrobial activities and act by disrupting the microbial cell membrane (Marcotte *et al.*, 2005; Wessels and Ingmer, 2013), resulting in leakage of cellular contents at concentrations above the minimum inhibitory concentrations (Tischer *et al.*, 2012).

The antifungal activities of QACs are determined by their molecular structure. Cell electrophoretic mobility measurements determined that Cetyltrimethylammonium bromide (CTAB) exerted its antifungal effect by reversing the cell surface charges from negative to positive (Carmona-Ribeiro *et al.*, 2006), while Oosterhof *et al.*, (2006) demonstrated that hyphae formation on prosthesis was impeded when coated with QAC compared to untreated prosthesis.

QACs are widely used in wound dressings eradicating bacterial infection and providing an ideal environment for tissue regeneration (Tran *et al.*, 2015). Being cationic in nature, they bind to the carboxyl-, phosphate and hydroxyl- groups of negatively charged surfaces and are thus capable of binding to the oral mucosal surface contributing to its anti-biofilm effects (Baker *et al.*, 1978; Moran and Addy, 1984).

1.7 K21 antimicrobial compound

K21, an antimicrobial compound developed by Dr. Kirk Kimmerling in 2011 (Ablashi *et al.*, 2015), derives its activity from the incorporation of DC5700, a silica quaternary ammonium compound (SiQAC) developed by Dow Corning. SiQAC, which, being an antimicrobial

quaternary ammonium silane (QAS), has been widely used as antimicrobial coatings of fabrics (Murray *et al.*, 1988; Song and Baney, 2011) and medical devices (Oosterhof *et al.*, 2006; Yuen and Yung, 2013).

The characteristic antimicrobial property of organosilicon quaternary ammonium chloride-3(trimethoxysilyl)-propyldimethyl-octadecyl ammonium chloride (the methoxy version of SiQAC), is due to the presence of a long, lipophilic carbon 18 alkyl chain acting on the bacterial cell membrane. The direct contact and leaching of the compound to intracellular components results in bacterial cell death (Ahlström *et al.*, 1999). However, the hydrolysis and condensation of SiQAC releases methanol that appeared to be toxic for intraoral use (Ghannoum *et al.*, 2014). As a result, to enhance the antimicrobial activity, SiQAC has been substituted with -3(triethoxysilyl)-propyldimethyloctadecyl ammonium chloride (the ethoxy version of SiQAC or Et-SiQAC) coupled with Tetra Ethyl Ortho Silicate (TEOS) by sol-gel synthesis, leading to the development of an ethanol- or acetone- soluble, fully hydrolysed, partially condensed quaternary ammonium silane (QAS), code-named K21. The inclusion of TEOS as the networkforming agent enables a three-dimensional organically modified silicate to be produced by condensation of additional tetra- and triethoxysilane molecules with remnant silanol groups within the molecule. The synthesis involves blending of 2.08 g TEOS with 29.89 g Et-SiQAC and 5 mL ethanol and hydrolysed by 10.08 g of 0.02M HCL-acidified water yielding a yellow solution mixture. The yellow solution was then maintained at 80° C for 6 hours to remove the reaction byproducts of ethanol and water until a pale, partially condensed solid material was produced (Daood *et al.*, 2017).

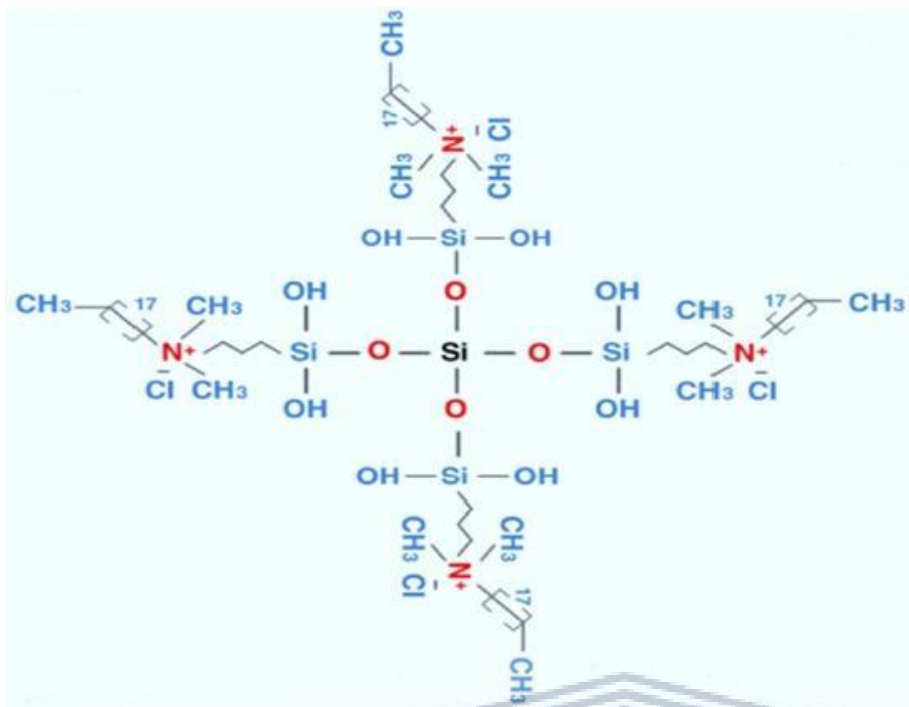


Figure 1.2: Chemical structure of K21 (Ablashi *et al.*, 2015). Formula weight =1840.86 g/mol Molecular formula = $C_{92}H_{204}Cl_4N_4O_{12}Si_5$ (1-octadecanaminium,N,N'-[[3,3-bis[[[3-(dimethyloctadecylammonio)propyl]dihydroxysilyl]oxy]-1,1,5,5-tetrahydroxy-1,5-trisiloxanediyl]di-3,1-propanediyl]bis[N,N-dimethyl-chloride).

Figure 1.2 shows the structure of the K21 compound with four arms of SiQAC on a silica core. The positive charges on K21 act to draw the negatively charged microbe towards the material while the long 18 carbon chain tails pierce the cell walls causing lysis.

The process of hydrolysis and condensation of K21 with TEOS produced a 3-dimensional antimicrobial macromolecule consisting of multiple arms with a potential of rupturing the membrane (Prusty *et al.*, 2014). The four quaternary ammonium arms of K21 provide four positive charges to the compound, thus favouring its antimicrobial activity. Such QACs are reported to cause the disruption of cytoplasmic and bacterial cell wall electrostatic interactions resulting in bacterial death (Melo *et al.*, 2014).

A partially-condensed form of QAS was synthesized in order to dissolve the products in ethanol and acetone. The partially-condensed K21 was immediately dissolved in absolute ethanol to obtain the desired weight percentage of QAS solutions. Figure 1.3 shows a diagrammatic representation of the hydrolysis and condensation of K21.

Depending on the form of the SiQAC starting material either methanol, if methacryloxy SiQAC, or ethanol, if ethacryloxy SiQAC, is generated as a by-product, thus the ethacryloxy SiQAC derived K21 is preferred for materials being placed in the oral cavity as an intra oral cavity disinfectant and potential protease inhibitor (Daood *et al.*, 2017). In a recent double-blind randomized clinical trial by Liu *et al.*, (2016b), the antimicrobial activity of methacryloxy SiQAC revealed contact-killing antimicrobial activity against plaque biofilms and was indicated for fabricating removable acrylic dentures.



Figure 1.3: Hydrolysis and condensation of K21. A) Yellow solution obtained after complete hydrolysis of the reaction mixture B) Partially condensed solid after heating of the completely hydrolysed solution (Daood *et al.*, 2017).

A study by Ablashi *et al.*, (2015) reported the inhibitory action of K21 on enveloped and non-enveloped DNA and RNA viruses. Being a potent inhibitor of enveloped RNA virus, K21 inhibited the replication of influenza A virus at 0.025% concentrations, however, higher concentrations of 0.10% were required to inhibit non-enveloped RNA virus, Calcivirus. A cytotoxic study on K21 found no major toxic effects on primary human fibroblasts with the cytotoxic dose of (CC50) of 9.45 mM, indicating the competency in the application of the compound. To determine the plasma membrane integrity and permeability, the cells were analysed using flow cytometry by treating the cells with 1.35 μ M of K21, below the CC50 value. There was 15% cell death with the absence of any cytotoxic effects. Further experiments on freshly isolated PBMCs also did not show cytotoxicity at 1.35 μ M of K21 (Gulve *et al.*, 2016).

K21 has been reported to exhibit an inhibitory effect on the growth of *Porphyromonas gingivalis*, *Escherichia coli*, *Streptococcus mutans*, *Actinomyces naeslundii* and *Enterococcus faecalis* and K21-coated sutures are under development which may possibly provide the potential of reducing the incidence of post-operative infection and also bacteraemia (Gong *et al.*, 2012a; 2012b; 2014; Meghil *et al.*, 2015). The use of K21 as an antiviral against HSV-1 and HHV-6A and HHV-7 at non-toxic concentrations has also been reported (Gulve *et al.*, 2016).

1.8 Summary

In order to combat the ongoing antifungal resistance of *Candida* species, several natural and novel antimicrobial compounds have been investigated as an alternative to, or in combination with, fluconazole. The use of novel compounds as an alternative for fluconazole may alleviate the emergence of multidrug resistant microbes. Resistance of fungal species toward the azole drugs has been associated with the mutation of azole target enzymes and

overexpression of drug transporters responsible for azole efflux from the cells (Zavrel and White, 2015). The resistant pattern varies among different *Candida* species according to their geographical distribution (Falagas *et al.*, 2010). It is therefore crucial to scrutinize the resistance pattern of different *Candida* strains, thus avoiding the chances of improperly or inaccurately treated fungal infections (Godoy *et al.*, 2003). Several natural products, synthetic agents or polymeric materials have been proven to show *in vitro* antifungal activities (Spampinato and Leonardi, 2013).

There has been a tremendous rise in resistant fungal infections due to the delay in the development of new classes of standard antifungal agents since 2006 (Moriyama *et al.*, 2014; Kontoyiannis and Lewis, 2015; McCarthy *et al.*, 2017). Resistance to antifungal drugs by *Candida* have been recognized widely as a public health threat and therefore necessitates new methods to prevent and control infections. To our knowledge, the antifungal activity of the novel K21 compound has not been investigated, making this study the first of its kind in testing K21 activity against *Candida*.

1.9 Study Hypothesis

K21 acts as a potent antifungal agent against fluconazole-resistant *Candida* species.

1.10 Aims and Objectives

With its antiviral and antibacterial properties already reported, the aim of the existing study was to investigate the antifungal effect of K21 against various oral *Candida* species known to be resistant to fluconazole. The following are the objectives of the study;

1. To establish the antifungal effect of K21 against fluconazole-resistant *Candida* species.
2. To determine the rate of activity of K21 to kill the resistant *Candida* species over time.
3. To determine whether synergism or antagonism exists between K21 and fluconazole by checkerboard microdilution and time-kill assays.

4. To observe the action of K21 on the morphology of the *Candida* cells using scanning electron microscopy and transmission electron microscopy.
5. To demonstrate the mode of action and target of K21 on *Candida* cells by evaluating the Sap 1-3 and Sap 4-6 protein expression using post embedding immunogold labelling.



CHAPTER 2

A COMPARISON OF THE ANTIFUNGAL PROFILES OF CANDIDA USING FLUCONAZOLE AND A NOVEL QUATERNARY AMMONIUM SILANE COMPOUND, K21

2.1 INTRODUCTION

Candida is reported to be the 4th most common isolated pathogen causing nosocomial bloodstream infections (Budhavari, 2009). The increasing incidence of *Candida* infections by *C. albicans* over the recent years, has led to difficulties in providing proper treatment due to the increased growth of immunogenic diseases, disproportionate use of immunosuppressive drugs and broad spectrum antibiotics. The role of non-*albicans* species in causing infections has also become increasingly important in high-risk or severely ill patients.

Some of the yeasts are single-drug resistant whereas others are multi-drug resistant to the antifungals. Early baseline data in South Africa, reported 100% susceptibility of *C. albicans* to fluconazole (FCZ) along with non-*albicans* exhibiting innate resistance (Blignaut *et al.*, 2002). However, recent studies in South Africa reported emerging fluconazole resistance among the *Candida* species (Owotade *et al.*, 2016; Abrantes *et al.*, 2014). With FCZ being fungistatic in action, an effort to develop novel antifungal compounds with potent fungicidal action and reduced toxicity to the host tissues may be endeavoured. In order to follow the trail of existing trend in the increasing azole resistant *Candida* species in sub-Saharan Africa, a definite diagnosis of the fungal infections and the type of *Candida* and their antifungal susceptibility testing is a requisite. Several natural, synthetic and semi-synthetic compounds have shown to exhibit alternative therapies for treating *Candida* infections (Oro *et al.*, 2015; Oblak *et al.*, 2013; Neto *et al.*, 2014).

K21 is a novel quaternary ammonium silane compound with a wide range of antimicrobial properties. K21 is the ethoxylated version of quaternary ammonium compound created with an intention to inhibit the growth of microbes resulting in a broad spectrum antimicrobial activity. Oblak *et al.*, (2016) notified the effectiveness of QASs against enveloped viruses like HIV and HBV but not on non-enveloped viruses. Bis-quaternary ammonium salts consisted of two identical alkyipyridinium rings and a bridge structure linking the rings to each other and are reported to have an excellent safety profile with a potent antifungal property and are easy to manufacture (Kourai *et al.*, 2006).

The objectives of this chapter are to evaluate the antifungal response of K21 against FCZ-resistant, FCZ-intermediate and FCZ-susceptible *Candida* species and investigate the synergistic anticandidal or antifungal effect of K21 in combination with FCZ. This chapter also aims to determine the time required by K21 to inhibit the growth of *Candida* species.

2.2 MATERIALS AND METHODS

2.2.1 Study design and Sample size

An *in vitro* study was conducted using one hundred and forty three (n = 143) *Candida* species. Nine type strains such as *C. albicans* (ATCC 90028 and NCPF 3281), *C. krusei* (ATCC 2159), *C. glabrata* (ATCC 26512), *C. dubliniensis* (NCPF 3949a), *C. tropicalis* (ATCC 950), *C. parapsilosis* (ATCC 22019), *C. lusitaniae* (ATCC 34449) and *C. kefyr* (ATCC 4135) were included as quality controls for all the tests performed. *Candida* type strains were obtained from the American Type Culture Collections (ATCC, Manassas, VA) and National Collection of Pathogenic Fungi (NCPF, Public Health Culture Collections, England).

Oral isolates of *Candida* species were previously isolated from HIV-positive patients and stored with consent at -80°C in Pro-Lab Microbank microbial preservation vials (Catalogue. no. PL.170/M, Pro-Lab, Canada).

2.2.2 Resuscitation and confirmation of purity of *Candida* isolates

Sabourauds dextrose agar (Catalogue.no. 84088, Sigma, SA) was prepared by dissolving 65 g of agar in 1 litre distilled water and sterilised by autoclaving at 121°C for 15 minutes. The media was cooled, poured into sterile petri dishes and allowed to set.

The *Candida* species were thawed by gentle agitation in a water bath between 25°C and 30°C and the yeast cells were transferred to sterile test tubes containing 10 mL Sabourauds dextrose broth (Catalogue.no. CMO147, Oxoid, UK) and incubated at 37°C for 3-5 days to revive the *Candida* strains. To ensure purity, the cultures were streaked onto Sabourauds dextrose agar plates and incubated at 37°C for 24 hours.

Species confirmation and purity of stored cultures were achieved using Oxoid chromogenic *Candida* agar (Catalogue.no.CM1002A, Oxoid, UK) and morphology was confirmed by Gram staining and microscopic analysis using an Optikam B3 camera (1000X) attached to an optical microscope.

2.2.3 Antifungal susceptibility testing of K21

2.2.3.1 Preparation of Roswell Park Memorial Institute-1640 media (RPMI-1640)

RPMI 1640 media was prepared by adding 10.43 g RPMI powder with L-glutamine (Catalogue. no. R6504, Sigma Aldrich, SA), 18 g glucose (Catalogue. no. G8270, Sigma

Aldrich, SA) in 900 mL distilled water, buffered with 34.53 g MOPS (N-Morpholino-propanesulfonic acid) with a molarity of 0.165 M (Catalogue. no. M1254, Sigma Aldrich, SA). The solution was mixed by gentle stirring using a sterile magnetic pellet on a Crison GLP21 plate stirrer (Barcelona, Spain). Once dissolved, the pH of the media was adjusted to pH 7 by adding 1N sodium hydroxide (Catalogue. no. S2770, Sigma Aldrich, SA). The solution was immediately filtered into a sterile bottle using a disposable membrane filter with a porosity of 0.22 microns (Catalogue. no. 25NS, MSI filters, USA).

2.2.3.2 Preparation of K21 dilutions for assays

A solution of K21 in 50% ethanol was obtained from KHG fiteBac technology (USA) and diluted as outlined in Figure 2.1. Stock solutions were prepared by dissolving 1 mL of the compound in 19 mL acetone yielding 20 mL smooth milky white solution (stock suspension). The 1 mL stock was then further diluted in 49 mL sterile distilled water to obtain a 50 mL working solution of 499.79 $\mu\text{g/mL}$.

UNIVERSITY of the
WESTERN CAPE

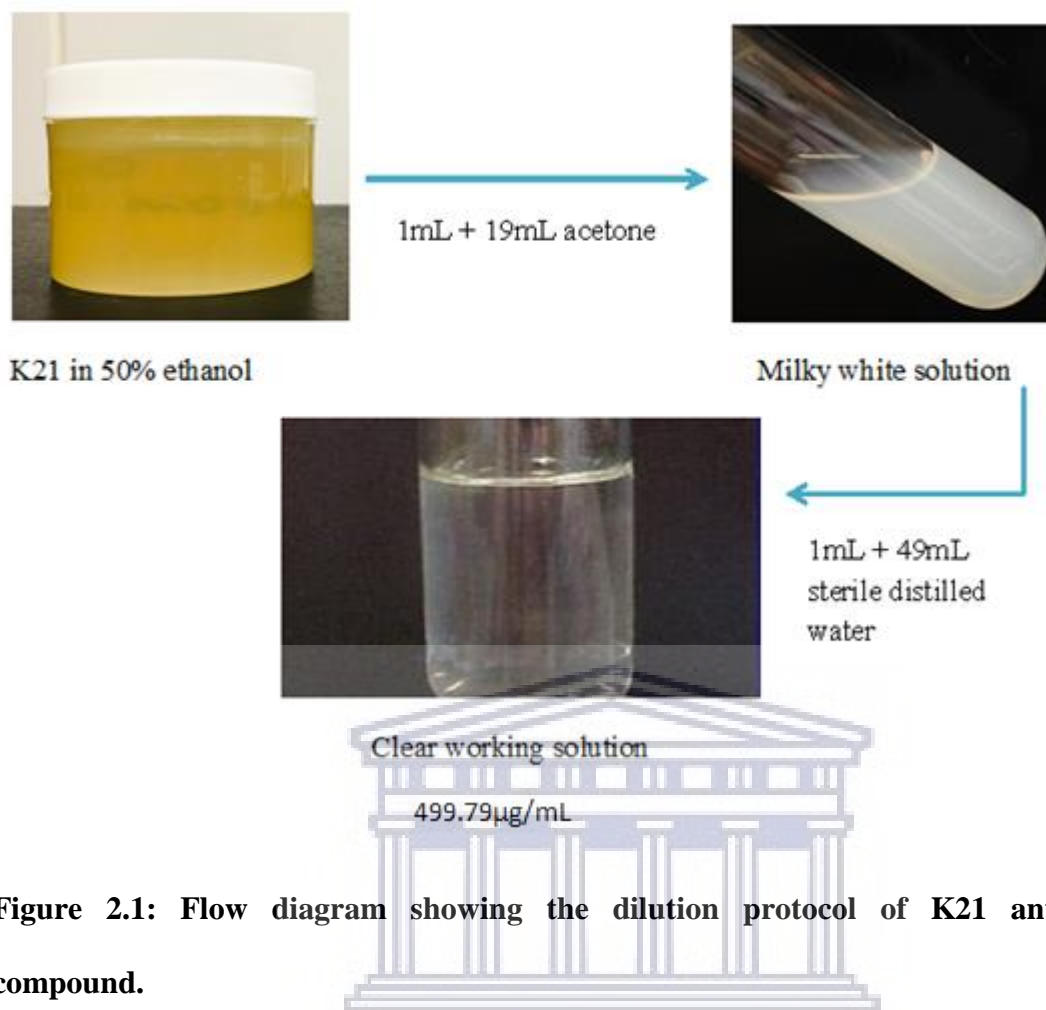


Figure 2.1: Flow diagram showing the dilution protocol of K21 antimicrobial compound.

2.2.3.3 Microdilution susceptibility assays

Broth microdilution assays were performed according to the Clinical and Laboratory Standards Institute M27A3 approved standard protocol (CLSI, 2008). Broth microdilution assays were performed on type strains before proceeding with the stored clinical isolates. The type strains such as *C. albicans* (ATCC 90028 and NCPF 3281), *C. krusei* (ATCC 2159), *C. glabrata* (ATCC 26512), *C. dubliniensis* (NCPF 3949a), *C. tropicalis* (ATCC 950), *C. parapsilosis* (ATCC 22019), *C. lusitaniae* (ATCC 34449) and *C. kefyr* (ATCC 4135) were also used as quality controls for the studies.

The cultures were grown on SDA incubated at 37°C for 24 hours. Fresh colonies of *Candida* from SDA plates were suspended in sterile saline solution (0.85% NaCl) and the cell density adjusted to 0.5 McFarland standard. The working suspension was prepared by making a 1:50 dilution of the stock suspension followed by a 1:20 dilution with RPMI 1640 medium resulting in an inoculum concentration of 1×10^3 - 5×10^3 CFU/mL. The microdilution test was performed in 96-well microtiter plates containing 100 μ L of RPMI medium from well 1 - well 9. This was followed by the addition of 100 μ L of a double concentration of K21 (499.79 μ g/mL) to the well 1. Broth microdilutions were carried out by the 2-fold serial dilutions of K21 in 100 μ L RPMI medium from well 1 - well 9 using a multichannel pipette. The plates were then inoculated with 100 μ L of the inoculum and sealed using sealing film and incubated for 24 hours at 37°C. The concentration range of K21 was 0.98 μ g/mL - 249.89 μ g/mL (Schwalbe *et al.*, 2007; Wong *et al.*, 2014). The experiments were conducted in triplicate.

Row A (wells 11 and 12) formed the negative control with 200 μ L RPMI alone. The FCZ-resistant *Candida* included 50 μ L of 25 μ g/mL of FCZ in 50 μ L inoculum and 100 μ L RPMI (Row B, wells 11 and 12), while 100 μ L inoculum in 100 μ L RPMI without K21 served as the positive control (Row G, wells 11 and 12). Solvent control was 50 μ L of ethanol and 50 μ L of acetone in 100 μ L RPMI (Row D, wells 11 and well 12).

The MIC values were recorded both visually and spectrophotometrically using an Anthos 2010 spectrophotometer (Biochrom Ltd, Cambridge CB4 0FJ, UK) at 450 nm. MICs were defined as the lowest concentration of K21 inhibiting the visible growth or 100% of the microorganism. Based on CLSI criteria, 100% growth inhibition was observed as clear wells in the plates. Antimicrobial activity was confirmed by the lack of growth after transferring 10 μ L of the sample from the clear wells onto a SDA plate and incubating at 37°C for 24 hours.

The readings were also interpreted by adding 40 μL iodinitrotetrazolium chloride (INT) calorimetric dye (Catalogue. no. 18377, Sigma-Aldrich, USA) at a concentration of 0.2 mg/mL into all the wells and incubating for a further 2 hours at 37°C. The MIC values were read by the change in colour. This technique relied on the ability of the viable cells to reduce the tetrazolium salt from yellow to pink/red. The INT dye acts as electron acceptor and is reduced by biologically active microbes resulting in the colour change observed (Eloff, 1998).

Disk diffusion assays were not performed in the present study due to the inability of K21 to diffuse into the agar media.

2.2.4 Antifungal susceptibility testing of Fluconazole

Minimum inhibitory concentration values for fluconazole (FCZ) against the isolates were previously performed (Abrantes *et al.*, 2014). The FCZ (Catalogue. no. 8929, Sigma Aldrich, USA) drug concentration ranged from 0.12 $\mu\text{g/mL}$ - 256 $\mu\text{g/mL}$ with sensitivity to FCZ indicated by CLSI approved breakpoint MIC values of ≤ 8 $\mu\text{g/mL}$, intermediate or dose-dependent susceptibility MIC between 16 $\mu\text{g/mL}$ - 32 $\mu\text{g/mL}$ and resistance MIC ≥ 64 $\mu\text{g/mL}$ (Eraso *et al.*, 2008).

The isolates were previously tested for FCZ susceptibility using Yeast Nitrogen Base Agar (YNBA). The TREK Sensititre YO9 drug panel exhibited MIC values of the FCZ-resistant isolates as 256 $\mu\text{g/mL}$ (Abrantes *et al.*, 2014). Since the *Candida* species were resistant to FCZ with a higher MIC, the present study included the above oral isolates for the susceptibility testing of K21.

2.2.5 Comparison of the antimicrobial activity of FCZ, K21 and FCZ/K21

2.2.5.1 Time-kill and Synergy assay

A time-kill assay was conducted to assess the rate of fungicidal activity of K21. The study was performed by a method previously described and evaluated by Klepser *et al.*, (1998). Broth microdilution was performed with a starting inoculum of $1-5 \times 10^5$ CFU/mL and K21 was tested at concentrations equal to MIC, 0.5MIC and 0.25MIC obtained by the microdilution checkerboard method. Plates were incubated at 37°C for 24 hours prior to removing a sample for the determination of colony counts at predetermined time points of 0, 2, 4, 6, 8, 12 and 24 hours. A 40 μ L sample was streaked onto sterile SDA plates. Colony counts were performed using a Gallenkamp 20/CX-300 colony counter (Gallenkamp Co. Ltd., UK). K21 was considered to have fungicidal activity when there was a reduction in microbial growth of $\geq 3 \log_{10}$ decrease in colony count after 24 hours, resulting in about 99.9% reduction in CFU/mL relative to the initial inoculum. Fungistatic activity was considered as a reduction in growth lower than 99.9% or $< 3 \log_{10}$ in CFU/mL from the initial inoculum after 24 hours (Locke *et al.*, 2018).

2.2.5.2 Checkerboard assay

We compared single-agent activity of K21 and FCZ along with a combination of K21/FCZ to define synergistic combinations *in vitro* using the time-kill assay and the checkerboard assay.

C. albicans (ATCC 90028 and NCPF 3281), *C. glabrata* (ATCC 26512), and *C. dubliniensis* (NCPF 3949a) were used in the assays. Using the time kill method, the rows in the microtiter plates were challenged with K21 and FCZ alone and with K21 and FCZ in a 1:1 combination

at their final concentrations of 0.5MIC and 0.25MIC. The plates were incubated at 37°C for 24 hours prior to removing a sample for the determination of colony counts at predetermined time points of 0, 2, 4, 6, 8, 12 and 24 hours (Bag and Chattopadhyay, 2017). The positive control included 100 µL RPMI and 100 µL inoculum (Row A, well 12) and negative control included 200 µL RPMI alone (Row B, well 12).

“Synergy” was defined as ≥ 2 log reduction in colony count for a given combination compared to the colony count obtained with the most active single agent and “Antagonism” was defined as ≥ 2 log increase in colony count for a given combination compared to the colony count obtained with the most active single agent (Zusman *et al.*, 2013), while a > 2 log and < 2 log increase or decrease in colony count at 24 hours with the combination compared with that of the most active single agent alone was reported as “Indifference” (Johnson *et al.*, 2004).

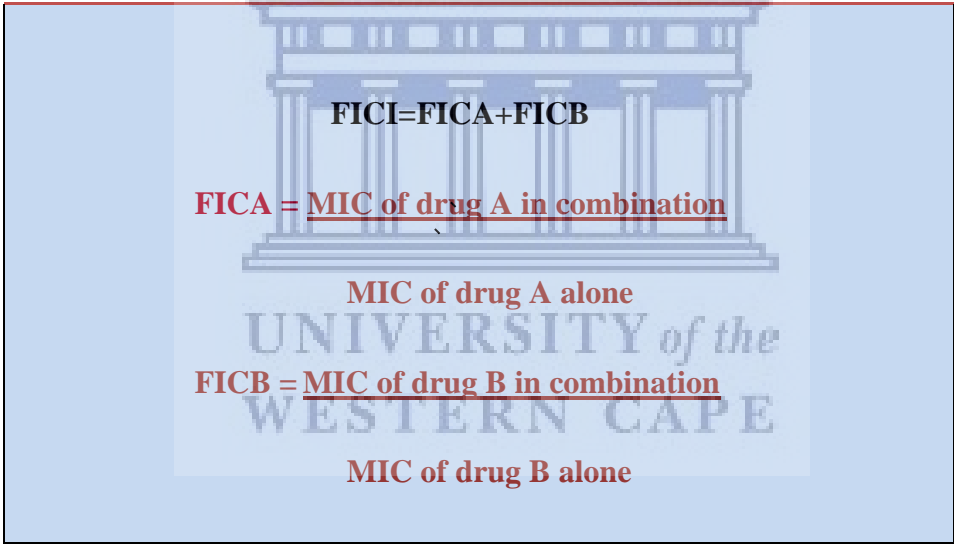
Using the checkerboard technique (Sopirala *et al.*, 2010), along with CLSI M27A2 and CLSI M27A3 guidelines for yeasts (CLSI, 2002; CLSI, 2008), synergism between K21 and FCZ was determined. The MIC values for K21 alone, FCZ alone and the combinations of K21 and FCZ were observed.

A starting inoculum was prepared by inoculating a tube of saline with fresh colonies of *Candida* and adjusting to 0.5 McFarland standard. A 1:10 dilution was done by adding 1 mL aliquot of inoculum to 9 mL RPMI yielding a working inoculum of $1-5 \times 10^5$ CFU/mL. Broth microdilutions involving 2-fold serial dilutions was performed in a microtiter plate with K21 and FCZ alone in row A and row C respectively and double concentrations of K21 and FCZ in combination in row E, well 1, so that serial dilutions in row E contained various concentrations of the combinations of the K21 and FCZ. The concentration range of K21 in row A was 0.49 µg/mL - 249.89 µg/mL and for FCZ in Row C was 0.12 µg/mL - 64 µg/mL. A positive growth control for each isolate included 100 µL RPMI + 100 µL inoculum (Row

A, well 12) and negative control included 200 μ L RPMI alone (Row B, well12). The plates were incubated at 37°C for 24 hours.

MIC or the inhibition of cell growth was observed by the appearance of clear wells in the plate and was confirmed by the absence of cell growth after transferring 10 μ L from the clear wells on to a SDA plate and incubating for 24 hours at 37°C. Turbidity in the wells and the colour change observed by the addition of 40 μ L INT dye indicated the growth of the cells. To assess the interactions of drug combinations, the data obtained by visual reading were further analysed using the fractional inhibitory concentration index (FICI).

FICI was evaluated for K21 in combination with fluconazole using the formula below;


$$\text{FICI} = \text{FICA} + \text{FICB}$$

FICA = MIC of drug A in combination
MIC of drug A alone

FICB = MIC of drug B in combination
MIC of drug B alone

FICI values were interpreted as follows: $\text{FICI} \leq 0.5$ = Synergy; > 0.5 to ≤ 4 = Indifference;

> 4 = Antagonism (Johnson *et al.*, 2004).

2.2.6 Statistical analysis

Data were analysed using SPSS software programme (SPSS Version 24, SPSS Inc, Chicago, IL, USA). All laboratory data were entered in a computer spread sheet programme, Microsoft Excel 2010. Data were expressed as the mean \pm standard deviation of at least three independent experiments. Mann-Whitney U-test which is a non-parametric test, was employed to evaluate the significant comparison between K21 and FCZ results. Two-factor analysis of variance (ANOVA) was used to test the differences between the combinations and single concentrations of K21 and FCZ over time. A Tukey test for post hoc analysis was used to determine the significance of time from 0-24 hours at different concentrations. A p value < 0.05 was considered statistically significant.



2.3 RESULTS

2.3.1 Confirmation of purity and distribution of *Candida* species

On chromogenic media *C. albicans* grew as light opaque green colonies. *C. glabrata* appeared as smooth beige or yellow/brown colonies whereas *C. krusei* appeared as pink/brown fuzzy colonies. *C. dubliniensis* and *C. tropicalis* grew as dark shiny green colonies and metallic blue colonies respectively. *C. parapsilosis*/*C. lusitaniae* and *C. kefyr* appeared as natural pigment colonies. Microscopic analysis demonstrated *Candida* cells as spherical to sub-spherical budding blastoconidia with the exception of *C. krusei* exhibiting larger elongated cells.

Among the 143 *Candida* isolates, 81.8% were *C. albicans* (n = 108), 11.2% were *C. glabrata* (n = 16), 2.8% were *C. dubliniensis* (n = 4), while *C. krusei* and *C. tropicalis* each constituted 2.1% (n = 3) (Figure 2.2).

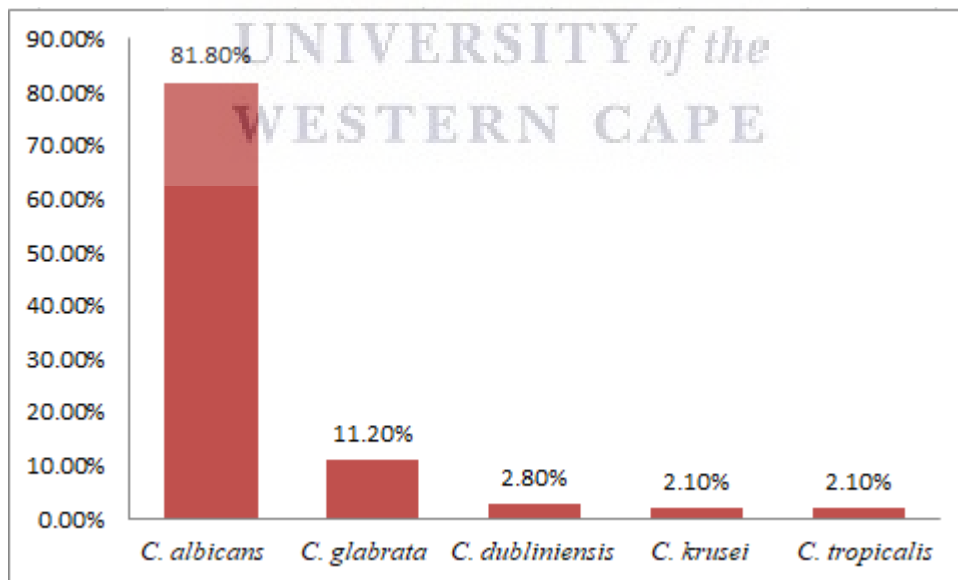


Figure 2.2: Species distribution of the *Candida* species investigated

2.3.2 Antifungal profiles of *Candida* species exposed to FCZ

Figure 2.3 shows the distribution of the FCZ-resistant *Candida* species with 96.10% of *C. albicans*, 1% of *C. dubliniensis* and *C. glabrata* and 1.9% *C. krusei*.

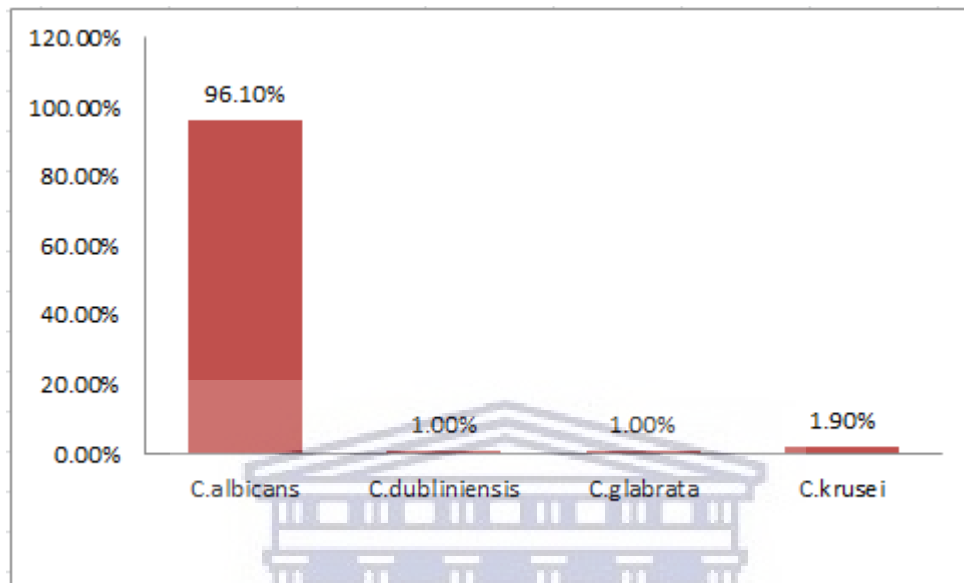


Figure 2.3: *Candida* species resistant to FCZ

FCZ-intermediate *Candida* species were 84.60% of *C. glabrata* and 15.40% of *C. albicans* (Figure 2.4). About 59.30% of *C. albicans*, 14.80% of *C. glabrata*, and 3.70% of *C. krusei* were FCZ-susceptible. Rest of the FCZ-susceptible *Candida* species were 11.10% of *C. dubliniensis* and *C. tropicalis* (Figure 2.5).

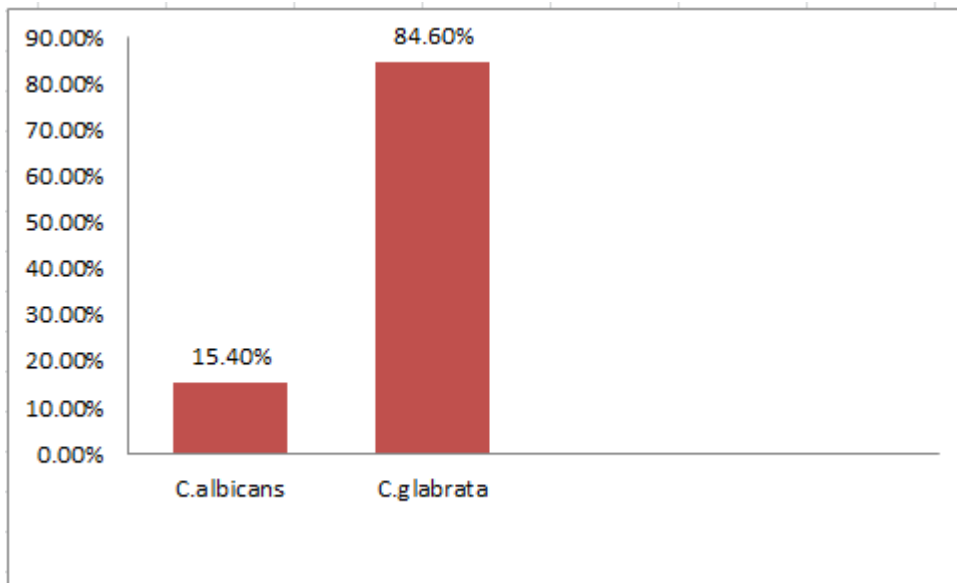


Figure 2.4: *Candida* species intermediate to FCZ

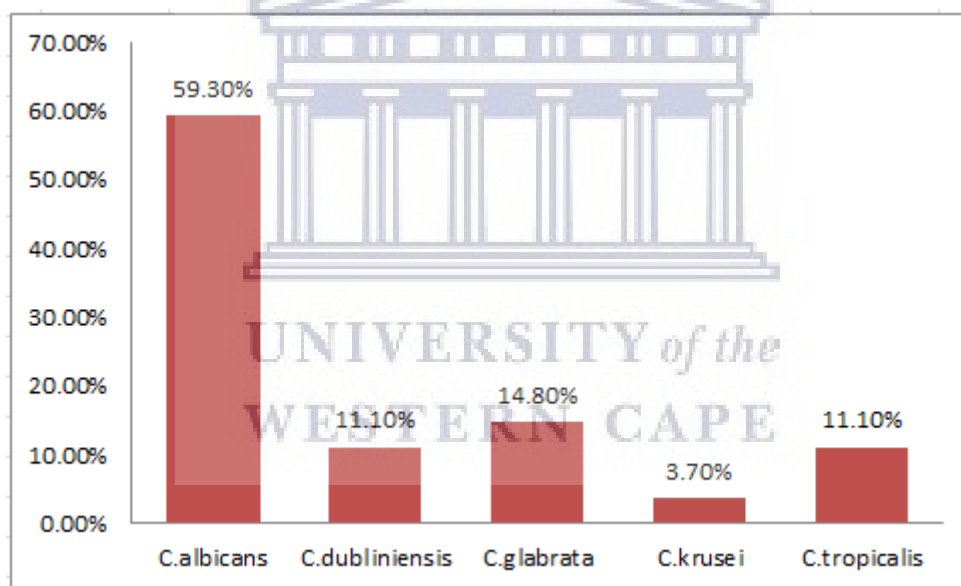


Figure 2.5: *Candida* species susceptible to FCZ

2.3.2.1 Broth microdilution assay for K21

The broth microdilution assay assisted in the quantitative measurement of the *in vitro* activity against *Candida* species and determined the minimum inhibitory concentrations of K21. The growth of the different *Candida* species was inhibited to some degree when treated with K21

showing the susceptibility of the species to K21. Clear wells in the microtiter plates indicated the minimum inhibitory concentration (MIC) of K21 for the *Candida* species and the presence of viable cells was indicated by turbid cells which turned red after the addition of INT dye (Figure 2.6). The broth microdilution assay for K21 against *C. albicans* showed a MIC of 31.24 $\mu\text{g/mL}$ (Figure 2.4, well 4). The K21 concentrations ranged from the highest to the lowest (249.89 $\mu\text{g/mL}$ - 0.98 $\mu\text{g/mL}$) from well 1- well 9. The experiments were done in triplicate.

The RPMI media that served as the negative control showed no colour change indicating the absence of *C. albicans* (Row A, wells 11 and well 12). The growth of the cells with colour change indicated the presence of FCZ-resistant *C. albicans* species (Row B, well 11 and well 12). The solvent control showed a colour change to red, indicating that the presence of ethanol and acetone in the solvent did not inhibit the growth of the *Candida* cells and that the inhibition of cell growth was due to the action of K21 alone (Row D, well 11 and well 12). The positive control in RPMI media indicated the active growth of *Candida* cells without the treatment of K21 or FCZ (Row G, well 11 and well 12).

UNIVERSITY of the
WESTERN CAPE

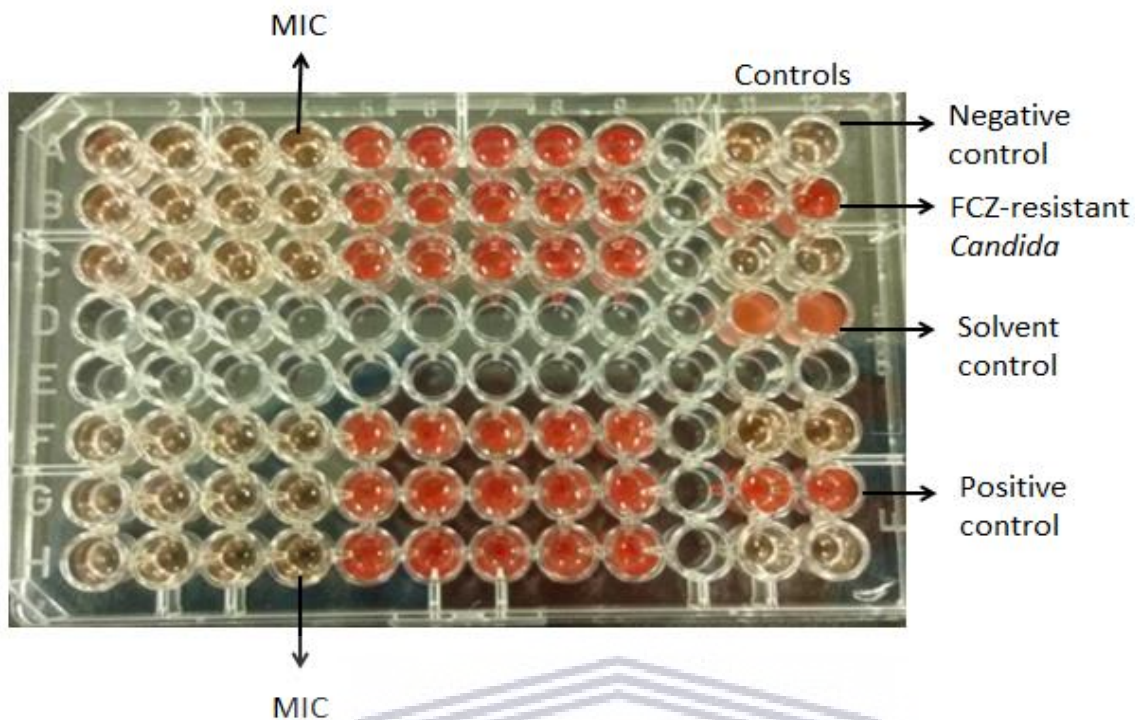


Figure 2.6: Broth microdilution assay for K21 (MIC 31.24 $\mu\text{g}/\text{mL}$) against *C. albicans*. Wells 1-9 contains 2-fold serial dilutions of K21 in RPMI. Negative control shows no growth (Row A, wells 11 and 12); FCZ-resistant *Candida* shows growth (Row B, wells 11 and 12); Solvent control shows growth (Row D, wells 11 and 12); Positive control shows growth (Row G, wells 11 and 12).

Table 2.1 shows the collective susceptibility patterns of *Candida* as determined by K21 and FCZ. About 103 species of *Candida* were resistant and 13 were intermediate to FCZ with a MIC range between 64 $\mu\text{g}/\text{mL}$ - 256 $\mu\text{g}/\text{mL}$ and 16 $\mu\text{g}/\text{mL}$ - 32 $\mu\text{g}/\text{mL}$ respectively. However, the majority of the *Candida* species ($n = 86$) were intermediate to K21 with a MIC range between 62.48 $\mu\text{g}/\text{mL}$ - 124.95 $\mu\text{g}/\text{mL}$ and only 9 of the *Candida* species were found resistant to K21 with a MIC value of ≥ 249.89 $\mu\text{g}/\text{mL}$. The *Candida* species susceptible to FCZ were 27 with a MIC range between 0.03 $\mu\text{g}/\text{mL}$ - 8 $\mu\text{g}/\text{mL}$ while 48 of them were susceptible to K21 exhibiting a MIC value ≤ 31.24 $\mu\text{g}/\text{mL}$. The MIC values of the *Candida* species for K21 and FCZ are displayed in the Appendix A.

Table 2.1: Collective susceptibility patterns of *Candida* as determined by K21 and FCZ

Species	K21		FCZ	
<i>Candida</i>	Susceptible = $\leq 31.24 \mu\text{g/mL}$	n = 48	Susceptible = $0.03 \mu\text{g/mL}$	n = 27
	Intermediate = $62.48 \mu\text{g/mL}$	n = 86	- $8 \mu\text{g/mL}$	
	- $124.95 \mu\text{g/mL}$		Intermediate = $16 \mu\text{g/mL}$	n = 13
	Resistant = $\geq 249.89 \mu\text{g/mL}$	n = 9	32 $\mu\text{g/mL}$	
			Resistant = $64 \mu\text{g/mL}$	n = 103
			256 $\mu\text{g/mL}$	

2.3.2.2 Effect of Fluconazole (FCZ)

The clinical isolates of *C. albicans* (96.1%) formed the majority of the FCZ-resistant *Candida* species followed by *C. krusei* (1.9%). There was only one resistant isolate of *C. dubliniensis* and one *C. glabrata* (Table 2.2).

The mean MIC of *C. albicans* was $251.47 \mu\text{g/mL}$ with a MIC range between $64 \mu\text{g/mL}$ - $256 \mu\text{g/mL}$. The median of *C. albicans* and *C. krusei* was $256 \mu\text{g/mL}$ and $64 \mu\text{g/mL}$ respectively.

Table 2.2: MIC ranges of FCZ-resistant *Candida*

Antifungal	<i>Candida</i>				
		<i>C. albicans</i> (n = 99)	<i>C. dubliniensis</i> (n = 1)	<i>C. krusei</i> (n = 2)	<i>C. glabrata</i> (n = 1)
FCZ	Mean MIC (SD)	251.4 µg/mL (±26.26)	-	64 µg/mL (±0.00)	-
	Median	256 µg/mL	-	64 µg/mL	-
	MIC range	64 - 256 µg/mL	-	-	-

Approximately 84.6% of the FCZ-intermediate *Candida* species were *C. glabrata* and 15.4% were *C. albicans* (Table 2.3). FCZ-intermediate *Candida* species refers to the species with dose-dependent antifungal activity.

The mean MIC of *C. albicans* and *C. glabrata* was 16 µg/mL and 18.9 µg/mL respectively, with a similar median of 16 µg/mL. *C. glabrata* showed a MIC range of 16 µg/mL - 32 µg/mL.

Table 2.3: MIC ranges of FCZ-intermediate *Candida*

Antifungal	<i>Candida</i>		
		<i>C. albicans</i> (n = 2)	<i>C. glabrata</i> (n = 11)
FCZ	Mean MIC (SD)	16 µg/mL (±0.00)	18.9 µg/mL (±6.47)
	Median	16 µg/mL	16 µg/mL
	MIC range (µg/mL)	-	16 - 32 µg/mL

Among the FCZ-susceptible *Candida* species, 59.3% were *C. albicans* and 14.8% were *C. glabrata*. Only 3.7% were *C. krusei* and the rest (11.1%) were *C. dubliniensis* and *C. tropicalis* (Table 2.4).

The mean MIC of *C. albicans* and *C. glabrata* was 2.77 µg/mL and 3.25 µg/mL with a MIC range of 0.12 µg/mL - 8 µg/mL and 0.5 - 8 µg/mL respectively. *C. dubliniensis* exhibited a lower mean MIC of 0.34 µg/mL and the single isolate of *C. krusei* showed a mean MIC of 4 µg/mL. The MIC range of *C. tropicalis* was 1 µg/mL - 2 µg/mL with a mean MIC of 1.66 µg/mL.

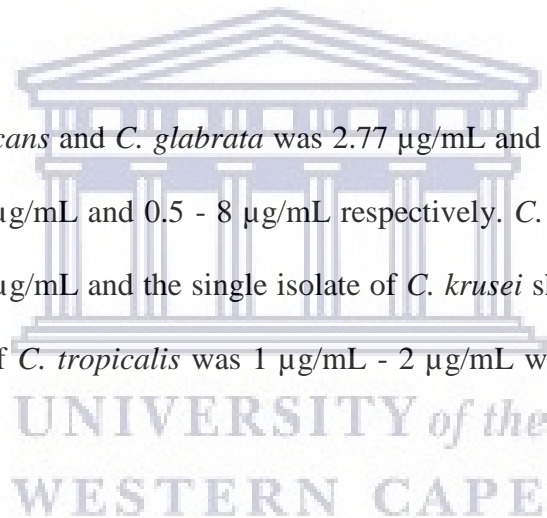


Table 2.4: MIC ranges of FCZ- susceptible *Candida*

Antifungal	<i>Candida</i>					
		<i>C. albicans</i> (n = 16)	<i>C. glabrata</i> (n = 4)	<i>C. krusei</i> (n = 1)	<i>C. dubliniensis</i> (n = 3)	<i>C. tropicalis</i> (n = 3)
FCZ	Mean MIC	2.77 µg/mL	3.25 µg/mL	4 µg/mL	0.34 µg/mL	1.66 µg/mL
	(SD)	(±3.00)	(±3.57)		(±0.27)	(±0.57)
	Median	0.75 µg/mL	2.25 µg/mL	4 µg/mL	0.5 µg/mL	2 µg/mL
	MIC range	0.12 – 8 µg/mL	0.5 - 8µg/mL	-	0.03 - 0.5µg/mL	1 - 2 µg/mL

2.3.2.3 Effect of K21

On treatment with K21, *C. albicans* exhibited a MIC range of 31.24 µg/mL - 249.89 µg/mL with a mean MIC value of 75.09 µg/mL. The mean MIC and median of *C. dubliniensis* and *C. krusei* was 124.95 µg/mL and of *C. glabrata* was 62.48 µg/mL (Table 2.5).

Table 2.5: K21 MIC ranges for FCZ-resistant *Candida*

Antifungal	<i>Candida</i>				
		<i>C. albicans</i> (n = 99)	<i>C. dubliniensis</i> (n = 1)	<i>C. krusei</i> (n = 2)	<i>C. glabrata</i> (n = 1)
K21	Mean MIC	75.09 µg/mL	124.95 µg/Ml	124.95 µg/mL	62.48 µg/mL
	(SD)	(±54.45)		(±0.00)	
	Median	62.48 µg/mL	124.95 µg/mL	124.95 µg/mL	62.48 µg/mL
	MIC range	31.24 - 249.89 µg/mL	-	-	-

When exposed to K21, the mean MIC of *C. glabrata* was high (136.30 µg/mL) when compared with *C. albicans* exhibiting the mean MIC of 31.24 µg/mL. The median of *C. glabrata* was also high (124.95 µg/mL) with a MIC range between 62.48 µg/mL - 249.89 µg/mL (Table 2.6).

Table 2.6: K21 MIC ranges for FCZ intermediate *Candida*

Antifungal	<i>Candida</i>	
	<i>C. albicans</i> (n = 2)	<i>C. glabrata</i> (n = 11)
K21	Mean MIC	31.24 µg/mL
	(SD)	(±0.00)
	Median	31.24 µg/mL
	MIC range	-

The mean MIC was high for *C. krusei* and *C. dubliniensis* (62.48 µg/mL) and low for *C. tropicalis* (31.24 µg/mL). *C. albicans* showed a mean MIC of 41.00 µg/mL and *C. glabrata* showed a mean MIC of 62.47 µg/mL with MIC ranging between 31.24 µg/mL - 62.48 µg/mL and 31.24 µg/mL - 124.95 µg/mL respectively. The median of *C. krusei* and *C. dubliniensis* was similar with a value of 62.48 µg/mL (Table 2.7).

Table 2.7: K21 MIC ranges of FCZ-susceptible *Candida*

Antifungal	<i>Candida</i>					
	<i>C. albicans</i> (n = 16)	<i>C. glabrata</i> (n = 4)	<i>C. krusei</i> (n = 1)	<i>C. dubliniensis</i> (n = 3)	<i>C. tropicalis</i> (n = 3)	
K21	Mean MIC	41.00 µg/mL	62.47 µg/mL	62.48 µg/mL	62.48 µg/mL	31.24 µg/mL
	(SD)	(±14.95)	(±44.17)		(±0.00)	(±0.00)
	Median	31.24 µg/mL	46.86 µg/mL	62.48 µg/mL	62.48 µg/mL	31.24 µg/mL
	MIC range	31.24 - 62.48 µg/mL	31.24 - 124.95 µg/mL	-	-	-

2.3.2.4 Comparison of FCZ with K21

Mann-Whitney U test determined the comparison between FCZ and K21 demonstrating a significant p value = 0.000 (Table 2.8). The whisker box plot displays the data variations against K21 and FCZ. The MIC of FCZ was significantly higher than K21 and have the same value of 256 for median and maximum (Figure 2.7).

Table 2.8: FCZ versus K21

FCZ ($\mu\text{g/mL}$)	K21 ($\mu\text{g/mL}$)	p value
256.00 (0.03 - 256) ^a	62.48 (31.24 - 249.89) ^a	0.000

^aMedian (range) of the MICs

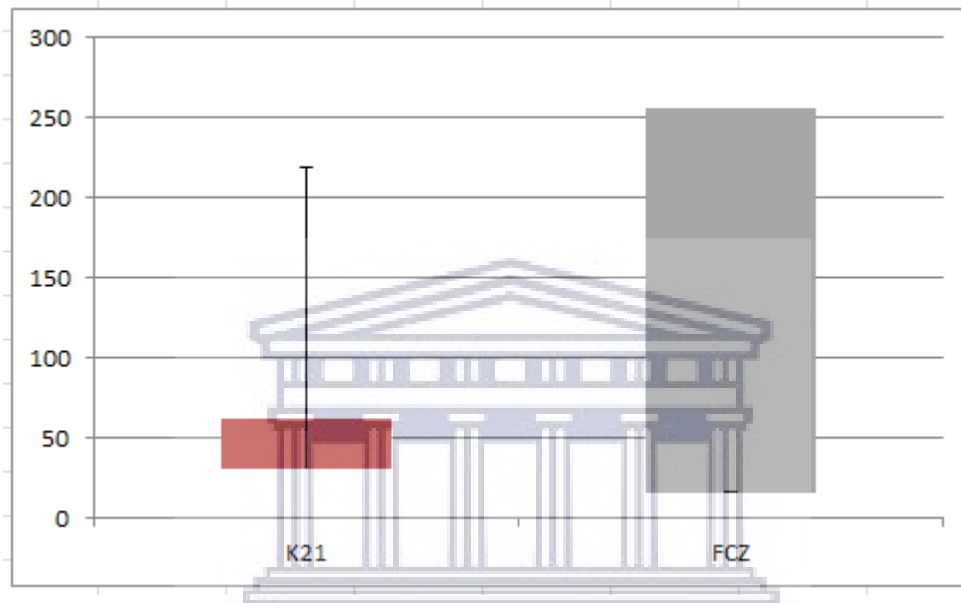


Figure 2.7: Whisker Box-plot showing the variations of the data against K21 and FCZ

2.3.2.5 Synergistic effect of FCZ/K21

Table 2.9 displays the MIC values of K21 and FCZ against type strains of *Candida* and their FIC indices. The individual MICs of the type strains against K21 were 62.48 $\mu\text{g/mL}$ except for *C. lusitaniae* (ATCC 34449) and *C. kefyr* (ATCC 4135) showing a MIC of 124.95 $\mu\text{g/mL}$. FCZ exhibited antifungal activity at a higher concentration of 64 $\mu\text{g/mL}$ against *C. glabrata* (ATCC 26512) and *C. krusei* (ATCC 2159), followed by *C. albicans* (NCPF 3281) (32 $\mu\text{g/mL}$) and *C. albicans* (ATCC 90028) (16 $\mu\text{g/mL}$). *C. dubliniensis* (NCPF 3949a) and *C. parapsilosis* (ATCC 22019) shared a similar MIC of 2 $\mu\text{g/mL}$, while *C. tropicalis* (ATCC

950), *C. lusitaniae* (ATCC 34449) and *C. kefyr* (ATCC 4135) shared a similar MIC of 1 µg/mL, when treated with FCZ.

FICI of the 9 type strains gave indifferent or synergistic profiles when K21 was combined with FCZ. A synergistic effect was observed for *C. dubliniensis* (NCPF 3949a), *C. tropicalis* (ATCC 950) and *C. lusitaniae* (ATCC 34449). Synergy was noted at 0.03 µg/mL K21 plus 0.25 µg/mL FCZ for *C. dubliniensis* (NCPF 3949a) and 0.01 µg/mL K21 plus 0.25 µg/mL FCZ for *C. tropicalis* (ATCC 950) and 0.007 µg/mL K21 plus 0.25 µg/mL FCZ for *C. lusitaniae* (ATCC 34449). The MICs and the FICI for *C. glabrata* (ATCC 26512) and *C. krusei* (ATCC 2159) appeared identical for both K21 and FCZ. The reason may be due to the resistant nature of both the strains. All other dose pairs displayed indifferent effects. No antagonistic effects were found in any of the combinations.

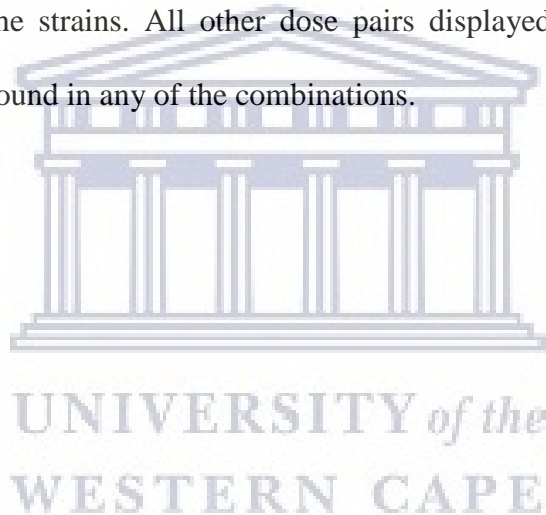


Table 2.9: Microdilution checkerboard values to determine FCZ/K21 synergy

Species	Individual MICs		Combination MICs		ΣFICI	Interpretation
			FIC A	FIC B		
<i>Candida</i>	FCZ MIC (µg/mL)	K21 MIC (µg/mL)	FCZ MIC (µg/mL)	K21 MIC (µg/mL)		
<i>C. albicans</i> (ATCC 90028)	16	62.48	0.5	0.5	1	Indifference
<i>C. albicans</i> (NCPF 3281)	32	62.48	0.5	1	1.5	Indifference
<i>C. krusei</i> (ATCC 2159)	64	62.48	0.25	1	1.25	Indifference
<i>C. glabrata</i> (ATCC 26512)	64	62.48	0.25	1	1.25	Indifference
<i>C. dubliniensis</i> (NCPF 3949a)	2	62.48	0.25	0.03	0.28	Synergy
<i>C. tropicalis</i> (ATCC 950)	1	62.48	0.25	0.01	0.26	Synergy
<i>C. parapsilosis</i> (ATCC 22019)	2	62.48	0.5	0.06	0.56	Indifference
<i>C. lusitaniae</i> (ATCC 34449)	1	124.95	0.25	0.007	0.25	Synergy
<i>C. kefyr</i> (ATCC 4135)	1	124.95	0.5	0.01	0.51	Indifference

≤0.5=synergy, >0.5 to ≤4 = indifference (Johnson *et al.*, 2004)

Figure 2.8 demonstrates the MIC of K21 in rows A and B and the MIC of FCZ in rows C and D against *C. albicans* (ATCC 90028) by the broth microdilution checkerboard assay. Rows E and F represents the combination MICs of K21 and FCZ. The MIC of K21 and FCZ was 62.48 µg/mL and 16 µg/mL respectively. With the combination of concentrations, the MICs of both K21 and FCZ were dropped to 31.24 µg/mL and 8 µg/mL. A positive control

containing the inoculum without K21 and FCZ showed cell growth and a negative control consisting of RPMI alone showed absence of cell growth.

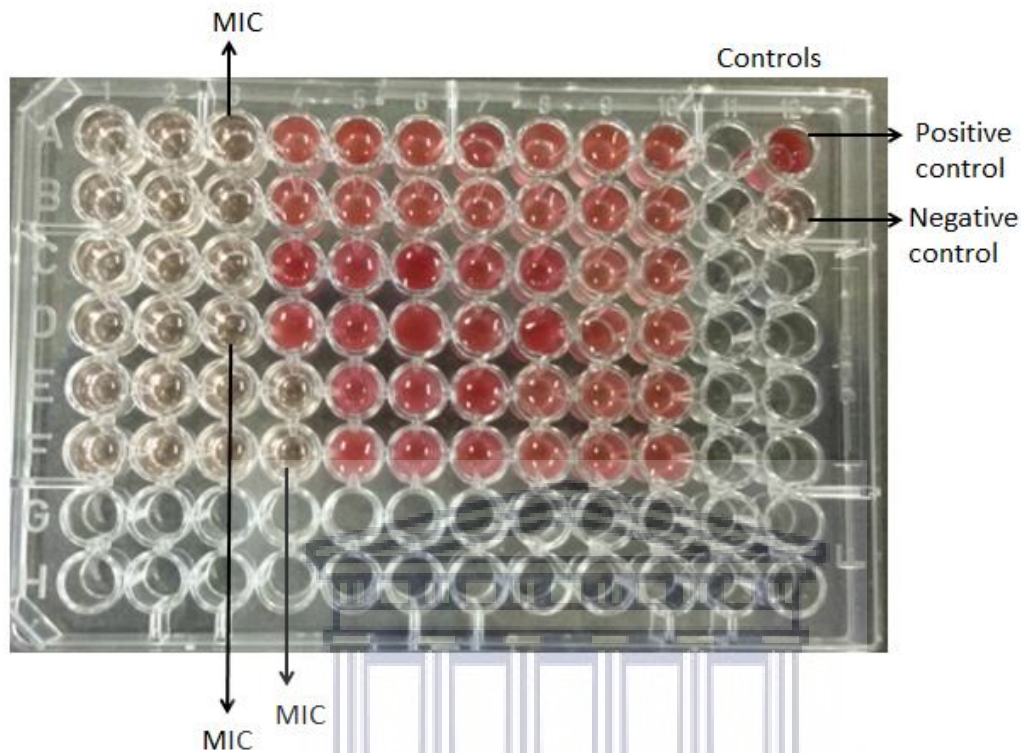


Figure 2.8: Broth microdilution checkerboard assay results of *C. albicans* (ATCC 90028) showing an indifferent effect. Rows A and B, wells 1-10 contains 2-fold serial dilutions of K21 in RPMI. Rows C and D, wells 1-10 contains 2-fold serial dilutions of FCZ. Rows E and F, wells 1-10 contains double concentrations of K21/FCZ in 1:1 combination. Wells 12 in rows A and B contains positive and negative controls.

Figure 2.9 shows the broth microdilution checkerboard assay results of *C. albicans* (NCPF 3281) with the individual MIC of 62.48 $\mu\text{g/mL}$ of K21 and 32 $\mu\text{g/mL}$ of FCZ. The combination MICs were 62.48 $\mu\text{g/mL}$ and 16 $\mu\text{g/mL}$ for K21 and FCZ respectively, indicating an indifferent effect. Rows A and B showed MIC of K21 and rows C and D showed MIC of FCZ, while rows E and F showed the combination concentrations of K21 and FCZ. The positive control with the inoculum without K21 and FCZ exhibited cell growth, while the negative control with RPMI alone showed no cell growth.

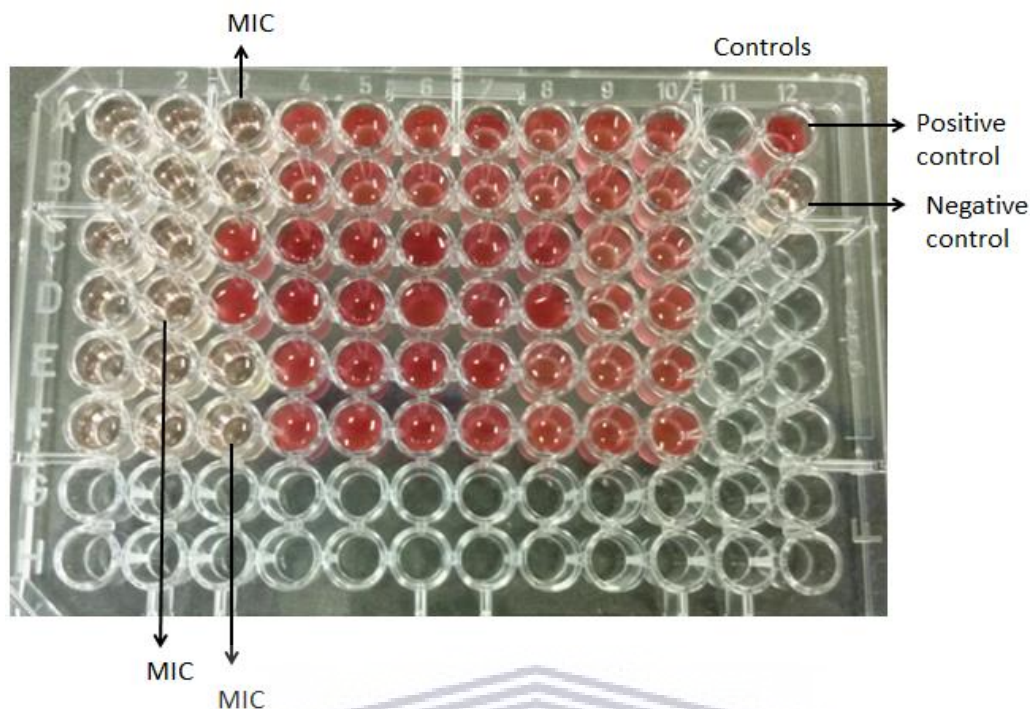


Figure 2.9: Broth microdilution checkerboard assay results of *C. albicans* (NCPF 3281) showing an indifferent effect. Rows A and B, wells 1-10 contains 2-fold serial dilutions of K21 in RPMI. Rows C and D, wells 1-10 contains 2-fold serial dilutions of FCZ. Rows E and F, wells 1-10 contains double concentrations of K21/FCZ in 1:1 combination. Wells 12 in rows A and B contains positive and negative controls.

A synergistic effect was exhibited for *C. dubliniensis* (NCPF 3949a) when treated with combination MICs of K21 and FCZ (Figure 2.10). The MIC of *C. dubliniensis* (NCPF 3949a) was 62.48 $\mu\text{g/mL}$ for K21 and 2 $\mu\text{g/mL}$ for FCZ. In combination, the MIC values for K21 and FCZ dropped to 1.95 $\mu\text{g/mL}$ and 0.5 $\mu\text{g/mL}$ respectively, indicating synergy when K21 and FCZ were combined.

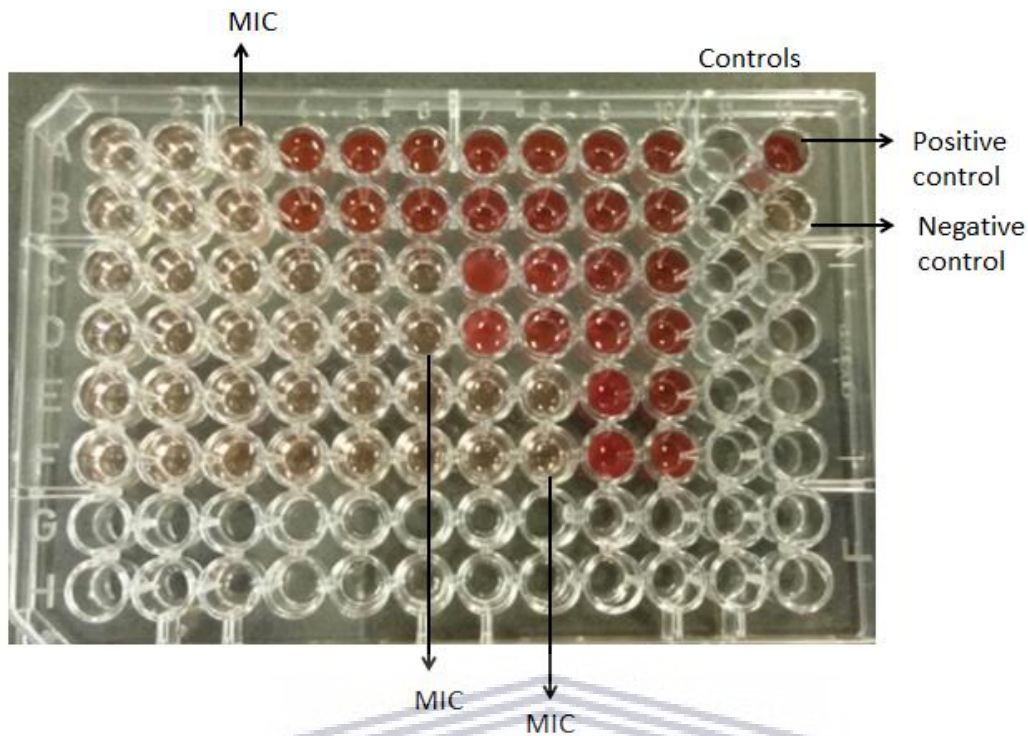


Figure 2.10: Broth microdilution checkerboard assay results of *C. dubliniensis* (NCPF 3949a) showing a synergistic effect. Rows A and B, wells 1-10 contains 2-fold serial dilutions of K21 in RPMI. Rows C and D, wells 1-10 contains 2-fold serial dilutions of FCZ. Rows E and F, wells 1-10 contains double concentrations of K21/FCZ in 1:1 combination. Rows A and B, wells 12 shows positive and negative controls.

Figure 2.11 represents the broth microdilution checkerboard assay results of *C. lusitaniae* (ATCC 34449). The MIC of K21 was 124.95 $\mu\text{g/mL}$ for K21 and 1 $\mu\text{g/mL}$ for FCZ and when combined, their MICs were effectively reduced to 0.97 $\mu\text{g/mL}$ and 0.25 $\mu\text{g/mL}$ for K21 and FCZ respectively. A definite synergism existed between K21 and FCZ when *C. lusitaniae* (ATCC 34449) was treated with a combination of different concentrations of K21 and FCZ.

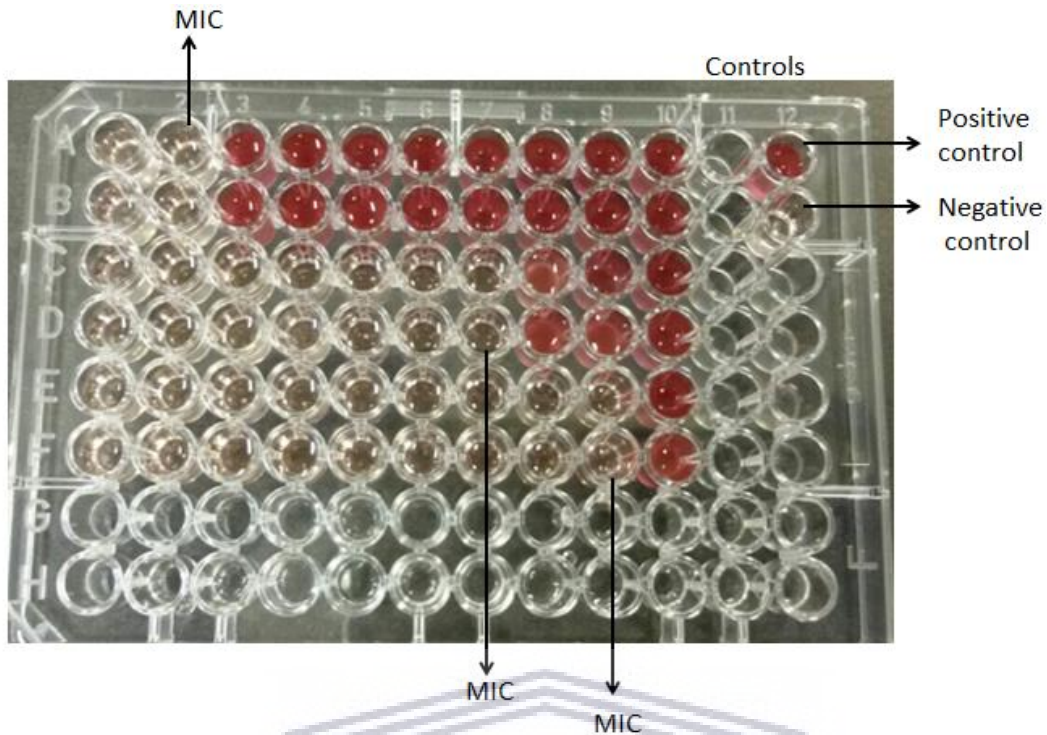


Figure 2.11: Broth microdilution checkerboard assay results of *C. lusitaniae* (ATCC 34449) showing a definite synergism. Rows A and B, wells 1-10 contains 2-fold serial dilutions of K21 in RPMI. Rows C and D, wells 1-10 contains 2-fold serial dilutions of FCZ. Rows E and F, wells 1-10 contains double concentrations of K21/FCZ in 1:1 combination. Rows A and B, wells 12 shows positive and negative controls.

The resistant *C. glabrata* showed a MIC of 62.48 $\mu\text{g/mL}$ and a MIC of 64 $\mu\text{g/mL}$ for K21 and FCZ respectively. There was a little drop in the MIC values when K21 and FCZ were combined. In combination, the MIC for K21 remained the same at 62.48 $\mu\text{g/mL}$ and FCZ was reduced to 16 $\mu\text{g/mL}$ (Figure 2.12).

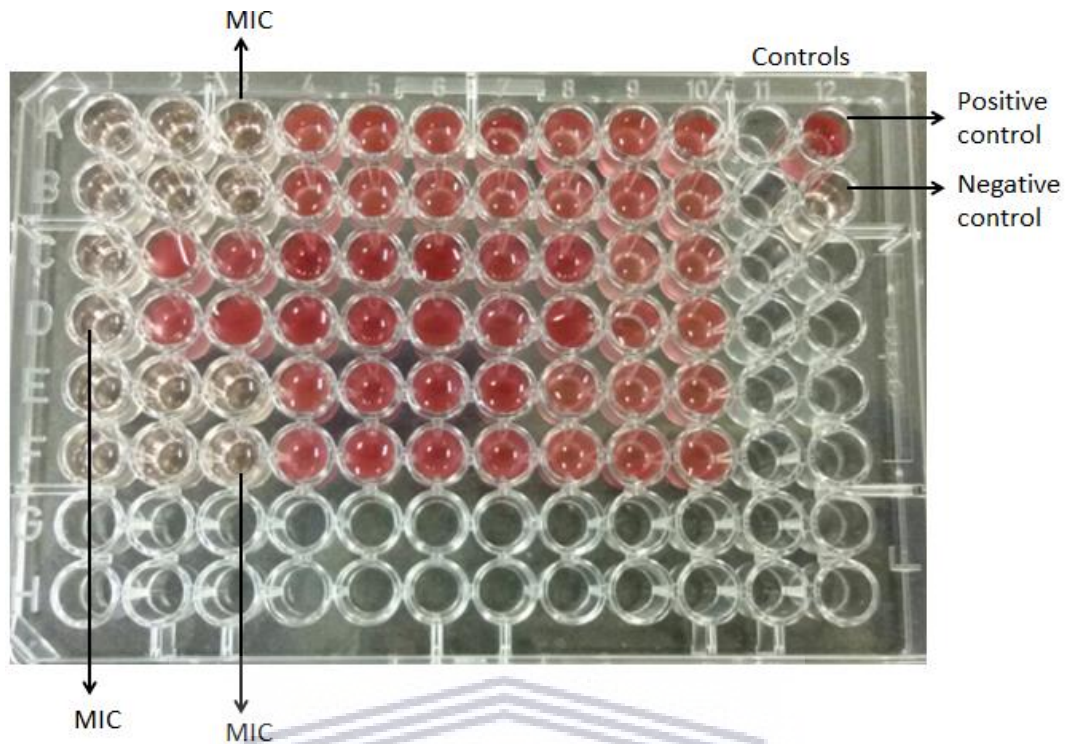


Figure 2.12: Broth microdilution checkerboard assay results of *C. glabrata* (ATCC 26512) showing an indifferent effect. Rows A and B, wells 1-10 contains 2-fold serial dilutions of K21 in RPMI. Rows C and D, wells 1-10 contains 2-fold serial dilutions of FCZ. Rows E and F, wells 1-10 contains double concentrations of K21/FCZ in 1:1 combination. Rows A and B, wells 12 shows positive and negative controls.

2.3.2.6 Time-kill assay for K21

The time-kill assay was performed to study the rate of inhibition of the growth of *Candida* species after contact with K21 at certain time periods. The rate of fungicidal activity of K21 was tested against *C. albicans* (ATCC 90028) and *C. glabrata* (ATCC 26512) at their MIC concentrations.

Figure 2.13 shows the time kill curve plotted for FCZ-susceptible *C. albicans* (ATCC 90028) along with 0.5MIC and 0.25MIC concentrations of K21. Analysis of the curve showed a

steady growth for *C. albicans* reaching a plateau at around 10 hours. The MIC concentration showed a reduction in fungal growth at 2 hours ($\geq 3\log_{10}$ of CFU/mL or lower than 99.9% reduction in microbial growth of the initial inoculum) which continued for 24 hours. There was no detection of viable cells at the MIC concentrations after 24 hours of incubation. The 0.5MIC showed a rapid growth curve up to 6 hours with slower growth continuing up to 24 hours. A similar curve was obtained for 0.25MIC. The killing curve showed that the growth of *C. albicans* (ATCC 90028) without any treatment (negative control) increased by the time of incubation.

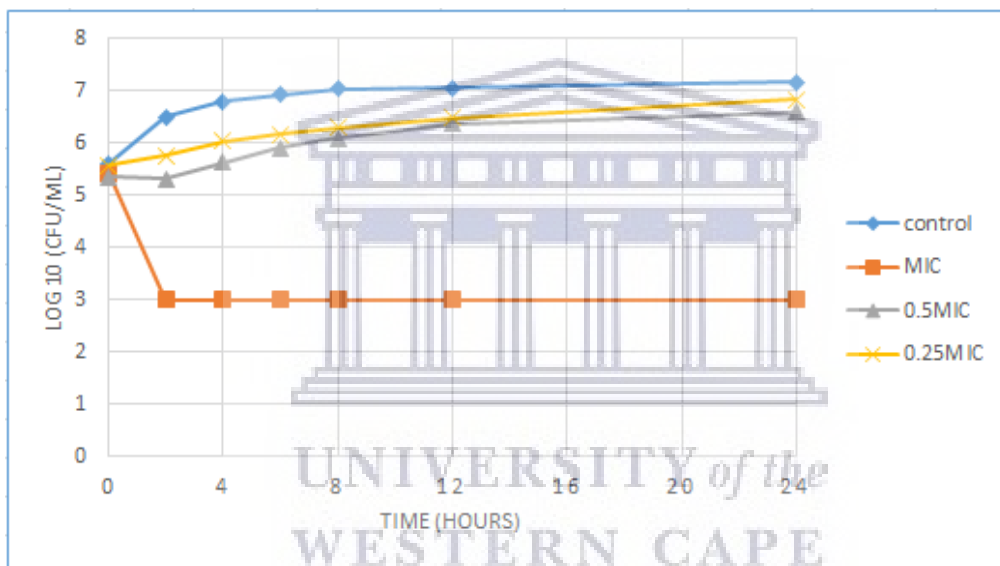


Figure 2.13: Time-kill curve plotted for *C. albicans* (ATCC 90028). Fungicidal effect of K21 was observed at 2 hours.

Analysis of the time-kill curve (Figure 2.14) showed a steady growth curve for the FCZ-resistant control *C. glabrata* (ATCC 26512) up to 6 hours after which it plateaued. The 0.5MIC and 0.25MIC concentrations of K21 presented a growth peak up to 6 hours of exposure showing a fungistatic activity with a reduction in microbial growth of $\leq 3\log_{10}$ of CFU/mL or lower than 99.9% of the initial inoculum. At 2 hours, the MIC showed fungicidal

activity with a reduction $\geq 3\log_{10}$ of CFU/mL or about 99.9% reduction in microbial growth relative to the initial inoculum. No viable cells were detected after 24 hours indicating the fungicidal effect of K21. The negative control without any treatment showed a steady increase in growth with the incubation time.

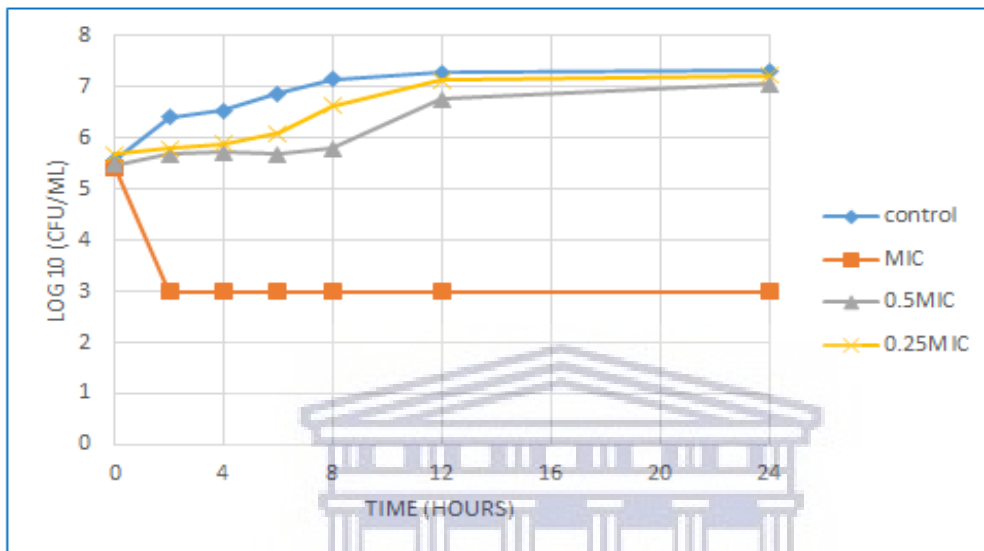


Figure 2.14: Time-kill curve plotted for *C. glabrata* (ATCC 26512). Fungicidal activity of K21 was observed at 2 hours.

UNIVERSITY of the
WESTERN CAPE

2.3.2.7 Time-kill assay for Synergy

C. albicans (ATCC 90028 and NCPF 3281), *C. glabrata* (ATCC 26512) and *C. dubliniensis* (NCPF 3949a) were tested for synergy by the time-kill assay.

2.3.2.7.1 Synergy of *C. albicans* (ATCC 90028 and NCPF 3281) determined by time-kill assay

The time-kill curve of K21 and FCZ for *C. albicans* (ATCC 90028) are presented in Figure 2.15. Exposure to both K21 and FCZ individually at their 0.5MIC and 0.25MIC concentrations decreased the cell growth in the first 2 hours. However there was an increased cell growth noted up to 24 hours. When K21 and FCZ were tested at combinations of 0.5MIC and 0.25MIC, there was a reduction in the growth of *C. albicans* (ATCC 90028) from 4 hours till 8 hours. There was a $2\log_{10}$ of CFU/mL reduction in the growth in 0.5MIC combinations of K21 and FCZ compared with killing by the most active single agent. At 0.25MIC combinations, a $2.5\log_{10}$ difference was observed compared to both K21 and FCZ alone. The negative control without the treatment showed a continuous increase in cell growth up to 24 hours. The combination of K21 and FCZ showed synergistic effects against *C. albicans* (ATCC 90028).

Figure 2.16 shows *C. albicans* (NCPF 3281) at 0.25MIC concentrations of K21 and FCZ combinations with a reduction of cell growth seen at 8 hours and an increase in cell growth at 12 hours, continuing till 24 hours. At 0.25MIC combinations, growth reduced at 4 hours with growth increasing from 12 hours to 24 hours. There was an approximate $2.8\log_{10}$ difference and $2.5\log_{10}$ difference in the viable cell counts at 0.5MIC and 0.25MIC combinations respectively, compared with the cells treated with either K21 or FCZ alone. Synergism between K21 and FCZ at both their combinations of 0.5MIC and 0.25MIC was demonstrated.

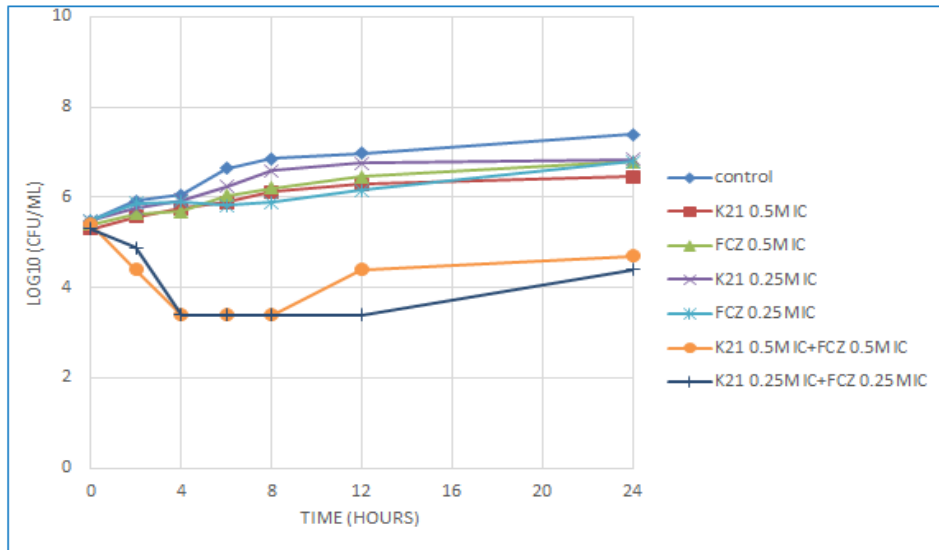


Figure 2.15: Time-kill curve of K21 and FCZ alone and in combinations against *C. albicans* (ATCC 90028).

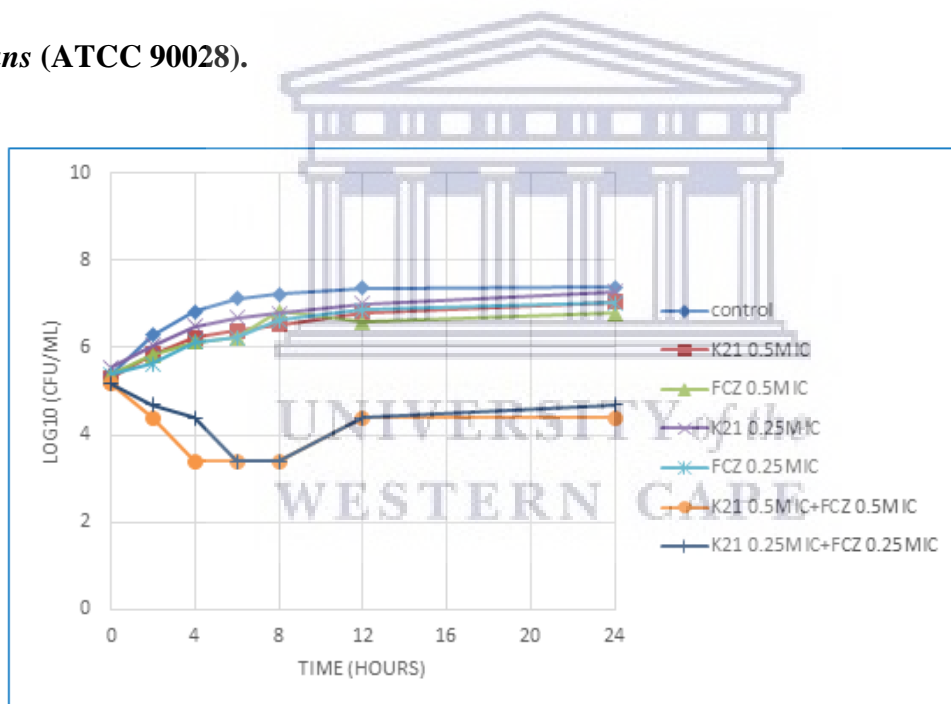


Figure 2.16: Time-kill curve of K21 and FCZ alone and in combinations against *C. albicans* (NCPF 3281).

Table 2.10 shows a 2-way ANOVA result of *C. albicans* (ATCC 90028) demonstrating a significant difference between the concentrations of K21 and FCZ alone and in combination ($p < 0.0001$).

The Tukey post hoc test located the site of significant difference between the concentrations with time (Table 2.11). At 8 hours a significant difference was shown between the control and the combinations of K21 and FCZ at 0.5MIC and 0.25MIC concentrations. At 12 hours a significant difference was noted between the control and combination of K21 and FCZ at 0.25MIC concentrations. At 12 hours a significant difference was exhibited between K21 at 0.25MIC concentration with the combination of K21 and FCZ at 0.25MIC. No significant difference was detected between any other concentrations with time.

Table 2.10: K21 and FCZ concentrations over time for *C. albicans* (ATCC 90028)

ANOVA table	Sum of Squares	DF	Mean Square	F	p value
Row Factor	42.88	6	7.147	24.06	p <0.0001
Residual	10.69	36	0.2971		

Table 2.11: K21 and FCZ concentrations relative to time for *C. albicans* (ATCC 90028)

Time	Variables	Mean diff	Significance
8 hours	Control K21 0.5MIC + FCZ 0.5MIC	3.455	p = 0.000
	Control K21 0.25MIC + FCZ 0.25MIC	3.455	
12 hours	Control K21 0.25MIC + FCZ 0.25MIC	3.568	p = 0.000
12 hours	K21 0.25MIC K21 0.25MIC + FCZ 0.25MIC	3.364	p = 0.000

Table 2.12 reveals a statistically significant result ($p < 0.0001$) between K21 and FCZ alone and in combination for *C. albicans* (NCPF 3281).

Table 2.13 displays the existence of significance across various concentrations using the Tukey post hoc test. At 4 hours significant difference was shown between the control and K21 and FCZ combinations at 0.5MIC concentrations. At 6 hours significant differences were noted between control and K21 and FCZ combinations at their 0.5MIC and 0.25MIC concentrations. Significant differences were also noted at 8 hours between the control and combinations of K21 and FCZ at 0.5MIC and 0.25MIC concentrations. FCZ at 0.5MIC concentration displayed a significant difference between 0.5MIC and 0.25MIC combinations of K21 and FCZ at 8 hours. The rest of the K21/FCZ concentrations did not show a significant difference with time.

Table 2.12: K21 and FCZ concentrations over time for *C. albicans* (NCPF 3281)

ANOVA table	Sum of Squares	DF	Mean Square	F	p value
Row Factor	52.02	6	8.670	28.04	p < 0.0001
Residual	11.13	36	0.3092		

Table 2.13: K21 and FCZ concentrations relative to time for *C. albicans* (NCPF 3281)

Time	Variables			Mean diff	Significance
4 hours	Control	K21 0.5MIC +	3.423	p = 0.000	
		FCZ 0.5MIC			
6 hours	Control	K21 0.5MIC +	3.735	p = 0.000	
		FCZ 0.5MIC			
	K21 0.25MIC +	3.735			
	FCZ 0.25MIC				
8 hours	Control	K21 0.5MIC +	3.832	p = 0.000	
		FCZ 0.5MIC			
	FCZ 0.5MIC	K21 0.25MIC +	3.832	p = 0.000	
		FCZ 0.25MIC			
	FCZ 0.5MIC	K21 0.5MIC +	3.431		
		FCZ 0.5MIC			
FCZ 0.5MIC	K21 0.25MIC +	3.431			
	FCZ 0.25MIC				



2.3.2.7.2 Synergy of *C. glabrata* (ATCC 26512) determined by time-kill assay

Figure 2.17 demonstrates the time kill curve of the combinations of K21 and FCZ plotted for FCZ-resistant *C. glabrata* (ATCC 26512). There was a steady reduction in the growth of the cells till 12 hours at 0.5MIC and 0.25MIC combinations of K21 and FCZ. A $4.5\log_{10}$ difference at 0.5MIC combinations was shown when compared to the single agent and a $5.5\log_{10}$ difference to the starting inoculum. A synergistic effect at 0.5MIC combinations of K21 and FCZ was noted. However, at 0.25MIC combinations, a $<2\log_{10}$ reduction in the cell growth was observed. There was no synergy exhibited at 0.25MIC combinations of K21 and FCZ. The control without the treatment showed steady growth up to 24 hours.

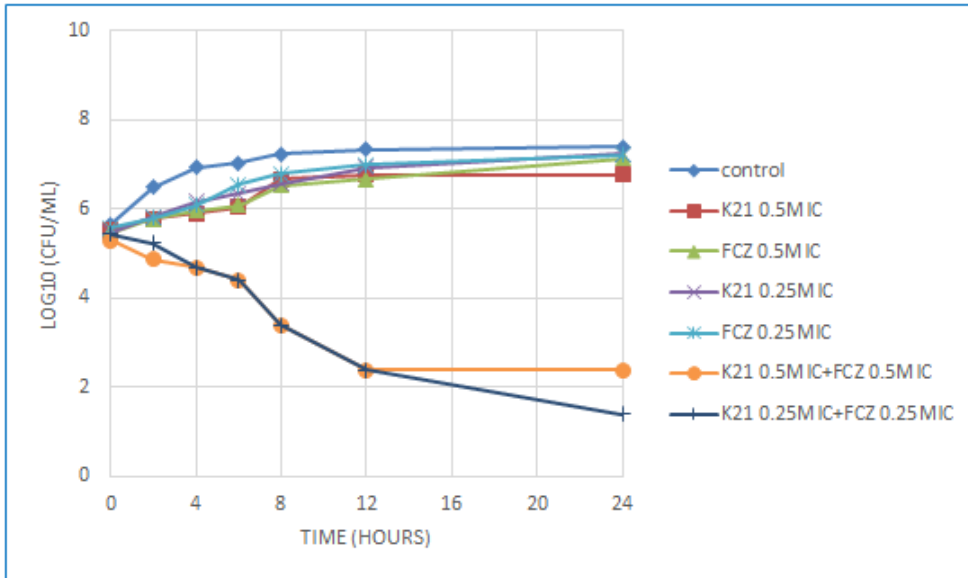


Figure 2.17: Time-kill curve of K21 and FCZ alone and in combinations for *C. glabrata* (ATCC 26512).

Table 2.14 shows a statistical significant difference for *C. glabrata* (ATCC 26512) with K21 and FCZ alone and in combination ($p < 0.0001$). The significance was noted at 24 hours between the control and the combination of K21 and FCZ at 0.5MIC concentrations. At 24 hours, a significant result was also noted between K21 0.5MIC and the combination of K21 and FCZ at 0.5MIC (Table 2.15), using the Tukey post hoc test. There was no significant difference found between any other K21/FCZ concentrations with time.

Table 2.14: K21 and FCZ concentrations over time for *C. glabrata* (ATCC 26512)

ANOVA table	Sum of Squares	DF	Mean Square	F	p value
Row Factor	66.01	6	11.00	12.30	p <0.0001
Residual	32.21	36	0.8948		

Table 2.15: K21 and FCZ concentrations relative to time for *C. glabrata* (ATCC 26512)

Time	Variables	Mean diff	Significance
24 hours	Control K21 0.5MIC + FCZ 0.5MIC	5.996	p = 0.000
24 hours	K21 0.5MIC K21 0.5MIC + FCZ 0.5MIC	5.832	p = 0.000

2.3.2.7.3 Synergy of *C. dubliniensis* (NCPF 3949a) determined by time-kill assay

C. dubliniensis (NCPF 3949a) exhibited a $4.5 \log_{10}$ difference at both 0.5MIC and 0.25MIC combinations of the drugs to their single drug concentration (Figure 2.18). At 0.5MIC combinations, there was a reduction in the viable count at 4 hours which remained constant till 12 hours and reduced at 24 hours. A reduction in viable cells was observed at 0.25MIC combinations at 8 hours, remaining so at 12 hours and 24 hours. An approximate 3log difference was observed between the combinations with the starting inoculum. K21 and FCZ at their 0.5MIC and 0.25MIC concentrations alone, showed a reduced growth till 8 hours followed by a gradual increase in the growth till 24 hours along with the control.

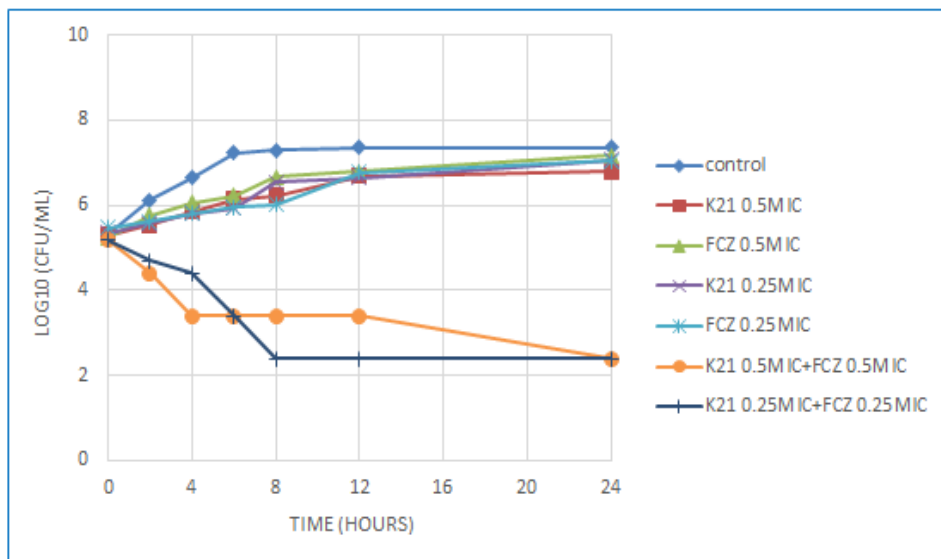


Figure 2.18: Time-kill curve of K21 and FCZ alone and in combinations for *C. dubliniensis* (NCPF 3949a).

Table 2.16 demonstrates a statistically significant result between K21 and FCZ alone and in combinations ($p < 0.0001$). A significant comparison result was found at 6 hours between the K21 0.25MIC and combinations of K21 and FCZ at 0.25MIC. A significant difference was also noted at 8 hours between the control and 0.25MIC combinations of K21 and FCZ (Table 2.17), using the Tukey post hoc test.

Table 2.16: K21 and FCZ concentrations over time for *C. dubliniensis* (NCPF 3949a)

ANOVA table	Sum of Squares	DF	Mean Square	F	p value
Row Factor	73.53	6	12.26	17.88	$p < 0.0001$
Residual	24.67	36	0.6854		

Table 2.17: K21 and FCZ concentrations relative to time for *C. dubliniensis* (NCPF 3949a)

Time	Variables		Mean diff	Significance
6 hours	K21 0.25MIC	K21 0.25MIC +	5.896	p = 0.000
		FCZ 0.25MIC		
8 hours	Control	K21 0.25MIC +	5.843	p = 0.000
		FCZ 0.25MIC		

2.4 DISCUSSION

When the FCZ-resistant *C. albicans* were treated with K21, the MIC of the species was 62.48 µg/mL with a MIC range of 31.24 µg/mL - 249.89 µg/mL. However, when treated with FCZ, the median was 256 µg/mL, with MIC ranging from 64 µg/mL - 256 µg/mL. This shows a promising antifungal effect of K21 compared to FCZ.

The majority of the *Candida* species were intermediate (n = 86) with a MIC range of 62.48 µg/mL - 124.95 µg/mL and only very few were resistant (n = 9) to K21 with a MIC value \geq 249.89 µg/mL, as determined by the susceptibility pattern. Apparently a majority of the *Candida* species were resistant (n = 103) and few were intermediate (n = 13) to FCZ. This demonstrates a major antifungal efficacy of K21 towards the FCZ- resistant *Candida* species. Moreover 48 of the *Candida* species were susceptible to K21 further highlighting the competency of the compound as a potent antifungal.

The FCZ-resistant *C. glabrata* and *C. krusei* were inhibited by K21 at a lesser concentration of 62.48 µg/mL and 124.95 µg/mL respectively, whereas with FCZ, *C. glabrata* was inhibited at a higher concentration of 256 µg/mL, with *C. krusei* inhibited at 64 µg/mL. The higher MIC concentrations could be due to the highly resistant nature of the species. It is

stated that *C. glabrata* develops resistance to FCZ after the exposure to the drug while *C. krusei* is intrinsically resistant to FCZ (Tercas *et al.*, 2017).

An *in vitro* study conducted by Calabrese *et al.*, (2013), established the antifungal activity of twoazole compounds CPA18 (1-(1-(biphenyl-4-yl)-3-(4-fluorophenyl)propan-2-yl)-1H-imidazole and CPA109 (1-(1-(biphenyl-4-yl)-3-(5-chlorothiophen-2-yl)propan-2-yl)-1H-imidazole against FCZ-susceptible and -resistant *C. albicans* strains. The fungicidal activities of the compound were explained as the secondary actions within the *C. albicans* cells that were not assigned by FCZ. Another study using a metal based drug such as a derivative of 1, 10-phenanthroline compounds, FEN ((1)-N-2-Methoxybenzyl-1, 10-phenanthroline Bromide), showed a MIC of 0.39 $\mu\text{g/mL}$ - 1.56 $\mu\text{g/mL}$ against *C. albicans* tested by the broth microdilution assay (Setiawati *et al.*, 2017).

The FCZ-susceptible *C. dubliniensis* showed a MIC range of 0.03 $\mu\text{g/mL}$ - 0.50 $\mu\text{g/mL}$ when treated with FCZ with the MIC for K21 established as 62.48 $\mu\text{g/mL}$. A study by Polacheck *et al.*, (2000) conducted on an Irish population reported the presence of *C. dubliniensis* in 26% of HIV-infected and 32% of AIDS patients with oral candidiasis. This demonstrates the increasing frequency of *C. dubliniensis* infections and the requirement of novel antifungal compounds in their treatment.

Even though *C. tropicalis* was considered difficult to treat (Barchiesi, 2000), their MIC was obtained at the lowest concentration of K21. However, FCZ exhibited its antifungal effect towards the species with a MIC range of 1.00 $\mu\text{g/mL}$ - 2.00 $\mu\text{g/mL}$. K21, with its unique antimicrobial properties towards various microorganisms, could be considered as a good candidate to overcome multi-drug infections.

Shinobu-Mesquita *et al.*, (2015) demonstrated an antifungal activity of hydroalcoholic extracts from *Sapindus saponaria*, with higher concentrations of the extract. In their study, the growth of *C. glabrata* and *C. tropicalis* was inhibited at MIC₅₀ of 780 $\mu\text{g/mL}$ and *C. albicans* was

inhibited at MIC₅₀ of 1560 µg/mL. Hence the higher MIC values of K21 in contrast to FCZ may not be limiting the use of K21 in managing fungal infections. Furthermore, K21 exhibited excellent antifungal activity in all the FCZ-resistant species in the study with lower a MIC compared to FCZ with a higher MIC of 256 µg/mL.

An *in vitro* study on bis (alkylpyridinium) alkanes established the fungicidal activity of the compounds potentially useful against common as well as more resistant emerging fungi (Chen *et al.*, 2010). A novel antifungal small molecule, SM21 inhibited the growth of *C. albicans*, *C. glabrata*, *C. krusei* with MIC values ranging from 0.2 µg/mL - 1.6 µg/mL (Wong *et al.*, 2014). Aminopiperidine derivatives demonstrated its antifungal effect by inhibiting the ergosterol biosynthesis of azoles in the C - 14 reduction catalyzed by Erg24p (Hata *et al.* 2010).

The present study relates to the study conducted by Aher (2014) that reports increased azole resistance in NAC species as compared to *C. albicans*. Since no susceptibility breakpoints have previously been reported for K21 against *Candida*, it was established that K21 inhibited the growth of all the FCZ-resistant and FCZ-intermediate *Candida* species with the MIC ranging from 31.24 µg/mL - 249.89 µg/mL and FCZ-susceptible *Candida* species with MIC ranging from 31.24 µg/mL - 62.48 µg/mL.

Resistance to FCZ may occur via the acquisition of a new resistant genotype of *C. albicans* or by the resistance emerging in a previously susceptible strain. Since oral candidiasis is an opportunistic infection in HIV-infected individuals, administration of appropriate drugs in the right proportions could prevent the possible occurrence of more resistant strains thus reducing infection and improving their quality of life.

In the combination therapy, the individual MIC concentrations of K21 and FCZ were drastically reduced to lower concentrations. Moreover, *C. dubliniensis* (NCPF 3949a), *C. tropicalis* (ATCC 950) and *C. lusitaniae* (ATCC 34449) exhibited definite synergism

between K21 and FCZ with Σ FICI values of 0.28, 0.26 and 0.25 respectively. The highlight of the study was that none of the strains exhibited antagonism. Even though Σ FICI displayed indifference between the combined MICs of K21 and FCZ for *C. albicans* (ATCC 90028 and NCPF 3281), the time-kill assay displayed synergism between them. There was also a significant difference observed along the concentrations over time.

K21 was identified as a fungicidal compound with a rapid activity at 2 hours against the susceptible *C. albicans* (ATCC 90028) and the resistant *C. glabrata* (ATCC 26512) determined by time-kill assay. However there was an increase in cell growth at 0.5MIC and 0.25MIC. The time-kill assay recognizes the count of the viable cells and determines the fungistatic or fungicidal effect of the drug on the cell growth, thus analysing the interaction between the drug and the *Candida* cells and the relationship between the concentration and activity over time (Klepser *et al.*, 1997).

A novel antimicrobial compound with a fast acting mechanism may be well accepted in this era of actively developing resistant species. Moreover, treatment of fungal infections with newer antimicrobial agents or a combination of antimicrobial therapies has become progressively dominant in the eradication of these infections due to the presence of the existing antimicrobial resistance among the *Candida* species to the current antifungal drugs. The ongoing inflation in the antifungal resistance re-sounds the need for novel, effective, non-toxic drugs for the complete eradication of the species. A thorough need for a better integration of old and new diagnostics and a well-designed strategy for antifungal management are imperative.

CHAPTER 3

MODE OF ACTION OF K21 AS OBSERVED BY ELECTRON MICROSCOPY

3.1 INTRODUCTION

The present chapter describes the changes in the ultrastructure of *Candida* cell morphology due to the action of K21 using scanning electron microscopy and transmission electron microscopy. The study also determines the mode of action and target of K21 on *Candida* species by demonstrating the expression pattern of Sap 1 - Sap 3 and Sap 4 - Sap 6 proteins using polyclonal antibodies specifically directed against Sap 1-3 and Sap 4-6, using post-embedding immunogold labelling.

3.2 MATERIALS AND METHODS

The strains included in the electron microscopy were *C. albicans* (ATCC 90028), *C. krusei* (ATCC 2159), *C. glabrata* (ATCC 26512), *C. dubliniensis* (NCPF 3949a) and *C. tropicalis* (ATCC 950). *C. albicans* (ATCC 90028), *C. krusei* (ATCC 2159) and *C. glabrata* (ATCC 26512) were included in the scanning electron microscopy. While the strains included in transmission electron microscopy and post-embedding immunogold labelling were *C. albicans* (ATCC 90028), *C. dubliniensis* (NCPF 3949a) and *C. tropicalis* (ATCC 950) due to their proteolytic activity.

3.2.1 Scanning electron microscopy

Scanning electron microscopy was performed by the standard protocol (Serpa *et al.*, 2012).

A Checkerboard assay was performed according to the Clinical and Laboratory Standards Institute M27A2 and M27A3 approved standard protocol (CLSI, 2002; 2008). The *Candida* species were treated with K21 alone, FCZ alone and K21 + FCZ (refer to Chapter 2, section 2.2.5.2). The concentration range of K21 in row A was 0.49 µg/mL - 249.89 µg/mL and for FCZ in Row C was 0.12 µg/mL - 64 µg/mL. For *C. albicans* (ATCC 90028), the concentration of K21 was 31.24 µg/mL, FCZ was 8 µg/mL and K21 + FCZ was 15.62 µg/mL + 4 µg/mL respectively. For *C. krusei* (ATCC 2159) and *C. glabrata* (ATCC 26512), the concentration of K21 was 31.24 µg/mL, FCZ was 32 µg/mL and K21 + FCZ was 31.24 µg/mL + 8 µg/mL respectively.

Following the checkerboard assay, 200 µL of the samples from 0.5MIC wells of K21, FCZ and K21 + FCZ were transferred to individual sterile Eppendorf tubes at 2 hours, 4 hours, 6 hours and 24 hours. The cells were harvested by centrifugation at 5000 x g for 10 minutes to obtain the microbial pellet. The supernatant was discarded. The microbial pellets were washed with 0.1M PBS (pH 7.4) three times for 5 minutes and the supernatant was discarded. Microbial cell pellets were chemically fixed in 2.5% glutaraldehyde (Catalogue no: G5882, Sigma Aldrich, South Africa) in PBS for 30 minutes, after which the fixative was removed by washing the pellets first in PBS and then in distilled water twice, for 5 minutes each, discarding the supernatant after every wash. The microbial pellets were dehydrated by re-suspending in a series of graded ethanol washes, namely, 50%, 70%, 90% (diluted in water) and 100% ethanol for 10 minutes each.

Following dehydration in 100% ethanol, the pellets were mounted on a carbon coated aluminium stub to be placed in the critical point dryer to remove any remnants of ethanol.

The *Candida* cells were sputter coated with gold-palladium for 60 seconds using a Quorum Q150T ES sputter coater system, and their morphology imaged using a Zeiss Auriga field-emission scanning electron microscope (FE-SEM) operated at 5 kV (Figure 3.1).

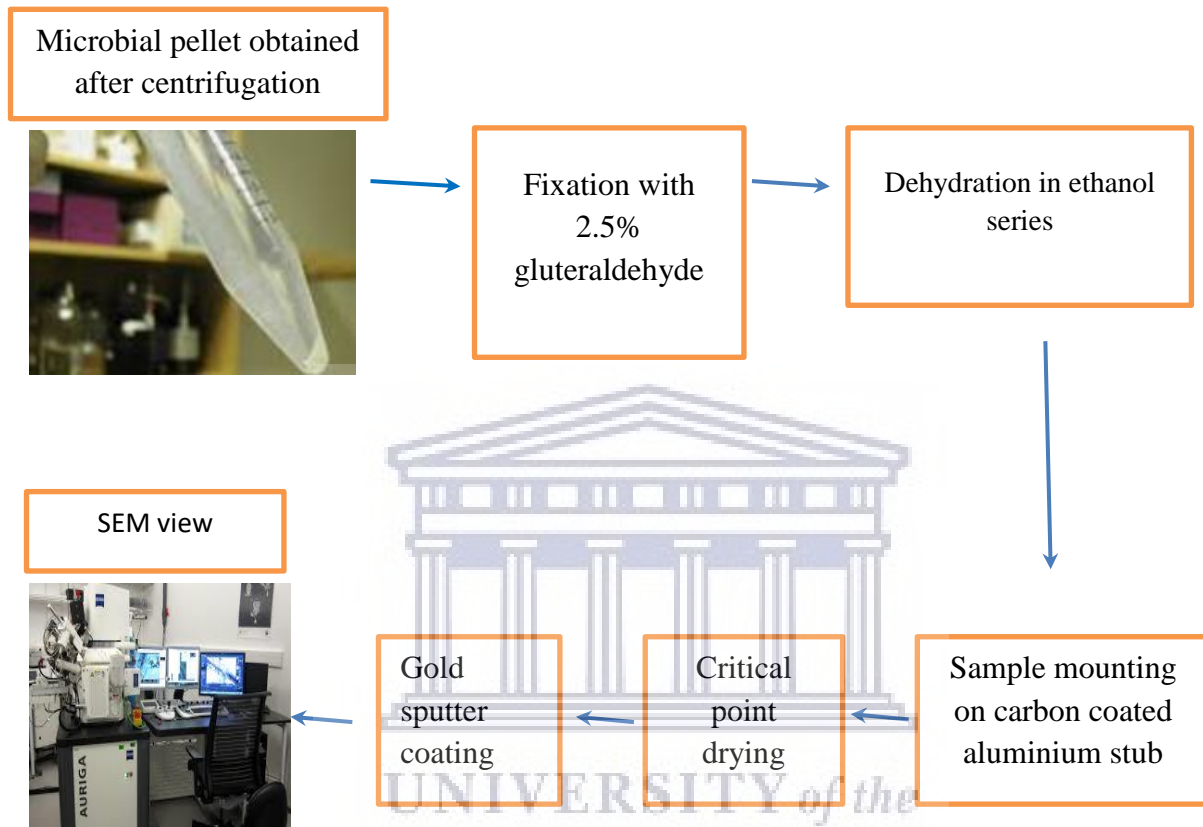


Figure 3.1: Diagrammatic representation of Scanning electron microscopy

3.2.2 Transmission electron microscopy

Transmission electron microscopy was performed according to the protocol by Kumar and Filippi (2016).

Following the incubation of the checkerboard assays described above, 800 μL of the samples at 2 hours, 4 hours, 6 hours and 24 hours from 0.5MIC wells of K21 (31.24 $\mu\text{g}/\text{mL}$) were

transferred to individual sterile Eppendorf tubes. The cells were harvested by centrifugation at 5000 x g for 10 minutes to obtain a microbial pellet and the supernatant discarded.

The microbial pellets were washed with 0.1M PBS (pH 7.4) buffer three times for 5 minutes, the supernatant discarded and the microbial cell pellets fixed in Karnovsky solution for overnight fixation. Karnovsky solution was prepared by adding 4 mL of 10% formaldehyde + 0.2 mL of 25% glutaraldehyde (Catalogue no. G5882, Sigma Aldrich, South Africa) in 1 mL of PBS 10x and diluted with distilled water to make up to 10 mL. Post fixation, the fixative was removed by washing the pellets in PBS buffer first and then in distilled water twice for 5 minutes each. The supernatant was discarded after every wash leaving the pellets suspended in 30 μ L of buffer.

The pellets were suspended in an equal amount (30 μ L) of low melting agarose (Catalogue no. A4018, Sigma Aldrich, South Africa) in distilled water and centrifuged in Eppendorf tubes at 1000 x g for 2 minutes, after which they were transferred to a box of ice for 30 minutes to solidify the agarose. Once the agarose was set, the pellets were removed from the Eppendorf tubes, sectioned with a scalpel and 1 mm size sections were suspended in PBS buffer. This was followed by 2 washes in water for 2 minutes each, followed by dehydration with ethanol (30%, 50%, 70%, 80%, 90%, 95%) for 5 minutes each and twice in 100% ethanol for 10 minutes. The pellets were embedded in a mixture of 50:50 of LR White (Catalogue no. L9774, Sigma Aldrich, South Africa) and ethanol, followed by 25:75 of LR White and ethanol and finally in 100% LR White. After embedding, 80 nm thick ultrathin sections were cut and mounted on nickel grids (Catalogue no. G5526, Sigma Aldrich, South Africa).

3.2.2.1 Double contrast staining of ultrathin sections

The grids with the cell sections were floated on drops of water on parafilm for 5 minutes, followed by staining with 2% uranyl acetate (Catalogue no. AGR1260A, Agar Scientific, UK) for 5 minutes and 2% lead citrate (Reynolds, 1963) for 5 minutes. The grids were examined using a FEI Tecnai 20 transmission electron microscope (FEI, Eindhoven, Netherlands) operating at 200 kV (Lab6 emitter) and fitted with a Gatan Tridiem energy filter and Gatan CCD camera (Gatan, UK) at magnifications of between 8000X and 34000X.

3.2.2.2 Immunogold labelling

Post embedding immunogold labelling was performed according to the protocol by Schaller *et al.*,(1999b). The sample preparation, fixation and dehydration with ethanol series were performed as above (Section 3.2.2).

A stock solution of 2 x BSA-PBS was prepared by adding 4 g of BSA-PBS (19.55 g) powder (Catalogue no. P3688, Sigma Aldrich, South Africa) in 100 mL water. 1 % BSA-PBS was prepared by 5 mL of stock solution + 5 mL water.

The immunogold labelling was carried out by placing the grids on two sheets of parafilm (Catalogue no. P7543, Sigma Aldrich, South Africa), one for Sap 1-3 antibody and the other for Sap 4-6 antibody. Immunogold labelling was individually performed on two sheets of parafilm with the grids as follows:

The grids were floated on drops of water for 5 minutes and then floated on 0.02M glycine (Catalogue no. 410225, Sigma Aldrich, South Africa) in PBS twice for 5 minutes (Figure 3.2), blocked with blocking buffer (5 mL stock solution + 0.5 mL of 0.5% FSG (Catalogue

no. G7765, Sigma Aldrich, South Africa) in 4.5 mL PBS), twice for 5 minutes, followed by washing in 0.1% BSA-PBS (0.5 mL stock solution in 9.5 mL PBS) twice for 5 minutes. The grids were then incubated with the anti-Sap polyclonal rabbit antibodies directed against Sap 1-3 (α -Sap 2) and Sap 4-6 (α -Sap 6F) diluted 1:100 in PBS supplemented with 5 mL stock solution + 0.1 mL of 0.1% TWEEN 20 (Catalogue no: P1379, Sigma Aldrich, South Africa) in 4.9 mL water, for overnight fixation at 4° C on their respective places on the parafilms (Figure 3.3).

After washing with 0.1% BSA-PBS, five times for 5 minutes, grids on both the parafilms were then incubated with 10 nm gold-conjugated goat anti-rabbit IgG (Catalogue no: G7402, Sigma Aldrich, South Africa) diluted 1:50 in 1% BSA-PBS for 1 hour at room temperature. Washing with 0.1% BSA-PBS, five times for 2 minutes was followed by 5 X 2 minute washes with PBS, fixation with 1% glutaraldehyde in PBS for 5 minutes, followed by 5 X 1 minute washes with PBS and 5 X 1 minute washes with water. This was followed by staining of the grids with 2% uranyl acetate and 2% lead citrate for 5 minutes each. The grids were examined using a FEI Tecnai 20 transmission electron microscope (FEI, Eindhoven, Netherlands) operating at 200 kV (Lab6 emitter) and fitted with a Gatan Tridiem energy filter and Gatan CCD camera (Gatan, UK) at magnifications between 8000X and 34000X. The anti-Sap polyclonal antibodies served as positive controls while in negative control cells the anti-Sap polyclonal antibodies were omitted.

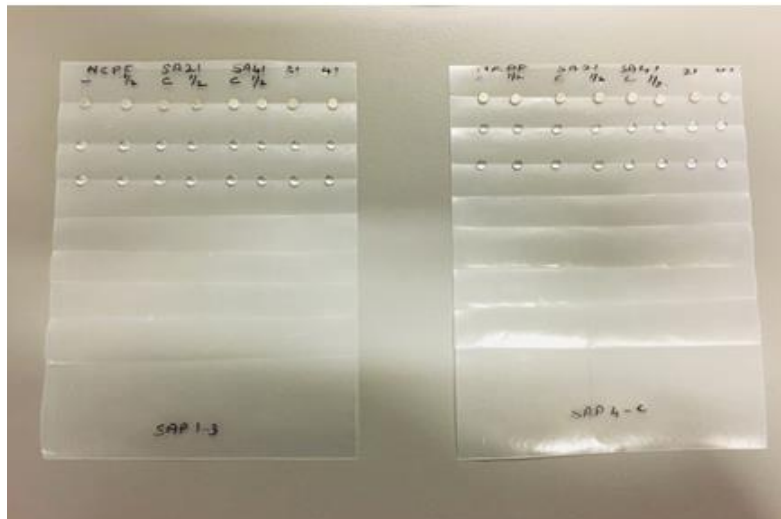


Figure 3.2: Post-embedding immunogold labelling. Nickel grids with the cells float on drops of water, followed by drops of glycine in two rows. The grids are on their respective parafilms for Sap 1-3 and Sap 4-6.

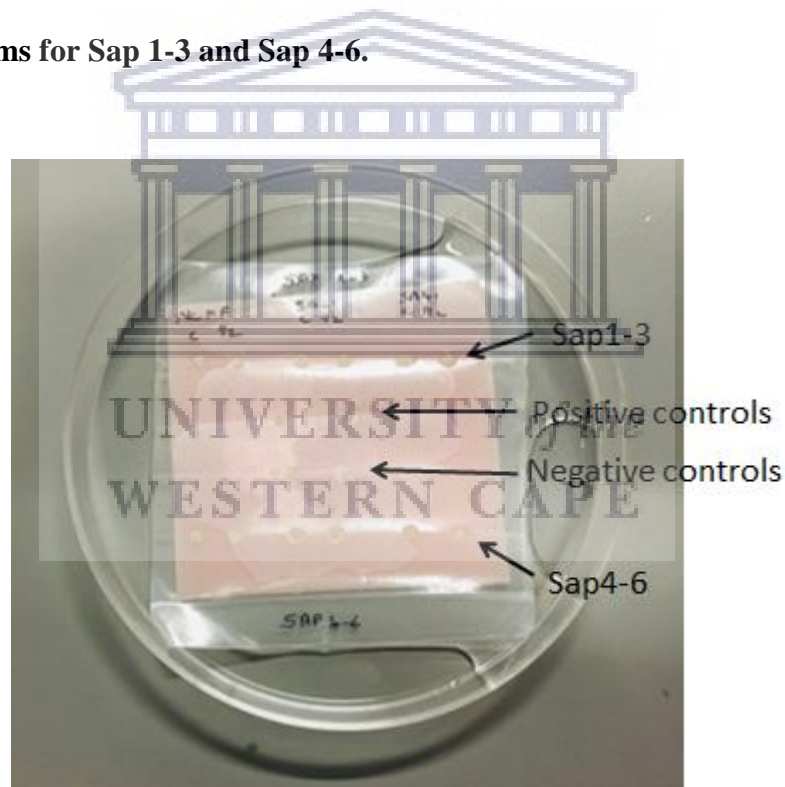


Figure 3.3: Primary antibody fixation. The nickel grids are floated on anti-Sap polyclonal antibodies directed against Sap 1-3 (first row) and Sap 4-6 (last row). Middle two rows formed the positive control and negative control respectively. The parafilm was placed in a plastic dish on a wax sheet with water supporting the parafilm in order to prevent the grids from drying, before placing for overnight fixation at 4°C.

3.3 RESULTS

3.3.1 Scanning electron microscopy

3.3.1.1 Cell surface changes following K21 exposure

C. albicans (ATCC 90028)

The untreated *C. albicans* (ATCC 90028) cells appeared round with smooth surfaces and polar bud scars (Figure 3.4 A). Some of the cells showed signs of budding into two daughter cells. After 2 hours exposure to K21 (31.24 µg/mL), some of the *Candida* cells began to show morphological changes while others remained as smooth cells (Figure 3.4 B). The cells were connected to each other by thin white threads and cell surfaces showed sparse extracellular vesicles.

Following 4 hours exposure to K21 (Figure 3.4 C), the *Candida* cells appeared elongated. There was a significant increase in extracellular material on the cell surface, and the cell surface appeared wrinkled and convoluted. The bud scars were placed without polar end positioning. At 6 hours (Figure 3.4 D), the cells appeared shrunken and deformed. More pronounced distortion of cells was observed with flocculent extracellular materials on the cell surface and extracellular vesicles which varied in size. Budding of the cells was disrupted and the cell surfaces appeared convoluted with cracks and depressions or holes.

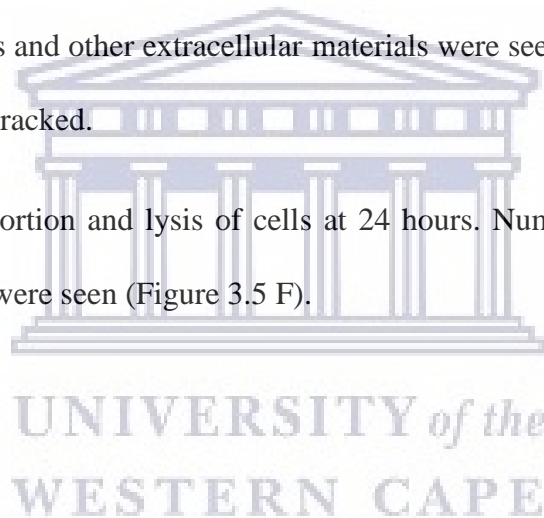
Following 24 hours exposure to K21 (Figure 3.4.E and F), there was complete distortion of the cells leading to cell lysis. There were cell remnants and abundant flocculent extracellular vesicles released by the lytic cells.

***C. krusei* (ATCC 2159)**

The control cells of *C. krusei* (ATCC 2159) possessed a slightly elongated shape compared to the usual round cells of *C. albicans*. The cells showed smooth cell surfaces with polar bud scars (Figure 3.5 A). *C. krusei* (ATCC 2159) was treated with K21 (31.24 µg/mL) and after 2 hours, the presence of white extracellular material was observed over the cells (Figure 3.5 B).

After 4 hours exposure, the cells appeared desiccated with multiple bud scars on some cells. An increase in extracellular materials was observed (Figure 3.5 C and D). Following 6 hours of treatment with K21, *C. krusei* exhibited a distorted appearance (Figure 3.5 E). The cell surface appeared highly convoluted. The multiple bud scars were not confined to the polar region. Flocculent deposits and other extracellular materials were seen on the cell surface and some cells were severely cracked.

K21 caused complete distortion and lysis of cells at 24 hours. Numerous cellular remnants and extracellular vesicles were seen (Figure 3.5 F).



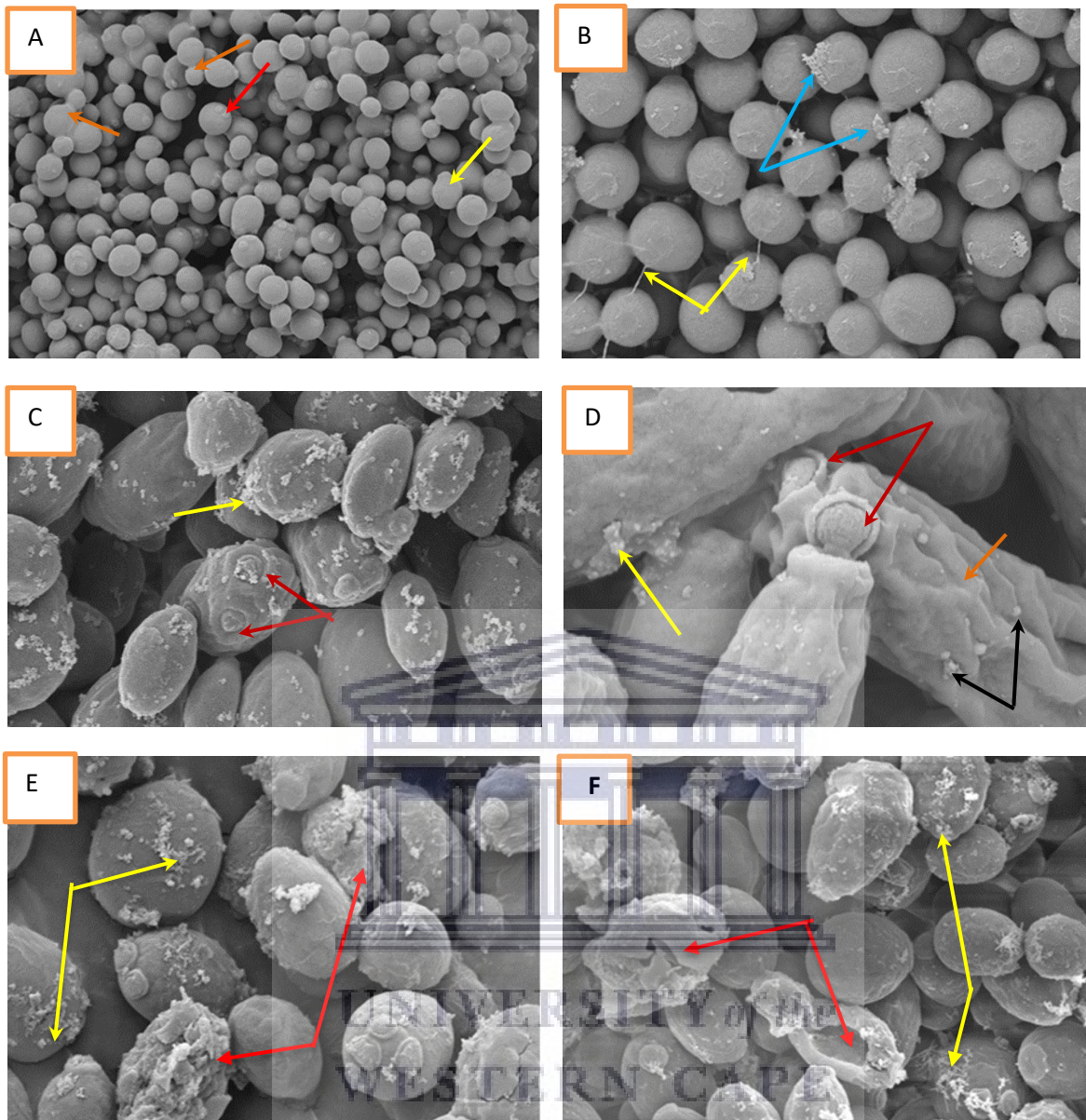


Figure 3.4: Scanning micrographs of *C. albicans* (ATCC 90028) without treatment (A) and after 2, 4, 6 and 24 hours exposure to K21 (B-F). (A) Budding yeast cells (orange arrows) with round and smooth cell surfaces (yellow arrow) and polar buds (red arrow) viewed at 2.00 K X magnification. After 2 hours (B), the cells appeared to be connected with thin white bands (yellow arrows) with sparse extracellular vesicles (blue arrows) on the cell surface viewed at 2.00 K X magnification. After 4 hours (C), cell surfaces appeared wrinkled, with increased extracellular materials (yellow arrow) and bud scars not confined to polar end positioning (red arrows) viewed at 10.00 K X magnification. After 6 hours (D), cell surface depression and convoluted cell surfaces (orange arrow) and flocculent extracellular materials (yellow arrow) as well as disrupted budding (red arrows) with extracellular vesicles of various sizes (black arrows) viewed at 20.00 K X magnification. After 24 hours (E and F), cells were distorted and lysed (red arrows) with heavy deposits of extracellular vesicles (yellow arrows), viewed at 11.10 K X and 10.00 K X magnifications respectively.

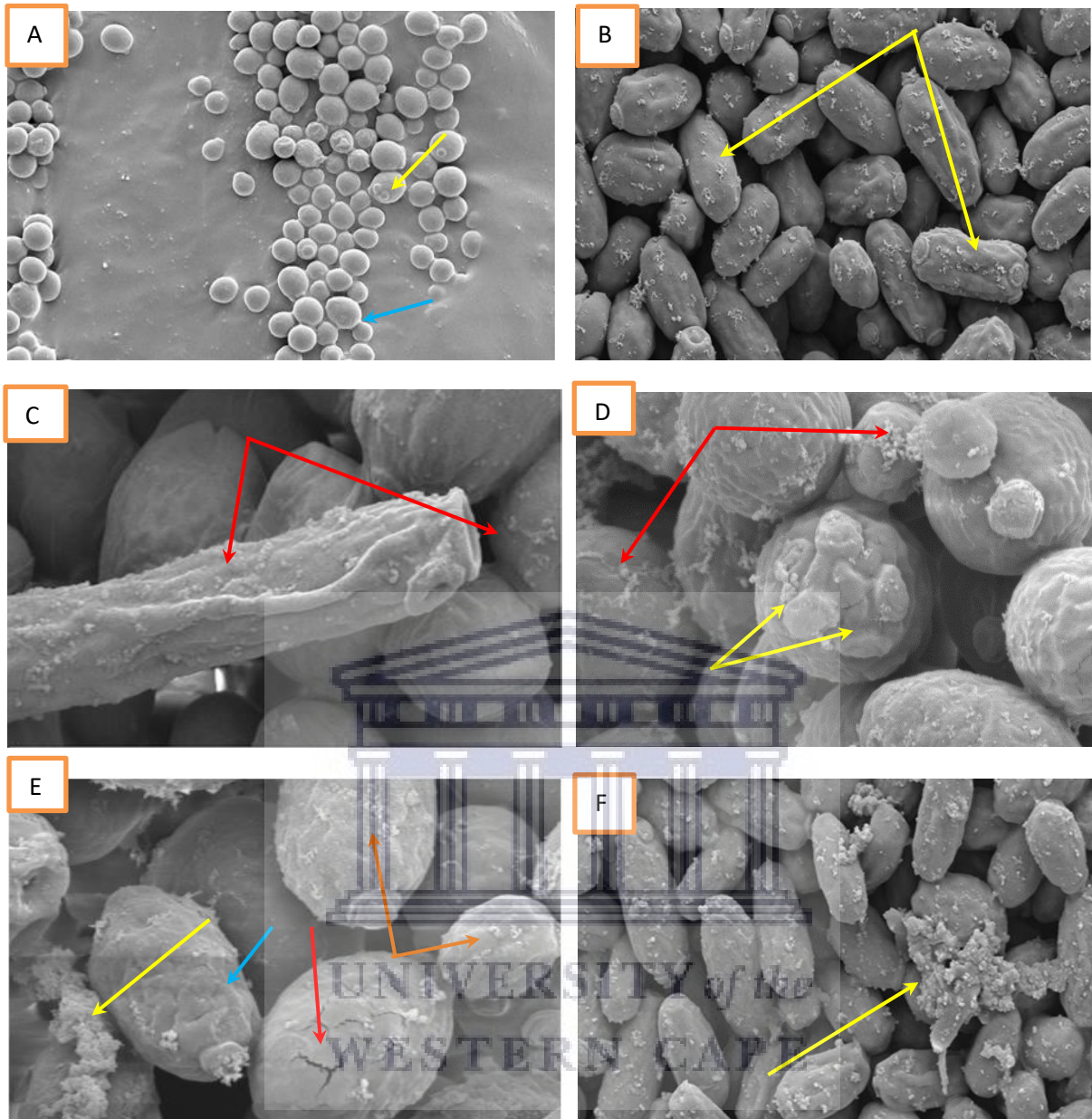


Figure 3.5: Scanning micrographs of *C. krusei* (ATCC 2159) without treatment (A) and after 2, 4, 6 and 24 hours exposure to K21 (B-F). (A) Smooth cells with polar bud scars (yellow arrow) and actively budding cells observed (blue arrow) viewed at 2.00 K X magnification. After 2 hours (B) extracellular vesicles (yellow arrows) were present over the elongated cells, viewed at 5.00 K X magnification. After 4 hours (C and D), Elongated cells with extracellular vesicles (red arrows) and multiple polar buds (yellow arrows) viewed at 10.00 K X and 20.00 K X magnifications respectively. After 6 hours (E), cracked cell (red arrow) with convoluted surfaces (blue arrow) and abundant extracellular vesicles (yellow arrow), with some sparse flocculent deposits (orange arrows) viewed at 20.00 K X magnification. After 24 hours (F) complete distortion of cells with masses of extracellular vesicles and cellular remnants (yellow arrow) viewed at 5.00 K X magnification.

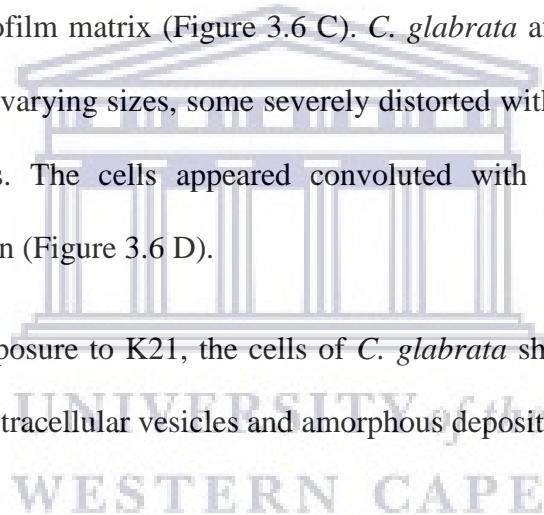
***C. glabrata* (ATCC 26512)**

Untreated cells of *C. glabrata* (ATCC 26512) appeared as round cells with smooth cell surface similar to the *C. albicans*. The cells showed bud scars at the poles with the budding process giving rise to the daughter cells (Figure 3.6 A).

After treatment with K21 (31.24 µg/mL) for 2 hours, some of the cells appeared swollen with an increase in the size of the cells. Sparse extracellular vesicles were present on the cell surfaces (Figure 3.6 B).

At 4 hours, the cell surfaces appeared cracked and desiccated with bud scars and flocculent materials resembling a biofilm matrix (Figure 3.6 C). *C. glabrata* after 6 hours of treatment with K21 showed cells of varying sizes, some severely distorted with some flocculent matter and extracellular vesicles. The cells appeared convoluted with multiple bud scars not confined to the polar region (Figure 3.6 D).

Finally, after 24 hours exposure to K21, the cells of *C. glabrata* showed cell distortion and cell lysis with abundant extracellular vesicles and amorphous deposits (Figure 3.6 E and F).



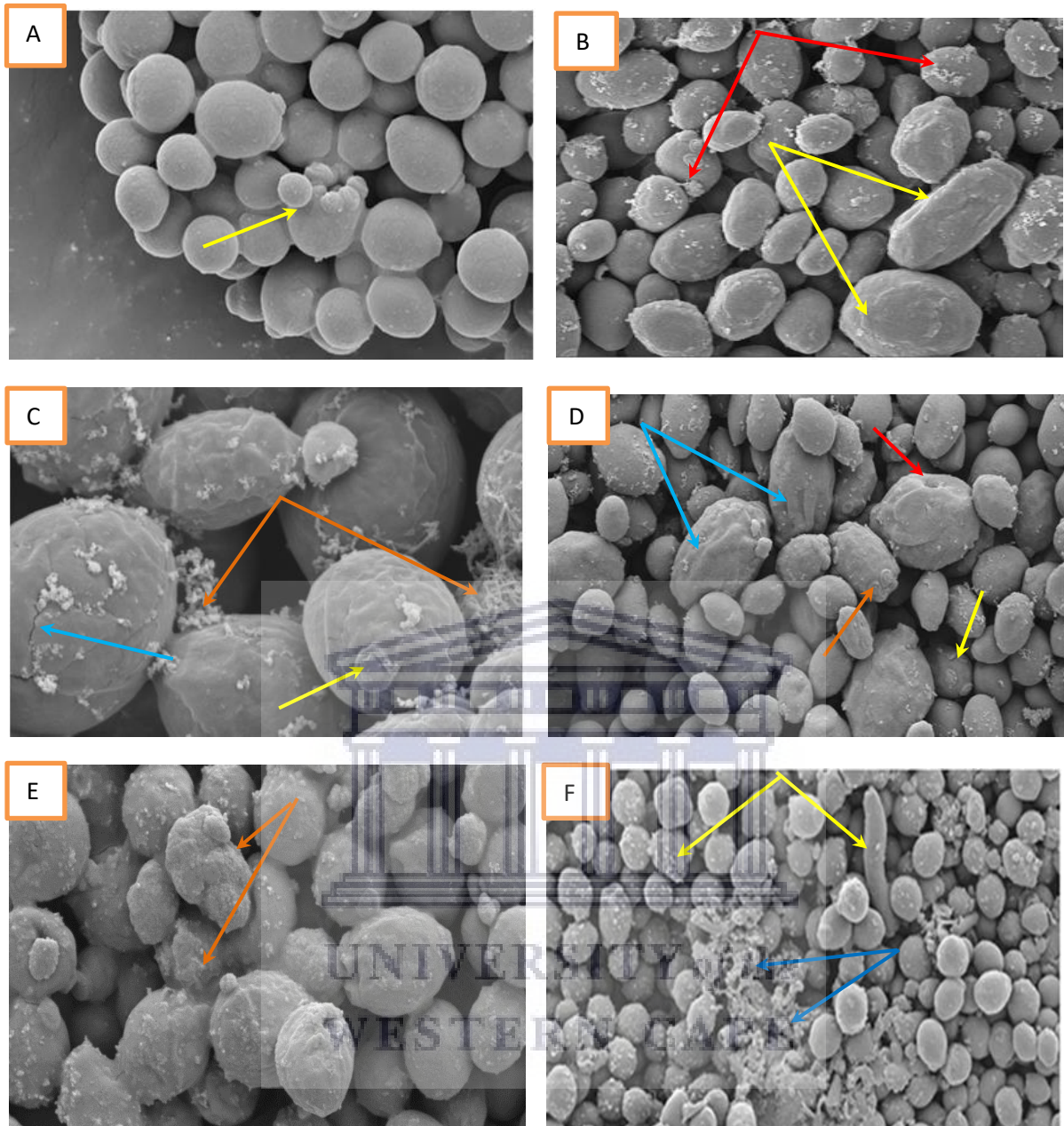


Figure 3.6: Scanning micrographs of *C. glabrata* (ATCC 26512) without treatment (A) and after 2, 4, 6 and 24 hours exposure to K21 (B-F). (A) Round smooth cells showing budding (yellow arrow) viewed at 5.00 K X magnification. After 2 hours (B) Cells appeared swollen (yellow arrows) with extracellular vesicles (red arrows) viewed at 2.00 K X magnification. After 4 hours (C) Flocculent extracellular vesicles (orange arrows) seen over the cracked (blue arrow) cell surface with presence of polar bud scars (yellow arrow) viewed at 20.00 K X magnification. After 6 hours (D) Cells showed variable morphology (blue arrows), with cavitation (red arrow) and multiple bud scars (orange arrow) not confined to the polar region (yellow arrow) viewed at 5.00 K X magnification. Some flocculent matter and tiny extracellular vesicles were present. After 24 hours (E and F), cells appeared distorted (orange arrows) along with cells of various shapes and sizes (yellow arrows) amidst a matrix of extracellular vesicles (blue arrows) viewed at 5.00 K X and 2.00 K X magnification respectively.

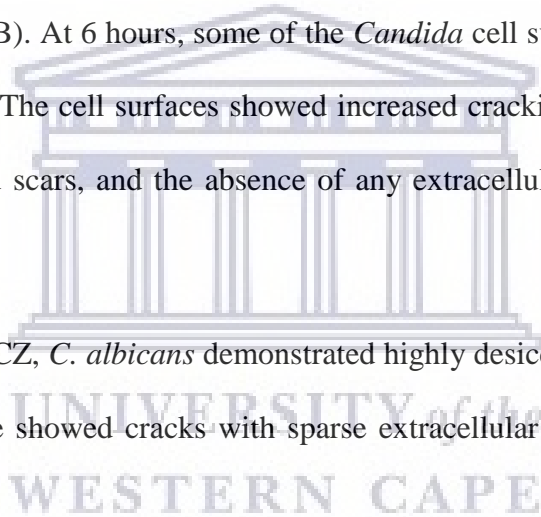
3.3.1.2 Cell surface changes following FCZ exposure

C. albicans (ATCC 90028)

The *C. albicans* (ATCC 90028) were treated with FCZ at (8 µg/mL), and at 2 hours, the surface of the cells appeared rough and shrunken with changes in morphology when compared to the smooth and round untreated cells. Cells were elongated with convoluted surfaces and bud scars were evident along with sparse extracellular vesicles (Figure 3.7 A).

At 4 hours treatment with FCZ, *Candida* cells exhibited a desiccated appearance, evidenced by the appearance of cracked and shrunken cells and the presence of multiple polar bud scars on some cells (Figure 3.7 B). At 6 hours, some of the *Candida* cell surfaces treated with FCZ exhibited deep cavitation. The cell surfaces showed increased cracking and shrinkage. Some cells showed multiple bud scars, and the absence of any extracellular materials (Figure 3.7 C).

At 24 hours exposure to FCZ, *C. albicans* demonstrated highly desiccated distorted cells with cell lysis. The cell surface showed cracks with sparse extracellular vesicles and polar buds (Figure 3.7 D).



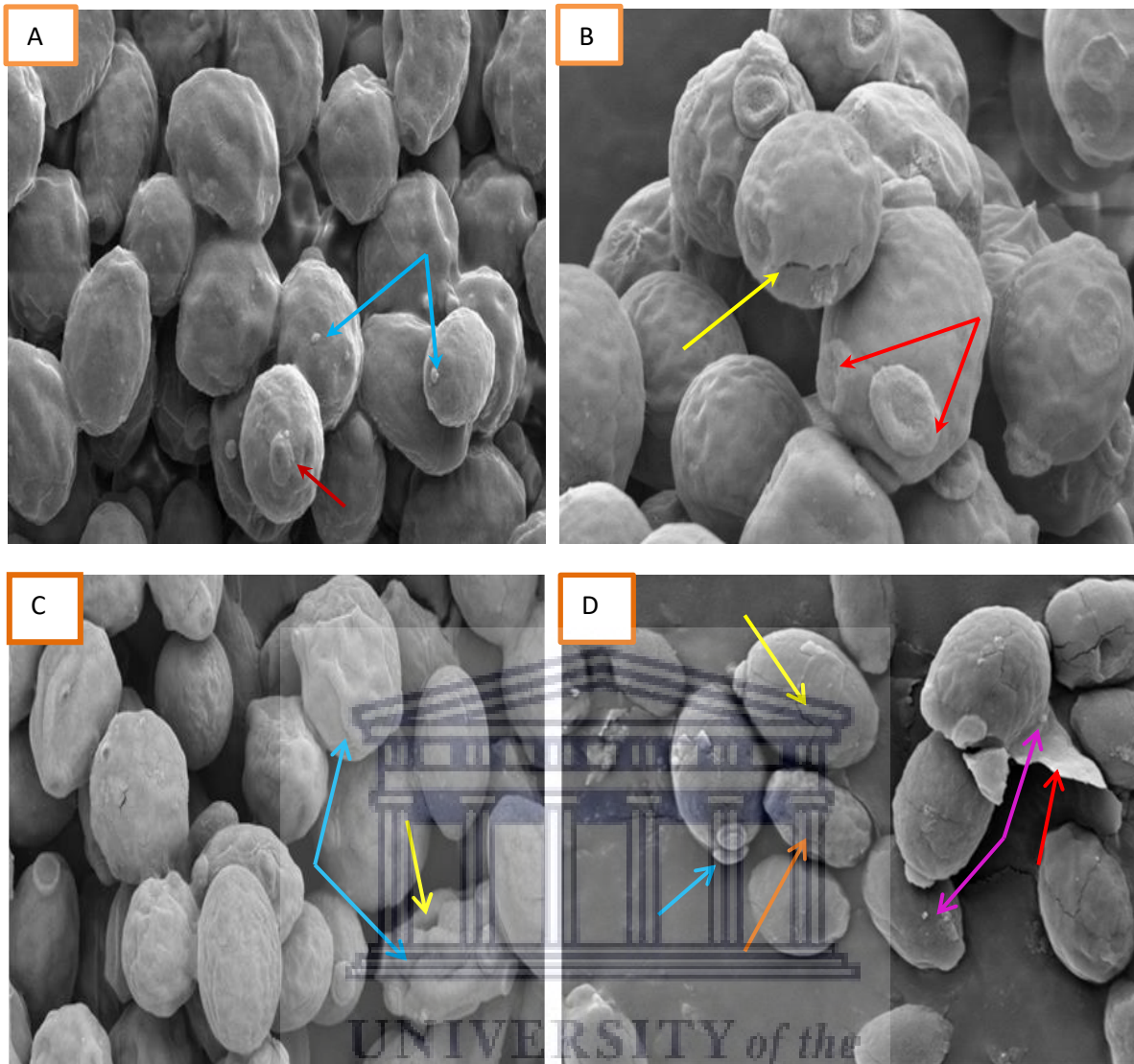


Figure 3.7: Scanning micrographs of *C. albicans* (ATCC 90028) treated with FCZ at 2, 4, 6 and 24 hours. At 2 hours (A) Cells appeared shrunken and wrinkled with bud scars (red arrow) and sparse extracellular vesicles (blue arrows) viewed at 5 K X magnification. At 4 hours (B) Desiccated cells with cracks on the cell surface (yellow arrow) and multiple bud scars on some cells (red arrows) viewed at 10.00 K X magnification. At 6 hours (C) Shrunken distorted cells (blue arrows) with deep cavitation (yellow arrow) on cell surface, viewed at 5 K X magnification. At 24 hours treatment (D) Cracked (yellow arrow) and lysed (red arrow) *Candida* cells with sparse extracellular vesicles (pink arrows). Some cells are distorted (orange arrow) and others are with polar buds (blue arrow) viewed at 10.00 K X magnification.

***C. krusei* (ATCC 2159)**

At 2 hours exposure of *C. krusei* (ATCC 2159) to FCZ (32 µg/mL), the cells appeared wrinkled with a rough convoluted cell surface (Figure 3.8 A). Sparse extracellular vesicles and bud scars were also observed.

At 4 hours, the cell surfaces of *C. krusei* appeared highly convoluted and shrunken. There were cracks on some cells with multiple bud scars (Figure 3.8 B). At 6 hours, the cells were desiccated and shrunken, demonstrating deep furrows and cavitations. Cell morphology was completely distorted (Figure 3.8 C).

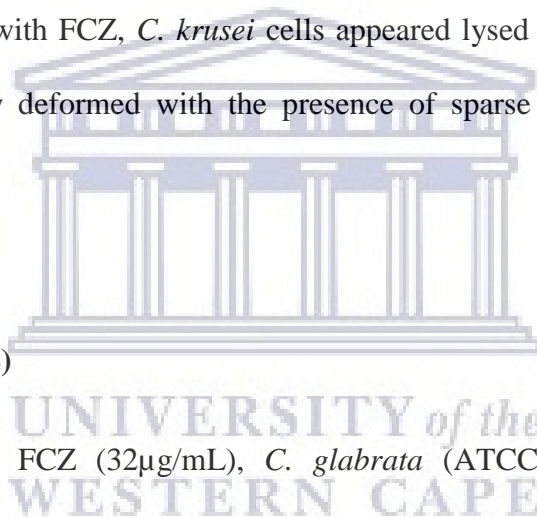
After 24 hours treatment with FCZ, *C. krusei* cells appeared lysed and desiccated. Some of the cells were completely deformed with the presence of sparse amount of extracellular vesicles (Figure 3.8 D).

***C. glabrata* (ATCC 26512)**

On 2 hours exposure to FCZ (32µg/mL), *C. glabrata* (ATCC 26512) cells appeared desiccated with mildly deformed, slightly shrunken and wrinkled, with bud scars (Figure 3.9 A).

At 4 hours, the cell surfaces appeared desiccated with deep cracks. Multiple bud scars appeared to be damaged and not confined to the polar region of cells (Figure 3.9 B). At 6 hours of exposure to FCZ, the cells were completely distorted and shrunken with sparse extracellular vesicles. Some cells had undergone lysis (3.9 C).

A 24 hour treatment with FCZ resulted in the distortion and lysis of the *C. glabrata* cells. There was a presence of sparse extracellular vesicles (Figure 3.9.D).



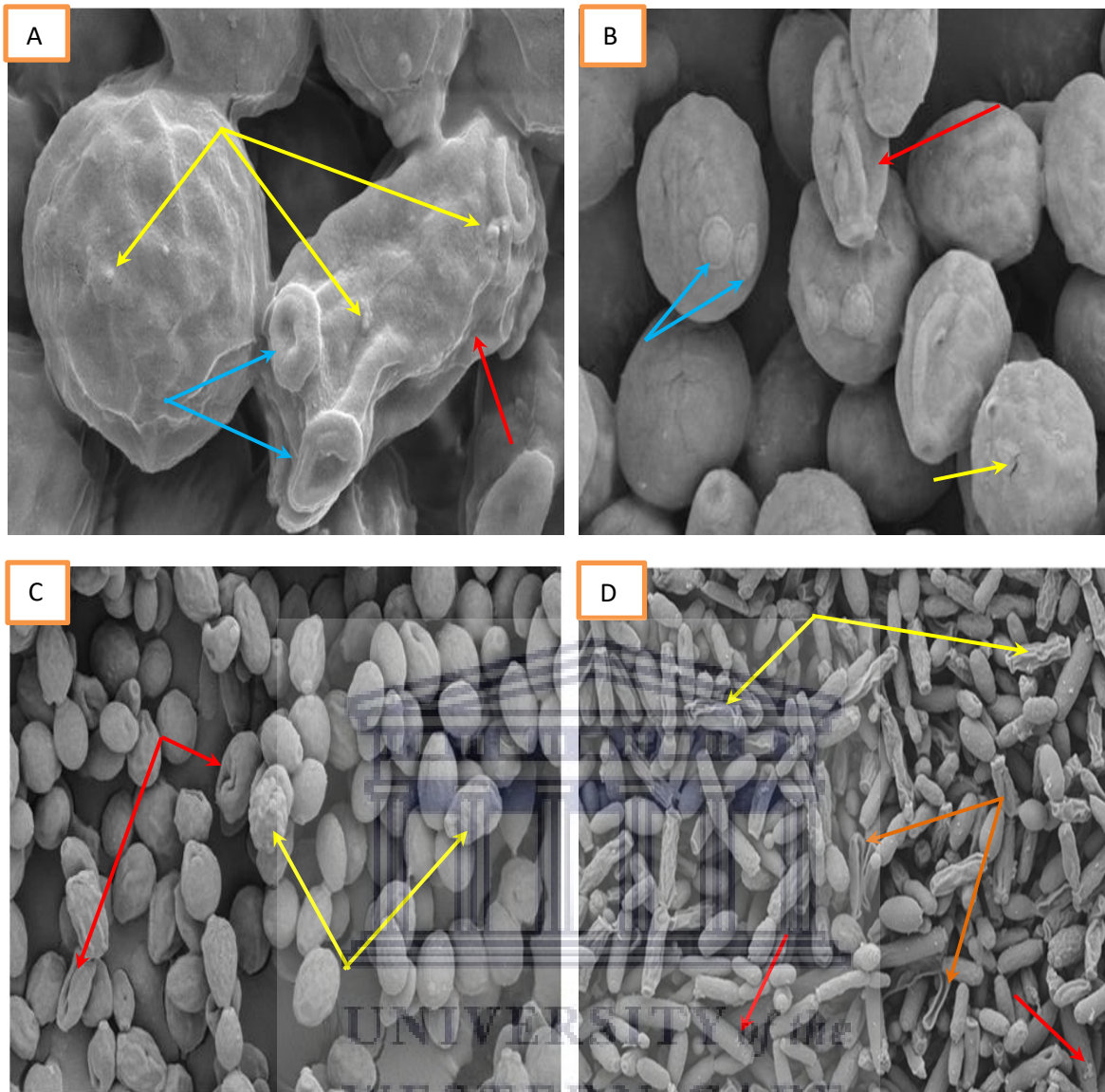


Figure 3.8: Scanning micrographs of *C. krusei* (ATCC 2159) treated with FCZ at 2, 4, 6 and 24 hours. At 2 hours (A) Cells showed a rough texture with wrinkled appearance (red arrow) and sparse extracellular vesicles (yellow arrows) and bud scars (blue arrows), viewed at 10.00 K X magnification. At 4 hours (B) Cells appeared cracked (yellow arrow) and shrunken (red arrow) with multiple bud scars not confined to the polar region (blue arrows), viewed at 5.00 K X magnification. At 6 hours (C) Highly distorted cells (yellow arrows) with cavitations (red arrows), viewed at 2.00 K X magnification. At 24 hours (D) Lysed and desiccated cells (orange arrows), some totally deformed cells (yellow arrows) and others with sparse extracellular vesicles (red arrows) viewed at 2.00 K X magnification.

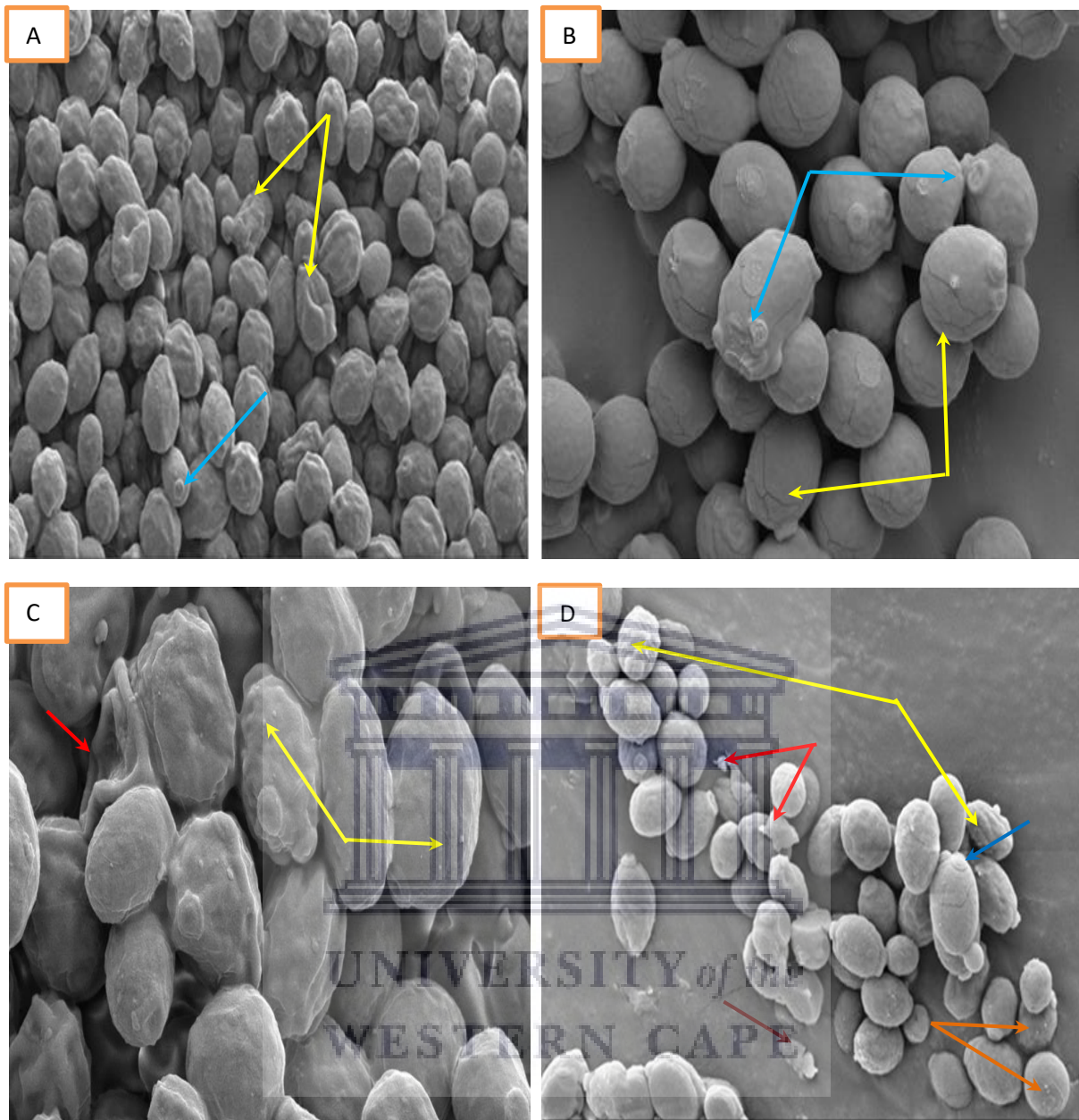


Figure 3.9: Scanning micrographs of *C. glabrata* (ATCC 26512) treated with FCZ at 2, 4, 6 and 24 hours. At 2 hours (A) Shrunken, wrinkled and desiccated cells (yellow arrows) with bud scars (blue arrow) viewed at 2.00 K X magnification. At 4 hours (B) Desiccated cracked cells (yellow arrows) appeared with multiple bud scars (blue arrows) viewed at 5.00 K X magnification. At 6 hours (C) Severely distorted cells (red arrow) with sparse extracellular vesicles (yellow arrows) viewed at 5.00 K X magnification. At 24 hours (D) Cracked deformed (yellow arrows), and lysed cells (red arrows), along with cell remnants (brown arrow) and polar bud scars (blue arrow) and sparse extracellular vesicles (orange arrows) viewed at 5.00 K X magnification.

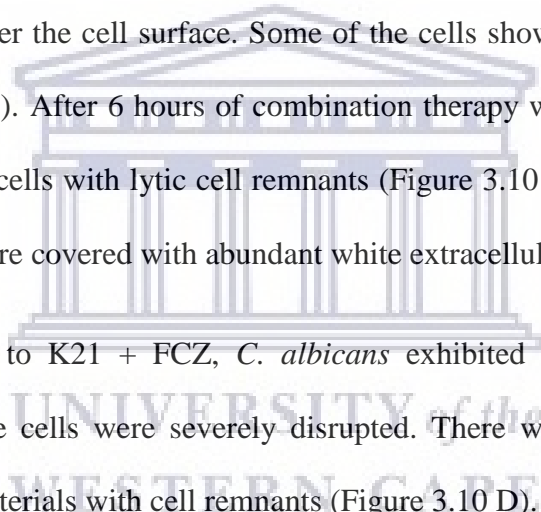
3.3.1.3 Cell surface changes following K21 + FCZ exposure

C. albicans (ATCC 90028)

After 2 hours exposure to the combination therapy with K21 (15.62 µg/mL) + FCZ (4 µg/mL), some cells of *C. albicans* (ATCC 90028) appeared interconnected with thick appendages, with abundant flocculent extracellular material observed on the cell surfaces (Figure 3.10 A). The bud scars increased in numbers and were not limited to polar end positioning.

At 4 hours, the cells appeared severely deformed. Thick extracellular flocculent materials and vesicles were observed over the cell surface. Some of the cells showed cracks and appeared dehydrated (Figure 3.10 B). After 6 hours of combination therapy with K21 and FCZ, there was evidence of *Candida* cells with lytic cell remnants (Figure 3.10 C). The totally distorted and disintegrating cells were covered with abundant white extracellular vesicles.

After 24 hours exposure to K21 + FCZ, *C. albicans* exhibited aggregated cells with a crumbled appearance. The cells were severely disrupted. There were abundant masses of flocculent extracellular materials with cell remnants (Figure 3.10 D).



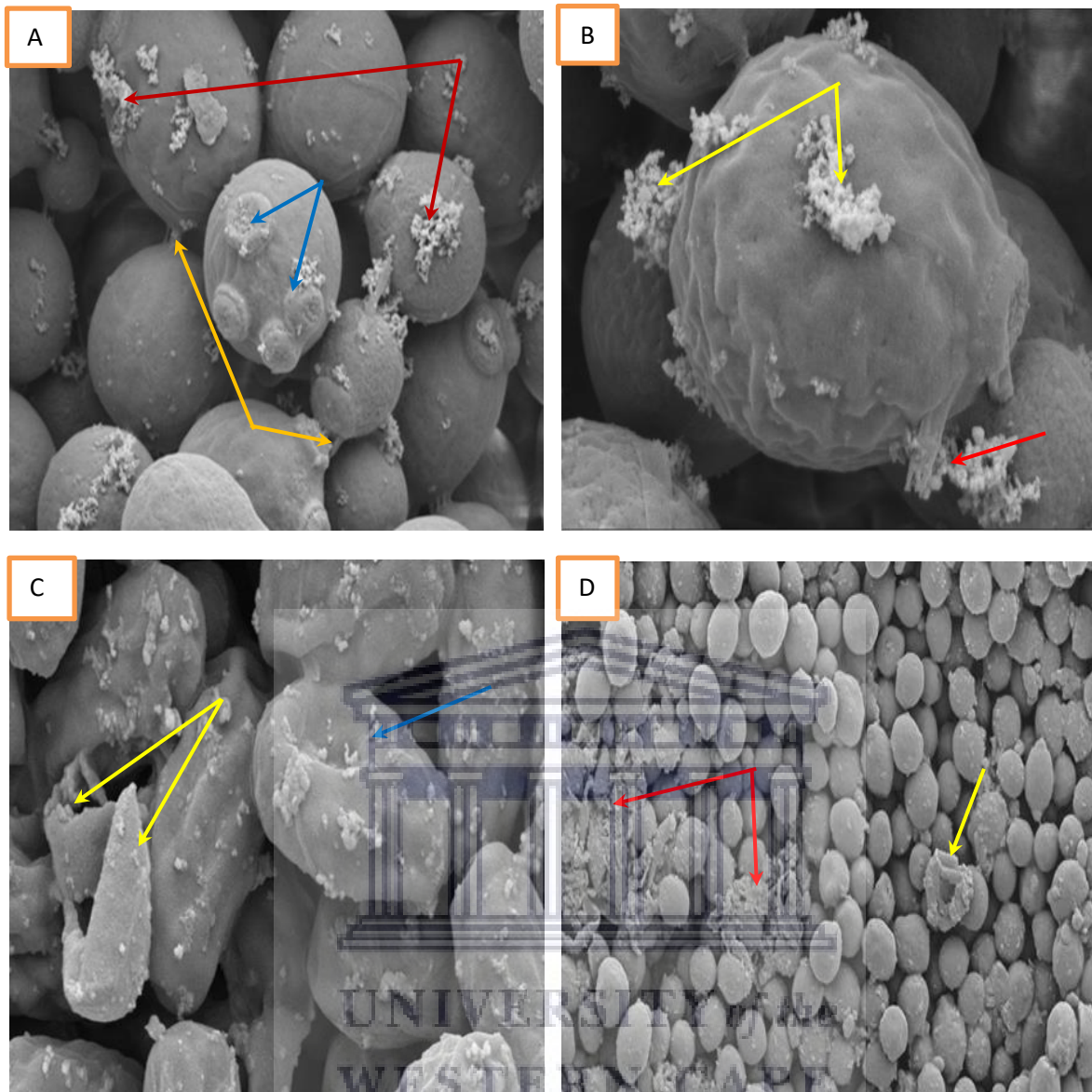


Figure 3.10: Scanning micrographs of *C. albicans* (ATCC 90028) treated with K21 + FCZ at 2, 4, 6 and 24 hours. At 2 hours (A) Thick appendages connecting some cells (yellow arrows) with flocculent extracellular materials (red arrows) on cell surfaces, multiple bud scars not limited to polar end positioning (blue arrows) viewed at 10.00 K X magnification. At 4 hours. (B) Breakage of thick appendages that connected the cells and severely distorted and convoluted cells with flocculent deposits (red arrow) and extracellular vesicles (yellow arrows) viewed at 20.00 K X magnification. After 6 hours of combination therapy with K21 and FCZ (C) Distorted and disintegrating cells (blue arrow) with lytic cell remnants (yellow arrows) viewed at 10.00 K X magnification. At 24 hours, (D) Cells with masses of extracellular materials (yellow arrow) and cell remnants (red arrows) were found, viewed at 2.00 K X magnification.

***C. krusei* (ATCC 2159)**

After 2 hours of exposure to K21 (31.24 µg/mL) + FCZ (8 µg/mL), *C. krusei* (ATCC 2159) showed the presence of flocculent deposits of extracellular vesicles on the cell surface. There were multiple bud scars not confined to the polar ends only (Figure 3.11 A).

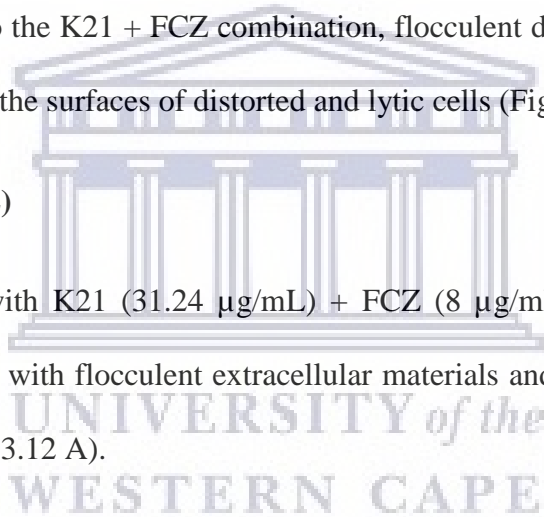
At 4 hours, the cells appeared wrinkled, shrunken and deformed with extracellular vesicles on the cell surface (Figure 3.11 B). A 6-hour exposure to K21 + FCZ resulted in the destruction of *C. krusei* cells with increased extracellular vesicles, bud scars and cellular remnants observed (Figure 3.11 C).

After 24 hours exposure to the K21 + FCZ combination, flocculent deposits and extracellular vesicles were observed on the surfaces of distorted and lytic cells (Figure 3.11 D).

***C. glabrata* (ATCC 26512)**

After 2 hours exposure with K21 (31.24 µg/mL) + FCZ (8 µg/mL), *C. glabrata* (ATCC 26512) cells were covered with flocculent extracellular materials and some tiny vesicles and multiple bud scars (Figure 3.12 A).

At 4 hours, the cells exhibited a variation in sizes and shapes. Cells exhibited convoluted cell surfaces with flocculent deposits, extracellular vesicles and multiple bud scars observed (Figure 3.12 B). After 6 hours, the cells appeared distorted, lysed and elongated Cellular remnants and multiple bud scars were evident (Figure 3.12 C). A 24 hour treatment with K21 + FCZ resulted in total cell lysis of some cells with release of large deposits of lytic cell remnants (Figure 3.12 D).



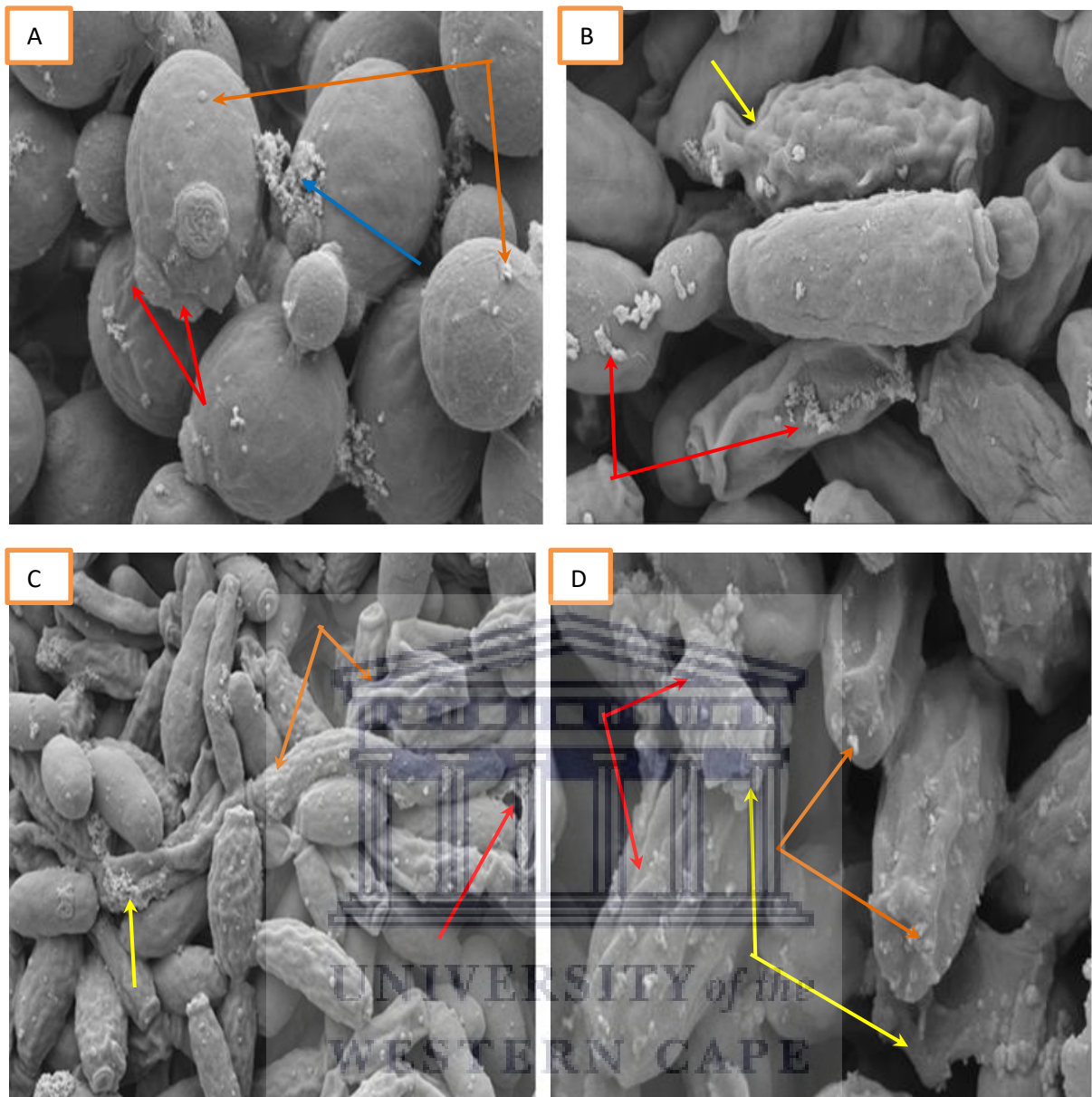


Figure 3.11: Scanning micrographs of *C. krusei* (ATCC 2159) treated with K21 + FCZ at 2, 4, 6 and 24 hours. At 2 hours (A) Cells showed flocculent deposits (orange arrows) and extracellular vesicles (blue arrow) with multiple bud scars (red arrows) viewed at 10.00 K X magnification. At 4 hours (B) Deformed and shrunken cells (yellow arrow) with extracellular vesicles (red arrows) viewed at 10.00 K X magnification. At 6 hours (C) Elongated and distorted cells entangled each other (orange arrows) with numerous extracellular vesicles (yellow arrow) and lytic cell remnants (red arrow) viewed at 5.00 K X magnification. At 24 hours (D) Distorted cells with lytic cell remnants (yellow arrows), flocculent deposits (orange arrows) and extracellular vesicles (red arrows) found, viewed at 10.00 K X magnification.

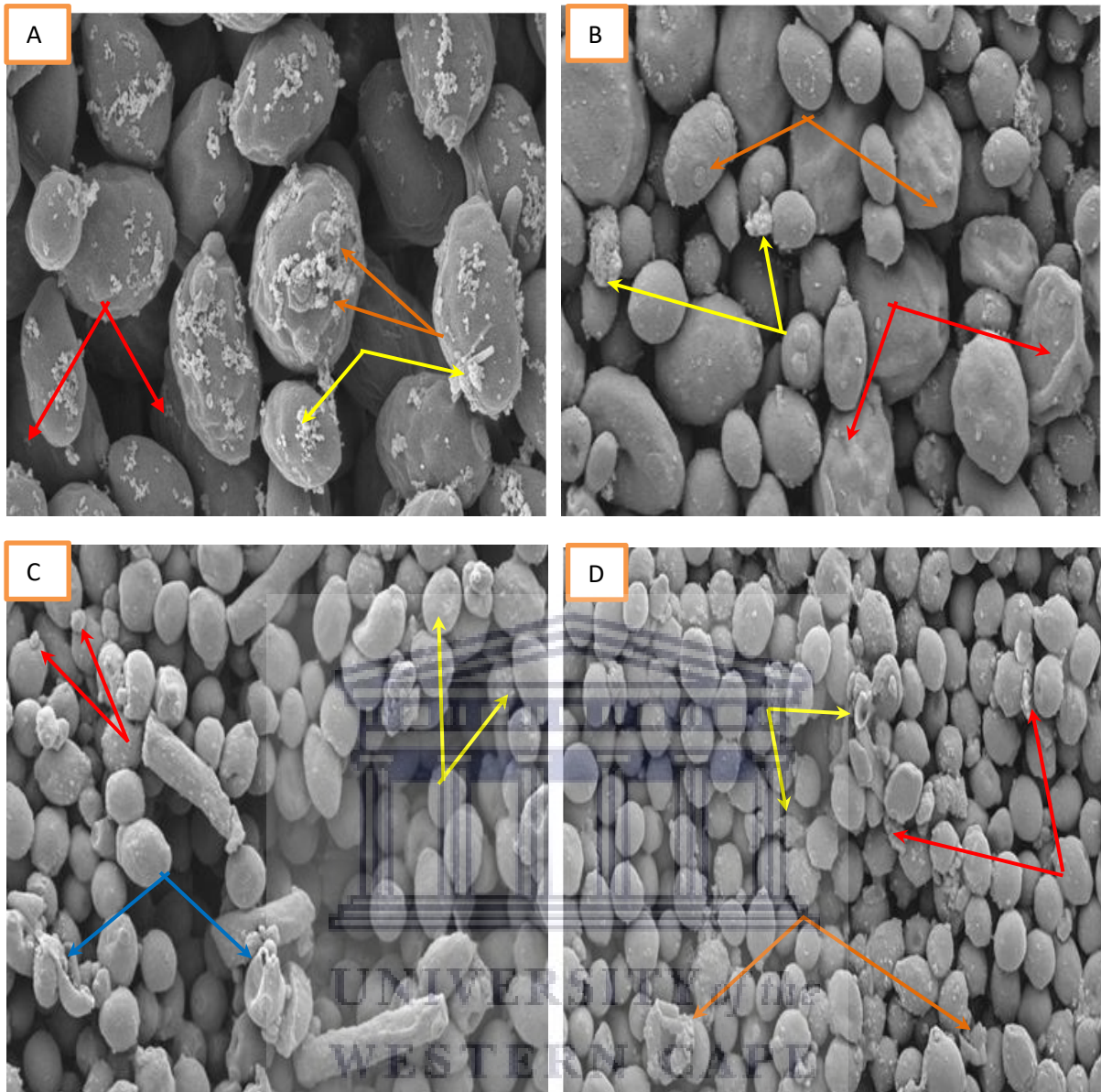


Figure 3.12: Scanning micrographs of *C. glabrata* (ATCC 26512) treated with K21 + FCZ at 2, 4, 6 and 24 hours. At 2 hours (A) Flocculent deposits of extracellular vesicles (yellow arrows) with multiple bud scars (orange arrows) and tiny extracellular vesicles (red arrows) present, viewed at 10.00 K X magnification. At 4 hours (B) Deformed cells with convoluted cell surfaces (red arrows) bud scars (orange arrows) flocculent deposits of extracellular vesicles (yellow arrows) present, viewed at 5.00 K X magnification. At 6 hours (C) Various shapes and sizes were observed with some lysed cells (blue arrows), extracellular vesicles (yellow arrows) and bud scars (red arrows), viewed at 5.00 K X magnification. At 24 hours (D) Severely cracked and distorted cells (yellow arrows) with cell lysis (orange arrows) and large deposits of cellular remnants (red arrows) found, viewed at 2.00 K X magnification.

3.3.2 Transmission electron microscopy

3.3.2.1 Ultrastructural changes at different time intervals of K21 exposure

C. albicans (ATCC 90028)

The untreated *C. albicans* (ATCC 90028) displayed an intact regular cell wall and a cell membrane close to the cell wall. The cell ultrastructure revealed intracellular components such as mitochondria, a well-defined nucleus and an electron dense body (Figure 3.13).

Figure 3.14 shows transmission micrographs of *C. albicans* (ATCC 90028) after treatment with K21 at different time intervals. After 2 hours of treatment with K21 (31.24 µg/mL), the cells showed an intact cell wall but separated with blebs at the margins of cytoplasm (Figure 3.14 A). The cytoplasm displayed lipid deposits and some amorphous electron dense material along with what appeared to be an early endosome. Shrinkage of the nucleus and a few secretory vesicles were observed.

After 4 hours of treatment with K21, the cell wall exhibited an increase in thickness and cell membrane disruption with the formation of blebs along the margins. The cytoplasm displayed a thick deposition of lipids along with electron dense material and melanin deposition along the membrane margins (Figure 3.14 B).

A 6 hour exposure to K21 resulted in the cell membrane separating from the cell wall. There was an increased amount of lipid deposition and electron dense deposits intracellularly. The cell wall and the membrane exhibited increased deposition of melanin. There was condensation of chromatin observed in the cytoplasm (Figure 3.14 C). At 24 hours, K21 caused complete deformation of the cell wall and cell membrane. Some areas showed separation of the cell wall from the cell membrane with the release of blebs. Intracellularly, the cell showed an increase in vacuole formation and lipid deposition (Figure 3.14 D).

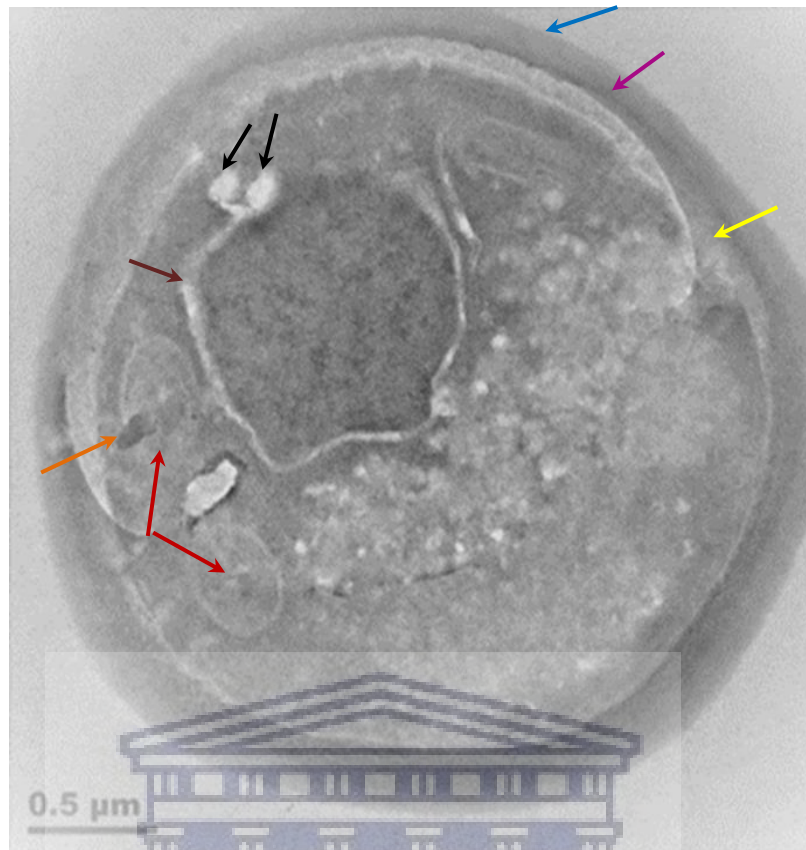


Figure 3.13: Transmission micrographs of *C. albicans* (ATCC 90028) without K21 treatment, viewed at 22.00 K X magnification. Untreated control cell shows intact cell wall (blue arrow) attached to the cytoplasmic membrane (pink arrow), mitochondria (red arrows), a nucleus (brown arrow), an electron dense body (orange arrow), lipid deposits (black arrows) and a secretory vesicle (yellow arrow).

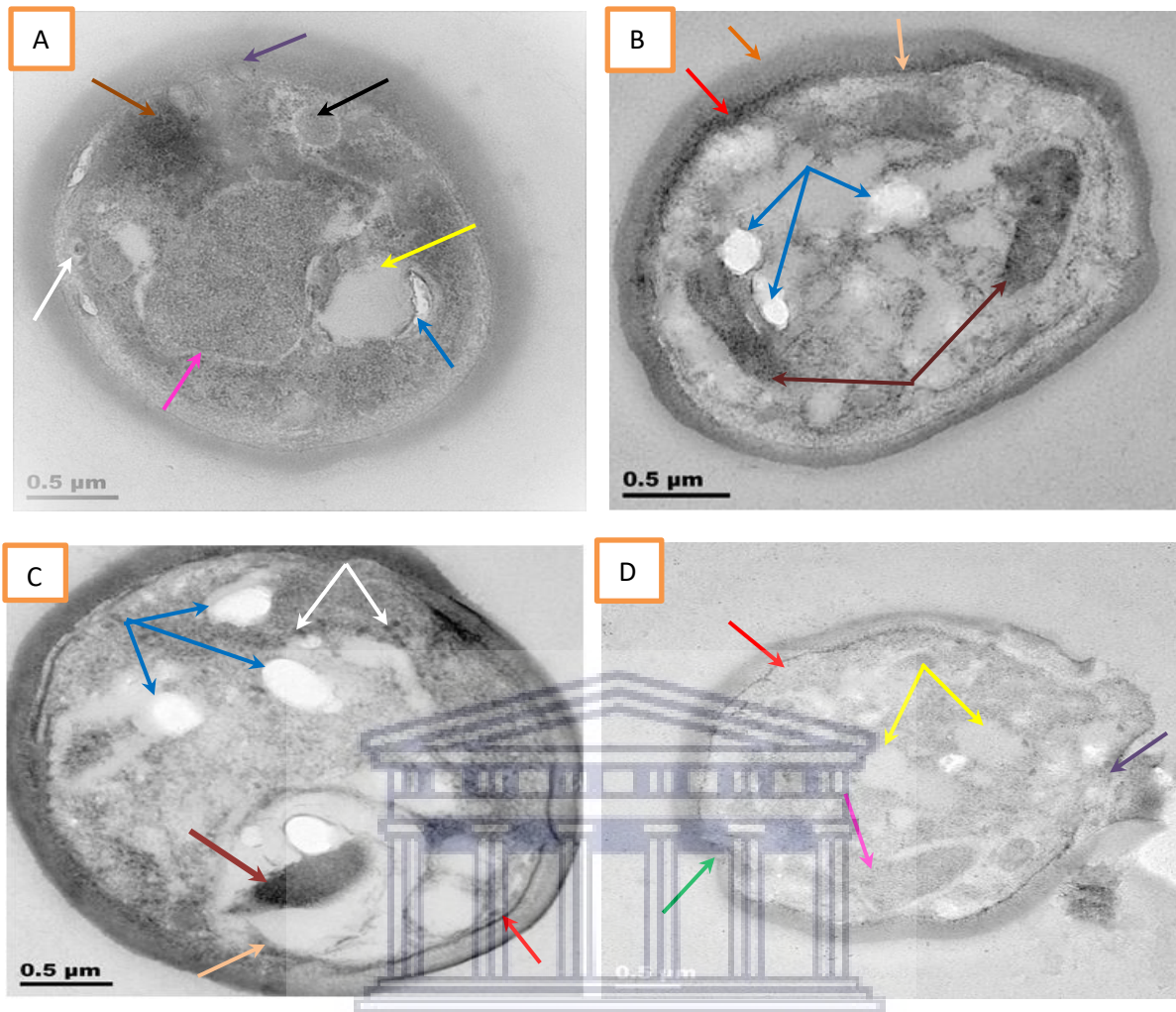


Figure 3.14: Transmission micrographs of *C. albicans* (ATCC 90028) treated with K21 at 2, 4, 6 and 24 hours. At 2 hours (A) Presence of blebs along the periphery of the cell membrane (violet arrow), shrunken nucleus (pink arrow), lipid deposits (blue arrow) observed. The cytoplasm showed mitochondria (black arrow) vacuoles (yellow arrow) with amorphous electron dense material (brown arrow) and a tiny vesicle with electron dense centre (white arrow). At 4 hours (B) Increased thickness of the cell wall (orange arrow) with cell membrane disruption (beige arrow) and melanin deposition (red arrow) with thick deposition of lipids (blue arrows) and electron dense deposits (brown arrows) in the cytoplasm. At 6 hours (C) Destruction of cell membrane (beige arrow) and heavy deposits of melanin (red arrow) along the cell wall and cell membrane with abundant lipid deposition (blue arrows) and electron dense ribosome-like deposits (orange arrows), chromatin condensation (brown arrow) in the cytoplasm. At 24 hours (D) Thick melanin deposition (red arrow) observed along the cell membrane with indentation of the cell wall and membrane (green arrow) and release of blebs (violet arrow). The nucleus showed shrinkage (pink arrow) with abundant vacuoles (yellow arrows). Magnification (A, B, C and D) - 22.00 K X.

3.3.2.2 Immunogold labelling of Sap after exposure to K21

C. albicans (ATCC 90028)

After 24 hours incubation with K21 (31.24 µg/mL), the *C. albicans* (ATCC 90028) cells were post embedded with Sap 1-3 and Sap 4-6 for the localization of Sap expression evaluated by the presence of gold particles on the cell surface.

The positive control with Sap 1-3 showed immunogold labelling on the cell membrane, cytoplasm, cell wall and in the vacuoles (Figure 3.15 A). There was an absence of gold labelling in the negative control without the addition of polyclonal Sap 1-3 (Figure 3.15 B).

Profound deposition of Sap 1-3 proteins was observed along the cell membrane and in the cytoplasm, with less displayed along the cell wall. The *Candida* cell was in active budding stage and an enhanced deposition of Sap 1-3 proteins was observed along the bud cell membrane. A shrunken nucleus and increased lipid deposition were observed. There was an increase in the thickness of the cell wall with some extracellular vesicles observed in the extracellular space (Figure 3.15 C and D).

Figure 3.16 demonstrates the localisation of Sap 4-6 proteins in *C. albicans* (ATCC 90028) along with the positive and negative controls.

Very sparse gold particles were observed in the cytoplasm of the positive control, indicating the limited expressions of Sap 4-6 antigens (Figure 3.16 A), while no gold labelling was seen in negative control without the addition of polyclonal antibodies (Figure 3.16 B).

The expression of Sap 4-6 proteins was very limited across the cells. Very few gold particles were observed confined to the cell membrane and cytoplasm indicating the poor expression of Sap 4-6. The cell membrane showed increased deposition of melanin with heavy deposition of lipids intracellularly (Figure 3.16 C and D).

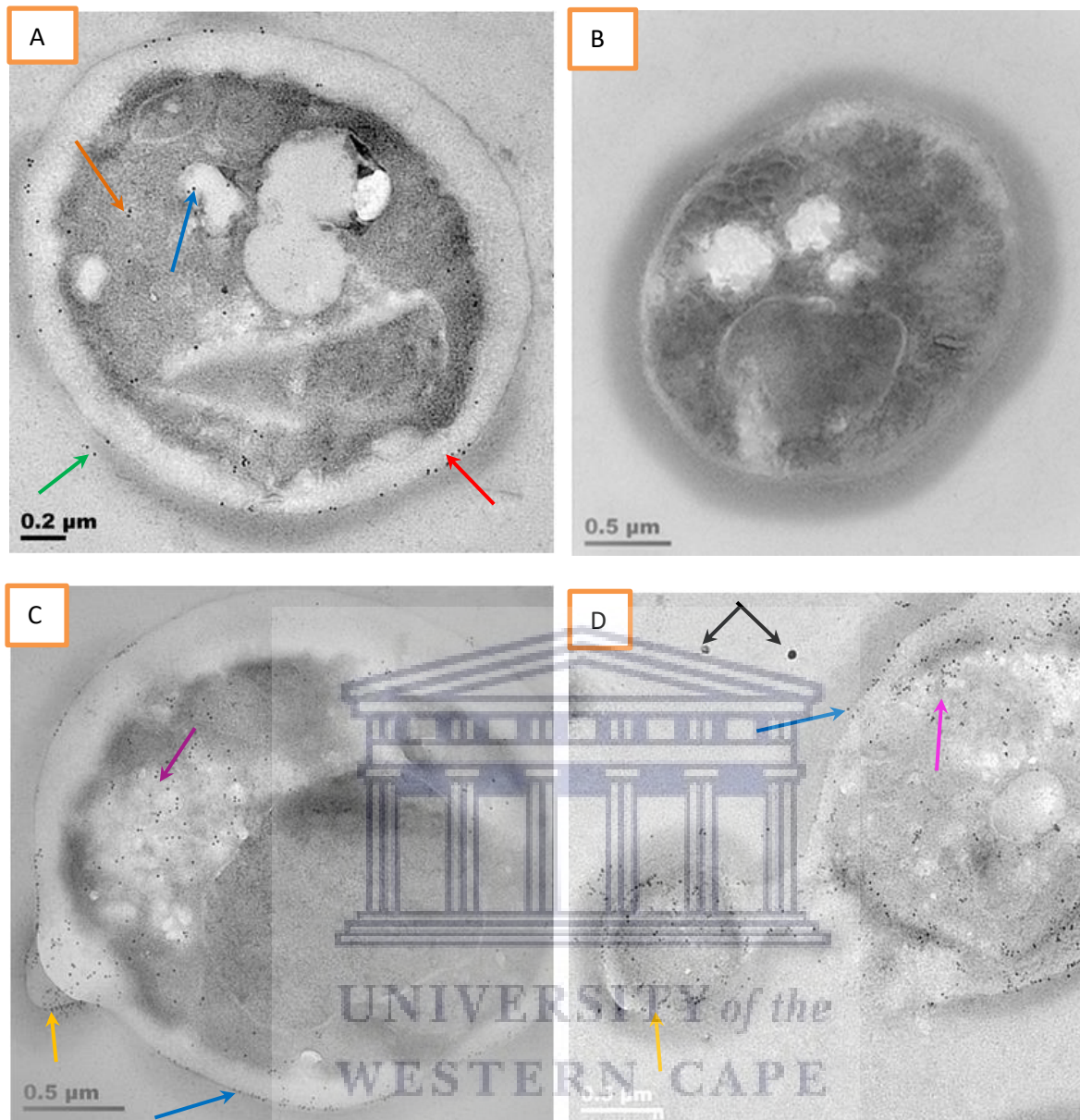


Figure 3.15: Immunogold labelling of *C. albicans* (ATCC 90028) with Sap 1-3 antibodies when treated with K21

(A) Positive control - Gold particles confined to the cell wall (green arrow), cell membrane (red arrow) and cytoplasm (orange arrow) with few gold particles found in the vacuole (blue arrow). Magnification - 30.00 K X (B) Negative control - No gold particles observed in the cell without the addition of Sap 1-3 antibodies. Magnification - 22.00 K X. (C and D) Localisation of Sap 1-3 proteins - Gold particles were observed on the cell wall, where bleb formation appeared to be starting along the cell wall and budding had occurred (yellow arrows). Gold particles were also observed along the cell membrane (blue arrows), and in parts of the cytoplasm adjacent to the nucleus (pink arrows). Extracellular vesicles were evident in the extracellular space (black arrows). Magnification - 22.00 K X.

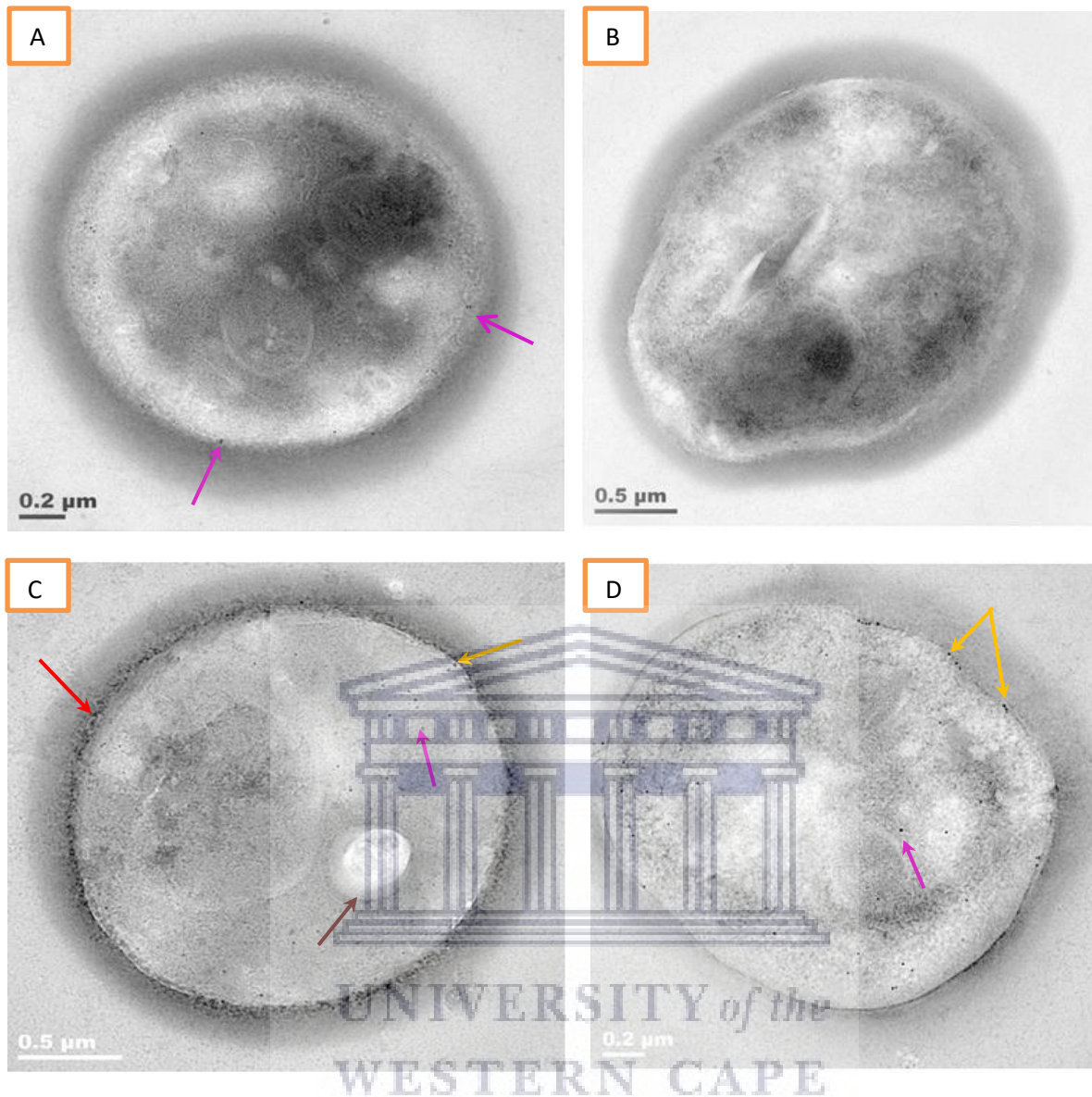


Figure 3.16: Immunogold labelling of *C. albicans* (ATCC 90028) with Sap 4-6 antibodies when treated with K21.

(A) Positive control - Extremely few non-specific gold particles were observed within the cell membrane (pink arrows). Magnification - 30.00 K X. (B) Negative control - Total absence of gold particles observed. Magnification - 22.00 K X. (C and D) Localisation of Sap 4-6 proteins - (C) Very few non-specific gold particles were observed along the cell membrane (yellow arrow) and in the cytoplasm (pink arrow). Increased melanin deposition along the membrane (red arrow) and lipid deposition were observed intracellularly (brown arrow). Magnification - 22.00 K.X. (D) A few gold particles confined to the cell membrane (yellow arrows) and cytoplasm (pink arrow). Magnification - 30.00 K X.

***C. dubliniensis* (NCPF 3949a)**

C. dubliniensis (NCPF 3949a) was treated with K21 at 31.24 µg/mL and postembedding of the cells was performed after 24 hours incubation with Sap 1-3 and Sap 4-6 polyclonal antibodies.

In the positive control, untreated *C. dubliniensis* (NCPF 3949a) was labelled with the Sap 1-3 and Sap 4-6 polyclonal antibodies respectively and in the negative control the Sap polyclonal antibodies were omitted.

Positive and negative controls confirmed the localization of Sap 1-3 antigens in *C. dubliniensis* (NCPF 3949a). In the positive control, specific gold labelling was observed along the cell membrane and few along the cell wall with an increase in cell wall thickness (Figure 3.17 A). In the negative control no specific gold labelling was observed (Figure 3.17 B).

Abundant gold particles were found along the cell membrane and cytoplasm, while few were found in the cell wall indicating the expression of Sap 1-3. Deformed nucleus and heavy deposition of lipids were observed intracellularly (Figure 3.17 C and D).

There was no gold labelling found in the positive control with Sap 4-6 (Figure 3.18 A) and in the negative control without Sap 4-6 (Figure 3.18 B).

Immunogold labelling of Sap 4-6 in *C. dubliniensis* (NCPF 3949a) did not show any expression of Sap 4-6 in the cell. There was deformation of the cell with cell membrane disruption and increased thickness of cell wall (Figure 3.18 C).

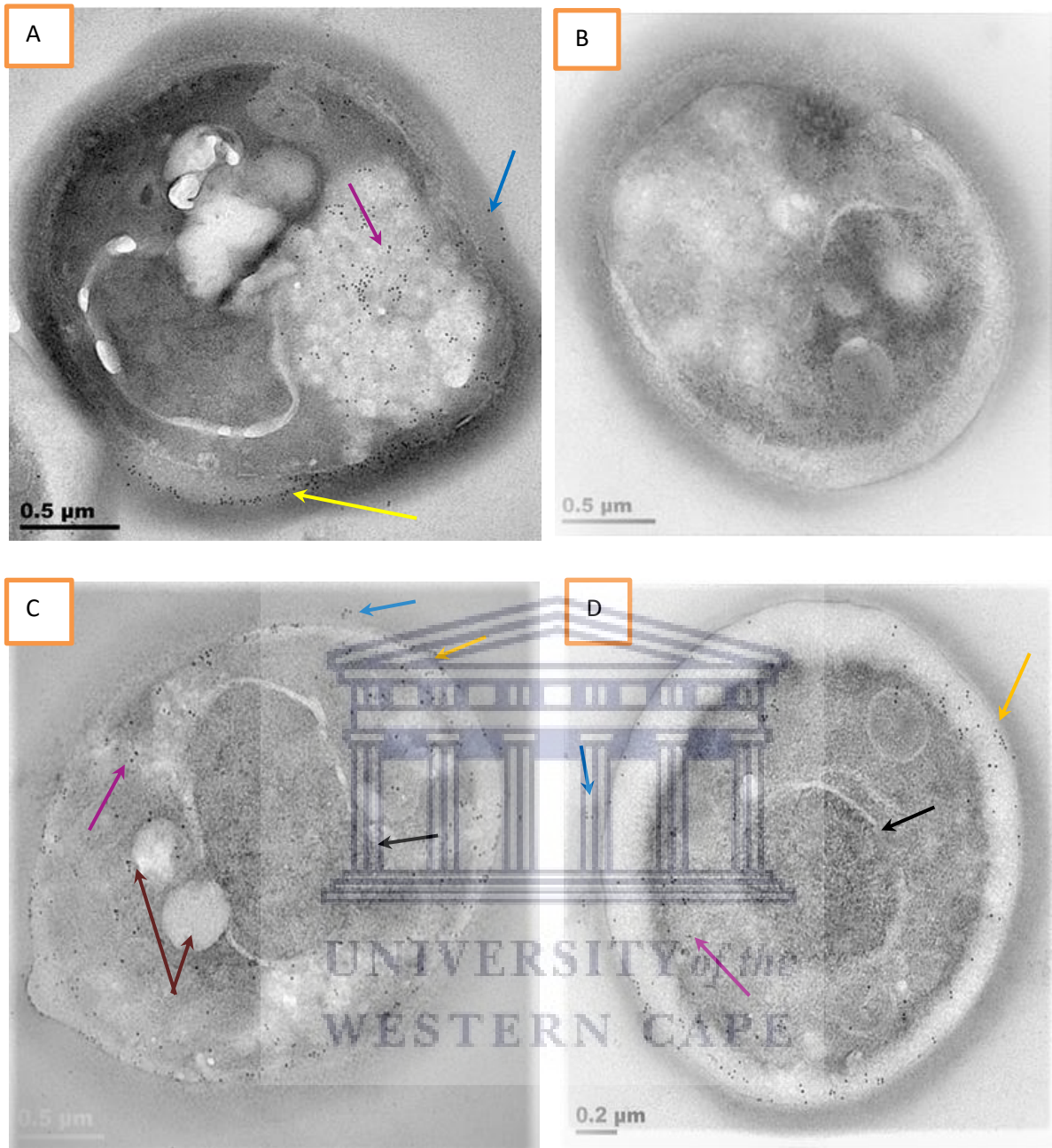


Figure 3.17: Immunogold labelling of *C. dubliniensis* (NCPF 3949a) with Sap 1-3 antibodies when treated with K21.

(A) Positive control - Gold particles found on the cell membrane (yellow arrow) and in the cytoplasm (pink arrow) and few gold particles found on the cell wall (blue arrow). (B) Negative control - No specific gold labelling or Sap 1-3 expression observed. Magnification (A and B) - 22.00 K X. (C and D) Localisation of Sap 1-3 proteins - Profound gold particles observed along the cell membrane (yellow arrows), cytoplasm (pink arrows) with few gold particles in the cell wall (blue arrows). The cytoplasm showed a deformed shrunken nucleus (black arrows) and vacuole formation (brown arrows). (C) Magnification - 22.00 K X (D) Magnification - 30.00 K X.

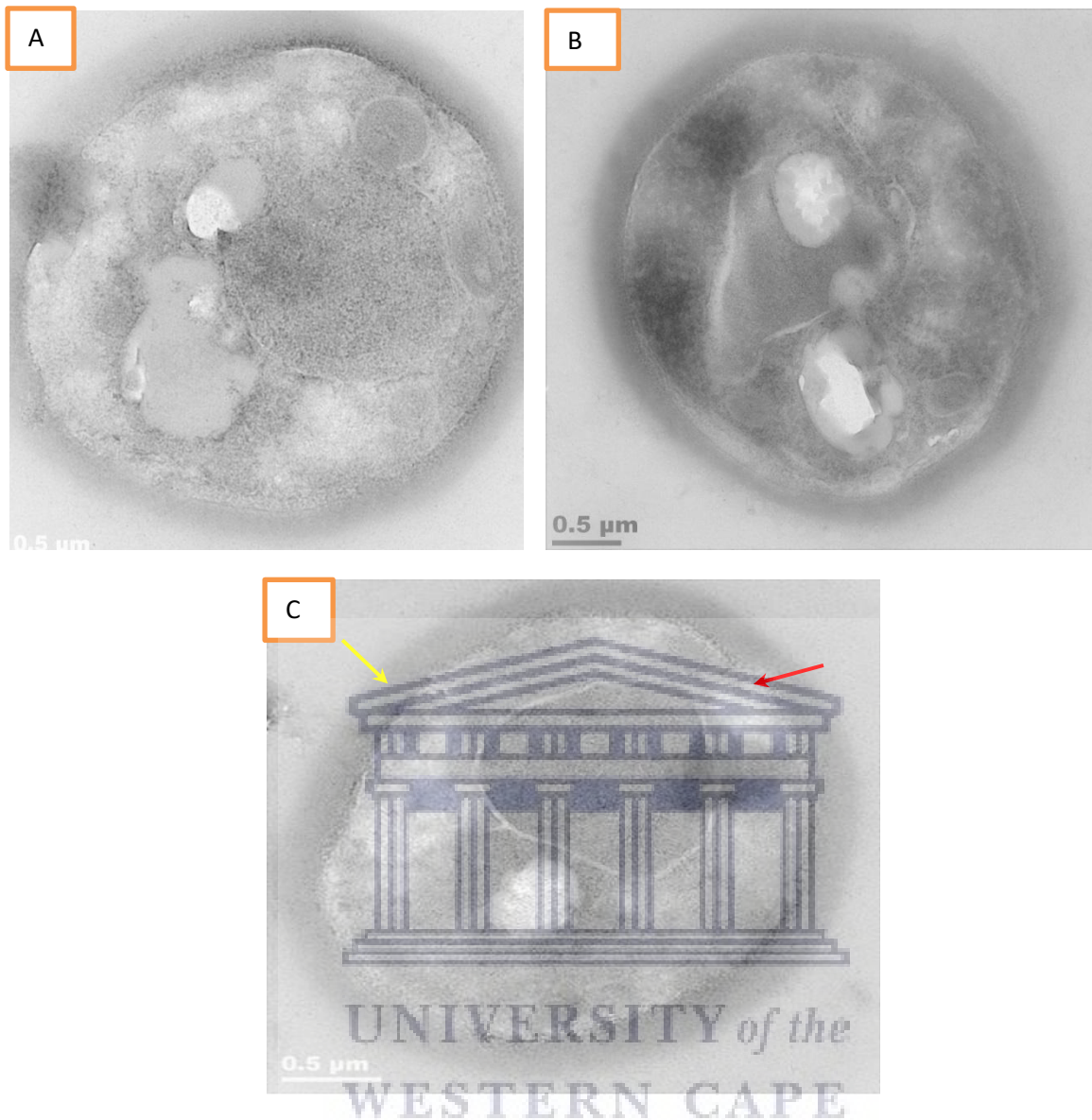


Figure 3.18: Immunogold labelling of *C. dubliniensis* (NCPF 3949a) with Sap 4-6 antibodies when treated with K21.

(A and B) Positive and Negative controls - No gold labelling was found (C) Localisation of Sap 4-6 proteins - Disruption of cell membrane (red arrow) and increased thickness in cell wall (yellow arrow) observed with the absence of gold particles. Magnification (A, B and C) - 22.00 K X.

***C. tropicalis* (ATCC 950)**

C. tropicalis (ATCC 950) was treated with K21 at 31.24 µg/mL and after 24 hours of incubation, postembedding of the cells was performed with Sap 1-3 and Sap 4-6 polyclonal antibodies.

Figure 3.19 displays the localisation of Sap 1-3 proteins and the positive and negative control for *C. tropicalis* (ATCC 950).

In the positive control, the Sap 1-3 polyclonal antibodies were included and in the negative control the Sap polyclonal antibodies were omitted. The positive control showed a limited presence of gold particles confined to the cell membrane and cytoplasm (Figure 3.19 A).

The cell wall did not exhibit any gold particles, but an electron dense vesicle was found in the cell wall. Increased melanin deposition was found along the cell membrane. The negative control did not show any gold particles (Figure 3.19 B).

C. tropicalis (ATCC 950) immunolabelled with Sap 1-3 polyclonal antibodies showed limited expression of Sap 1-3. There were gold particles present in the cytoplasm and along the cell membrane with membrane disruption, but no gold particles were found in the cell wall (Figure 3.19 C).

Figure 3.20 demonstrates the localisation of Sap 4-6 proteins and the positive and negative controls of *C. tropicalis* (ATCC 950).

In the positive control, Sap 4-6 polyclonal antibodies were included and in the negative control the Sap polyclonal antibodies were omitted. There was no gold labelling found in the positive control (Figure 3.20 A) nor in the negative control (Figure 3.20 B). Postembedding of the cells with Sap 4-6 did not show any gold labelling in the cell. This indicated the absence of Sap 4-6 expression in the cell (Figure 3.20 C).

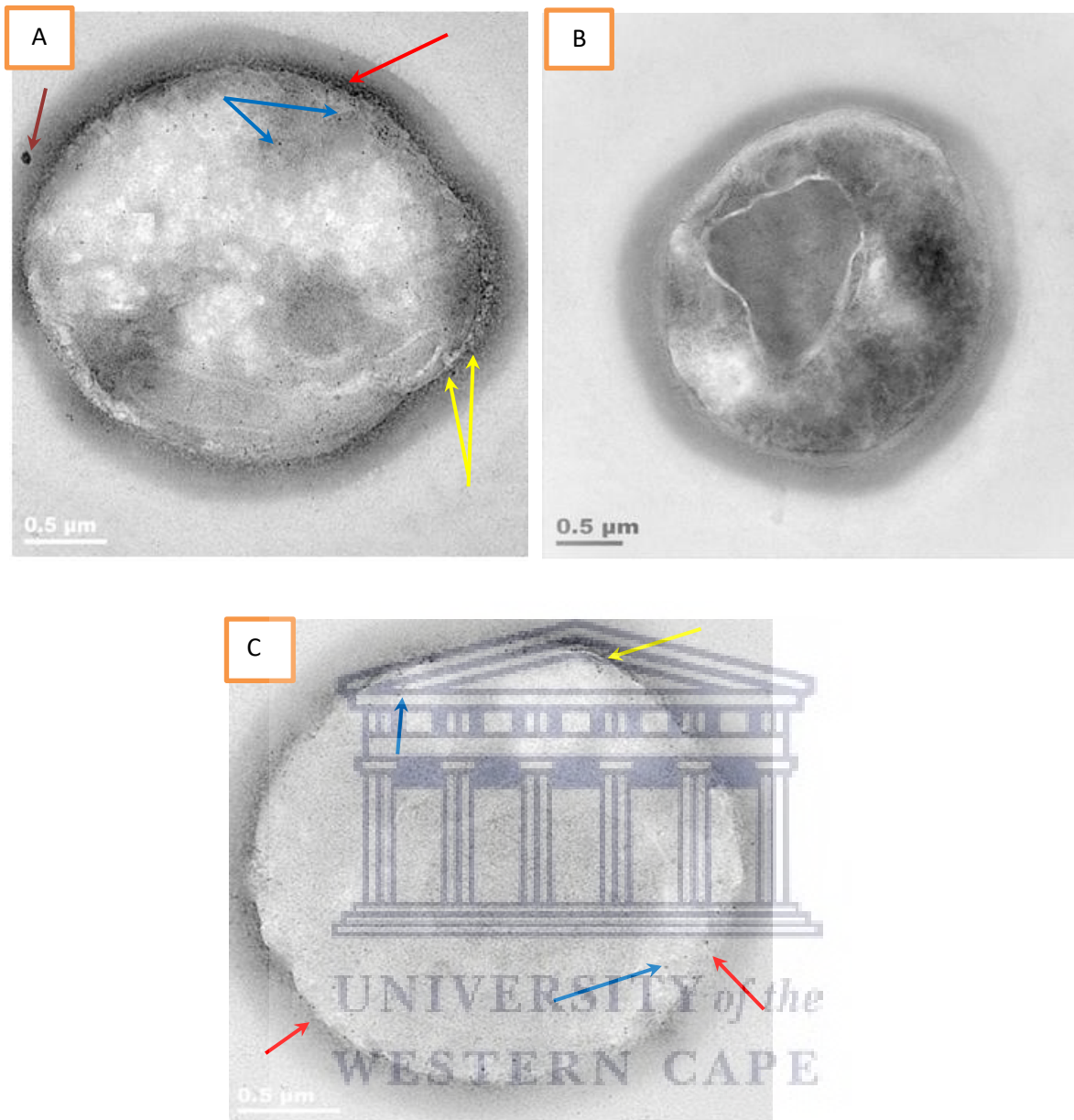


Figure 3.19: Immunogold labelling of *C. tropicalis* (ATCC 950) with Sap 1-3 antibodies when treated with K21.

(A) Positive control - Gold particles confined to the cell membrane (yellow arrows) and cytoplasm (blue arrows). Melanin deposits on the membrane (red arrow) with extracellular vesicle in the cell wall (brown arrow). (B) Negative control - No gold particles observed. (C) Localisation of Sap 4-6 proteins - Very limited gold particles observed along the cell membrane (red arrows) and cytoplasm (blue arrows). Melanin granules prominent around the cell (yellow arrow). Magnification (A, B and C) - 22.00 K X.

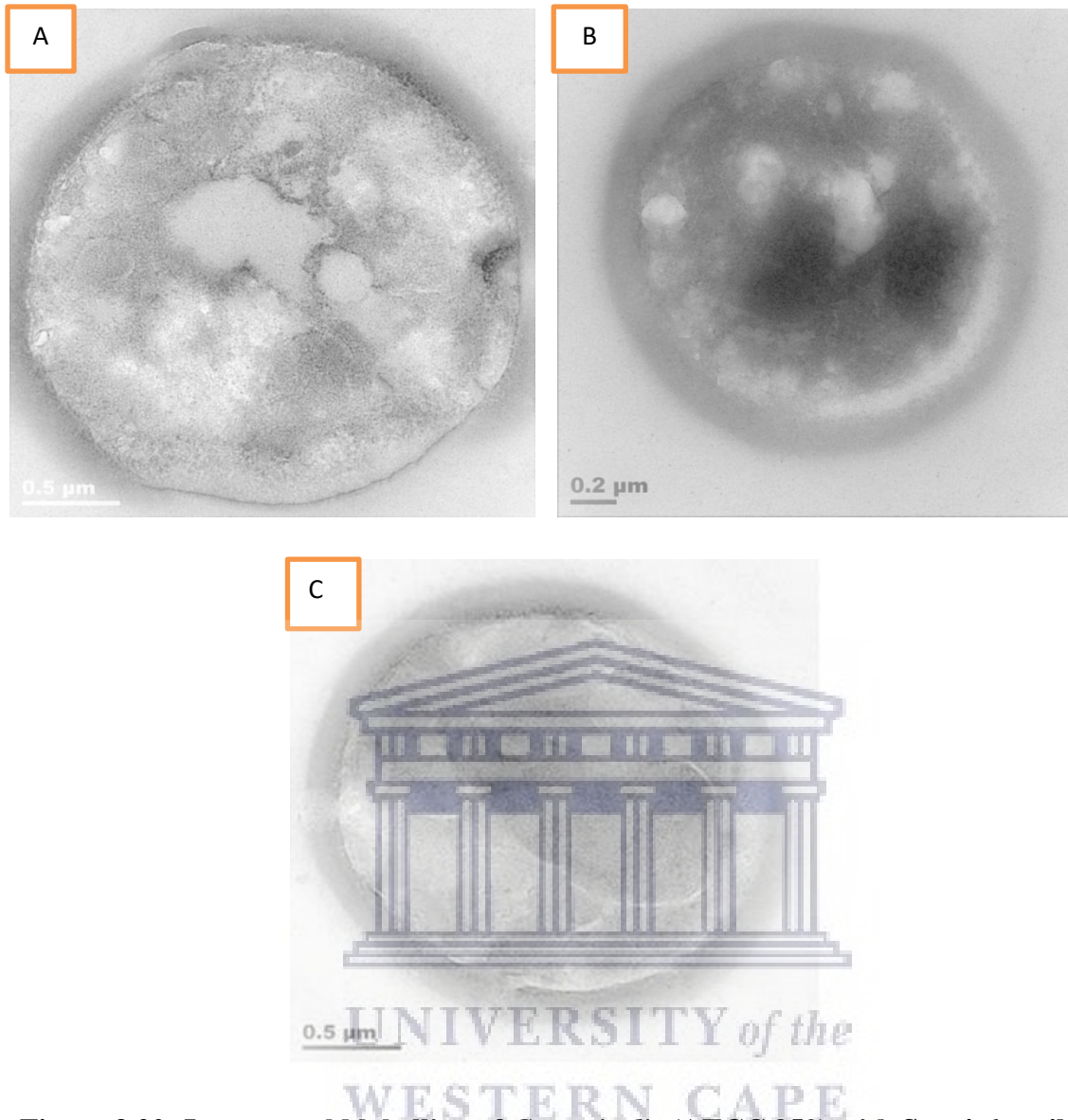


Figure 3.20: Immunogold labelling of *C. tropicalis* (ATCC 950) with Sap 4-6 antibodies when treated with K21.

(A and B) Positive and Negative controls - No gold labelling was found (C) Localisation of Sap 4-6 proteins - Absence of gold particles in the cell. Magnification (A, B and C) - 22.00 K X.

3.4 DISCUSSION

Scanning electron microscopy determined the major alterations in the microstructure of the *Candida* species revealing the characteristics of the antifungal agents.

Initially at 2 hours of exposure to K21, the homogeneous regular cells of *C. albicans* (ATCC 90028) were seen connected to each other by thin threads and the cell surface was found to be covered by sparse amounts of extracellular vesicles. The extracellular material plays characteristic roles in surface adhesion and cell cohesion (Flemming and Wingender, 2010; Chandra *et al.*, 2001) and resistance to antifungal agents (Baillie and Douglas, 2000) that may seed disseminated infections. The extracellular materials in the present study progressively increased in the following hours leading up to 24 hours. The increased presence of the lytic broken cells on the cell surface may indicate the release of intracellular granulated contents from the fungal cells due to disruption of the cell wall (Ellis, 2002).

The cell surface morphology was altered after 4 hours and 6 hours of exposure to K21 with extracellular vesicles abundantly present on the cell surface and at the bud scars. The increase in the bud scars at various regions on the cell surface suggested that K21 may affect the normal division process of *Candida* cells, similar to the study reported by Li *et al.*, (2011) in which the profound increase in the bud scars were related to the action of the compound hindering the normal *Candida* cell division process.

After 24 hours exposure with K21, it was observed that the compound acted on the cell wall with complete disruption of the cells. K21 inhibited the growth of the cells even at 0.5MIC resulting in dead cells. The collapsed and flocculent extracellular vesicles over the dead cells could be due to the leakage of the lytic material from the cell lysis as previously described by Latha *et al.*, (2011). Moreover, the cells of *C. glabrata* appeared swollen and double in size than the normal spherical *C. glabrata* control cells after exposure to the antifungals. Our

results were in agreement with the reports on the antifungal effect of CF661 demonstrating morphological alterations of *C. albicans* such as profound increase in the cell size and the interconnection of cells holding it together. The researchers considered the formation of cells in clusters as the antifungal activity of CF661. Moreover, they also reported a three times prominent increase in the size of the *C. albicans* cells after 30 minutes exposure to CF661 (Li *et al.*, 2011). Hence, the interconnected cells in the current study may be considered as the antifungal mechanisms of K21 and were distinctly vivid by the morphological changes examined by scanning electron microscopy.

The NCAC species are thought to be less pathogenic and cause candidiasis of less virulence due to the fact that they lack (totally or partially) some of the virulence factors in comparison to *C. albicans* (Moran *et al.*, 2002). In the present study, the cells of *C. krusei* and *C. glabrata* showed similar destructive morphological changes when exposed to K21 at each time interval with the presence of flocculent extracellular materials.

With FCZ, the *Candida* cells showed a different morphological appearance after the treatment exhibiting a highly desiccated and wrinkled cell surface with cavitations and indentations on the cell surface and collapsed cells at 24 hours. The wrinkled cells with cavitations on the cell surface may be due to the cell wall perturbation and the disruption of the cell membrane resulting in the collapse of the cells. The fungal cell morphology deteriorated with the increased time intervals. The most distinguishing feature was the absence of the flocculent appearance of extracellular material around the cells.

In the combination therapy of K21 + FCZ, the cells displayed a destructive behaviour suggesting the effectiveness of a combination therapy rather than treating the species with a single agent alone. Combination therapy is indeed an effective remedy for treating the fluconazole-resistant and innate-resistant *C. albicans* and non-*C. albicans Candida* species.

The flocculent presence of extracellular materials was found only when the cells were treated with K21 alone and also with the K21 + FCZ while not with FCZ. A study conducted by Serpa *et al.*, (2012) also stated the presence of flocculent extracellular materials interconnecting the cells of *C. albicans*, *C. parapsilosis* and *C. tropicalis*. In their study, they found the presence of abundant extracellular materials with baicalein alone and baicalein in combination with fluconazole at MIC₅₀. The material was absent among the cells with fluconazole alone. The extracellular materials were related to the structure of the biofilm matrix forming a complex interaction of different components. It is reported that biofilm exhibits resistance to the commonly used antifungals by restricting the penetration of the drug with reduced susceptibility to the host immune system (Douglas, 2003). This further indicates the utmost need for novel antifungal drugs and K21 with its superior fungicidal activity may act as an effective treatment strategy in treating the resistant *Candida* species.

Most of the cells were covered with the extracellular flocculent materials when K21 was treated alone and in combination with FCZ. França *et al.*, (2011) reported the presence of extracellular materials in *C. tropicalis* as a biofilm-like colony indicating its correlation with the complex architecture of *Candida* colonies.

Dead cells of the *Candida* species appeared at 6 hours of the combined therapy with K21 + FCZ, whereas, in treatment with a single agent the dead cells were only observed at 24 hours. This may further emphasize the effectiveness of treating the *Candida* species with appropriate dosages of two antifungal agents combined together.

It is obligatory for a pathogen to cause proteinase secretion in order to deteriorate the tissue barriers and acquire nutrition at the site of infection for their survival. The transmission electron microscopy revealed that the untreated cells of *C. albicans* (ATCC 90028) exhibited a well-defined cell wall around the structure of the *Candida* cell, with the cytoplasmic

membrane closely located to each other. The control cells exhibited the classic *Candida* cell with a regular and intact cell wall with an outer electron dense layer and a continuous inner cell membrane attached. However the treated cells with K21 showed a rupture in the cell membrane continuity. The fungal cell wall is a vital structure for the cell integrity and forms the first point of contact with the host protecting it from the extracellular environmental changes with any discontinuity in the cell wall making the cells osmotically delicate.

The transmission electron micrographs of *C. albicans* (ATCC 90028) demonstrated a homogenous cytoplasm with cell membrane, attached to an intact cell wall. However, after the exposure to K21 at 24 hours, the cell wall integrity was lost, leading to the extracellular leakage of the cytoplasmic contents. This was similar to the study conducted by Leng *et al.*, (2017) which demonstrated the anticandidal efficacy of alginate-enclosed chitosan-calcium phosphate-loaded Fe-bovine lactoferrin nanocapsules in *C. albicans*. In their study, the nanocapsules inhibited the growth of *C. albicans* and the SEM and TEM micrographs revealed the deterioration of the cell ultrastructure starting with 12 hours up to 36 hours. It was reported that the cells lost their metabolic functions and the intracellular leakage of the cytoplasmic contents through the pores on the cell wall, eventually leading to cell death.

C. albicans is a known producer of hydrolytic enzymes responsible for its virulence behaviour when compared with the less pathogenic *Candida* species (Moran *et al.*, 2011). *C. albicans* Saps can be organized in six families such as Sap 1-3, Sap 4-6, Sap 7, Sap 8, Sap 9 and Sap 10 and the presence of SAP genes correlates with the virulence of *C. albicans* and its level of Sap activity (Naglik *et al.*, 2003). In the current study, *C. albicans* (ATCC 90028) exhibited an abundant expression of Sap 1-3 mainly along the cell membrane and in the cytoplasm. Sap 1-3 found on the cell wall was very few which may suggest the limited action of K21 on the cell wall and a stronger action on the cell membrane. The cell membrane and the cytoplasm of *C. dubliniensis* (NCPF 3949a) showed Sap 1-3 expressions similar to *C.*

albicans. An intense and regular distribution of Sap 1-3 proteins was expressed along the cytoplasmic membrane and the membrane of the budding cells. The similar types of Sap 1-3 expression were expected in *C. dubliniensis* because of the phenotypically alike behaviour of *C. dubliniensis* with *C. albicans*. However, *C. tropicalis* (ATCC 950) showed very little expression of Sap 1-3 proteins along the cell membrane of the cell. K21 exhibited its antifungal action in all the *Candida* cells targeting the virulence factor of the species, Sap proteins. Some of the electron-dense and electron-lucent vacuoles within the cytoplasm were labelled with gold particles suggesting the target of Sap 1-3 expressions in the *Candida* cell.

Immunogold labelling of *C. albicans* with the polyclonal antibodies directed against Sap 4-6 showed very few specific gold particles on the cell membrane and the cytoplasm in contrast to the abundant deposition of Sap 1-3. However, the Sap 4-6 expression was completely absent in *C. dubliniensis* (NCPF 3949a) and *C. tropicalis* (ATCC 950) included in the study. The negative expression of Sap 4-6 in *C. dubliniensis* and *C. tropicalis* may be due to the absence of *C. albicans* orthologues Sap 5 and Sap 6 in *C. dubliniensis* and Sap 4-Sap 6 in *C. tropicalis* respectively, since Sap 4-6 is highly associated with hyphae formation and not yeast cells (Monod *et al.*, 2010). Regulation of Sap expression by the cell morphotypes and environmental factors indicate the expression of Sap 1-3 in yeast cells and that of Sap 4-6 in hyphal cells (Naglik *et al.*, 2003; Staniszezwska *et al.*, 2013).

The secreted hydrolytic enzymes affect the epithelial cell-cell junctions facilitating cell membrane degradation (Naglik *et al.*, 2011). The mechanism of direct virulence of the *Candida* species includes hydrolysing host cell membrane proteins contributing to the adherence and fungal epithelial penetration leading to cell damage of the host defence system, eventually avoiding or resisting the strike of antimicrobial agents (Monod and Borg-von Zepelin, 2002). However, a recent study reported Sap 6 as an important virulence factor

in oral candidiasis and the regulation of the structure or function of Sap 6 may form an alternative therapeutic modality for candidiasis (Kumar *et al.*, 2015).

The process of Sap secretion forms a secretory pathway system and the distribution of Sap proteins within the cytoplasm may be regarded as the initial step of a *Candida* cell infection followed by their presence in the space between the cytoplasmic membrane and the cell wall and their secretion into the extracellular space. The extracellular secretion occurs as a result of fusion of the vesicles with the plasma membrane causing invaginations at the inner side of the fungal cell wall exhibited by the presence of gold immunolabelling at the invaginations (Schaller *et al.*, 1998; Reid, 1991). These reports coincide with our results showing the presence of gold particles at the cell membrane invaginations indicating the release of the proteins into the periplasmic space.

The present study showed the presence of bilayered membranous extracellular vesicles inside the cell wall and in the extra-cellular environment. Even though Sap 1-3 immunoreactivity was associated with the presence of extracellular vesicles, no specific gold labelling was found within the vesicle. The vesicles in the extra-cellular environment appeared to be in various sizes and were found between the adjacent cells in a haphazard manner. K21 acts on the *Candida* cells resulting in apoptosis of the cells that released apoptotic bodies into the extracellular space and appeared as the extracellular vesicles in the outer space. The complex intravesicular structure of the apoptotic bodies prompted the use of transmission electron microscopy to reveal the presence and appearance of the vesicles (Andaloussi *et al.*, 2013; Cline and Radic, 2004; György *et al.*, 2011). Studies by Oblak *et al.*, (2003, 2010), also demonstrated the influence of QASs on the plasma membrane of yeasts using transmission electron microscopy, while Wolf *et al.*, (2014) demonstrated the transfer of single and multiple vesicles to the extracellular environment by crossing the cell wall. It is reported that the secretory extracellular vesicles may be responsible for the release of virulence

determinants extra-cellularly by transporting the virulence associated components such as proteins (lipases, proteases), nucleic acids and polysaccharides to the extra cellular medium indicating its key role in pathogenesis (Peres da Silva *et al.*, 2015; Vallejo *et al.*, 2011).

In the present study, images obtained by transmission electron microscopy supported and elaborated on the morphological changes of the *Candida* cell observed by scanning electron microscopy. It was determined that K21 exhibited a stronger fungicidal activity on the FCZ-resistant and FCZ-susceptible *Candida* species when compared to FCZ, by acting on the cell membrane of the species. Moreover, the combination therapy of K21 and FCZ resulted in a highly powerful outcome with the fungicidal activity initiating at 6 hours rather than 24 hours.



CHAPTER 4

GENERAL DISCUSSION

4.1 BACKGROUND

Candidiasis, caused by *Candida*, originates by the interactions of endogenic commensal strains inhabiting the oral cavity, gastrointestinal tract and genitourinary system (Bharathi and Rani, 2011). The frequency of fungal infections varies in different countries and the inherent host factors establish the infections. Since *Candida* infections are mostly seen in high risk and ill patients, early identification of specific *Candida* strains causing candidiasis could prevent any delay in the provision of appropriate antifungal drugs. A study conducted by Magalhaes *et al.*, (2015) in Sao Luis-Maranhao hospital, Brazil, exhibited the prevalence of invasive fungal infections among patients in the hospital environment and re-inforced the need for *Candida* species identification and improved treatment options. The prolonged immunosuppressive therapies, indwelling intravascular devices and concomitant use of wide spectrum antibiotics may result in selective pressure on the commensal flora leading to yeast overgrowth, causing systemic and oral candidiasis in hospitalized patients. The ongoing increase in antifungal resistant *Candida* species, the deficient drug import to the cells and the reduced number of available drugs has led to the exploration of advanced antifungal compounds with a significant role in overcoming drug resistance.

4.2 Antifungal Susceptibility Testing

The azole, fluconazole, being fungistatic creates an opportunity for the development of acquired resistance among the *Candida* species during long term treatment (Berkow and

Lockhart, 2017). Studies have reported poorer outcomes among patients with antifungal drug resistant *Candida* infections compared to those suffering with antifungal drug susceptible *Candida* infections (Alexander *et al.*, 2013; Baddley *et al.*, 2008). Resistance to FCZ occurs via acquisition of a new resistant genotype of *C. albicans* or by the resistance which emerged in a previously susceptible strain.

K21 is a quaternary ammonium silane with its antimicrobial properties thus inhibiting the growth of various virulent microbes. According to study reports, the antifungal mechanism of QACs exhibits an electrostatic interaction with the fungal cell membrane ultimately causing cell lysis (Leclercq *et al.*, 2012; Nurdin *et al.*, 1993). A new class of amphiphilic compounds, gemini quaternary ammonium chlorides with 10 carbon atoms within the alkyl chain, inhibited the action of *C. albicans* by lysis of the cell membrane and prevents biofilm formation on host tissues (Oblak *et al.*, 2013). It is documented that the pathogens when treated with QACs, display a sequence of events such as the initial absorption and penetration of the compound into the cell and its reaction with the cell membrane, leading to membrane disorganisation and extracellular leakage of the low molecular weight material with protein and nucleic acid degradation. All these events eventually result in lysis of the cell wall by the action of autolytic enzymes (McDonnell and Russell, 1999).

Due to the exhaustive use of antifungal therapies, in the prophylaxis of immunosuppressed HIV-infected individuals, the chances of azole drug resistance continue to emerge. With patients suffering with severe HIV infections and their progression to AIDS, introduction of K21 as a novel antifungal agent in inhibiting the growth of pathogenic *Candida* species and preventing their infections will be a boon to the emerging field of drug discovery.

The results outlined in this study are encouraging because they demonstrate the antifungal action of K21 against a wide range of FCZ-resistant, FCZ-intermediate and FCZ-susceptible

Candida species, thus establishing the effectiveness of K21 to eliminate *Candida*. K21 was found to have a stronger antifungal effect on the *C. albicans* and non-*C. albicans* species tested in the study with a lesser MIC concentration when compared to the higher MIC concentrations of FCZ, especially on the FCZ-resistant *Candida* species. Some of the present antifungal drugs cause host toxicities and in severely compromised patients, interactions with other drugs and host toxicities cannot be permitted (Perfect, 2016). The fact that K21 has been found to be non-toxic to human cells could be regarded as a superior property of the compound in the quest to obtain outstanding treatment or management outcomes. Gulve *et al.*, (2016) established the absence of K21 cytotoxicity at 1.35 μ M or lower concentrations on SupT-1 cell and on freshly isolated PBMCs even after 5 days of exposure. Though the antimicrobial properties of QACs are not well understood, it has been stated that they solubilize the phospholipid bilayers leading to cell lysis (Salton, 1968). Furthermore, Daood *et al.*, (2017), in his study on pre-treatment of dentin with K21, revealed that 2% QAS exhibited less cytotoxicity to human dental pulp stem cells when compared to 2% chlorhexidine. Quaternary ammonium methacryloxy silicate molecule (QAMS) incorporated orthodontic acrylic resins has contact-killing antimicrobial properties and are proven to be non-cytotoxic to the host tissues (Gong *et al.*, 2012b). The solubilized K21 in a mixture of 0.025% mixture of ethanol and 0.95% acetone was reported to be non-toxic to human cells (Chernos *et al.*, 1972; Gulve *et al.*, 2016).

C. albicans (ATCC 90028) and *C. glabrata* (ATCC 26512) were elected to determine the rate of fungicidal action of K21, because these are the predominant species responsible for causing widespread fungal infection in both healthy and immunocompromised patients (Leroy *et al.*, 2009), with *C. glabrata* being extremely difficult to treat due to its high resistance to FCZ. K21 exhibited its fungicidal activity at 2 hours with a MIC of 62.48

$\mu\text{g/mL}$, while an increase in cell growth was noted at 0.5MIC and 0.25MIC along with the control.

According to Klepser *et al.*, (1997), the time-kill assay recognizes the count of the viable cells and determines the fungistatic or fungicidal effect of the drug on the cell growth, thus analysing the interaction between the drug and the *Candida* cells and the relationship between the concentration and activity over time. The time-kill assay conducted on SCY-078, a novel oral glucan synthase inhibitor, exhibited 50% reduction in CFU/mL of *Candida* species growth in 1 - 2.8 hours and a fungicidal effect at 12.1 - 21.8 hours at $\geq 4\text{MIC}$ (Scoreaux *et al.*, 2017). In their study, *C. albicans* (ATCC 90028) showed 1.7log₁₀ reduction in CFU/mL and FCZ showed a fungistatic effect on *Candida* growth. Leite *et al.*, (2014) in an evaluation on the antifungal effect of Citral by broth microdilution assay, reported a MIC of 64 $\mu\text{g/mL}$ against *C. albicans* with a fungicidal activity at 4 hours. Citral was found to exhibit its antifungal activity by targeting the fungal cell membrane (Harris, 2002). K21 could be considered superior to these studies by means of its fungicidal action at 2 hours.

Multidrug therapy makes the biological targets less competent to counteract with the simultaneous action of two or more drugs and makes the treatment highly efficient and superior than the mono-target drugs. The concept of synergy has become a present-day challenge in the evolution of new therapeutic agents (Lehar *et al.*, 2007). The FIC indices established the stronger antifungal action of K21 and FCZ in combination rather than the individual treatment with K21 and FCZ. There was a substantial reduction in the individual MICs of K21 and FCZ when they were used as a combination therapy. Treatment of fungal infections with newer antimicrobial agents or combination of antimicrobial therapies has become progressively dominant in the eradication of these infections due to the presence of

the existing antimicrobial resistance among the *Candida* species to the current antifungal drugs.

The Σ FICI of *C. albicans* (ATCC 90028) was 1 $\mu\text{g/mL}$ and the lowest effective concentrations of the combinations therapy for the species were 31.24 $\mu\text{g/mL}$ of K21 plus 8 $\mu\text{g/mL}$ of FCZ. However, synergy of combinations determined by the time-kill assay revealed a statistical significance for *C. albicans* (ATCC 90028) between the various concentrations and the time. A statistical significance in the growth of the cells was identified at combined concentrations of 0.5MIC and 0.25MIC between K21 and FCZ at 8 hours, compared to the growth of the cells without any treatment. This shows that at lower concentrations the combination of K21 and FCZ could provide a beneficial result by eliminating *Candida*. Moreover, at 12 hours, 0.25MIC of K21 showed a significant difference with the combination therapy. This further explains that combination therapy is more effective than administering the single agent alone. There were no significant differences recognized at other concentrations.

Similar synergy has previously been reported. An *in vitro* study by Yu *et al.*, (2011) reported a synergistic interaction between Triclosan, an antimicrobial compound with FCZ against *C. albicans*. Liu *et al.*, (2016c) reported an *in vitro* synergistic action between FCZ and calcium channel blockers amlodipine, nifedipine, benidipine and flunarizine against FCZ-resistant *C. albicans* isolates through a process not related to the inactivation of efflux pumps. Shekhar-Guturja *et al.*, (2016) described an effective interaction between the natural substance beauvericin with traditional antifungals such as azoles, in FCZ-resistant *C. albicans* by inhibiting their efflux pump and morphogenesis. Several natural molecules manifesting antifungal activity exhibit synergism with traditional antifungal drugs *in vitro*.

In the current study, a significant result was also noted for *C. albicans* (NCPF 3281) with a significance along the rows ($p < 0.0001$) and the columns ($p = 0.0151$) suggesting synergism by the time-kill assay, in contrast to the Σ FICI showing indifference. At 4 hours, a difference was found between the control and the combinations at 0.5MIC followed by 0.5MIC and 0.25MIC at 6 hours and 8 hours. The combination therapy acted at early hours reduced the cell growth while the control showed a steady increase in the growth of the cells up to 24 hours.

The FICI in the present study demonstrated the effectiveness of combination therapy over monotherapy and are crucial due to the development of increased frequency in cross-resistance among the *Candida* species. The highlight was the absence of antagonism between the concentrations of K21 and FCZ in any of the strains tested. This could indicate that K21 and FCZ interact efficiently with each other and thus a combination therapy with a synergistic effect hampers the resistance of the microorganisms against certain drugs and benefits the health of the host by reducing the antimicrobial dosages, as well as any adverse or toxic side-effects that may be caused by the over usage of the antimicrobials, while also making it more cost effective for the patients (Bag and Chattopadhyay., 2017; Sardi *et al.*, 2016; Wang *et al.*, 2016). Reports have indicated a successful correlation of Σ FIC indices by checkerboard dilutions with clinical evidence of optimal outcomes in refractory *Candida* infections (Soares *et al.*, 2008).

When the growth of the resistant *C. glabrata* (ATCC 26512) was analysed at various concentrations over time, a difference was found in the cell growth at 0.25MIC combination therapy at 24 hours compared with monotherapy. It is to be noted that, even though the individual MIC of the resistant *C. glabrata* (ATCC 26512) and *C. krusei* (ATCC 2159) for K21 and FCZ was high, the growth of the cells were inhibited at a relatively lower MIC concentration when treated in combination with K21 and FCZ.

Our study also agrees with the *in vitro* study determining the antifungal and synergistic effect of Glabridin, an active isoflavane, with FCZ. Glabridin exhibited its broad spectrum antifungal activity at high concentrations of MIC ranging from 16 µg/mL - 64 µg/mL. The combination therapy with FCZ revealed a potent synergistic antifungal effect against drug-resistant *C. tropicalis*, *C. albicans*, *C. krusei* and *C. parapsilosis* at lower MIC concentrations ranging from 1 µg/mL - 16 µg/mL, as interpreted by FICI (Liu *et al.*, 2014).

Based on the FICI, a definite synergistic effect was observed against *C. dubliniensis* (NCPF 3949a), *C. tropicalis* (ATCC 950) and *C. lusitaniae* (ATCC 34449) between the combined concentrations of K21 and FCZ. Low MIC values were observed at ΣFICI for all of the 9 type strains indicating the potency of combination therapy over monotherapy. As per the results of the study, K21 enhances the antifungal effect of FCZ.

Invasive candidiasis caused by NAC species such as *C. glabrata*, *C. krusei*, *C. tropicalis* or *C. parapsilosis* create a concern due to the higher incidence of mortality and antifungal resistance compared to those by *C. albicans* and therefore, exacerbates the need for new antifungal drugs or new treatments against *Candida* infection (Sardi *et al.*, 2013; Silva *et al.*, 2012). Similar to the higher MICs found in the antifungal susceptibility assay for K21, the indifferent interaction shown by the checkerboard assay between K21 and FCZ with *C. krusei* (ATCC 2159) and *C. glabrata* (ATCC 26512) may be due to the resistant mechanisms of the strains. In other studies, Menezes *et al.*, (2012) reported a synergistic effect between simvastatin and fluconazole against *C. albicans* using the broth microdilution assay FIC indices, while Liu *et al.*, (2016) established a synergistic effect of fluconazole with calcium channel blockers by conducting the broth microdilution and time-kill assays.

The azole-resistant and azole-susceptible *Candida* species were synergistically inhibited by K21 + FCZ combinations, though their exact mechanisms when acting synergistically needs to be explored. The lower MICs of the combinations were obtained with concentrations nearly one-half to a quarter lower than concentration of the individual compounds. An *in vitro* study on the activities of two novel azole compounds (aryl-1, 2, 4-triazol-3-ylthio analogues of FCZ [ATTAF-1 and ATTAF-2]) also exhibited synergistic effects in combination therapy with FCZ against the FCZ-resistant and FCZ-susceptible clinical *Candida* isolates (Fakhim *et al.*, 2017). With the introduction of combination therapy of antifungal agents, a close interaction between the drugs takes place enhancing the action of one by another. There may be pharmacological benefits with one drug eliminating the infection from one site of the body while the other eliminates it from a different site of the body, thus aiming to prevent or delay the occurrence of new resistant pathogenic species *in vivo*. Evidence of time-kill studies have enlightened the rate and extent of antifungal activities of the drugs and the associated potential synergism or antagonism between the antifungal agents administered.

To determine the antifungal combinations against *Candida* species, time-kill assays are considered superior to checkerboard studies, though the procedure is time consuming and labour intensive (Lewis *et al.*, 2002; Klepser *et al.*, 1998). Even though an indifferent effect was demonstrated for *C. glabrata* (ATCC 26512) and *C. dubliniensis* (NCPF 3949a) based on the FICI, a synergistic effect was observed along the various concentrations over time as depicted by the time-kill assay.

Administration of highly-active antiretroviral therapy in HIV-infected people has reduced the severity of oral *Candida* infection in the developed countries. However the majority of HIV-infected individuals found in the developing country are deprived of HAART and antifungal therapies and therefore, are at risk of severe increase in HIV associated *Candida* infections. A

desperate requirement of novel antifungal compounds is obligatory to prevent any possible systemic *Candida* infections and also to avoid transmission of drug-resistant *Candida* to the family members (Porter, 2003).

Various studies have been conducted with the intention of the development of novel antifungal agents with better quality and efficacy. A recent study by Lakota *et al.*, (2018), reported the *in vitro* antifungal activity of Rezafungin (CD101), a novel echinocandin antifungal agent that is currently in development, against azole-resistant and echinocandin-resistant isolates of *C. albicans* and *C. glabrata*. Another recent study by Hargrove *et al.*, (2017), reported the antifungal efficacy of VT-1161 (oteseconazole;(R)-2-(2,4-difluorophenyl)-1,1-difluoro-3-(1H-tetrazol-1-yl)-1-(5-(4-(2,2,2-trifluoroethoxy)phenyl)pyridin-2-yl)propan-2-ol) against the intrinsically FCZ-resistant *C. krusei* and *C. glabrata*. It has been reported that structural variations in the azoles have been responsible for the development of cross-resistance among the *Candida* species (Cuenca-Estrella *et al.*, 2006). Novel compounds such as APX001A and APX2020 in combination with FCZ exhibited synergism with FICI of 0.37 for both the compounds. APX001A and its prodrug APX001, that is currently in clinical development, showed *in vitro* antifungal activity against invasive fungal infections (Shaw *et al.*, 2018). An *in vitro* study on the synergism between calcium channel blockers such as amlodipine, nifedipine, benidipine and flunarizine with FCZ exhibited FICI<0.5 (Liu *et al.*, 2016c). In a combination study including 16 µg/mL of licofelone and 1 µg/mL of FCZ, a strong synergistic antifungal activity against resistant *C. albicans* was demonstrated (Liu *et al.*, 2017). Cyclosporin A, an immunosuppressant drug, exhibited synergism with FCZ showing a 2.51 log₁₀ reduction in the growth of resistant *C. albicans* compared with FCZ alone (Li *et al.*, 2008).

To our knowledge, there is no investigation performed on the antifungal effect of the ethoxylated version of K21 and the combination of K21 and FCZ to determine their synergistic action. To date, since no susceptibility breakpoints have been established for K21,

this is the first study that determines the MIC values of K21 using the CLSI broth microdilution antifungal susceptibility testing. As per the study, K21 alone or in combination with FCZ has proven its effectiveness against FCZ-resistant, FCZ-intermediate and FCZ-susceptible *Candida* species. Hence it can be considered that the present study renders the evolution of the novel compound K21 as a possible alternative to FCZ.



4.3 Electron microscopy and Sap protein expression of *Candida*

Antifungal agents exert their antifungal activity by targeting multiple sites on the fungal cell. The pathogenicity of *Candida* would be distinctly clear by understanding the virulence determinants of these species and the exploration of novel classes of antifungal drugs. In addition, drug targets may be improved by the characterization of *Candida* virulence factors, since most of the antimicrobials are either synthesized from natural products or they are chemically synthesized with specific activity towards the unique targets of the pathogens (Harvey *et al.*, 2015).

The scanning and transmission electron microscopy in this study, demonstrated the mode of action of K21 on the structure of the *Candida* cells with different events taking place at different hours. As a result, it was established that K21 is undeniably beneficial in the elimination of FCZ-resistant *Candida* species due to its fungicidal activity by acting on the fungal cell membrane and disruption of the fungal cells.

4.3.1 Scanning Electron Microscopy

Any surface alterations or morphological changes in the *Candida* cells after treatment with the antifungal drugs may be observed by microscopic analysis, determining the action of the drug. Furlaneto *et al.*, (2012a) used scanning electron microscopy to analyse the architecture of whole colonies of *C. tropicalis* as it reveals the ultrastructural characteristics and morphology of *Candida* species. Scanning electron microscopic analysis demonstrated the presence of flocculent extracellular materials concealing the cell surface of *C. tropicalis* connecting the neighbouring cells similar to the results of the present study exhibiting the

morphology of *Candida* cells with extracellular material deposits on the cell surface connecting the neighbouring cells after treatment with K21 and K21 + FCZ.

Scanning electron microscopy revealed that exposure to K21 resulted in total lysis of the cells with a flocculent release of extracellular vesicles at 24 hours. Extracellular vesicles released by the fungal cells has been associated with the presence of atypical molecules on the cell wall and serves as a cellular communication with the transport of virulence associated factors to the extracellular space resulting in an interaction between fungi with other organisms or with the fungal cell themselves, thus being involved in pathogenesis and commensalism (Nimrichter *et al.*, 2016; Rizzo *et al.*, 2017; Vargas *et al.*, 2015). They are divided into three major compartments such as endosomes that are formed by the invagination of the endosomal membrane, microvesicles formed by the outward budding of the plasma membrane and lastly, the apoptotic bodies that are formed by the blebbing of the plasma membranes which may result in the release of apoptotic bodies extracellularly (Pugholm *et al.*, 2015). The cells in the present study exhibited the budding of plasma membrane with the release of blebs and apoptotic bodies extracellularly.

Similar to the present study exhibiting the rough and wrinkled cell surface of the *Candida* species due to the treatment with FCZ, several other studies reported that *C. albicans* exposed to FCZ or antimycotics exhibited a rough and wrinkled cell surface with an absence of hyphae formation (Bachmann *et al.*, 2002; Nasution and Basri, 2017; Samaranayake *et al.*, 2005). Following 24 hours of treatment with K21 + FCZ in this study, the *Candida* cells appeared flatter and elongated with irregularities in the bud scars on the cell surface, similar to the study by Rajeh *et al.*, (2010) which reported that affected cells demonstrated a lying position with changes in the appearance of buds when subjected to antifungal treatments.

The combination therapy of K21 and FCZ with *C. albicans* (ATCC 90028), *C. glabrata* (ATCC 26512) and *C. krusei* (ATCC 2159) exhibited considerable morphological alterations

with cells undergoing different stages of cell distortion and cell death. An osmotic imbalance may be created by fluconazole by inducing permeability changes resulting in the disruption of the fluidity of the cell wall and the cytoplasm. The morphological alterations of the cells such as cell distortion and changes in cell size may be due to the cell permeability. De Nollin and Borgers, (1975) stated that initial ultrastructural alterations are usually localized at the cell wall or the cell membrane followed by changes in the interior of the cells.

A 12 hour exposure of *C. albicans* (MIC 64 µg/mL), *C. glabrata* (MIC 16 µg/mL) and *C. dubliniensis* (MIC 32 µg/mL) to magnolol, a natural compound, exhibited similar morphological changes of the *Candida* cells such as cell deformation with convolutions, deep furrows and wrinkled cell surfaces with the presence of lytic material in the form of vesicles (Behbehani *et al.*, 2017). Shinobu-Mesquita *et al.*, (2015) determined the cellular structural changes in *C. albicans* (ATCC 90028) by scanning electron microscopy, following the treatment with the hydroalcoholic extract from *Sapindus saponaria L* and reported that the *C. albicans* reduced in amount after 30 minutes and showed convolutions and irregularities on the cell surface after 120 minutes.

UNIVERSITY of the
WESTERN CAPE

4.3.2 Transmission Electron Microscopy

The transmission micrographs of *Candida* cells demonstrated the fungicidal action of K21 with cell membrane disruption that appeared detached from the cell wall. There were alterations in the assembly of intracellular organelles with nucleus shrinkage and electron-dense accumulation. The plasma membrane forms the primary target for quaternary ammonium salts by reacting with the phospholipids components in the membrane exhibiting higher plasma membrane permeability for the extrusion of cell content.

Since the *Candida* cells were examined at their 0.5MIC sub-inhibitory concentrations, some of the cells were dead and others were deformed by the action of K21. The cells treated with K21 showed disruption of the cell interior with a lytic appearance and the deposition of fats or lipids within the cytoplasm. Lipids may also be considered as a virulence factor in fungal pathogenesis, being implicated in drug resistance, biofilm formation and vesicle formation (Szwarc *et al.*, 2018).

The vesicles that were found in the cell wall and in the extracellular space appeared in various sizes and patterns may be supported by the explanation that the sequential sections involved in the transmission electron microscopy alter the dimensional accuracy of the extracellular vesicles (Vargas *et al.*, 2015) and the variations in the vesicular density may suggest the heterogeneity in vesicular contents. A study conducted by Albuquerque *et al.*, (2008) demonstrated the presence of extracellular vesicles related to the transport of macromolecules and virulence in fungi and suggested that the process could be a target for the development of novel therapeutics. Similarly the release of extracellular vesicles by the *Candida* cell may also act as a target for the antifungal action of K21 and could determine the pathogenesis of the infection by *Candida*. Their reports on the transmission micrographs of *C. albicans*, and *C. parapsilosis* exhibited the presence of vesicular secretion inside the cell

wall and the extracellular environment with the presence of the vesicles indicating the pathogenesis of *C. albicans*.

Vargas *et al.*, (2015) used extracellular vesicles from *C. albicans* as a pre-treatment in a *Galleria mellonella* model of infection minimizing the cell viability. In their study, they demonstrated the vesicles of *C. albicans* as structurally complex and immunologically active and the transmission micrographs demonstrated the presence of extracellular vesicles in the periplasmic and extracellular spaces. The formation of extracellular vesicles in fungi involves the contribution of multivesicular bodies and budding of the membrane (Rodrigues *et al.*, 2000; Wolf *et al.*, 2014) which was evident in our study. Wolf and colleagues (2014) used electron microscopy to demonstrate the interaction of single and multiple vesicles with the extracellular environment by crossing the cell wall. Baltazar *et al.*, (2016) reported that binding of monoclonal antibodies targeting Hsp60 to fungal cells, altered the vesicular size and the activity of the vesicular enzymes which in turn may alter the host defence susceptibility. It was established that echinocandins target the cell wall and fluconazole targets the plasma membrane inducing various stresses causing the formation of reactive oxygen species that plays a pivotal role in apoptosis (Sharon *et al.*, 2009).

An investigation of resistant mutant cells of *Saccharomyces cerevisiae* by quaternary ammonium salt, IM ((N-(dodecyloxycarbonylmethyl)-N,N,N-trimethyl ammonium chloride) revealed an increased cell wall thickness, deposition of lipid droplets and detachment of cell wall from the cytoplasm (Oblak *et al.*, 2016; 2010). They reported that the increased amount of unsaturated fatty acids in the cytoplasm may be associated with the amount of drug penetrating the cell causing cell growth inhibition. A comparison of our study with these studies, suggests that the presence of fatty deposits in the cytoplasm may be related to the amount of K21 penetrating the cell causing cell death.

On treatment with K21, the fungal cells showed the presence of melanin deposits along the cell membrane which may indicate the virulence properties of melanin since melanin plays a role in antifungal resistance and survival of the cells by making the pathogens less susceptible to the antimicrobial agents (Nosanchuk *et al.*, 2015).

The results of the present study were also in agreement with the *in vitro* study conducted by Martínez *et al.*, (2014), that reported on the action of essential oils containing terpenes and their effect on the morphology of *C. albicans* with total destruction of the fungal cells. The scanning and transmission micrographs of the combination of terpenes and Coe-Comfort tissue conditioner demonstrated similar findings such as an increase in cell size with the presence of intracytoplasmic vacuoles. In another study (Jothy *et al.*, 2012), a 24 hour exposure of *C. albicans* to *Cassia fistula* seed extract showed irregular cells with a rough appearance and surface invaginations in the scanning electron micrographs and disruption of the cytoplasmic membrane with cell wall alterations in the transmission electron micrographs. Moreover, the cells were present in clusters of interconnected cells, similar to the cells which appeared in the present study when exposed to K21 and FCZ.

As revealed in the reports of Weerasinghe and Buja, (2012) and Kroemer *et al.*, (2009), the fungal cells in the current study underwent several events leading to the death of the cells. The cells initially exhibited a mechanism of autophagy in an attempt to survive by budding and forming biofilms. The cell surface showed the presence of flocculent deposits of extracellular vesicles and multiple bud scars, later followed by the disruption of the cell membrane with bleb formation resulting in oncosis of the cells. Eventually there was apoptosis of the cell with considerable cell shrinkage and the release of apoptotic bodies or lytic cell remnants extracellularly.

The increased lipid deposition and vacuoles with condensation of chromatin and the dysfunction of mitochondria along with electron dense deposits intracellularly, indicate the process of apoptosis of the *Candida* cells due to the treatment with K21. Apoptosis is associated with the response of the cells to oxidative stress at the plasma membrane and the cell wall, suggesting the loss of cell viability due to the antifungal treatment (Kannan and Jain, 2000).



4.3.3 Effect of K21 on Sap expression in *Candida*

C. albicans strains produce high amounts of proteinase which intensely adhere to the human buccal epithelial cells compared to the strains producing low proteinase (Ghannoum and Elteen, 1986). Saps are considered to be among the most important virulence factors of *C. albicans* (Moran *et al.*, 2011). Because they are involved in the adhesion of *C. albicans* to tooth surfaces and the degradation of extracellular matrix and proteins, they have been associated with caries formation (Li *et al.*, 2014). The adherence of *Candida* cells takes place by using Saps to target the host cell structure thus altering the surface proteins or ligands of epithelial cells (Monod *et al.*, 2010). An *in vitro* study by Mayr *et al.* (2005) exhibited an antifungal effect of 5-Hydroxytryptamine by inhibiting the growth of *C. albicans* and reducing the production of Saps. The present study investigated whether K21 would inhibit Sap production, thereby enhancing the activity of K21.

Saps 1-3 are capable of being active at a pH 2.0-7.0 while Saps 4-6 are active at a pH 5.0-7.0 (Calderone and Fonzi, 2001; Dalle *et al.*, 2010; Naglik *et al.*, 2004;) and based on structural analysis, it has been reported the Saps 1-8 are secreted extracellularly (Naglik *et al.*, 2003). There are four SAP genes in *C. tropicalis* (Sapt 1 - Sapt 4), eight in *C. dubliniensis* (Sapcd 1 - Sapcd 4; Sapcd 7 - Sapcd 10) and three in *C. parapsilosis* (Sapp 1 - Sapp 3) (Pichová *et al.*, 2001). *C. tropicalis* Sapt 4 belongs to the Sap 1 - Sap 3 of *C. albicans* family whereas Sapt 1 belongs to Sap 8 family and Sapt 2 and Sapt 3 have apparently no orthologues in *C. albicans*. Moreover, *C. tropicalis* do not possess Sap 4 - Sap 6 and Sap 7. *C. dubliniensis* show orthologues in *C. albicans* and belongs to Sap 1 - Sap 3 while Sap 5 and Sap 6 genomes are missing in *C. dubliniensis* except only for the presence of Sap 4 (SAPD 4). Apparently, *C. parapsilosis* possess only Sap 8, Sap 9 and Sap 10 genes and did not possess Sap 1 - Sap 3 and Sap 4 - Sap 6 genes of *C. albicans* and hence no expression reported (Monod *et al.*,

2010). The studies indicated that only *C. dubliniensis* and *C. tropicalis* are related to the Sap 1 - Sap 3 in *C. albicans* family. Correspondingly, the findings of the current study showed the presence of Sap 1-3 and absence of Sap 4-6 in *C. dubliniensis* and *C. tropicalis*, while in *C. albicans* there were abundant expressions of Sap 1-3 proteins with appearance of few non-specific Sap 4-6 proteins.

C. albicans strains isolated from HIV-positive patients with oral candidiasis showed increased Sap activity compared to the HIV-negative patients (Wu *et al.*, 1996). Naglik *et al.*, (2003) reported the dissimilarity between HIV-positive and HIV-negative individuals in the production of Sap proteins which may be due to the direct binding of HIV proteins to *Candida* cells, since HIV proteinases and *Candida* proteinases belong to the same aspartyl proteinase family. Borg-von Zepelin (2002) reported on the increased adherence of *C. dubliniensis* in HIV-infected patients treated with fluconazole, associated with increased proteinase antigen expression. The increased Sap expression in HIV patients enduring with oral candidiasis may be controlled by treating with K21 considering its fungicidal property.

Many studies have reported the introduction of HIV aspartic protease inhibitors mainly pepstatin A, used in HAART for AIDS patients, as a treatment for mucosal candidiasis acting as Sap 1-3 inhibitors (Arribas *et al.*, 2000; Egger *et al.*, 1997; Ledergerber *et al.*, 1999). It was due to the indirect action of HIV aspartic protease inhibitors on inhibiting the *C. albicans* Saps that leads to a decline in the oropharyngeal candidiasis along with an improvement in their immune system. Other HIV protease inhibitors such as ritonavir and saquinavir had characteristic properties of inhibiting *Candida* strains expressing Sap 1-3, however they did not have an inhibitory effect on other Sap expressing *Candida* strains (Monod *et al.*, 2010).

In the current study, immuno-electron microscopy of K21 treated *Candida* species with two polyclonal antibodies specifically directed against Sap 1-3 and Sap 4-6, exhibited significant

immunolabelling of the *Candida* cells indicating Sap enzyme expression. *C. albicans* showed increased expression of Sap 1-3 with increased deposits of gold particles along the cell membrane and in the cytoplasm and also along the cell membrane of the budding cells. Labelling with the Sap 1-3 antibody demonstrated immunoreactivity localised and restricted to the cell membrane in contrast to the cell wall where a limited amount of labelling was noted. Hajjar *et al.*, (2015) demonstrated inhibition of Saps in *C. albicans* by exposure to triangular gold nanoparticles. The results of our study confirmed that the mode of action of K21 is predominantly on the cell membrane and cytoplasm with the expression of Saps marked by the deposition of gold particles. A study by Shirai *et al.*, (2009) on the antifungal activity of a quaternary ammonium salt, demonstrated destruction of the intracellular organelles of the yeast cell with the preservation of the outer structure of the cell. The fungal cell membrane acts as a barrier to environmental stress and therefore cell membrane integrity is essential for the cell survival.

Sap 1-3 and Sap 4-6 proteins facilitate the virulence of *C. albicans* in superficial candidiasis and systemic infections respectively suggesting that Sap 1-3 may be primarily responsible for the pathogenicity during oral or cutaneous infections caused by *C. albicans* (Schaller *et al.*, 2001). An *in-vitro* study focused on SAP gene expression demonstrated that Sap 1 and Sap 3 are expressed in the switching phase of the yeast while Sap 2 is specifically expressed in media with proteins as the sole nitrogen source (White and Agabian, 1995).

The Sap 4-6 proteins in *C. albicans* consist of a tripeptide called, RGD motif, a cell surface receptor for interaction, which explains the expression of SAP 4-6 genes on the adherent hyphal cells (Hube *et al.*, 1994; White and Agabian, 1995). The very little amount of non-specific gold labelling of Sap 4-6 in *C. albicans* indicated that the pattern of Sap 4-6 expression may be relevant only during hyphal invasion or penetration. It could also indicate that the Sap proteins were not able to eliminate the action of K21. However, our study did not

exhibit any specific gold labelling in *C. tropicalis* and *C. dubliniensis* indicating the absence of Sap 4-6 expression.

A study by Ikonomova *et al.*, (2018) evaluated the susceptibility of the peptide variants of Histatin 5 to proteolysis by *C. albicans* Saps because Saps are known to eliminate the antifungal properties of Histatin 5. The results of their study reported resistance of the peptide variants to proteolysis with a prolonged antimicrobial efficiency in presence of Saps. Keikha *et al.*, (2017) reported reduction in SAP 4 - SAP 6 genes expression of *C. albicans* after treatment with designed NK95 peptide and Caspofungin. Jalal *et al.*, (2019) and Hamid *et al.*, (2018) demonstrated the inhibition of Saps in *Candida albicans* and non-*albicans* species by the antifungal action of silver nanoparticles. The above studies demonstrated the inhibition of Sap expression by the action of the antifungal compounds. Likewise it may be considered that the ethoxylated version of K21 may inhibit the expression of Saps continuing its antimicrobial efficiency in the elimination of fungal infections.

Even though *C. dubliniensis* are so phenotypically alike to *C. albicans*, several systemic and mucosal comparative studies clearly indicated the highly significant and pathogenic behaviour of *C. albicans* compared to *C. dubliniensis* (Koga-Ito *et al.*, 2011; Spiering *et al.*, 2010). The pattern of Sap expression during oral and cutaneous candidiasis and in *C. albicans* pleomorphic forms has been demonstrated at the ultrastructural level by labelling with the antibodies (Schaller *et al.*, 2001; Staniszewska *et al.*, 2012b).

It is stated that, during infection all Sap proteins (Sap 1-10) are expressed where each Sap protein exhibits multiple functions such as cell growth are induced by Sap 2 while phenotypic switching of the cells are induced by Sap 1 and Sap 3 and the expression of Sap 4, Sap 5 and Sap 6 are associated with the hyphal formation. However, the time and the level of Sap expression may vary with different stages of infection (Naglik *et al.*, 2008; 2004). According to the current study, it is distinctly vivid that with the increase in the stages of HIV infection,

there will be an increase in the expression of Sap proteins indicating the virulence of the Saps.

Schaller *et al* (1999a), in an *in vivo* study, suggested the expression of Sap 1-3 within the cell cytoplasm might be an initial stage towards the infection process and Sap secretion was achieved by the fusion of the vesicles with the plasma membrane causing membrane invaginations and protein transport. They reported intensive gold labelling on the cytoplasm and in close proximity between the plasma membrane and the cell wall of the *Candida* cells localizing the Sap 1-3 expression during human oropharyngeal candidiasis using a monoclonal antibody directed against the proteins. Similar to the present study, Schaller *et al.*, (2001) conducted an *in vivo* study localising the expression of Sap 1-3 and Sap 4-6 using post-embedding immunogold labelling. Specific polyclonal antibodies to Sap 1-3 (α - Sap 2) and Sap 4-6 (α - Sap 6F) revealed the intense Sap 1-3 localisation adjacent to the cell wall and the cytoplasmic membrane of *C. albicans* and Sap 4-6 showing very little gold particles in a few *C. albicans* cells during oral candidiasis infection. As a result of their study, it was reported that Sap 1-3 plays a direct role in superficial infections while Sap 4-6 plays its role in penetrating into deeper tissues. Ultrastructural localisation of Sap 1-3 was reported during reconstituted human epithelium infection in the fungal cell wall close to the epithelial cells and may cause tissue damage in the epithelium and also during human oropharyngeal candidiasis in HIV patients (Schaller *et al.*, 1999a; 1999b).

In agreement with the above study, our study exhibited expression of Sap 1-3 along the cell cytoplasm. However, they did not expose the cells to any antifungal agent in contrast to our study where the cells were treated with K21 determining its antifungal action and its effect on the virulence of Saps which makes our study unique. The heavy expression of Sap 1-3 proteins within the cells after 24 hours of treatment with K21 may show the virulent behaviour of Saps. Our results further established that K21 antimicrobial compound targets

predominantly on the cytoplasm and cell membrane of the *Candida* cells with modest action on the cell wall suggesting the mode of fungicidal action of the compound by cell lysis indicated by the cell membrane disruption. This could further suggest that K21 acts on the Sap expression intracellularly and along the cell membrane resulting in the death of the cells. Blockage of *C. albicans* Saps may debilitate the pathogenic action of the *Candida* thus reducing the infection. Since, the immense growth of *Candida* and fungal infections are due to the highly resistant mechanisms of the species towards the existing antifungal agents, recent approaches are focused on the development of novel antifungal agents that target the virulence mechanisms of the species and are indispensable without identification of a molecular target. Morphological profiling of the species further aids in the emergence of new antifungal drugs (Gebre *et al.*, 2015). Due to the scarcity in the development of novel classes of antifungal drugs and the paucity of molecular targets, combination therapy increases the possibility of multiple targets against the effective novel agents (Mukherjee *et al.*, 2005). Therefore, our study coincides with the above reports and targets one of the key virulent factors namely, Saps, which has a pivotal role in the initial stage of fungal infection and further aids in the identification of the mode of antifungal action of K21 acting on the Sap expression.

To the best of our knowledge, this is the first *in vitro* study conducted to determine the mode of action of an antifungal agent by targeting the expression of Sap proteins using immunogold labelling in a *Candida* cell. Development of a novel antifungal agent by identifying and locating the virulence factor causing the infection is indeed an ideal strategy. Based on the results of the electron microscopic study, it could be determined that K21 performs its antifungal activity by distorting the cell membrane of the *Candida* species. K21 could be a replacement or an alternative for FCZ against treating the FCZ-resistant *Candida* species and thus may form a highly beneficial antifungal agent, especially when combined

with FCZ. Moreover, K21 with its fungicidal activity in 2 hours further establishes the competency of the compound.

The ongoing inflation in antifungal resistant *Candida* infections re-sounds the need for novel, effective, non-toxic drugs for the complete elimination of the species. A thorough need for a better integration of old and new diagnostics and a well-designed strategy for antifungal management are imperative. Antifungal susceptibility testing has become an indispensable tool for assessing the activity of antimicrobials against *Candida* and acts as an indicator in the selection of an appropriate antifungal agent capable of providing appropriate therapy in the treatment of disseminated *Candida* infections. The need for the development of innovative antifungal agents with a rapid killing action is critical to prevent the spread of invasive fungal infections and the long-term use of antifungals. K21 may be considered as a curative therapy for reducing or preventing the emergence of resistant *Candida* species and all forms of fungal diseases, particularly in HIV-associated opportunistic infections. The present work opens further avenues to explore the the key targets for the development of an exceedingly productive antimicrobial agent.

4.4 Limitations of the Study

Limitations of the study include our failure to determine whether a similar *in vitro* efficacy of K21 with other antifungal drugs besides fluconazole. The antifungal efficiency of K21 was established, but it is difficult to compare with the effective doses of the antifungals from different studies due to the lack of a standard protocol. Electron micrographs displayed that K21 could be targeting the fungal cell wall and the cell membrane. Moreover, the synergy assay of K21 was not conducted with other novel antifungals which could have determined the potential of K21 by comparing their efficiency in inhibiting the growth of *Candida*. The

combination therapy of K21 with other antifungal drugs may play a significant part in diminishing the antifungal resistance in immunocompromised patients.



UNIVERSITY *of the*
WESTERN CAPE

CHAPTER 5

CONCLUSION

The escalating antifungal drug resistance due to the increased incidence and spectrum of invasive fungal infections has become the paramount consideration in the management of patients. Turnidge and Paterson (2007) defined antifungal resistance as microbiologic resistance or clinical resistance, or as a combination of the two. The emerging resistance to the azole drugs especially FCZ renders it ineffective against the treatment of *C. albicans* and non-*C. albicans* species which led to the development and introduction of novel antifungal compounds or agents with specific targets. To track the resistance in *Candida* species in sub-Saharan Africa, it is mandatory for a proper fungal diagnosis and accurate antifungal susceptibility testing (Mushi *et al.*, 2017) that could aid in the evolution of new and improved antifungal agents.

In the present study, the antifungal susceptibility of a novel antimicrobial compound, K21 against the FCZ-resistant clinical isolates of *Candida* species obtained from HIV-positive patients was evaluated by the broth microdilution method. K21 was established as an effective antifungal agent against the FCZ-resistant, FCZ-intermediate and FCZ-susceptible *Candida* species with a statistically significant result (p value = 0.000) between FCZ and K21. The antifungal efficiency of K21 may be considered beneficial in the development of a novel antifungal agent for the management and therapy of *Candida* infections especially in immunocompromised patients and may be useful as an alternative to FCZ in the treatment of oral candidiasis.

A definite synergism between K21 and FCZ was established in this study with a distinct absence of antagonism between K21 and FCZ. This is the first *in vitro* study conducted on

the antifungal efficacy of ethoxylated quaternary ammonium silane, K21 and to determine the synergistic activity between K21 and FCZ. A potent antifungal agent with a rapid fungicidal activity (within 2 hours) with little or no host toxicity (Gulve *et al.*, 2016) may be considered as an added advantage in considering K21 as an antifungal agent.

The mechanism of action of antifungal drugs takes place by targeting the unique structures of the fungal cell (Roemer and Krysan, 2014). The morphological evaluation of the *Candida* strains was determined by scanning electron microscopy at different time intervals. By 24 hours, the treatment of cells with K21 exhibited complete lysis of the cells demonstrated by cell membrane damage with the presence of flocculent extracellular vesicles on the surface that were believed to be the result of cell lysis. The scanning micrographs of K21 + FCZ demonstrated severely distorted and disintegrated cells with the presence of extracellular vesicles and flocculent extracellular material deposition on the cells.

The mode of action of K21 was confirmed by the transmission electron microscopy of the K21 treated *Candida* cells and clearly indicated that the mechanism of action of K21 was on the cell membrane leading to leakage of the cellular contents. The Sap proteins were considered as the virulent factor of *C. albicans* and therefore, in the study the Sap protein expression was evaluated by post-embedding immunogold labelling of Sap 1-3 and Sap 4-6 proteins in the *Candida* cell. As a result it was observed that there was intensive Sap 1-3 expression on the cell membrane and cytoplasm of the cell while less on the cell wall. However, Sap 4-6 expression was found little or few non-specific in the *Candida* cells. Expression of Sap 1-3 inside the *Candida* cell indicated that the antifungal action of K21 occurred by damaging the cell membrane of the cell leading to cell death.

In the current scenario with the dramatically increasing antimicrobial resistant microbes, the restricted availability of antifungal drugs and the limited number of novel antimicrobials that

are in pre-clinical development or are enduring clinical trials (Denning and Bromley, 2015; Ostrosky-Zeichner *et al.*, 2010), there is indeed an urgent requirement for the development of novel antifungal drugs. The alarmingly high use of antifungal therapies in the prophylaxis of immunosuppressed HIV-infected individuals, the chances of azole drug resistance continues to emerge.

Though it may be accepted that QACs disrupt the cell membrane integrity resulting in cellular content leakage, studies have reported the occurrence of QAC-related antimicrobial resistance at sub-inhibitory concentrations through intrinsic and acquired resistance mechanisms and development of co-resistance and cross resistance between QACs and antibiotics (Buffet-Bataillon *et al.*, 2012; Hegstad *et al.*, 2010). However, more data may be required to determine the contributory factors and the underlying mechanisms causing the antimicrobial resistance by QACs. QACs with lower cytotoxicity with enhanced antimicrobial properties may be well accepted (Jiao *et al.*, 2017).

In the present study, the disruption in the fungal cell membrane and cell structure due to K21, inhibited the cell growth and morphogenesis leading to cell lysis and cell death. The outcome of the study demonstrated K21, as a rapidly acting fungicidal agent. The present study has set a platform for future studies on the development of K21 for *in vivo* studies. Further pharmacological and biochemical evaluations will be beneficial in developing K21 antimicrobial compound as a therapeutic agent, along with investigations on the chronic toxicity studies to ensure the safety of the compound on patients and the potential dosages to be prescribed.

REFERENCES

Abegg, M.A., Lucietto, R., Alabarse, P.V., Mendes, M.F. and Benfato, M.S., 2011. Differential resistance to oxidants and production of hydrolytic enzymes in *Candida albicans*. *Mycopathologia*. 171(1): p35-41.

Ablashi, D., Prusty, B.K., Kimmerling, K., Tay, F.R., Schader, S. and Krueger, G., 2015. *The Antimicrobial Compound, K21, Inhibits Replication of Enveloped and Non-Enveloped DNA and RNA Viruses*. 5th World Congress on Virology. Atlanta, GA. p74.

Abrantes, P.M.D.S., McArthur, C.P. and Africa, C.W.J., 2014. Multi-drug resistant oral *Candida* species isolated from HIV-positive patients in South Africa and Cameroon. *Diagnostic microbiology and infectious disease*. 79(2): p222-227.

Abubakar, I.I., Tillmann, T. and Banerjee, A., 2015. Global, regional, and national age-sex specific all-cause and cause-specific mortality for 240 causes of death, 1990-2013: a systematic analysis for the Global Burden of Disease Study 2013. *Lancet*. 385(9963): p117-171.

Aher, C.S., 2014. Species distribution, virulence factors and antifungal susceptibility profile of *Candida* isolated from oropharyngeal lesions of HIV-infected patients. *Int. J. Curr. Microbiol. App. Sci*. 3(1): p453-460.

Ahlström, B., Thompson, R.A. and Edebo, L., 1999. Loss of bactericidal capacity of long-chain quaternary ammonium compounds with protein at lowered temperature. *Apmis*. 107(1-6): p606-612.

Ajenjo, M.H., Aquevedo, A.S., Guzmán, A.D., Poggi, H.M., Calvo, M.A., Castillo, C.V., León, E.C., Andresen, M.H. and Labarca, J.L., 2011. Epidemiological profile of invasive candidiasis in intensive care units at a university hospital. *Revista chilena de infectología: Organo oficial de la Sociedad Chilena de Infectología*. 28(2): p118-122.

Akpan, A. and Morgan, R., 2002. Oral candidiasis. *Postgrad Med J*. 78(922): p455-9.

Albuquerque, P.C., Nakayasu, E.S., Rodrigues, M.L., Frases, S., Casadevall, A., Zancope-Oliveira, R.M., Almeida, I.C. and Nosanchuk, J.D., 2008. Vesicular transport in *Histoplasma capsulatum*: an effective mechanism for trans-cell wall transfer of proteins and lipids in ascomycetes. *Cellular microbiology*. 10(8): p1695-1710.

Alexander, B.D., Johnson, M.D., Pfeiffer, C.D., Jiménez-Ortigosa, C., Catania, J., Booker, R., Castanheira, M., Messer, S.A., Perlin, D.S. and Pfaller, M.A., 2013. Increasing echinocandin resistance in *Candida glabrata*: clinical failure correlates with presence of FKS mutations and elevated minimum inhibitory concentrations. *Clinical infectious diseases*. 56(12): p1724-1732.

Almirante, B., Rodríguez, D., Park, B.J., Cuenca-Estrella, M., Planes, A.M., Almela, M., Mensa, J., Sanchez, F., Ayats, J., Gimenez, M. and Saballs, P., 2005. Epidemiology and predictors of mortality in cases of *Candida* bloodstream infection: results from population-based surveillance, Barcelona, Spain, from 2002 to 2003. *Journal of Clinical Microbiology*. 43(4): p1829-1835.

Andaloussi, S.E., Mäger, I., Breakefield, X.O. and Wood, M.J., 2013. Extracellular vesicles: biology and emerging therapeutic opportunities. *Nature reviews Drug discovery*. 12(5): p.347-357.

Arribas, J.R., Hernández-Albujar, S., González-García, J.J., Peña, J.M., Gonzalez, A., Cañedo, T., Madero, R., Vazquez, J.J. and Powderly, W.G., 2000. Impact of protease inhibitor therapy on HIV-related oropharyngeal candidiasis. *Aids*. 14(8): p979-985.

Ashley, E.S.D., Lewis, R., Lewis, J.S., Martin, C. and Andes, D., 2006. Pharmacology of systemic antifungal agents. *Clinical infectious diseases*. 43(S1): pS28-S39.

Ayukekbong, J.A., Ntemgwa, M. and Atabe, A.N., 2017. The threat of antimicrobial resistance in developing countries: causes and control strategies. *Antimicrobial Resistance & Infection Control*. 6(1): p47.

Bachmann, S.P., VandeWalle, K., Ramage, G., Patterson, T.F., Wickes, B.L., Graybill, J.R. and López-Ribot, J.L., 2002. *In vitro* activity of caspofungin against *Candida albicans* biofilms. *Antimicrobial agents and chemotherapy*. 46(11): p3591-3596.

Baddley, J.W., Patel, M., Bhavnani, S.M., Moser, S.A. and Andes, D.R., 2008. Association of fluconazole pharmacodynamics with mortality in patients with candidemia. *Antimicrobial agents and chemotherapy*. 52(9): p3022-3028.

Bag, A. and Chattopadhyay, R.R., 2017. Synergistic antibiofilm efficacy of a gallotannin 1, 2, 6-tri-O-galloyl- β -D-glucopyranose from *Terminalia chebula* fruit in combination with gentamicin and trimethoprim against multidrug resistant uropathogenic *Escherichia coli* biofilms. *PloS one*. 12(5): p.e0178712.

Baillie, G.S. and Douglas, L.J., 2000. Matrix polymers of *Candida* biofilms and their possible role in biofilm resistance to antifungal agents. *Journal of Antimicrobial Chemotherapy*. 46(3): p397-403.

Baker, P.J., Coburn, R.A., Genco, R.J. and Evans, R.T., 1978. The *in vitro* inhibition of microbial growth and plaque formation by surfactant drugs. *Journal of periodontal research*. 13(5): p474-485.

Baltazar, L.M., Nakayasu, E.S., Sobreira, T.J., Choi, H., Casadevall, A., Nimrichter, L. and Nosanchuk, J.D., 2016. Antibody binding alters the characteristics and contents of extracellular vesicles released by *Histoplasma capsulatum*. *Mosphere*, 1(2): p.e00085-15.

Barchiesi, F., Calabrese, D., Sanglard, D., Di Francesco, L.F., Caselli, F., Giannini, D., Giacometti, A., Gavaudan, S. and Scalise, G., 2000. Experimental induction of fluconazole resistance in *Candida tropicalis* ATCC 750. *Antimicrobial agents and chemotherapy*. 44(6): p1578.

Batavia, A.S., Secours, R., Espinosa, P., Juste, M.A.J., Severe, P., Pape, J.W. and Fitzgerald, D.W., 2016. Diagnosis of HIV-associated oral lesions in relation to early versus delayed antiretroviral therapy: results from the CIPRA HT001 trial. *Plos one*. 11(3): p.e0150656.

Behbehani, J., Shreaz, S., Irshad, M. and Karched, M., 2017. The natural compound magnolol affects growth, biofilm formation, and ultrastructure of oral *Candida* isolates. *Microbial pathogenesis*. 113: p209-217.

Belazi, M., Velegraki, A., Koussidou-Eremondi, T., Andreadis, D., Hini, S., Arsenis, G., Eliopoulou, C., Destouni, E. and Antoniadis, D., 2004. Oral *Candida* isolates in patients undergoing radiotherapy for head and neck cancer: prevalence, azole susceptibility profiles and response to antifungal treatment. *Oral microbiology and immunology*. 19(6): p347-351.

Berkow, E.L. and Lockhart, S.R., 2017. Fluconazole resistance in *Candida* species: a current perspective. *Infection and drug resistance*. 10: p237-244.

Bharathi, M. and Rani, A.U., 2011. Pathogenic fungal isolates in sputum of HIV positive patients. *Journal of AIDS and HIV Research*. 3(6): p107-113.

Blignaut, E., Messer, S., Hollis, R.J. and Pfaller, M.A., 2002. Antifungal susceptibility of South African oral yeast isolates from HIV/AIDS patients and healthy individuals. *Diagnostic microbiology and infectious disease*. 44(2): p169-174.

Borg-von Zepelin, M., Beggah, S., Boggian, K., Sanglard, D. and Monod, M., 1998. The expression of the secreted aspartyl proteinases Sap 4 to Sap 6 from *Candida albicans* in murine macrophages. *Molecular microbiology*. 28(3): p543-554.

Borg-von Zepelin, M., Niederhaus, T., Gross, U., Seibold, M., Monod, M. and Tintelnot, K., 2002. Adherence of different *Candida dubliniensis* isolates in the presence of fluconazole. *Aids*. 16(9): p1237-1244.

Budhavari, S., 2009. What's new in diagnostics? Fungitell®: 1, 3 beta-D Glucan assay. *Southern African Journal of Epidemiology and Infection*. 24(1): p37-38.

Buffet-Bataillon, S., Tattevin, P., Bonnaure-Mallet, M. and Jolivet-Gougeon, A., 2012. Emergence of resistance to antibacterial agents: the role of quaternary ammonium compounds-a critical review. *International journal of antimicrobial agents*. 39(5): p381-389.

Byadarahally, R. S. and Rajappa, S., 2011. Isolation and identification of *Candida* from the oral cavity. *ISRN dentistry*. 2011: p7.

Calabrese, E.C., Castellano, S., Santoriello, M., Sgherri, C., Quartacci, M.F., Calucci, L., Warrilow, A.G., Lamb, D.C., Kelly, S.L., Milite, C. and Granata, I., 2013. Antifungal activity of azole compounds CPA18 and CPA109 against azole-susceptible and -resistant strains of *Candida albicans*. *Journal of Antimicrobial Chemotherapy*. 68(5): p1111-1119.

Calderone, RA. (ed.) 2002. *Candida and candidiasis*. ASM Press. Washington D.C.

Calderone, R.A. and Fonzi, W.A., 2001. Virulence factors of *Candida albicans*. *Trends in microbiology*. 9(7): p327-335.

Carmona-Ribeiro, A.M., Vieira, D.B. and Lincopan, N., 2006. Cationic surfactants and lipids as anti-infective agents. *Anti-Infective Agents in Medicinal Chemistry (Formerly Current Medicinal Chemistry-Anti-Infective Agents)*. 5(1): p33-51.

Casadevall, A., 2007. Determinants of virulence in the pathogenic fungi. *Fungal biology reviews*. 21(4): p130-132.

Casadevall, A. and Pirofski, LA. 1999. Host-pathogen interactions: redefining the basic concepts of virulence and pathogenicity. *Infect Immun* . 67(8): p3703.

Cassone, A. and Cauda, R., 2012. *Candida* and candidiasis in HIV-infected patients: where commensalism, opportunistic behaviour and frank pathogenicity lose their borders. *Aids*, 26(12): p1457-1472.

Chaffin, W.L., López-Ribot, J.L., Casanova, M., Gozalbo, D. and Martínez, J.P., 1998. Cell wall and secreted proteins of *Candida albicans*: identification, function, and expression. *Microbiology and Molecular Biology Reviews*. 62(1): p130-180.

Chandra, J., Kuhn, D.M., Mukherjee, P.K., Hoyer, L.L., McCormick, T. and Ghannoum, M.A. 2001. Biofilm formation by the fungal pathogen *Candida albicans*: development, architecture, and drug resistance. *Journal of bacteriology*. 183(18): p5385.

Chen, S.C.A., Biswas, C., Bartley, R., Widmer, F., Pantarat, N., Obando, D., Djordjevic, J.T., Ellis, D.H., Jolliffe, K.A. and Sorrell, T.C., 2010. *In vitro* antifungal activities of bis (alkylpyridinium) alkane compounds against pathogenic yeasts and molds. *Antimicrobial agents and chemotherapy*. 54(8): p3233-3240.

Chen, X., Ren, B., Chen, M., Liu, M.X., Ren, W., Wang, Q.X., Zhang, L.X. and Yan, G.Y., 2014. ASDCD: antifungal synergistic drug combination database. *PloS one*. 9(1): p.e86499.

Chen, Y.C., Wu, C.C., Chung, W.L. and Lee, F.J.S., 2002. Differential secretion of Sap 4-6 proteins in *Candida albicans* during hyphae formation. *Microbiology*. 148(11): p3743-3754.

Chernos, V.I., Libshits, B.A., Yakobson, E. and Ghendon, Y.Z., 1972. Mechanism of antiviral action of acetone on rabbitpox virus replication. *Journal of virology*. 9(2): p251-257.

Cleveland, A.A., Farley, M.M., Harrison, L.H., Stein, B., Hollick, R., Lockhart, S.R., Magill, S.S., Derado, G., Park, B.J. and Chiller, T.M., 2012. Changes in incidence and antifungal drug resistance in candidemia: results from population-based laboratory surveillance in Atlanta and Baltimore, 2008–2011. *Clinical infectious diseases*. 55(10): p1352-1361.

Cline, A.M. and Radic, M.Z., 2004. Apoptosis, subcellular particles, and autoimmunity. *Clinical Immunology*. 112(2): p175-182.

Clinical and Laboratory Standards Institute. 2002. *Reference method for broth dilution susceptibility testing of yeasts*: approved standard-2nd ed. CLSI document M27-A2. Clinical and Laboratory Standards Institute, Wayne, PA.

Clinical and Laboratory Standards Institute. 2008. *Reference method for broth dilution antifungal susceptibility testing of yeasts*; approved standard-3rd ed. CLSI document M27-A3. Clinical and Laboratory Standards Institute, Wayne, PA.

Como, J.A. and Dismukes, W.E., 1994. Oral azole drugs as systemic antifungal therapy. *New England Journal of Medicine*. 330(4): p263-272.

Correia, A., Lermann, U., Teixeira, L., Cerca, F., Botelho, S., da Costa, R.M.G., Sampaio, P., Gärtner, F., Morschhäuser, J., Vilanova, M. and Pais, C., 2010. Limited role of secreted aspartyl proteinases Sap 1 to Sap 6 in *Candida albicans* virulence and host immune response in murine hematogenously disseminated candidiasis. *Infection and immunity*. 78(11): p4839-4849.

Cowen, L.E., Sanglard, D., Howard, S.J., Rogers, P.D. and Perlin, D.S., 2015. Mechanisms of antifungal drug resistance. *Cold Spring Harbor perspectives in medicine*. 5(7): p.a019752.

Cuenca-Estrella, M., Gomez-Lopez, A., Mellado, E., Buitrago, M.J., Monzon, A. and Rodriguez-Tudela, J.L., 2006. Head-to-head comparison of the activities of currently available antifungal agents against 3,378 Spanish clinical isolates of yeasts and filamentous fungi. *Antimicrobial Agents and Chemotherapy*. 50(3): p917-921.

Cuenca-Estrella, M., Lee-Yang, W., Ciblak, M.A., Arthington-Skaggs, B.A., Mellado, E., Warnock, D.W. and Rodriguez-Tudela, J.L., 2002. Comparative evaluation of NCCLS M27-A and EUCAST broth microdilution procedures for antifungal susceptibility testing of *Candida* species. *Antimicrobial agents and chemotherapy*. 46(11): p3644-3647.

Dalle, F., Wächtler, B., L'ollivier, C., Holland, G., Bannert, N., Wilson, D., Labruère, C., Bonnin, A. and Hube, B., 2010. Cellular interactions of *Candida albicans* with human oral epithelial cells and enterocytes. *Cellular microbiology*. 12(2): p248-271.

Daood, U., Yiu, C.K.Y., Burrow, M.F., Niu, L.N. and Tay, F.R., 2017. Effect of a novel quaternary ammonium silane on dentin protease activities. *Journal of dentistry*. 58: p19-27.

da Silva Dantas, A., Lee, K.K., Raziunaite, I., Schaefer, K., Wagener, J., Yadav, B. and Gow, N.A., 2016. Cell biology of *Candida albicans*–host interactions. *Current opinion in microbiology*. 34: p111-118.

Denning, D.W. and Bromley, M.J., 2015. How to bolster the antifungal pipeline? *Science*. 347(6229): p1414-1416.

De Nollin, S. and Borgers, M., 1975. Scanning electron microscopy of *Candida albicans* after *in vitro* treatment with miconazole. *Antimicrobial agents and chemotherapy*. 7(5): p704-711.

Desai, C., Mavrianos, J. and Chauhan, N., 2011. *Candida glabrata* Pwp7p and Aed1p are required for adherence to human endothelial cells. *FEMS yeast research*. 11(7): p595-601.

De Viragh, P.A., Sanglard, D., Togni, G., Falchetto, R. and Monod, M., 1993. Cloning and sequencing of two *Candida parapsilosis* genes encoding acid proteases. *Microbiology*. 139(2): p335-342.

Domagk, G., 1935. A new class of disinfectants. *Deut. Med. Wochenschr*. 61: p829-832.

Dostál, J., Hamal, P., Pavlíčková, L., Souček, M., Ruml, T., Pichová, I. and Hrušková-Heidingsfeldová, O., 2003. Simple method for screening *Candida* species isolates for the presence of secreted proteinases: a tool for the prediction of successful inhibitory treatment. *Journal of clinical microbiology*. 41(2): p712-716.

Douglas, L.J., 2003. *Candida* biofilms and their role in infection. *Trends in microbiology*. 11(1): p30-36.

Dupont, B., Graybill, J.R., Armstrong, D., Laroche, R., Touze, J.E. and Wheat, L.J., 1992. Fungal infections in AIDS patients. *Journal of Medical and Veterinary Mycology*. 30(s1): p19-28.

Egger, M., Hirschel, B., Francioli, P., Sudre, P., Wirz, M., Flepp, M., Rickenbach, M., Malinverni, R., Vernazza, P. and Battegay, M., 1997. Impact of new antiretroviral combination therapies in HIV infected patients in Switzerland: prospective multicentre study. *Bmj*. 315(7117): p1194-1199.

Ellis, D., 2002. Amphotericin B: spectrum and resistance. *Journal of Antimicrobial Chemotherapy*. 49(1): p7-10.

Eloff, J.N., 1998. A sensitive and quick microplate method to determine the minimal inhibitory concentration of plant extracts for bacteria. *Planta medica*. 64(08): p711-713.

Epstein, J.B., Gorsky, M. and Caldwell, J., 2002. Fluconazole mouthrinses for oral candidiasis in postirradiation, transplant, and other patients. *Oral Surgery, Oral Medicine, Oral Pathology, Oral Radiology, and Endodontology*. 93(6): p671-675.

Eraso, E., Ruesga, M., Villar-Vidal, M., Carrillo-Muñoz, A.J., Espinel-Ingroff, A. and Quindós, G., 2008. Comparative evaluation of ATB Fungus 2 and Sensitre Yeast One panels for testing *in vitro* *Candida* antifungal susceptibility. *Revista iberoamericana de micología*. 25(1): p3-6.

Espinel-Ingroff, A., Pfaller, M.A., Bustamante, B., Canton, E., Fothergill, A., Fuller, J., Gonzalez, G.M., Lass-Flörl, C., Lockhart, S.R., Martin-Mazuelos, E. and Meis, J.F., 2014. Multilaboratory study of epidemiological cut off values for detection of resistance in eight *Candida* species to fluconazole, posaconazole, and voriconazole. *Antimicrobial agents and chemotherapy*. 58(4): p2006-2012.

Fakhim, H., Emami, S., Vaezi, A., Hashemi, S.M., Faeli, L., Diba, K., Dannaoui, E. and Badali, H., 2017. *In vitro* activities of novel azole compounds ATTAF-1 and ATTAF-2 against fluconazole-susceptible and-resistant isolates of *Candida* species. *Antimicrobial agents and chemotherapy*. 61(1): p.e01106-16.

Falagas, M.E., Roussos, N. and Vardakas, K.Z., 2010. Relative frequency of *albicans* and the various non-*albicans* *Candida* spp among candidemia isolates from inpatients in various parts of the world: a systematic review. *International journal of infectious diseases*. 14(11): p.e954-e966.

Felk, A., Kretschmar, M., Albrecht, A., Schaller, M., Beinhauer, S., Nichterlein, T., Sanglard, D., Korting, H.C., Schäfer, W. and Hube, B., 2002. *Candida albicans* hyphal formation and the expression of the Efg1-regulated proteinases Sap 4 to Sap 6 are required for the invasion of parenchymal organs. *Infection and immunity*. 70(7): p3689-3700.

Fichtenbaum, C.J., Koletar, S., Yiannoutsos, C., Holland, F., Pottage, J., Cohn, S.E., Walawander, A., Frame, P., Feinberg, J., Saag, M. and Van der Horst, C., 2000. Refractory mucosal candidiasis in advanced human immunodeficiency virus infection. *Clinical Infectious Diseases*. 30(5): p749-756.

Flemming, H.C. and Wingender, J., 2010. The biofilm matrix. *Nature reviews microbiology*. 8(9): p.623.

Fotedar, R. and Al-Hedaithy, S.S.A., 2005. Comparison of phospholipase and proteinase activity in *Candida albicans* and *C. dubliniensis*. *Mycoses*. 48(1): p62-67.

Fournier, P., Schwebel, C., Maubon, D., Vesin, A., Lebeau, B., Foroni, L., Hamidfar-Roy, R., Cornet, M., Timsit, J.F. and Pelloux, H., 2011. Antifungal use influences *Candida* species distribution and susceptibility in the intensive care unit. *Journal of antimicrobial chemotherapy*. 66(12): p2880-2886.

França, E.J., Andrade, C.G., Furlaneto-Maia, L., Serpa, R., Oliveira, M.T., Quesada, R.M. and Furlaneto, M.C., 2011. Ultrastructural architecture of colonies of different morphologies produced by phenotypic switching of a clinical strain of *Candida tropicalis* and biofilm formation by variant phenotypes. *Micron*. 42(7): p726-732.

Fredell, D.L., 1994. "Biological properties and applications of cationic surfactants" In Cationic surfactants, J. Cross & E. J. Singer (eds). Marcel Dekker, New York. p31-60.

Furlaneto, M.C., Andrade, C.G.T.J., Aragão, P.H.A., França, E.J.G., Moralez, A.T.P. and Ferreira, L.C.S., 2012a. Scanning electron microscopy as a tool for the analysis of colony architecture produced by phenotypic switching of a human pathogenic yeast *Candida tropicalis*. In *Journal of Physics: Conference Series* IOP Publishing. 371(1): p012022.

Garcia-Cuesta, C., Sarrion-Pérez, M.G. and Bagán, J.V., 2014. Current treatment of oral candidiasis: A literature review. *Journal of Clinical and Experimental dentistry*. 6(5): p.e576-e582.

Gebre, AA, Okada, H, Kim, C, Kubo, K, Ohnuki, S, Ohya, Y. 2015. Profiling of the effects of antifungal agents on yeast cells based on morphometric analysis. *FEMS yeast research*. 15(5).

Ghannoum, M. and Elteen, K.A., 1986. Correlative relationship between proteinase production, adherence and pathogenicity of various strains of *Candida albicans*. *Journal of Medical and Veterinary Mycology*. 24(5): p407-413.

Ghannoum, M., Hoffman, R.S., Mowry, J.B. and Lavergne, V., 2014. Trends in toxic alcohol exposures in the United States from 2000 to 2013: a focus on the use of antidotes and extracorporeal treatments. *In Seminars in dialysis*. 27(4): p395-401.

Goins, R.A., Ascher, D., Waecker, N., Arnold, J. and Moorefield, E., 2002. Comparison of fluconazole and nystatin oral suspensions for treatment of oral candidiasis in infants. *The Pediatric infectious disease journal*. 21(12): p1165-1167.

Godoy, P., Tiraboschi, I.N., Severo, L.C., Bustamante, B., Calvo, B., Almeida, L.P.D., Matta, D.A.D. and Colombo, A.L., 2003. Species distribution and antifungal susceptibility profile of *Candida* spp. bloodstream isolates from Latin American hospitals. *Memorias do Instituto Oswaldo Cruz*. 98(3): p401-405.

Gong, S.Q., Epasinghe, J., Rueggeberg, F.A., Niu, L.N., Mettenberg, D., Yiu, C.K., Blizzard, J.D., Wu, C.D., Mao, J., Drisko, C.L. and Pashley, D.H., 2012a. An ORMOSIL-containing orthodontic acrylic resin with concomitant improvements in antimicrobial and fracture toughness properties. *PloS one*. 7(8): p.e42355.

Gong, S.Q., Huang, Z.B., Shi, W., Ma, B., Tay, F.R. and Zhou, B., 2014. *In vitro* evaluation of antibacterial effect of AH Plus incorporated with quaternary ammonium epoxy silicate against *Enterococcus faecalis*. *Journal of endodontics*. 40(10): p1611-1615.

Gong, S.Q., Niu, L.N., Kemp, L.K., Yiu, C.K., Ryou, H., Qi, Y.P., Blizzard, J.D., Nikonov, S., Brackett, M.G., Messer, R.L. and Wu, C.D., 2012b. Quaternary ammonium silane-functionalized, methacrylate resin composition with antimicrobial activities and self-repair potential. *Acta biomaterialia*. 8(9): p3270-3282.

Gonzales, F.P. and Maisch, T., 2012. Photodynamic inactivation for controlling *Candida albicans* infections. *Fungal biology*. 116(1): p1-10.

Greenberg, M.S., Glick, M. and Ship, J.A., 2008. *Burket's Oral Medicine*. (11th ed). Hamilton: BC Decker Inc. p79-84.

Grover, N.D., 2010. Echinocandins: A ray of hope in antifungal drug therapy. *Indian journal of pharmacology*. 42(1): p9-11.

Gudlaugsson, O., Gillespie, S., Lee, K., Berg, J.V., Hu, J., Messer, S., Herwaldt, L., Pfaller, M. and Diekema, D., 2003. Attributable mortality of nosocomial candidemia, revisited. *Clinical Infectious Diseases*. 37(9): p1172-1177.

Gulve, N., Kimmerling, K., Johnston, A.D., Krueger, G.R., Ablashi, D.V. and Prusty, B.K., 2016. Anti-herpesviral effects of a novel broad range anti-microbial quaternary ammonium silane, K21. *Antiviral research*. 131: p166-173.

Guo, F., Yang, Y., Kang, Y., Zang, B., Cui, W., Qin, B., Qin, Y., Fang, Q., Qin, T., Jiang, D. and Li, W., 2013. Invasive candidiasis in intensive care units in China: a multicentre prospective observational study. *Journal of Antimicrobial Chemotherapy*. 68(7): p1660-1668.

György, B., Szabó, T.G., Pásztói, M., Pál, Z., Misják, P., Aradi, B., László, V., Pállinger, E., Pap, E., Kittel, A. and Nagy, G., 2011. Membrane vesicles, current state-of-the-art: emerging role of extracellular vesicles. *Cellular and molecular life sciences*. 68(16): p2667-2688.

Hajjar, F.H.E., Jebali, A. and Hekmatimoghaddam, S., 2015. The inhibition of *Candida albicans* secreted aspartyl proteinase by triangular gold nanoparticles. *Nanomed J*. 2: p54–59.

Hamid, S., Zainab, S., Faryal, R., Ali, N. and Sharafat, I., 2018. Inhibition of secreted aspartyl proteinase activity in biofilms of *Candida* species by mycogenic silver nanoparticles. *Artificial cells, nanomedicine, and biotechnology*. 46(3): p551-557.

Hargrove, T.Y., Friggeri, L., Wawrzak, Z., Qi, A., Hoekstra, W.J., Schotzinger, R.J., York, J.D., Guengerich, F.P. and Lepesheva, G.I., 2017. Structural analyses of *Candida albicans* sterol 14 α -demethylase complexed with azole drugs address the molecular basis of azole-mediated inhibition of fungal sterol biosynthesis. *Journal of Biological Chemistry*. 292(16): p6728-6743.

Harris, R., 2002. Progress with superficial mycoses using essential oils. *International Journal of Aromatherapy*. 12(2): p.83-91.

Harvey, A.L., Edrada-Ebel, R. and Quinn, R.J., 2015. The re-emergence of natural products for drug discovery in the genomics era. *Nature reviews drug discovery*. 14(2): p111-129.

Hata, M., Ishii, Y., Watanabe, E., Uoto, K., Kobayashi, S., Yoshida, K.I., Otani, T. and Ando, A., 2010. Inhibition of ergosterol synthesis by novel antifungal compounds targeting C-14 reductase. *Medical mycology*. 48(4): p613-621.

Hegstad, K., Langsrud, S., Lunestad, B.T., Scheie, A.A., Sunde, M. and Yazdankhah, S.P., 2010. Does the wide use of quaternary ammonium compounds enhance the selection and spread of antimicrobial resistance and thus threaten our health? *Microbial drug resistance*. 16(2): p91-104.

Hirata, C.H.W., 2015. Oral manifestations in AIDS. *Brazilian journal of otorhinolaryngology*. 81(2): p120-123.

Hube, B., 2004. From commensal to pathogen: stage- and tissue-specific gene expression of *Candida albicans*. *Current opinion in microbiology*. 7(4): p336-341.

Hube, B., Monod, M., Schofield, D.A., Brown, A.J.P. and Gow, N.A.R., 1994. Expression of seven members of the gene family encoding secretory aspartyl proteinases in *Candida albicans*. *Molecular microbiology*. 14(1): p87-99.

Hube, B. and Naglik, J., 2001. *Candida albicans* proteinases: resolving the mystery of a gene family. *Microbiology*. 147(8): p1997-2005.

Ikonomova, S.P., Moghaddam-Taaheri, P., Jabra-Rizk, M.A., Wang, Y. and Karlsson, A.J., 2018. Engineering improved variants of the antifungal peptide histatin 5 with reduced susceptibility to *Candida albicans* secreted aspartic proteases and enhanced antimicrobial potency. *The FEBS journal*. 285(1): p146-159.

Jabra-Rizk, M.A., Kong, E.F., Tsui, C., Nguyen, M.H., Clancy, C.J., Fidel, P.L. and Noverr, M., 2016. *Candida albicans* pathogenesis: fitting within the host-microbe damage response framework. *Infection and immunity*. 84(10): p2724-2739.

James, W.D., Berger, T.G., Elston, D.M. and Neuhaus, I., 2006. "Andrews" *Diseases of the Skin: Clinical Dermatology*. Philadelphia: Saunders Elsevier. p308.

Jalal, M., Ansari, M.A., Alzohairy, M.A., Ali, S.G., Khan, H.M., Almatroudi, A. and Siddiqui, M.I., 2019. Anticandidal activity of biosynthesized silver nanoparticles: effect on growth, cell morphology, and key virulence attributes of *Candida* species. *International journal of nanomedicine*. 14: p4667-4679.

Jayatilake, J.A.M.S., Samaranyake, Y.H. and Samaranyake, L.P., 2005. An ultrastructural and a cytochemical study of candidal invasion of reconstituted human oral epithelium. *Journal of oral pathology & medicine*. 34(4): p240-246.

Jennings, M.C., Minbiole, K.P. and Wuest, W.M., 2015a. Quaternary ammonium compounds: an antimicrobial mainstay and platform for innovation to address bacterial resistance. *ACS infectious diseases*. 1(7): p288-303

Jennings, M.C., Buttaro, B.A., Minbiole, K.P. and Wuest, W.M., 2015b. Bioorganic investigation of multicationic antimicrobials to combat QAC-resistant *Staphylococcus aureus*. *ACS infectious diseases*. 1(7): p304-309.

Jiao, Y., Niu, L.N., Ma, S., Li, J., Tay, F.R. and Chen, J.H., 2017. Quaternary ammonium-based biomedical materials: State-of-the-art, toxicological aspects and antimicrobial resistance. *Progress in Polymer Science*. 71: p53-90.

Johnson, M.D., MacDougall, C., Ostrosky-Zeichner, L., Perfect, J.R. and Rex, J.H., 2004. Combination antifungal therapy. *Antimicrobial agents and chemotherapy*. 48(3): p693-715.

Jothy, S.L., Zakariah, Z., Chen, Y. and Sasidharan, S., 2012. *In vitro*, *in situ* and *in vivo* studies on the anticandidal activity of *Cassia fistula* seed extract. *Molecules*. 17(6): p6997.

Junqueira, J.C., Vilela, S.F., Rossoni, R.D., Barbosa, J.O., Costa, A.C.B., Rasteiro, V., Suleiman, J.M. and Jorge, A.O.C., 2012. Oral colonization by yeasts in HIV-positive patients in Brazil. *Revista do Instituto de Medicina Tropical de Sao Paulo*. 54(1): p17-24.

Kannan, K. and Jain, S.K., 2000. Oxidative stress and apoptosis. *Pathophysiology*. 7(3): p153-163.

Karkowska-Kuleta, J., Rapala-Kozik, M. and Kozik, A., 2009. Fungi pathogenic to humans: molecular bases of virulence of *Candida albicans*, *Cryptococcus neoformans* and *Aspergillus fumigatus*. *Acta Biochimica Polonica*. 56(2): p211-224.

Kathiravan, M.K., Salake, A.B., Chothe, A.S., Dudhe, P.B., Watode, R.P., Mukta, M.S. and Gadhwe, S., 2012. The biology and chemistry of antifungal agents: a review. *Bioorganic & medicinal chemistry*. 20(19): p5678-5698.

Keikha, N., Yadegari, M.H., Rajabibazl, M. and Amani, J., 2017. Investigation of the Inhibitory Effects of the Designed NK95 Peptide on Expression of SAP4-SAP6 Genes of *Candida albicans* in Comparison with Caspofungin. *Iranian Red Crescent Medical Journal*. 19(12). p9.

Khan, M.S.A., Ahmad, I., Aqil, F., Owais, M., Shahid, M. and Musarrat, J., 2010. Virulence and pathogenicity of fungal pathogens with special reference to *Candida albicans*. In *Combating Fungal Infections*. Springer, Berlin, Heidelberg. p21-45.

Kim, J. and Sudbery, P., 2011. *Candida albicans*, a major human fungal pathogen. *The Journal of Microbiology*. 49(2): p171.

Klepser, M.E., Wolfe, E.J., Jones, R.N., Nightingale, C.H. and Pfaller, M.A., 1997. Antifungal pharmacodynamic characteristics of fluconazole and amphotericin B tested against *Candida albicans*. *Antimicrobial Agents and Chemotherapy*. 41(6): p1392-1395.

Klepser, M.E., Ernst, E.J., Lewis, R.E., Ernst, M.E. and Pfaller, M.A., 1998. Influence of test conditions on antifungal time-kill curve results: proposal for standardized methods. *Antimicrobial Agents and Chemotherapy*. 42(5): p1207-1212.

Koga-Ito, C.Y., Komiyama, E.Y., de Paiva Martins, C.A., Vasconcellos, T.C., Cardoso Jorge, A.O., Carvalho, Y.R., do Prado, R.F. and Balducci, I., 2011. Experimental systemic virulence of oral *Candida dubliniensis* isolates in comparison with *Candida albicans*, *Candida tropicalis* and *Candida krusei*. *Mycoses*. 54(5): p278-285.

Konaté, K., Mavoungou, J.F., Lepengué, A.N., Aworet-Samseny, R.R., Hilou, A., Souza, A., Dicko, M.H. and M'Batchi, B., 2012. Antibacterial activity against β -lactamase producing Methicillin and Ampicillin-resistant *Staphylococcus aureus*: fractional Inhibitory Concentration Index (FICI) determination. *Annals of clinical microbiology and antimicrobials*. 11(1): p18.

Konstantyner, T.C.R.D.O., Silva, A.M.D., Tanaka, L.F., Marques, H.H.D.S. and Latorre, M.D.R.D.D., 2013. Factors associated with time free of oral candidiasis in children living with HIV/AIDS, São Paulo, Brazil. *Cadernos de saude publica*. 29: p2197-2207.

Kontoyiannis, D.P. and Lewis, R.E., 2015. Treatment principles for the management of mold infections. *Cold Spring Harbor perspectives in medicine*. 5(4): p.a019737.

Kontoyiannis, D.P. and Lewis, R.E., 2002. Antifungal drug resistance of pathogenic fungi. *The Lancet*. 359(9312): p1135-1144.

Kourai, H., Yabuhara, T., Shirai, A., Maeda, T. and Nagamune, H., 2006. Syntheses and antimicrobial activities of a series of new bis-quaternary ammonium compounds. *European journal of medicinal chemistry*. 41(4): p437-444.

Kroemer, G., Galluzzi, L., Vandenabeele, P., Abrams, J., Alnemri, E. S., Baehrecke, E. H., Blagosklonny, M.V., El-Deiry, W.S., Golstein, P., Green, D.R., Hengartner, M., Knight, R.A., Kumar, S., Lipton, S.A., Malorni, W., Nuñez, G., Peter, M.E., Tschopp, J., Yuan, J., Piacentini, M., Zhivotovsky, B. and Melino, G., 2009. Classification of cell death: recommendations of the Nomenclature Committee on Cell Death 2009. *Cell Death Differ.* 16: p3-11.

Kumamoto, C.A., 2002. *Candida* biofilms. *Current opinion in microbiology.* 5(6): p608-611.

Kumar, S. and Filippi, M.D., 2016. An Alternative Approach for Sample Preparation with low cell number for TEM analysis. *JoVE (Journal of Visualized Experiments)*, (116): p.e54724.

Kumar, R., Saraswat, D., Tati, S. and Edgerton, M., 2015. Novel aggregation properties of *Candida albicans* secreted aspartyl proteinase Sap6 mediate virulence in oral candidiasis. *Infection and immunity.* 83(7): p2614-2626.

Lakota, E.A., Ong, V., Flanagan, S. and Rubino, C.M., 2018. Population pharmacokinetic analyses for rezafungin (CD101) efficacy using phase 1 data. *Antimicrobial agents and chemotherapy.* 62(6): p.e02603-17.

Latha, L.Y., Darah, I., Jain, K. and Sasidharan, S., 2011. Effects of *Vernonia cinerea* less methanol extract on growth and morphogenesis of *Candida albicans*. *European review for medical and pharmacological sciences.* 15(5): p543-549.

Lebeaux, D., Ghigo, J.M. and Beloin, C., 2014. Biofilm-related infections: bridging the gap between clinical management and fundamental aspects of recalcitrance toward antibiotics. *Microbiol. Mol. Biol. Rev.* 78(3): p510-543.

Leclercq, L., Lubart, Q., Dewilde, A., Aubry, J.M. and Nardello-Rataj, V., 2012. Supramolecular effects on the antifungal activity of cyclodextrin/di-n-decyldimethylammonium chloride mixtures. *European Journal of Pharmaceutical Sciences.* 46(5): p336-345.

Ledergerber, B., Egger, M., Opravil, M., Telenti, A., Hirschel, B., Battegay, M., Vernazza, P., Sudre, P., Flepp, M., Furrer, H. and Francioli, P., 1999. Clinical progression and virological failure on highly active antiretroviral therapy in HIV-1 patients: a prospective cohort study. *The Lancet*. 353(9156): p863-868.

Lehár, J., Zimmermann, G.R., Krueger, A.S., Molnar, R.A., Ledell, J.T., Heilbut, A.M., Short, G.F., Giusti, L.C., Nolan, G.P., Magid, O.A. and Lee, M.S., 2007. Chemical combination effects predict connectivity in biological systems. *Molecular systems biology*. 3(1): p80.

Leite, M.C.A., Bezerra, A.P.D.B., Sousa, J.P.D., Guerra, F.Q.S. and Lima, E.D.O., 2014. Evaluation of antifungal activity and mechanism of action of citral against *Candida albicans*. *Evidence-Based Complementary and Alternative Medicine*. 2014: p9.

Leng, K.M., Vijayarathna, S., Jothy, S.L., Sasidharan, S. and Kanwar, J.R., 2017. *In vitro* and *in vivo* anticandidal activities of alginate-enclosed chitosan-calcium phosphate-loaded Fe-bovine lactoferrin nanocapsules. *Future science OA*. 4(2): p.FSO257.

Leroy, O., Gangneux, J.P., Montravers, P., Mira, J.P., Gouin, F., Sollet, J.P., Carlet, J., Reynes, J., Rosenheim, M., Regnier, B. and Lortholary, O., 2009. Epidemiology, management, and risk factors for death of invasive *Candida* infections in critical care: a multicenter, prospective, observational study in France (2005–2006). *Critical care medicine*. 37(5): p1612-1618.

Lewis, K., 2007. Persister cells, dormancy and infectious disease. *Nature Reviews Microbiology*. 5(1): p48-56.

Lewis, R.E., Diekema, D.J., Messer, S.A., Pfaller, M.A. and Klepser, M.E., 2002. Comparison of Etest, chequerboard dilution and time-kill studies for the detection of synergy or antagonism between antifungal agents tested against *Candida* species. *Journal of Antimicrobial Chemotherapy*. 49(2): p345-351.

Liao, X., Qiu, H., Li, R., Guo, F., Liu, W., Kang, M., Kang, Y. and China-SCAN Team, 2015. Risk factors for fluconazole-resistant invasive candidiasis in intensive care unit patients: an analysis from the China Survey of Candidiasis study. *Journal of critical care*. 30(4): p862e1-862e5.

Li, X., Hou, Y., Yue, L., Liu, S., Du, J. and Sun, S., 2015. Potential targets for antifungal drug discovery based on growth and virulence in *Candida albicans*. *Antimicrobial agents and chemotherapy*. 59(10): p5885-5891.

Li, L., Redding, S. and Dongari-Bagtzoglou, A., 2007. *Candida glabrata*, an emerging oral opportunistic pathogen. *Journal of dental research*. 86(3): p204-215.

Li, Y., Sun, S., Guo, Q., Ma, L., Shi, C., Su, L. and Li, H., 2008. *In vitro* interaction between azoles and cyclosporin A against clinical isolates of *Candida albicans* determined by the checkerboard method and time-kill curves. *Journal of antimicrobial chemotherapy*. 61(3): p577-585.

Li, W., Yu, D., Gao, S., Lin, J., Chen, Z. and Zhao, W., 2014. Role of *Candida albicans*-secreted aspartyl proteinases (Saps) in severe early childhood caries. *International journal of molecular sciences*. 15(6): p10766-10779.

Li, X., Yu, H.Y. and Quan, C.S., 2011. Candidacidal action of CF66I, an antifungal compound produced by *Burkholderia cepacia*. *Tropical Journal of Pharmaceutical Research*. 10(5): p577-585.

Lipp, H.P., 2008. Antifungal agents-clinical pharmacokinetics and drug interactions. *Mycoses*. 51: p7-18.

Liu, F., Fan, X., Auclair, S., Ferguson, M., Sun, J., Soong, L., Hou, W., Redfield, R.R., Birx, D.L., Ratto-Kim, S. and Robb, M.L., 2016a. Sequential dysfunction and progressive depletion of *candida albicans*-specific CD4 T cell response in HIV-1 infection. *PLoS pathogens*. 12(6): p.e1005663.

Liu, W., Li, L.P., Zhang, J.D., Li, Q., Shen, H., Chen, S.M., He, L.J., Yan, L., Xu, G.T., An, M.M. and Jiang, Y.Y., 2014. Synergistic antifungal effect of glabridin and fluconazole. *PLoS one*. 9(7): p.e103442.

Liu, S.Y., Tonggu, L., Niu, L.N., Gong, S.Q., Fan, B., Wang, L., Zhao, J.H., Huang, C., Pashley, D.H. and Tay, F.R., 2016b. Antimicrobial activity of a quaternary ammonium methacryloxy silicate-containing acrylic resin: a randomised clinical trial. *Scientific reports*. 6: p21882.

Liu, S., Yue, L., Gu, W., Li, X., Zhang, L. and Sun, S., 2016c. Synergistic effect of fluconazole and calcium channel blockers against resistant *Candida albicans*. *PLoS One*. 11(3): p.e0150859.

Liu, X., Li, T., Wang, D., Yang, Y., Sun, W., Liu, J. and Sun, S., 2017. Synergistic antifungal effect of fluconazole combined with licofelone against resistant *Candida albicans*. *Frontiers in microbiology*. 8: p2101.

Locke, J.B., Almaguer, A.L., Donatelli, J.L. and Bartizal, K.F., 2018. Time-Kill Kinetics of Rezafungin (CD101) in Vagina-Simulative Medium for Fluconazole-Susceptible and Fluconazole-Resistant *Candida albicans* and Non-*albicans* *Candida* Species. *Infectious diseases in obstetrics and gynaecology*. 2018: p10.

Loeffler, J. and Stevens, D.A., 2003. Antifungal drug resistance. *Clinical infectious diseases*. 36(Supplement_1): pS31-S41.

Lopez-Rangel, E. and Van Allen, M.I., 2005. Prenatal exposure to fluconazole: an identifiable dysmorphic phenotype. Birth Defects Research Part A: *Clinical and Molecular Teratology*. 73(11): p919-923.

Lushniak, B.D., 2014. Antibiotic resistance: a public health crisis. *Public Health Reports*. 129(4): p314-316.

Luque, A.G., Biasoli, M.S., Tosello, M.E., Binolfi, A., Lupo, S. and Magaró, H.M., 2009. Oral yeast carriage in HIV-infected and non-infected populations in Rosario, Argentina. *Mycoses*. 52(1): p53-59.

Magalhães, Y.C., Bomfim, M.R.Q., Melônio, L.C., Ribeiro, P., Cosme, L.M., Rhoden, C.R. and Marques, S.G., 2015. Clinical significance of the isolation of *Candida* species from hospitalized patients. *Brazilian Journal of Microbiology*. 46(1): p117-123.

Makarova, N.U., Pokrowsky, V.V., Kravchenko, A.V., Serebrovskaya, L.V., James, M.J., McNeil, M.M., Lasker, B.A., Warnock, D.W. and Reiss, E., 2003. Persistence of oropharyngeal *Candida albicans* strains with reduced susceptibilities to fluconazole among human immunodeficiency virus-seropositive children and adults in a long-term care facility. *Journal of clinical microbiology*. 41(5): p1833-1837.

Manzano-Gayosso, P., Mendez-Tovar, L.J., Hernandez-Hernandez, F. and Lopez-Martinez, R., 2008. Antifungal resistance: an emerging problem in Mexico. *Gaceta medica de Mexico*. 144(1): p23-26.

Marcotte, L., Barbeau, J. and Lafleur, M., 2005. Permeability and thermodynamics study of quaternary ammonium surfactants-phosphocholine vesicle system. *Journal of colloid and interface science*. 292(1): p219-227.

Martins, N., Barros, L., Henriques, M., Silva, S. and Ferreira, I.C., 2015. Activity of phenolic compounds from plant origin against *Candida* species. *Industrial Crops and Products*. 74: p648-670.

Martínez, A, Rojas, N, García, L, González, F, Domínguez, M, Catalán, A. 2014. *In vitro* activity of terpenes against *Candida albicans* and ultrastructural alterations. *Oral surgery, oral medicine, oral pathology and oral radiology*. 118(5): p553.

Mason, K.L., Downward, J.R.E., Mason, K.D., Falkowski, N.R., Eaton, K.A., Kao, J.Y., Young, V.B. and Huffnagle, G.B., 2012. *Candida albicans* and bacterial microbiota interactions in the cecum during recolonization following broad-spectrum antibiotic therapy. *Infection and immunity*. 80(10): p3371-3380.

Maurya, I.K., Thota, C.K., Sharma, J., Tupe, S.G., Chaudhary, P., Singh, M.K., Thakur, I.S., Deshpande, M., Prasad, R. and Chauhan, V.S., 2013. Mechanism of action of novel synthetic dodecapeptides against *Candida albicans*. *Biochimica et Biophysica Acta (BBA)-General Subjects*. 1830(11): p5193-5203.

Mayr, A., Hinterberger, G., Dierich, M.P. and Lass-Flörl, C., 2005. Interaction of serotonin with *Candida albicans* selectively attenuates fungal virulence *in vitro*. *International journal of antimicrobial agents*. 26(4): p335-337.

Mayers, DL, Sobel, JD, Ouellette, M, Kaye, KS. and Marchaim, D. (eds)., 2017. *Antimicrobial Drug Resistance. Clinical and Epidemiological Aspects*. Springer (Vol 2)

Mayer, F.L., Wilson, D. and Hube, B., 2013. *Candida albicans* pathogenicity mechanisms. *Virulence*. 4(2): p119-128.

McCarthy, M.W., Kontoyiannis, D.P., Cornely, O.A., Perfect, J.R. and Walsh, T.J., 2017. Novel agents and drug targets to meet the challenges of resistant fungi. *The Journal of infectious diseases*. 216(S3): pS474-S483.

McDonnell, G. and Russell, A.D., 1999. Antiseptics and disinfectants: activity, action, and resistance. *Clinical microbiology reviews*. 12(1): pp.147-179.

Meghil, M.M., Rueggeberg, F., El-Awady, A., Miles, B., Tay, F., Pashley, D. and Cutler, C.W., 2015. Novel coating of surgical suture confers antimicrobial activity against *Porphyromonas gingivalis* and *Enterococcus faecalis*. *Journal of periodontology*. 86(6): p788-794.

Melo, N.R., Taguchi, H., Jorge, J., Pedro, R.J., Almeida, O.P., Fukushima, K., Nishimura, K. and Miyaji, M., 2004. Oral *Candida* flora from Brazilian human immunodeficiency virus-infected patients in the highly active antiretroviral therapy era. *Memórias do Instituto Oswaldo Cruz*. 99(4): p425-431.

Melo, M.A., Wu, J., Weir, M.D. and Xu, H.H., 2014. Novel antibacterial orthodontic cement containing quaternary ammonium monomer dimethylaminododecyl methacrylate. *Journal of dentistry*. 42(9): p1193-1201.

Menezes, E.A., Vasconcelos Júnior, A.A.D., Silva, C.L.F., Plutarco, F.X., Cunha, M.D.C.D.S.O. and Cunha, F.A., 2012. *In vitro* synergism of simvastatin and fluconazole against *Candida* species. *Revista do Instituto de Medicina Tropical de São Paulo*. 54(4): pp197-199.

Michael, C.A., Dominey-Howes, D. and Labbate, M., 2014. The antimicrobial resistance crisis: causes, consequences, and management. *Frontiers in public health*. 2: p145.

Mohandas, V. and Ballal, M., 2011. Distribution of *Candida* species in different clinical samples and their virulence: biofilm formation, proteinase and phospholipase production: a study on hospitalized patients in southern India. *Journal of global infectious diseases*. 3(1): p4-8.

Monod, M., Togni, G., Hube, B. and Sanglard, D., 1994. Multiplicity of genes encoding secreted aspartic proteinases in *Candida* species. *Molecular microbiology*. 13(2): p357-368.

Monod, M., Hube, B., Hess, D. and Sanglard, D., 1998. Differential regulation of SAP8 and SAPS, which encode two new members of the secreted aspartic proteinase family in *Candida albicans*. *Microbiology*. 144(10): p2731-2737.

Monod, M. and Borg-von Zepelin, M., 2002. Secreted proteinases and other virulence mechanisms of *Candida albicans*. *Chem Immunol*. 81: p114-128.

Monod, M., Staib, P., Reichard, U. and Jousson, O., 2010. Fungal aspartic proteases as possible therapeutic targets. *Aspartic Acid Proteases as Therapeutic Targets*. 45: p573-606.

Moran, J. and Addy, M., 1984. The effect of surface adsorption and staining reactions on the antimicrobial properties of some cationic antiseptic mouthwashes. *Journal of periodontology*. 55(5): p278-282.

Moran, G.P., Coleman, D.C. and Sullivan, D.J., 2011. *Candida albicans* versus *Candida dubliniensis*: why is *C. albicans* more pathogenic? *International journal of microbiology*, 2012: p1-7.

Moran, G. P., Sullivan, D. J. and Coleman, D. C., 2002. Emergence of non-*Candida albicans* *Candida* species as pathogens. In R. A. Calderone (ed.), *Candida and candidiasis*. ASM Press. Washington, D.C. p37-53.

Moriyama, B., Gordon, L.A., McCarthy, M., Henning, S.A., Walsh, T.J. and Penzak, S.R., 2014. Emerging drugs and vaccines for candidemia. *Mycoses*. 57(12): p718-733.

Morschhäuser, J., 2016. The development of fluconazole resistance in *Candida albicans*-an example of microevolution of a fungal pathogen. *Journal of microbiology*. 54(3): p192-201.

Moyes, D.L. and Naglik, J.R., 2011. Mucosal immunity and *Candida albicans* infection. *Clinical and Developmental Immunology*, 2011.

Mukherjee, P.K. and Chandra, J., 2004. *Candida* biofilm resistance. *Drug Resistance Updates*. 7(4-5): p301-309.

Mukherjee, P.K., Sheehan, D.J., Hitchcock, C.A., Ghannoum, M.A., 2005. Combination treatment of invasive fungal infections. *Clin. Microbiol. Rev.*18(1): p163.

Murciano, C., Moyes, D.L., Runglall, M., Tobouti, P., Islam, A., Hoyer, L.L. and Naglik, J.R. 2012. Evaluation of the role of *Candida albicans* agglutinin-like sequence (Als) proteins in human oral epithelial cell interactions. *PLoS One*. 7(3): e33362

Murray, P.R., Niles, A.C. and Heeren, R.L., 1988. Microbial inhibition on hospital garments treated with Dow Corning 5700 antimicrobial agent. *Journal of clinical microbiology*. 26(9): p1884-1886.

Mushi, M.F., Bader, O., Taverne-Ghadwal, L., Bii, C., Groß, U. and Mshana, S.E., 2017. Oral candidiasis among African human immunodeficiency virus-infected individuals: 10

years of systematic review and meta-analysis from sub-Saharan Africa. *Journal of oral microbiology*. 9(1): p.1317579.

Mushi, M.F., Mtemisika, C.I., Bader, O., Bii, C., Mirambo, M.M., Groß, U. and Mshana, S.E., 2016. High Oral Carriage of Non-*albicans Candida* spp. among HIV-infected individuals. *International Journal of Infectious Diseases*. 49: p185-188.

Naglik, J., Albrecht, A., Bader, O. and Hube, B., 2004. *Candida albicans* proteinases and host/pathogen interactions. *Cellular microbiology*. 6(10): p915-926.

Naglik, J.R., Challacombe, S.J. and Hube, B., 2003. *Candida albicans* secreted aspartyl proteinases in virulence and pathogenesis. *Microbiol. Mol. Biol. Rev.* 67(3): p400-428.

Naglik, J.R., Moyes, D., Makwana, J., Kanzaria, P., Tsihchaki, E., Weindl, G., Tappuni, A.R., Rodgers, C.A., Woodman, A.J., Challacombe, S.J. and Schaller, M., 2008. Quantitative expression of the *Candida albicans* secreted aspartyl proteinase gene family in human oral and vaginal candidiasis. *Microbiology (Reading, England)*. 154(Pt 11): p3266-3280.

Naglik, J.R., Moyes, D.L., Wächtler, B. and Hube, B., 2011. *Candida albicans* interactions with epithelial cells and mucosal immunity. *Microbes and Infection*. 13(12): p963-976.

Nanteza, M., Tusiime, J.B., Kalyango, J. and Kasangaki, A., 2014. Association between oral candidiasis and low CD4+ count among HIV positive patients in Hoima Regional Referral Hospital. *BMC oral health*. 14(1): p143.

Nasution, A.I. and Basri, B., 2017. Scanning electron microscopy of *Candida albicans* cell wall on tooth surface after fluconazole-treated and incubated with guava (*psidium guajava* L). *Journal of Syiah Kuala Dentistry Society*. 2(2): p78-84.

Nemutandani, M.S., Hendricks, S.J.H. and Mulaudzi, F.M., 2016. Knowledge and beliefs about oral pseudomembranous candidiasis among traditional health practitioners in Limpopo Province, South Africa. *South African Dental Journal*. 71(6): p260-265.

Neto, J.B., da Silva, C.R., Neta, M.A., Campos, R.S., Siebra, J.T., Silva, R.A., Gaspar, D.M., Magalhães, H.I., de Moraes, M.O., Lobo, M.D. and Grangeiro, T.B., 2014. Antifungal activity of naphthoquinoidal compounds *in vitro* against fluconazole-resistant strains of different *Candida* species: a special emphasis on mechanisms of action on *Candida tropicalis*. *PLoS One*. 9(5): p.e93698.

Nosanchuk, J.D., Stark, R.E. and Casadevall, A., 2015. Fungal melanin: what do we know about structure? *Frontiers in microbiology*. 6: p1463.

Nimrichter, L., De Souza, M.M., Del Poeta, M., Nosanchuk, J.D., Joffe, L., Tavares, P.D.M. and Rodrigues, M.L., 2016. Extracellular vesicle-associated transitory cell wall components and their impact on the interaction of fungi with host cells. *Frontiers in microbiology*. 7: p1034.

Nuridin, N., Helary, G. and Sauvet, G., 1993. Biocidal polymers active by contact. III. Ageing of biocidal polyurethane coatings in water. *Journal of applied polymer science*. 50(4): p671-678.

Nweze, E.I. and Ogbonnaya, U.L., 2011. Oral *Candida* isolates among HIV-infected subjects in Nigeria. *Journal of Microbiology, Immunology and Infection*. 44(3): p172-177.

Oberoi, J.K., Wattal, C., Goel, N., Raveendran, R., Datta, S. and Prasad, K., 2012. Non-*albicans* *Candida* species in blood stream infections in a tertiary care hospital at New Delhi, India. *The Indian journal of medical research*. 136(6): p997-1003.

Obłak, E., Adamski, R.Y.S.Z.A.R.D. and Lachowicz, T.M., 2003. pH-dependent influence of a quaternary ammonium salt and an amino ester on the yeast *Saccharomyces cerevisiae* ultrastructure. *Cell. Mol. Biol. Lett*. 8: p105-110.

Obłak, E., Gamian, A., Adamski, R. and Ułaszewski, S., 2010. The physiological and morphological phenotype of a yeast mutant resistant to the quaternary ammonium salt N-(dodecyloxycarboxymethyl)-N, N, N-trimethyl ammonium chloride. *Cellular & molecular biology letters*. 15(2): p215-233.

Obłąk, E., Piecuch, A., Krasowska, A. and Łuczyński, J., 2013. Antifungal activity of gemini quaternary ammonium salts. *Microbiological research*. 168(10): p630-638.

Obłąk, E., Piecuch, A., Maciaszczyk-Dziubińska, E. and Wawrzycka, D., 2016. Quaternary ammonium salt N-(dodecyloxycarbonylmethyl)-N, N, N-trimethyl ammonium chloride induced alterations in *Saccharomyces cerevisiae* physiology. *Journal of biosciences*. 41(4): p601-614.

Odds, F.C., 1994. Pathogenesis of *Candida* infections. *Journal of the American Academy of Dermatology*. 31(3): p.S2-S5.

Oosterhof, J.J., Buijssen, K.J., Busscher, H.J., van der Laan, B.F. and van der Mei, H.C., 2006. Effects of quaternary ammonium silane coatings on mixed fungal and bacterial biofilms on tracheoesophageal shunt prostheses. *Appl. Environ. Microbiol.* 72(5): p3673-3677.

Oro, D., Heissler, A., Rossi, E.M., Scapin, D., da Silva Malheiros, P. and Boff, E., 2015. Antifungal activity of natural compounds against *Candida* species isolated from HIV-positive patients. *Asian Pacific Journal of Tropical Biomedicine*. 5(9): p781-784.

Osaigbovo, II., Lofor, P. and Oladele, R., 2017. Fluconazole resistance among oral *Candida* isolates from people living with HIV/AIDS in a Nigerian tertiary hospital. *Journal of Fungi*. 3(4), p.69.

Ostrosky-Zeichner, L., Casadevall, A., Galgiani, J.N., Odds, F.C. and Rex, J.H., 2010. An insight into the antifungal pipeline: selected new molecules and beyond. *Nature reviews Drug discovery*. 9(9): p719.

Owotade, F.J, Gulube, Z., Ramla, S. and Patel, M., 2016. Antifungal susceptibility of *Candida albicans* isolated from the oral cavities of patients with HIV infection and cancer. *South African Dental Journal*. 71(1): p8-11.

Owotade, F.J. and Patel, M., 2014. Virulence of oral *Candida* isolated from HIV-positive women with oral candidiasis and asymptomatic carriers. *Oral surgery, oral medicine, oral pathology and oral radiology*. 118(4): p455-460.

Owotade, F.J., Patel, M., Ralephenya, T.R. and Vergotine, G., 2013. Oral *Candida* colonization in HIV-positive women: associated factors and changes following antiretroviral therapy. *Journal of medical microbiology*. 62(1): p126-132.

Pappas, P.G., Rex, J.H., Lee, J., Hamill, R.J., Larsen, R.A., Powderly, W., Kauffman, C.A., Hyslop, N., Mangino, J.E., Chapman, S. and Horowitz, H.W., 2003. A prospective observational study of candidemia: epidemiology, therapy, and influences on mortality in hospitalized adult and pediatric patients. *Clinical Infectious Diseases*. 37(5): p634-643.

Parra-Ortega, B., Cruz-Torres, H., Villa-Tanaca, L. and Hernández-Rodríguez, C., 2009. Phylogeny and evolution of the aspartyl protease family from clinically relevant *Candida* species. *Memórias do Instituto Oswaldo Cruz*. 104(3): p505-512.

Park, M., Do, E. and Jung, W.H., 2013. Lipolytic enzymes involved in the virulence of human pathogenic fungi. *Mycobiology*. 41: p67-72.

Patil, S., Rao, R.S., Majumdar, B. and Anil, S., 2015. Clinical appearance of oral *Candida* infection and therapeutic strategies. *Frontiers in Microbiology*. 6: p1391.

Patton, L.L., Bonito, A.J. and Shugars, D.A., 2001. A systematic review of the effectiveness of antifungal drugs for the prevention and treatment of oropharyngeal candidiasis in HIV-positive patients. *Oral Surgery, Oral Medicine, Oral Pathology, Oral Radiology, and Endodontology*. 92(2): p170-179.

Peres da Silva, R., Puccia, R., Rodrigues, M.L., Oliveira, D.L., Joffe, L.S., César, G.V., Nimrichter, L., Goldenberg, S. and Alves, L.R., 2015. Extracellular vesicle mediated export of fungal RNA. *Sci Rep*. 5: p7763.

Perfect, J.R., 2016. "Is there an emerging need for new antifungals?" *Expert opinion on Emerging Drugs*. 21(2): p129-131.

Pfaller, M.A., Moet, G.J., Messer, S.A., Jones, R.N. and Castanheira, M., 2011. *Candida* bloodstream infections: comparison of species distributions and antifungal resistance patterns in community-onset and nosocomial isolates in the SENTRY Antimicrobial Surveillance Program, 2008-2009. *Antimicrobial agents and chemotherapy*. 55(2): p561-566.

Pfaller, M.A., 2012. Antifungal drug resistance: mechanisms, epidemiology, and consequences for treatment. *The American journal of medicine*. 125(1): pS3-S13.

Pfaller, M.A., Rhomberg, P.R., Messer, S.A., Jones, R.N. and Castanheira, M., 2015. Isavuconazole, micafungin, and 8 comparator antifungal agents' susceptibility profiles for common and uncommon opportunistic fungi collected in 2013: temporal analysis of antifungal drug resistance using CLSI species-specific clinical breakpoints and proposed epidemiological cut off values. *Diagnostic microbiology and infectious disease*. 82(4): p303-313.

Pichová, I., Pavlíčková, L., Dostál, J., Dolejší, E., Hrušková-Heidingsfeldová, O., Weber, J., Ruml, T. and Souček, M., 2001. Secreted aspartic proteases of *Candida albicans*, *Candida tropicalis*, *Candida parapsilosis* and *Candida lusitanae*: inhibition with peptidomimetic inhibitors. *European journal of biochemistry*. 268(9): p2669-2677.

Pinjon, E., Moran, G.P., Coleman, D.C. and Sullivan, D.J., 2005. Azole susceptibility and resistance in *Candida dubliniensis*. *Biochem Soc Trans*. 33(5): p1210-1214.

Polacheck, I., Strahilevitz, J., Sullivan, D., Donnelly, S., Salkin, I.F. and Coleman, D.C., 2000. Recovery of *Candida dubliniensis* from non-human immunodeficiency virus-infected patients in Israel. *Journal of clinical microbiology*. 38(1): p170-174.

Porter, S., 2003. Which antifungal agent is most effective in oropharyngeal candidiasis? *Evidence-Based Dentistry*. 4(1): p14.

Prusty, B.K., Niu, L., Kimmerling, K., Johnston, A.D., Tay, F., Krueger, G.R., Rudel, T. and Ablashi, D., 2014. *Novel antiviral compound K21 effective against HSV-1*. Conference: 3rd Antiviral Conference.

Pugholm, L.H., Revenfeld, A.L.S., Søndergaard, E.K.L. and Jørgensen, M.M., 2015. Antibody-based assays for phenotyping of extracellular vesicles. *BioMed Research International*. 2015. p15.

Rajeh, M.A.B., Zuraini, Z., Sasidharan, S., Latha, L.Y. and Amutha, S., 2010. Assessment of *Euphorbia hirta* L. leaf, flower, stem and root extracts for their antibacterial and antifungal activity and brine shrimp lethality. *Molecules*. 15(9): p6008-6018.

Ranjan, A. and Dongari-Bagtzoglou, A., 2018. Tipping the balance: *C. albicans* adaptation in polymicrobial environments. *Journal of Fungi*. 4(3): p112.

Rao, P.K., 2012. Oral candidiasis - A review. *Scholarly journal of Medicine*. 2(2): p26-30

Read, A.F. and Woods, R.J., 2014. Antibiotic resistance management. *Evolution, medicine, and public health*. 2014(1): p147.

Reid, G.A., 1991. Protein targeting in yeast. *Microbiology*. 137(8): p1765-1773.

Reynolds, E.S., 1963. The use of lead citrate at high pH as an electron-opaque stain in electron microscopy. *The Journal of cell biology*. 17(1): p208-212.

Reznik, D.A., 2005. Oral manifestations of HIV disease. *Topics in HIV medicine: a publication of the International AIDS Society, USA*. 13(5): p143-148.

Rhodus, N.L., 2012. Treatment of oral candidiasis. *Northwest Dentistry Journal*. 91(2): p32-34.

Rizzo, J., Nimrichter, L. and Rodrigues, M.L., 2017. What is new? Recent knowledge on fungal extracellular vesicles. *Current Fungal Infection Reports*. 11(4): p141-147.

Rodrigues, C.F., Silva, S. and Henriques, M., 2014. *Candida glabrata*: a review of its features and resistance. *European journal of clinical microbiology & infectious diseases*. 33(5): p673-688.

Rodrigues, M.L., Travassos, L.R., Miranda, K.R., Franzen, A.J., Rozental, S., de Souza, W., Alviano, C.S. and Barreto-Bergter, E., 2000. Human antibodies against a purified glucosylceramide from *Cryptococcus neoformans* inhibit cell budding and fungal growth. *Infection and immunity*. 68(12): p.7049-7060.

Roemer, T. and Krysan, D.J., 2014. Antifungal drug development: challenges, unmet clinical needs, and new approaches. *Cold Spring Harbor perspectives in medicine*. 4(5): p019703.

Rüchel, R., 1981. Properties of a purified proteinase from the yeast *Candida albicans*. *Biochimica et Biophysica Acta (BBA)-Enzymology*. 659(1): p99-113.

Rüchel, R., De Bernardis, F., Ray, T.L., Sullivan, P.A. and Cole, G.T., 1992. *Candida* acid proteinases. *Journal of Medical and Veterinary Mycology*. 30(sup1): p123-132.

Ruhnke, M., 2002. Skin and mucous membrane infections. *Candida and candidiasis*. ASM Press. Washington, DC, p307-325.

Sagatova, A.A., Keniya, M.V., Wilson, R.K., Monk, B.C. and Tyndall, J.D., 2015. Structural insights into binding of the antifungal drug fluconazole to *Saccharomyces cerevisiae* lanosterol 14 α -demethylase. *Antimicrobial agents and chemotherapy*. 59(8): p4982-4989.

Samaranayake, Y.H., Ye, J., Yau, J.Y.Y., Cheung, B.P.K. and Samaranayake, L.P., 2005. *In vitro* method to study antifungal perfusion in *Candida* biofilms. *Journal of clinical microbiology*. 43(2): p818-825.

Salton, M.R.J., 1968. Lytic agents, cell permeability, and monolayer penetrability. *The Journal of general physiology*. 52(1): p227-252.

Salwiczek, M., Qu, Y., Gardiner, J., Strugnell, R.A., Lithgow, T., McLean, K.M. and Thissen, H., 2014. Emerging rules for effective antimicrobial coatings. *Trends in Biotechnology*. 32(2): p82-90.

Sanglard, D., 2016. Emerging threats in antifungal-resistant fungal pathogens. *Frontiers in medicine*. 3: p11.

Sanglard, D., Coste, A. and Ferrari, S., 2009. Antifungal drug resistance mechanisms in fungal pathogens from the perspective of transcriptional gene regulation. *FEMS yeast research*. 9(7): p1029-1050.

Sanglard, D. and Odds, F.C., 2002. Resistance of *Candida* species to antifungal agents: molecular mechanisms and clinical consequences. *The Lancet infectious diseases*. 2(2): p73-85.

Sardi, J.D.C.O., Gullo, F.P., Freires, I.A., de Souza Pitangui, N., Segalla, M.P., Fusco-Almeida, A.M., Rosalen, P.L., Regasini, L.O. and Mendes-Giannini, M.J.S., 2016. Synthesis, antifungal activity of caffeic acid derivative esters, and their synergism with fluconazole and nystatin against *Candida* spp. *Diagnostic microbiology and infectious disease*. 86(4): p387-391.

Sardi, J.C.O., Scorzoni, L., Bernardi, T., Fusco-Almeida, A.M. and Giannini, M.M., 2013. *Candida* species: current epidemiology, pathogenicity, biofilm formation, natural antifungal products and new therapeutic options. *Journal of medical microbiology*. 62(1): p10-24.

Schaller, M., Borelli, C., Korting, H.C. and Hube, B., 2005. Hydrolytic enzymes as virulence factors of *Candida albicans*. *Mycoses*. 48(6): p365-377.

Schaller, M., Hube, B., Ollert, M.W., Schäfer, W., Borg-von Zepelin, M., Thoma-Greber, E., and Korting, H.C., 1999a. *In vivo* expression and localization of *Candida albicans* secreted aspartyl proteinases during oral candidiasis in HIV-infected patients. *J Invest Dermatol*. 112(3): p383-6.

Schaller, M., Januschke, E., Schackert, C., Woerle, B. and Korting, H.C., 2001. Different isoforms of secreted aspartyl proteinases (Sap) are expressed by *Candida albicans* during oral and cutaneous candidosis *in vivo*. *Journal of medical microbiology*. 50(8): p743-747.

Schaller, M., Korting, H.C., Schäfer, W., Bastert, J., Chen, W. and Hube, B., 1999b. Secreted aspartic proteinase (Sap) activity contributes to tissue damage in a model of human oral candidosis. *Molecular microbiology*. 34(1): p169-180.

Schaller, M., Schäfer, W., Korting, H.C. and Hube, B., 1998. Differential expression of secreted aspartyl proteinases in a model of human oral candidosis and in patient samples from the oral cavity. *Molecular microbiology*. 29(2): p605-615.

Schmalreck, A.F., Willinger, B., Haase, G., Blum, G., Lass-Flörl, C., Fegeler, W., Becker, K. and Antifungal Susceptibility Testing (AFST) Study Group, 2012. Species and susceptibility distribution of 1062 clinical yeast isolates to azoles, echinocandins, flucytosine and amphotericin B from a multi-centre study. *Mycoses*. 55(3): p124-137.

Schwalbe, R., Steele-Moore, L. and Goodwin, A.C., 2007. *Antimicrobial susceptibility testing protocols*. CRC Press, Boca Raton, FL

Scorneaux, B., Angulo, D., Borroto-Esoda, K., Ghannoum, M., Peel, M. and Wring, S., 2017. SCY-078 is Fungicidal in Time-Kill Studies against *Candida* Species. *Antimicrobial Agents and Chemotherapy*. 61(3): p01961.

Scorzoni, L., de Paula e Silva, A.C., Marcos, C.M., Assato, P.A., de Melo, W.C., de Oliveira, H.C., Costa-Orlandi, C.B., Mendes-Giannini, M.J. and Fusco-Almeida, A.M., 2017. Antifungal therapy: new advances in the understanding and treatment of mycosis. *Frontiers in microbiology*. 8: p36.

Scully, C., 2008. *Oral and Maxillofacial Medicine: the Basis of Diagnosis and Treatment*. 2nd ed. Edinburgh: Churchill Livingstone. p191.

Serpa, R., França, E.J., Furlaneto-Maia, L., Andrade, C.G., Diniz, A. and Furlaneto, M.C., 2012. *In vitro* antifungal activity of the flavonoid baicalein against *Candida* species. *Journal of medical microbiology*. 61(12): p1704-1708.

Setiawati, S., Nuryastuti, T., Ngatidjan, N., Mustofa, M., Jumina, J. and Fitriastuti, D., 2017. *In vitro* antifungal activity of (1)-N-2-Methoxybenzyl-1, 10-phenanthroline Bromide against *Candida albicans* and its effects on membrane integrity. *Mycobiology*. 45(1): p25-30.

Shah, R., Chaturvedi, P. and Pandya, H.P., 2014. Prevalence of *Candida* from sputum in HIV infected patients of Gujarat, India. *Int J Curr Microbiol App Sci*. 3(8): p345-57.

Sharon, A., Finkelstein, A., Shlezinger, N. and Hatam, I., 2009. Fungal apoptosis: function, genes and gene function. *FEMS Microbiology Reviews*. 33(5): p.833-854.

Shaw, K.J., Schell, W.A., Covell, J., Duboc, G., Giamberardino, C., Kapoor, M., Moloney, M., Soltow, Q.A., Tenor, J.L., Toffaletti, D.L. and Trzoss, M., 2018. *In vitro* and *in vivo* evaluation of APX001A/APX001 and other Gwt1 inhibitors against *Cryptococcus*. *Antimicrobial agents and chemotherapy*. 62(8): p.e 00523-18.

Shekhar-Guturja, T., Tebung, W.A., Mount, H., Liu, N., Köhler, J.R., Whiteway, M. and Cowen, L.E., 2016. Beauvericin potentiates azole activity via inhibition of multidrug efflux, blocks *Candida albicans* morphogenesis, and is effluxed via Yor1 and circuitry controlled by Zcf29. *Antimicrobial agents and chemotherapy*. 60(12): p7468-7480.

Sherman, R.G., Prusinski, L., Ravenel, M.C. and Joralmon, R.A., 2002. Oral candidosis. *Quintessence Int*. 33(7): p521-32

Shinobu-Mesquita, C., Bonfim-Mendonça, P., Moreira, A., Ferreira, I., Donatti, L., Fiorini, A. and Svidzinski, T., 2015. Cellular Structural Changes in *Candida albicans* caused by the Hydroalcoholic Extract from *Sapindus saponaria* L. *Molecules*. 20(5): p9405-9418.

Shirai, A., Sumitomo, T., Kurimoto, M., Maseda, H. and Kourai, H., 2009. The mode of the antifungal activity of gemini-pyridinium salt against yeast. *Biocontrol science*. 14(1): p13-20.

Sholapurkar, A.A., Pai, K.M. and Rao, S., 2009. Comparison of efficacy of fluconazole mouthrinse and clotrimazole mouthpaint in the treatment of oral candidiasis. *Australian dental journal*. 54(4): p341-346.

Silva, S., Negri, M., Henriques, M., Oliveira, R., Williams, D.W. and Azeredo, J., 2012. *Candida glabrata*, *Candida parapsilosis* and *Candida tropicalis*: biology, epidemiology, pathogenicity and antifungal resistance. *FEMS microbiology reviews*. 36(2): p288-305.

Singh, G. and Raksha, A.U., 2013. Candidal infection: Epidemiology, Pathogenesis and recent advances for diagnosis. *Bulletin of Pharmaceutical and Medical Sciences (BOPAMS)*. 1(1).

Soares, B.M., Assis Santos, D., Kohler, L.M., da Costa César, G., de Carvalho, I.R., Martins, M.D.A. and Cisalpino, P.S., 2008. Cerebral infection caused by *Cryptococcus gattii*: a case report and antifungal susceptibility testing. *Revista iberoamericana de micologia*. 25(4): p242-245.

Song, L. and Baney, R.H., 2011. Antibacterial evaluation of cotton textile treated by trialkoxysilane compounds with antimicrobial moiety. *Textile Research Journal*. 81(5): p504-511.

Sopirala, M.M., Mangino, J.E., Gebreyes, W.A., Biller, B., Bannerman, T., Balada-Llasat, J.M. and Pancholi, P., 2010. Synergy testing by Etest, microdilution checkerboard, and time-kill methods for pan-drug-resistant *Acinetobacter baumannii*. *Antimicrobial agents and chemotherapy*. 54(11): p4678-4683.

Souza, N.A.B., Lima, E.D.O., Guedes, D.N., Pereira, F.D.O., Souza, E.L.D. and Sousa, F.B.D., 2010. Efficacy of *Origanum* essential oils for inhibition of potentially pathogenic fungi. *Brazilian Journal of Pharmaceutical Sciences*. 46(3): p499-508.

Soysa, N.S., Samaranyake, L.P. and Ellepola, A.N.B., 2008. Antimicrobials as a contributory factor in oral candidosis—a brief overview. *Oral diseases*. 14(2): p138-143.

Spampinato, C. and Leonardi, D., 2013. *Candida* infections, causes, targets, and resistance mechanisms: traditional and alternative antifungal agents. *BioMed research international*. 2013. p13.

Spiering, M.J., Moran, G.P., Chauvel, M., MacCallum, D.M., Higgins, J., Hokamp, K., Yeomans, T., d'Enfert, C., Coleman, D.C. and Sullivan, D.J., 2010. Comparative transcript profiling of *Candida albicans* and *Candida dubliniensis* identifies SFL2, a *C. albicans* gene required for virulence in a reconstituted epithelial infection model. *Eukaryotic cell*. 9(2): p251-265.

Staib, F., 1966. Serum-proteins as nitrogen source for yeast like fungi. *Sabouraudia: Journal of Medical and Veterinary Mycology*. 4(3): p187-193.

Staniszewska, M., Bondaryk, M., Piłat, J., Siennicka, K., Magda, U. and Kurzatkowski, W., 2012a. Virulence factors of *Candida albicans*. *Przegląd epidemiologiczny*. 66(4): p629-33

Staniszewska, M., Bondaryk, M., Siennicka, K., Kurek, A., Orłowski, J., Schaller, M., and Kurzatkowski, W., 2012b. *In vitro* study of secreted aspartyl proteinases Sap 1 to Sap 3 and Sap 4 to Sap 6 expression in *Candida albicans* pleomorphic forms. *Pol J Microbiol*. 61(4): p247-256.

Staniszewska, M., Bondaryk, M., Swoboda-Kopec, E., Siennicka, K., Sygitowicz, G. and Kurzatkowski, W., 2013. *Candida albicans* morphologies revealed by scanning electron microscopy analysis. *Brazilian Journal of Microbiology*. 44(3): p813.

Stehr, F., Felk, A., Kretschmar, M., Schaller, M., Schäfer, W. and Hube, B., 2000. Extracellular hydrolytic enzymes and their relevance during *Candida albicans* infections. *Mycoses*. 43(S2): pS17-21.

Sun, L., Liao, K. and Wang, D., 2015. Effects of magnolol and honokiol on adhesion, yeast-hyphal transition, and formation of biofilm by *Candida albicans*. *PLoS One*. 10(2): p.e0117695.

Szwarc, P., Goldenberg, S. and Alves, L.R., 2018. Extracellular Vesicles in Fungi: Composition and Functions. *Current topics in microbiology and immunology*. Springer Nature. Switzerland.

Taillandier, J., Esnault, Y. and Alemanni, M., 2000. A comparison of fluconazole oral suspension and amphotericin B oral suspension in older patients with oropharyngeal candidosis. Multicentre Study Group. *Age and ageing*. 29(2): p117-123.

Tatsumi, Y., Nagashima, M., Shibanushi, T., Iwata, A., Kangawa, Y., Inui, F., Siu, W.J.J., Pillai, R. and Nishiyama, Y., 2013. Mechanism of action of efinaconazole, a novel triazole antifungal agent. *Antimicrobial agents and chemotherapy*. 57(5): p2405-2409.

Terças, A.L., Marques, S.G., Moffa, E.B., Alves, M.B., de Azevedo, C.M., Siqueira, W.L. and Monteiro, C.A., 2017. Antifungal drug susceptibility of *Candida* species isolated from HIV-positive patients recruited at a public hospital in São Luís, Maranhão, Brazil. *Frontiers in microbiology*. 8: p298.

Terézhalmy, G.T. and Huber, M.A., 2011. Oropharyngeal candidiasis: Etiology, epidemiology, clinical manifestations, diagnosis, and treatment. *Crest Oral-B at dentalcare.com Contin Educ Course*. p1-16.

Thompson III, G.R., Patel, P.K., Kirkpatrick, W.R., Westbrook, S.D., Berg, D., Erlandsen, J., Redding, S.W. and Patterson, T.F., 2010. Oropharyngeal candidiasis in the era of antiretroviral therapy. *Oral Surgery, Oral Medicine, Oral Pathology, Oral Radiology, and Endodontology*. 109(4): p488-495.

Tinoco-Araujo, J.E., Araújo, D.F.G., Barbosa, P.G., Santos, P.S.D.S. and Medeiros, A.M.C.D., 2013. Invasive candidiasis and oral manifestations in premature newborns. *Einstein (Sao Paulo)*. 11(1): p71-75.

Tischer, M., Pradel, G., Ohlsen, K. and Holzgrabe, U., 2012. Quaternary ammonium salts and their antimicrobial potential: targets or nonspecific interactions? *ChemMedChem*. 7(1): p22-31.

Togni, G., Sanglard, D., Falchetto, R. and Monod, M., 1991. Isolation and nucleotide sequence of the extracellular acid protease gene (ACP) from the yeast *Candida tropicalis*. *FEBS letters*. 286(1-2): p181-185.

Tongchusak, S., Brusica, V. and Chaiyaroj, S.C., 2008. Promiscuous T cell epitope prediction of *Candida albicans* secretory aspartyl protease family of proteins. *Infection, Genetics and Evolution*. 8(4): p467-473.

Tortorano, A.M., Prigitano, A., Dho, G., Grancini, A., Passera, M. and Ecm-Fimua Study Group, 2012. Antifungal susceptibility profiles of *Candida* isolates from a prospective survey of invasive fungal infections in Italian intensive care units. *Journal of medical microbiology*. 61(3): p389-393.

Tran, P.L., Hamood, A.N., de Souza, A., Schultz, G., Liesenfeld, B., Mehta, D. and Reid, T.W., 2015. A study on the ability of quaternary ammonium groups attached to a polyurethane foam wound dressing to inhibit bacterial attachment and biofilm formation. *Wound Repair and Regeneration*. 23(1): p74-81.

Treister, N.S. and Bruch, J.M., 2010. *Clinical oral medicine and pathology*. New York: Humana Press. p19-21.

Tsang, C.S.P., Chu, F.C.S., Leung, W.K., Jin, L.J., Samaranayake, L.P. and Siu, S.C., 2007. Phospholipase, proteinase and haemolytic activities of *Candida albicans* isolated from oral cavities of patients with type 2 diabetes mellitus. *Journal of medical microbiology*. 56(10): p1393-1398.

Turnidge, J. and Paterson, D.L., 2007. Setting and revising antibacterial susceptibility breakpoints. *Clinical microbiology reviews*. 20(3): p391-408.

UNAIDS. Joint United Nations Programme on HIV/AIDS. 2002. *Report on the global HIV/AIDS epidemic*. UNAIDS.

Vadlapatla, R.K., Patel, M., Paturi, D.K., Pal, D. and Mitra, A.K., 2014. Clinically relevant drug-drug interactions between antiretrovirals and antifungals. *Expert opinion on drug metabolism & toxicology*. 10(4): p561-580.

Vallejo, M.C., Matsuo, A.L., Ganiko, L., Medeiros, L.C.S., Miranda, K., Silva, L.S., Freymüller-Haapalainen, E., Sinigaglia-Coimbra, R., Almeida, I.C. and Puccia, R., 2011. The pathogenic fungus *Paracoccidioides brasiliensis* exports extracellular vesicles containing highly immunogenic α -Galactosyl epitopes. *Eukaryotic cell*. 10(3): p343-351.

Vargas, G., Rocha, J.D., Oliveira, D.L., Albuquerque, P.C., Frases, S., Santos, S.S., Nosanchuk, J.D., Gomes, A.M.O., Medeiros, L.C., Miranda, K. and Sobreira, T.J., 2015. Compositional and immunobiological analyses of extracellular vesicles released by *Candida albicans*. *Cellular microbiology*. 17(3): p389-407.

Vazquez, J.A., 2010. Optimal management of oropharyngeal and esophageal candidiasis in patients living with HIV infection. *HIV/AIDS (Auckland, NZ)*. 2: p89-101.

Vazquez, J.A., Lundstrom, T., Dembry, L., Chandrasekar, P., Boikov, D., Parri, M.B. and Zervos, M.J., 1995. Invasive *Candida guilliermondii* infection: *in vitro* susceptibility studies and molecular analysis. *Bone marrow transplantation*. 16(6): p849-853.

Verma, R. and Narang, R., 2014. An Update on Oral Candidiasis: An Opportunistic Infection. *Indian Journal of Public Health Research & Development*. 5(4): p112-117.

Wabe, N.T., Hussein, J., Suleman, S. and Abdella, K., 2011. *In vitro* antifungal susceptibility of *Candida albicans* isolates from oral cavities of patients infected with human immunodeficiency virus in Ethiopia. *J Exp Integr Med*. 1(4): p265-71.

Wächtler, B., Wilson, D., Haedicke, K., Dalle, F. and Hube, B., 2011. From attachment to damage: defined genes of *Candida albicans* mediate adhesion, invasion and damage during interaction with oral epithelial cells. *PloS one*. 6(2): p.e17046.

Wang, Y.H., Dong, H.H., Zhao, F., Wang, J., Yan, F., Jiang, Y.Y. and Jin, Y.S., 2016. The synthesis and synergistic antifungal effects of chalcones against drug resistant *Candida albicans*. *Bioorganic & medicinal chemistry letters*. 26(13): p3098-3102.

Weerasinghe, P. and Buja, L.M., 2012. Oncosis: an important non-apoptotic mode of cell death. *Experimental and molecular pathology*. 93(3): p302-308.

Wessels, S. and Ingmer, H., 2013. Modes of action of three disinfectant active substances: a review. *Regulatory Toxicology and Pharmacology*. 67(3): p456-467.

White, T.C. and Agabian, N., 1995. *Candida albicans* secreted aspartyl proteinases: isoenzyme pattern is determined by cell type, and levels are determined by environmental factors. *Journal of bacteriology*. 177(18): p5215-5221.

World Health Organization., 2014. Antimicrobial resistance: global report on surveillance. *World Health Organization*. Retrieved. May 9, 2015.

Williams, D., and Lewis, M. 2011. Pathogenesis and treatment of oral candidosis. *Journal of oral microbiology*. 3(1): p5771.

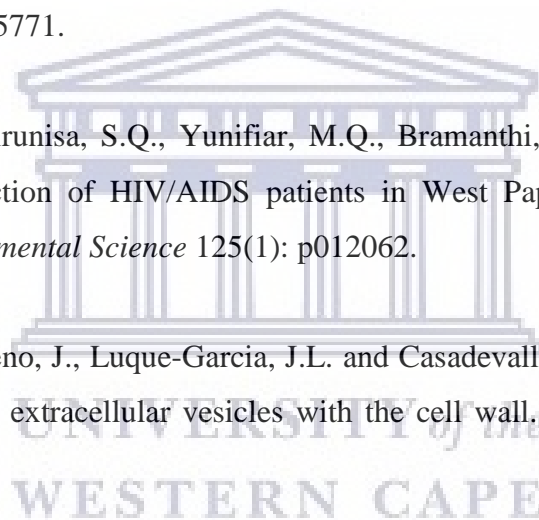
Witaningrum, A.M., Khairunisa, S.Q., Yunifiar, M.Q., Bramanthi, R. and Rachman, B.E., 2018. Opportunistic infection of HIV/AIDS patients in West Papua. In IOP Conference Series: *Earth and Environmental Science* 125(1): p012062.

Wolf, J.M., Espadas-Moreno, J., Luque-Garcia, J.L. and Casadevall, A., 2014. Interaction of *Cryptococcus neoformans* extracellular vesicles with the cell wall. *Eukaryotic cell*. 13(12): p1484-1493.

Wong, S.S.W., Kao, R.Y.T., Yuen, K.Y., Wang, Y., Yang, D., Samaranayake, L.P. and Seneviratne, C.J., 2014. *In vitro* and *in vivo* activity of a novel antifungal small molecule against *Candida* infections. *PLoS One*. 9(1): p.e85836.

Wu, T., Samaranayake, L.P., Cao, B.Y. and Wang, J., 1996. *In-vitro* proteinase production by oral *Candida albicans* isolates from individuals with and without HIV infection and its attenuation by antimycotic agents. *Journal of medical microbiology*. 44(4): p311-316.

Yu, L., Ling, G., Deng, X., Jin, J., Jin, Q. and Guo, N., 2011. *In vitro* interaction between fluconazole and triclosan against clinical isolates of fluconazole-resistant *Candida albicans* determined by different methods. *Antimicrobial agents and chemotherapy*. 55(7): p3609-3612.



Yuen, J.W.M. and Yung, J., 2013. Medical implications of antimicrobial coating polymers-Organosilicon quaternary ammonium chloride. *Modern chemistry & applications*. 1(3).

Zavrel, M. and White, T.C., 2015. Medically important fungi respond to azole drugs: an update. *Future microbiology*. 10(8): p1355-1373.

Zusman, O., Avni, T., Leibovici, L., Adler, A., Friberg, L., Stergiopoulou, T., Carmeli, Y. and Paul, M., 2013. Systematic review and meta-analysis of *in vitro* synergy of polymyxins and carbapenems. *Antimicrobial agents and chemotherapy*. 57(10): p5104-5111.

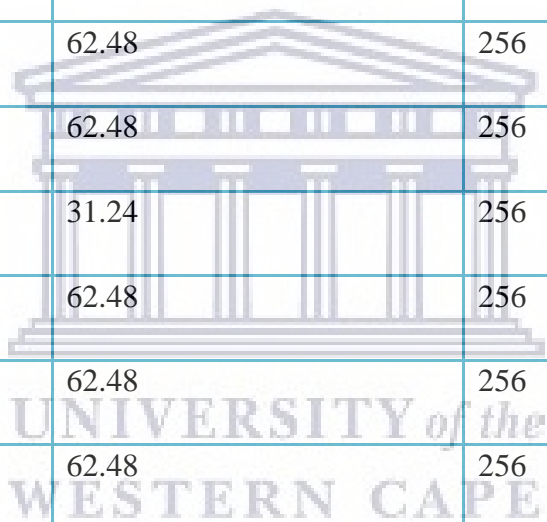


APPENDIX A

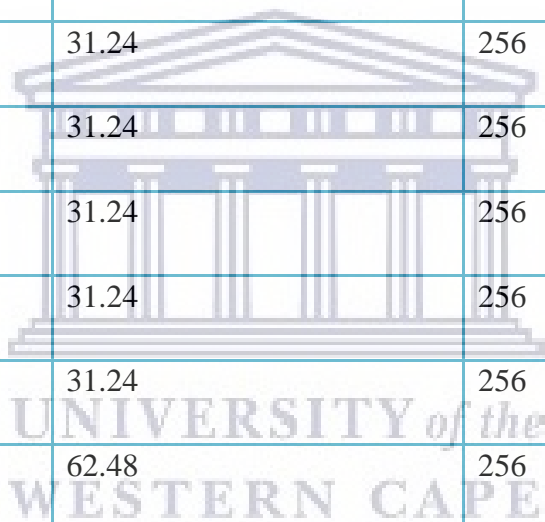
MIC values of K21 and FCZ against *Candida* isolates

FCZ-resistant <i>Candida</i>		
<i>C. albicans</i>		
Serial number	K21 MIC ($\mu\text{g/mL}$)	FCZ MIC ($\mu\text{g/mL}$)
1	62.48	256
2	124.95	256
3	124.95	256
4	124.95	256
5	62.48	256
6	124.95	256
7	62.48	256
8	62.48	256
9	124.95	256
10	124.95	256
11	62.48	256
12	62.48	256
13	124.95	256
14	62.48	256
15	249.89	256

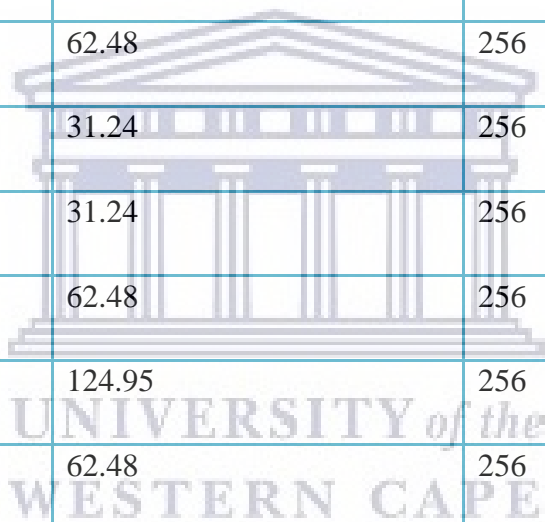
16	124.95	256
17	62.48	256
18	62.48	256
19	31.24	256
20	62.48	256
21	249.89	256
22	62.48	256
23	249.89	256
24	62.48	256
25	62.48	256
26	31.24	256
27	62.48	256
28	62.48	256
29	62.48	256
30	62.48	256
31	31.24	256
32	31.24	256
33	62.48	256
34	249.89	256
35	62.48	256
36	31.24	256



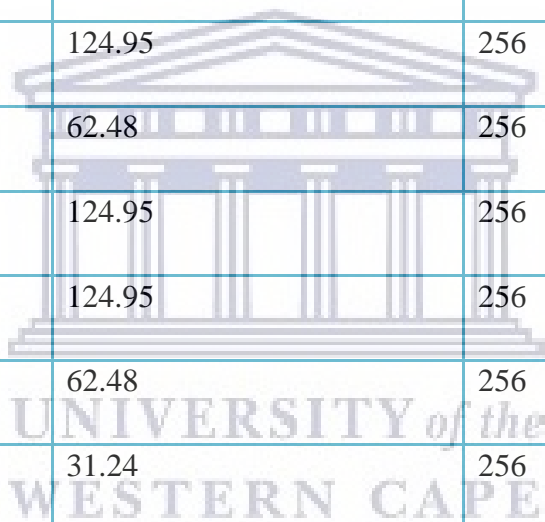
37	62.48	256
38	62.48	256
39	31.24	256
40	62.48	256
41	31.24	256
42	62.48	256
43	62.48	256
44	62.48	256
45	31.24	256
46	31.24	256
47	31.24	256
48	31.24	256
49	31.24	256
50	62.48	256
51	62.48	128
52	124.95	256
53	62.48	256
54	62.48	256
55	62.48	256
56	62.48	256
57	62.48	256



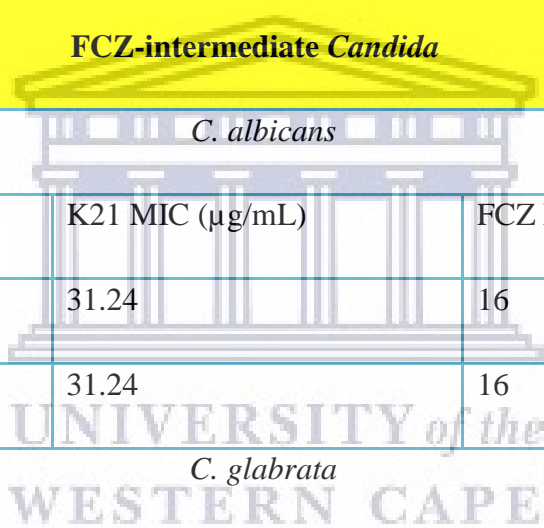
58	62.48	256
59	62.48	256
60	31.24	256
61	31.24	256
62	31.24	256
63	62.48	256
64	31.24	256
65	31.24	256
66	62.48	256
67	31.24	256
68	31.24	256
69	62.48	256
70	124.95	256
71	62.48	256
72	31.24	256
73	31.24	256
74	31.24	64
75	124.95	256
76	62.48	256
77	62.48	256
78	31.24	256



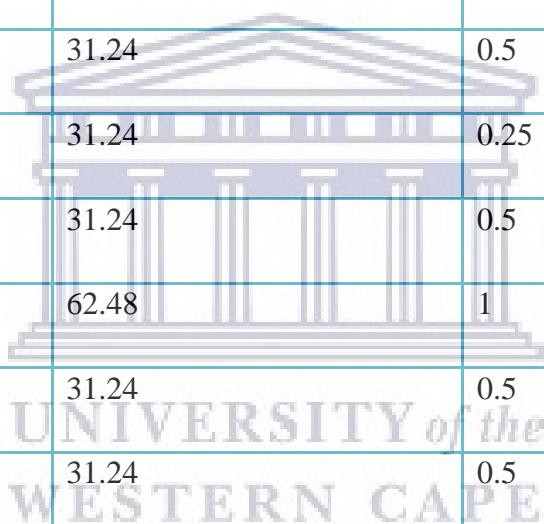
79	62.48	256
80	31.24	256
81	249.89	256
82	124.95	256
83	31.24	256
84	31.24	256
85	249.89	256
86	31.24	128
87	124.95	256
88	62.48	256
89	124.95	256
90	124.95	256
91	62.48	256
92	31.24	256
93	124.95	256
94	62.48	256
95	62.48	256
96	124.95	256
97	31.24	256
98	31.24	256
99	62.48	256



<i>C. dubliniensis</i>		
100	124.95	256
<i>C. krusei</i>		
101	124.95	64
102	124.95	64
<i>C. glabrata</i>		
103	62.48	256
FCZ-intermediate <i>Candida</i>		
<i>C. albicans</i>		
Serial number:	K21 MIC ($\mu\text{g/mL}$)	FCZ MIC ($\mu\text{g/mL}$)
1	31.24	16
2	31.24	16
<i>C. glabrata</i>		
3	249.89	32
4	62.48	16
5	124.95	16
6	249.89	32
7	249.89	16
8	62.48	16
9	124.95	16
10	124.95	16



11	62.48	16
12	62.48	16
13	124.95	16
FCZ-susceptible <i>Candida</i>		
<i>C. albicans</i>		
Serial number	K21 MIC ($\mu\text{g/mL}$)	FCZ MIC ($\mu\text{g/mL}$)
1	31.24	0.5
2	31.24	0.5
3	31.24	0.25
4	31.24	0.5
5	62.48	1
6	31.24	0.5
7	31.24	0.5
8	62.48	0.5
9	31.24	0.12
10	31.24	4
11	31.24	4
12	62.48	4
13	31.24	4
14	31.24	8



15	62.48	8
16	62.48	8
<i>C. glabrata</i>		
17	31.24	0.5
18	62.48	4
19	31.24	0.5
20	124.95	8
<i>C. dubliniensis</i>		
21	62.48	0.5
22	62.48	0.5
23	62.48	0.03
<i>C. krusei</i>		
24	62.48	4
<i>C. tropicalis</i>		
25	31.24	2
26	31.24	2
27	31.24	1

